ISSN:2067-3809

ACTA TECHNICA CORVINIENSIS

- Bulletin of Engineering

fascicule 2
[April - June]
tome X
[2017]

ISSN:2067-3809

INDEXES & DATABASES

We are very pleased to inform that our international scientific journal **ACTA TECHNICA CORVINIENSIS ■ Bulletin of Engineering** completed its nine years of publication successfully [**2008–2016, Tome I–IX**].
In a very short period the **ACTA TECHNICA CORVINIENSIS ■ Bulletin of Engineering** has acquired global presence and scholars from all over the world have taken it with great enthusiasm.
We are extremely grateful and heartily acknowledge the kind of support and encouragement from all contributors and all collaborators!

ACTA TECHNICA CORVINIENSIS ■ Bulletin of Engineering is accredited and ranked in the **"B+" CATEGORY Journal** by **CNCSIS – The National University Research Council's Classification of Romanian Journals, positionno. 940 (http://cncsis.gov.ro/).**
ACTA TECHNICA CORVINIENSIS ■ Bulletin of Engineering is a part of the **SCIPIO - The Romanian Editorial Platform (http://www.scipio.ro/).**

ACTA TECHNICA CORVINIENSIS ■ Bulletin of Engineering is indexed, abstracted and covered in the world-known bibliographical databases and directories including:

INDEX COPERNICUS – JOURNAL MASTER LIST
http://journals.indexcopernicus.com/
GENAMICSJOURNALSEEK Database
http://journalseek.net/
DOAJ – Directory of Open Access Journals
http://www.doaj.org/
EVISA Database
http://www.speciation.net/
CHEMICAL ABSTRACTS SERVICE (CAS)
http://www.cas.org/
EBSCO Publishing
http://www.ebscohost.com/
GOOGLE SCHOLAR
http://scholar.google.com
SCIRUS - Elsevier
http://www.scirus.com/
ULRICHSweb – Global serials directory
http://ulrichsweb.serialssolutions.com
getCITED
http://www.getcited.org
BASE - Bielefeld Academic Search Engine
http://www.base-search.net
Electronic Journals Library
http://rzblx1.uni-regensburg.de
Open J-Gate
http://www.openj-gate.com
ProQUEST Research Library
http://www.proquest.com
Directory of Research Journals Indexing
http://www.drji.org/
Directory Indexing of International Research Journals
http://www.citefactor.org/

ACTA TECHNICA CORVINIENSIS ■ Bulletin of Engineering is also indexed in the digital libraries of the following world's universities and research centers:

WorldCat – the world's largest library catalog
https://www.worldcat.org/
National Lybrary of Australia
http://trove.nla.gov.au/
University Library of Regensburg – GIGA German Institute of Global and Area Studies
http://opac.giga-hamburg.de/ezb/
Simon Fraser University – Electronic Journals Library
http://cufts2.lib.sfu.ca/
University of Wisconsin-Madison Libraries
http://library.wisc.edu/
University of Toronto Libraries
http://search.library.utoronto.ca/
The University of Queensland
https://www.library.uq.edu.au/
The New York Public Library
http://nypl.bibliocommons.com/
State Library of New South Wales
http://library.sl.nsw.gov.au/
University of Alberta Libraries - University of Alberta
http://www.library.ualberta.ca/
The University of Hong Kong Libraries
http://sunzi.lib.hku.hk/
The University Library - The University of California
http://harvest.lib.ucdavis.edu/

10th years ANNIVERSARY

ISSN:2067-3809

ACTA TECHNICA CORVINIENSIS
– Bulletin of Engineering
Tome X [2017]
Fascicule 2 [April – June]
ISSN: 2067 – 3809

ASSOCIATE EDITORS AND REGIONAL COLLABORATORS

The Editor and editorial board members do not receive any remuneration. These positions are voluntary. The members of the Editorial Board may serve as scientific reviewers.

We are very pleased to inform that our journal **ACTA TECHNICA CORVINIENSIS – Bulletin of Engineering** is going to complete its eight years of publication successfully. In a very short period it has acquired global presence and scholars from all over the world have taken it with great enthusiasm. We are extremely grateful and heartily acknowledge the kind of support and encouragement from you.

ACTA TECHNICA CORVINIENSIS – Bulletin of Engineering seeking qualified researchers as members of the editorial team. Like our other journals, **ACTA TECHNICA CORVINIENSIS – Bulletin of Engineering** will serve as a great resource for researchers and students across the globe. We ask you to support this initiative by joining our editorial team. If you are interested in serving as a member of the editorial team, kindly send us your resume to redactie@fih.upt.ro.

ISSN:2067-3809

ACTA TECHNICA CORVINIENSIS
– Bulletin of Engineering
Tome X [2017]
Fascicule 2 [April – June]
ISSN: 2067 – 3809

INTERNATIONAL SCIENTIFIC COMMITTEE MEMBERS AND SCIENTIFIC REVIEWERS

The Scientific Committee members and Reviewers do not receive any remuneration. These positions are voluntary.

We are extremely grateful and heartily acknowledge the kind of support and encouragement from all contributors and all collaborators!

ACTA TECHNICA CORVINIENSIS – Bulletin of Engineering is dedicated to publishing material of the highest engineering interest, and to this end we have assembled a distinguished Editorial Board and Scientific Committee of academics, professors and researchers.

ACTA TECHNICA CORVINIENSIS – Bulletin of Engineering publishes invited review papers covering the full spectrum of engineering. The reviews, both experimental and theoretical, provide general background information as well as a critical assessment on topics in a state of flux. We are primarily interested in those contributions which bring new insights, and papers will be selected on the basis of the importance of the new knowledge they provide.

ACTA TECHNICA CORVINIENSIS – Bulletin of Engineering encourages the submission of comments on papers published particularly in our journal. The journal publishes articles focused on topics of current interest within the scope of the journal and coordinated by invited guest editors. Interested authors are invited to contact one of the Editors for further details.

ACTA TECHNICA CORVINIENSIS – Bulletin of Engineering accept for publication unpublished manuscripts on the understanding that the same manuscript is not under simultaneous consideration of other journals. Publication of a part of the data as the abstract of conference proceedings is exempted.

Manuscripts submitted (original articles, technical notes, brief communications and case studies) will be subject to peer review by the members of the Editorial Board or by qualified outside reviewers. Only papers of high scientific quality will be accepted for publication. Manuscripts are accepted for review only when they report unpublished work that is not being considered for publication elsewhere. The evaluated paper may be recommended for:

- ✓ **Acceptance without any changes** – in that case the authors will be asked to send the paper electronically in the required .doc format according to authors' instructions;
- ✓ **Acceptance with minor changes** – if the authors follow the conditions imposed by referees the paper will be sent in the required .doc format;
- ✓ **Acceptance with major changes** – if the authors follow completely the conditions imposed by referees the paper will be sent in the required .doc format;
- ✓ **Rejection** – in that case the reasons for rejection will be transmitted to authors along with some suggestions for future improvements (if that will be considered necessary).

The manuscript accepted for publication will be published in the next issue of **ACTA TECHNICA CORVINIENSIS – Bulletin of Engineering** after the acceptance date.

All the authors and the corresponding author in particular take the responsibility to ensure that the text of the article does not contain portions copied from any other published material which amounts to plagiarism. We also request the authors to familiarize themselves with the good publication ethics principles before finalizing their manuscripts.

ISSN:2067-3809

ACTA TECHNICA CORVINIENSIS
– Bulletin of Engineering
Tome X [2017]
Fascicule 2 [April – June]
ISSN: 2067 – 3809

TABLE of CONTENTS

ACTA TECHNICA CORVINIENSIS
– Bulletin of Engineering
Tome X [2017],
Fascicule 2 [April – June]

Abstract: Primary goals of dimensioning and control of feed drives are on the one hand the exact tracing of a given target contour with low latency. On the other hand, static and dynamic disturbances, for example process forces, shall be optimally compensated. The dynamic behavior not only influences machining accuracy and manufacturing time, it also has an impact on wear and damages of machine and tool. To increase productivity and efficiency of industrial machine tools, one important aspect is the dynamic behavior of their feed drives. At the Institute for Control Engineering of Machine Tools and Manufacturing Units (ISW) of the University of Stuttgart, various approaches, based on constructive methods, control engineering or additional actuators were examined, which can influence the dynamic behavior in a positive way. In this paper, exemplary solutions are presented with their benefits and drawbacks to provide an overview on the currently ongoing research work. For validation and illustration of the different principles, simulative and experimental results are presented.
Keywords: machine tool feed drives, control, dynamic behavior

Abstract: This aim of this study is to identify failure mechanism of ethylene pyrolysis furnace tube after five year of operation. The tubes were manufactured from centrifugally cast heat resistant steel HK 40. Failure analysis of the radiant tubes was performed by careful visual inspection of the failed tubes, scanning electron microscopy observation of crack region samples, hardness and micro-hardness measurements. Selected specimens were prepared from the four samples, measurements was carried out at inner, middle and outer sides of the samples. The experimental results showed that the mode of tube failure was a combination of high temperature carburization attack and creep damage leading to intergranular cracking. Maximum hardness is associated with internally carburized zone where the amount of carbides is maximum in this region. The hardness of the radiant tubes decreases as the distance moves from the inner surface to the middle section. The metallurgical background of the combined action of carburization and creep ductility exhaustion have been investigated and are explained. Pyrolysis tube failures can be prevented by a combination of proper furnace operation, materials choice, regular inspections and good design.
Keywords: ethylene pyrolysis; furnace; tube; damage; inspection

Abstract: The influence of low-frequency electromagnetic field (LF EMF) on living organisms is widely discussed issue both in scientific area and in public. The paper deals with low frequency electromagnetic field effects on growth dynamics of yeast cells Saccharomyces cerevisiae. The current state of the research of electromagnetic field interactions with biological systems is briefly introduced. Several experiments are carried out in order to investigate influence of specifically adjusted artificial low frequency electromagnetic field on Saccharomyces cerevisiae growth dynamics. The experimental apparatus, materials, conditions and evaluation methods are described in the paper. The presented results indicate the differences in growth dynamics between cells exposed to magnetic field and the unexposed ones.
Keywords: electromagnetic field, yeast cells, exposed sample, control sample

Abstract: Manipulators of mobile machines represent multisegment kinematic chains with segments, in the form of lever, which are connected rotary or translational joints of the first class. The last segment in the kinematic chain of manipulators are different tools by which perform the basic functions of the machine. In paper is defined the optimization tribological criteria of the manipulators crank driving mechanisms of mobile machines. Criteria indicator is mechanical efficiency of driving mechanisms, which reflects the tribological loss power of machines driving system due to friction between the elements of kinematic pairs (joints) manipulator's driving mechanisms.
Keywords: driving mechanisms, optimization

Abstract: Because of the rapid development of precision machinery, the demands on the dimensional precision of cutting tools have much increased. In the investigation, a rotary axis measurement system with laser diodes and Position Sensitive Device (PSD) has been proposed. The parallel deviation between the spindle axis and correlated linear axis of the machine can be measured by the developed system. With the aid of this system, error of the rotation axis during installation or operation can be reduced Measurement results of the spindle axis with Y-axis have demonstrated that horizontal angle error is 5.557 arc-seconds and the vertical angle error comes to -19.961 arc-seconds.
Keywords: tool grinder, linear axis, rotation axis, parallel error

Abstract: The last past few decades have witnessed a considerable number of different attempts to design the Shell-and-tube heat exchangers have been developed. However, most of these designs focused on the thermal analysis of the heat exchanger without much consideration of the effects of the mechanical parts of the systems. Moreover, such complete designs have never been an easy "straight forward" task since it involves a lot of mathematical models, which are not easily and directly related to each other. A consequence of this is that, at the present time, there is no assurance of complete design of the equipment, but with the aid of Computer Aided Design which takes both Thermal and Mechanical design of the E type shell of the equipment into a deep consideration. Therefore this project aims at presenting a complete design with effective considerations of welding and analysis of stress of Shell-and-tube heat exchangers for different types of passes, flows, shapes and working fluids using Computer-Aided design with the aid of Visual Basic.Net. The computer-aided analysis and theoretical analysis are in agreement. It can be said that the developed computer program has some advantages to its credit which includes less skill requirement, high precision and accuracy of the design. It must be mentioned that the computer program can accept a design that satisfies the temperature correction factor, fouling factor, pressure drop and velocity of the fluid on both tube and shell side without investigating other options that may be more better, since the design parameters are been supplied. This programme will serve as a handy tool for designers who want to simulate various working process, conditions parameters and shape geometry.
Keywords: Shell and tube heat Exchanger, thermal and mechanical design

Abstract: This paper presents a simulation model through which the inventories in the warehouse can easily be followed and the appropriate value of the minimum stocks determined. The simulation model of the warehouse is based on the discrete events and built in the software package Tecnomatix Plant Simulation. A reasonable approach how to treat inventories of the existing situation as well as the inventories movement in the warehouse through its analysis is presented. In the article the analyses are carried out on the basis of the results of simulation suggestions and a new methodology is proposed together with guidelines for improving the material flow in the production and warehouse process.
Keywords: discrete event simulation, stock optimization, inventory tracking, minimum stocks, digital warehouse

Abstract: Systems approach in safety is applied during the analysis of complex safety systems and identification of key performance indicators. The integration of the safety system is necessary to enable efficient use of safety resources, and to take into consideration all technical, human and organizational aspects of safety. Safety lifecycle is an engineering process designed to optimize safety system and increase the level of safety. The main advantage of applying this model in real systems is increasing the effectiveness of the protection of employees and goods and the efficiency of safety resource use. In this paper, we describe the model for safety performance assessment of integrated safety systems, based on selected safety indicators and safety lifecycle.
Keywords: safety, safety performance, safety indicators, safety lifecycle, integrated safety system

Abstract: The paper deals with classification of objects in the urban area, particularly road surface, facades of buildings and pole-like objects. The attention is paid to processing of three-dimensional models generated and reconstructed on the base of two-dimensional mobile laser scanning. There are different methods available to classify scanned objects; however, various shortcomings and limitations are usually identified in relation to their practical usage. Most classification methods applied to the three-dimensional models are based on range data processing. We present our three-stage classification algorithm that has been proposed and implemented with motivation to explore how range and reflectivity data could be used separately or in fusion to classify certain objects. The paper shows results of practical experiments based on real data recordings and proving usability of the proposed algorithm.
Keywords: Laser, scanning, 3D model, algorithm, classification

Abstract: A purpose of power flow studies is to minimize the power distribution losses and the cost of power drawn from the substation, without affecting the voltage regulation. The current electrical power needs are increasing rapidly in line with technological developments. Optimal Power Flow (OPF) problem is to optimize a certain objective over power network variables under certain constraints. The variables may include real and reactive power outputs, bus voltages and angles, the objective may be the minimization of generation cost or maximization of user utilities and the constraints may be bounded on voltages or power levels, or that the line loading not exceeding thermal or stability limits. Optimal reactive power dispatch problem as a sub-problem of the Optimal Power Flow (OPF) is a very important optimization problem in power systems as proper management of reactive power injection into the power system can minimize losses in real power, voltage deviations and save voltage stability. The power system uses the simplified symbol such as a one-line diagram, per-unit system, moreover direct on various regard of alternating current power parameters, such as voltages, voltage angles, active power and reactive power. Researchers studied many different solutions have been proposed to solve the OPF problems. This paper presents a survey for Flexible Alternating Current Transmission Systems (FACTS) that can consider for OPF in power system.
Keywords: Power System, OPF, FACTS

Abstract: This paper presents an overview of current state of affairs in the Internet of Things (IoT) domain and briefly discusses its industrial applications. This has provided a motivation for the development of educational IoT laboratory setup based on legacy (mature) microcontroller-based control hardware, which should be easily upgraded by expanding it with a serial connection-equipped embedded network controller board such as ESP8266 module. The laboratory setup upgrade process is briefly outlined and Industrial IoT educational aspects implementable on such a platform are briefly discussed.

Keywords: Internet of Things, industrial computer control, education

Abstract: In the last period a high-speed main spindles, by modern machine tools, are used with basic goal - to increase efficiency. The prediction of thermal behavior of the spindle is essential for machining precision. The main source of heat on the spindle occurs due to friction torque on bearings with angular contact. The heat generated on the bearings transfers to the spindle and surrounding air, thus causing the thermal expansion of spindle elements. This paper presents a 3D FEM thermal model of the main spindle with hybrid angular contact ball bearings.

Keywords: angular contact ball bearings, FEM, main spindle, thermal behavior

Abstract: Today's wireless time brings some comfort, but on the other hand the impact of electromagnetic fields is serious threat to people. Many studies dealt with the effects of electromagnetic fields on living organisms, but the results are not completely clear. General and scientific public is increasingly focused on the impact of electromagnetic fields on living organisms. This is closely related limit values for parameters characterizing exposure to electromagnetic fields, depending on the frequency range, as defined by the Ministry of Health Decree 534/2007 Z.z. on the details and requirements for sources of electromagnetic radiation and exposure limits citizens to electromagnetic radiation in the environment. This contribution therefore focuses on mapping the electric and magnetic fields in the environment. The environment was selected area with a higher concentration of people in Prešov. The mapping was performed in two frequency ranges from 1 MHz to 1 GHz and 1 GHz to 2 GHz.

Keywords: electromagnetic field, electric field strength, magnetic flux density

Abstract: The design for the domain of CAD/CAM systems is a process of decision making where technical solutions have been applied in order to achieve predefined objectives. There are many factors influencing the production of a part that can affect the quality. This paper presents an expert system that provides support for the analysis of CAD model design and its transformation in order to improve production parameters. The system provides multiple analysis as the basis for proposing optimal solution of manufacturing process. Validation of results of the system model is verified through the use of reverse engineering techniques.

Keywords: CAD, expert system, additive technology, reverse engineering

Abstract: Many research work related to geopolymer are being carried out in the recent years because of its better environment friendly status than ordinary Portland cement. This paper attempts to study the microstructural behaviour of fly ash based geopolymer after exposed to elevated temperatures. FTIR, XRD, TGA and SEM analysis has been carried out on geopolymer mortar/paste specimens after they were exposed to 200°C, 400°C, 600°C and 800°C. Based on the present study, the mechanism of early strength loss and the subsequent strength gain of geopolymer during temperature exposure have been established. The difference between the mass loss characteristics of geopolymer paste and OPC mortar specimen when exposed to elevated temperatures has been identified. It has also been established that, the geopolymer will have lower crack width compared to OPC specimen when they are exposed to elevated temperatures.

Keywords: Geopolymer, Fly ash, High temperature, FTIR, XRD, SEM

Abstract: Automotive development is based on virtual product and process models and covers both the development of the car itself as well as of the corresponding production and assembling processes. Considering simultaneous engineering approaches, the integration of product-related and production-associated development plays an important role. Based on an exemplary application in automotive body-in-white development, the present paper introduces and discusses the efficient application of enhanced knowledge-based 3D-CAD methods, including data exchange and management. Target is to support data creation and processing through the implementation of specific algorithms. In this way, a continuous method is provided, which closes the gap between different design, simulation, and production engineering processes.

Keywords: automotive body in white, joining technology, enhanced design, knowledge-based engineering

Abstract: Presently, there are known various technologies for processing of waste tires and their components. Rubber materials are by separating devices processed into small pieces or granules, which are added to asphalt, concrete products and in railway sleepers. One disadvantage of these technology solutions is inefficient rubber materials evaluation and potential environmental hazards at their disposal. The paper is focused on therefore reducing the economic and environmental impact on the environment using fabrics components from waste tires. Recycling by itself plays an important role in meeting the objectives of the EU as regards the use of secondary raw materials, namely the reduction of energy consumption and their applications to the new material. Currently, processors of waste recycling systems are motivated to recovery for environmental solutions. There are research companies seeking to develop new more appropriate methods of processing waste tires, and the use of known methods of recovery and their constant innovation.

Keywords: Saving cost, waste tires, secondary raw materials, environment

Abstract: It is well known the role of bearings in the engineering industry, as well as elements for rotary motion, which are represented in almost all types of machines where rotation is the basic movement of the craft. Primarily used for supporting the shaft, thereby allowing rotation of the sleeve relative to the fixed support, while the transfer of appropriate load. Bearings, as a mechanical elements that allow relative movement of rotating parts while transferring loads between them, are primary in the most demanding sectors of machine industry, as automotive and aerospace industry, and they are required to have extremely high level of accuracy of manufacturing and meet the requirements prescribed by international standards. Producers specialized in the production of highly demanding types of bearings must prove eligibility criteria defined in ISO 281:2007 and ISO/TS 16281/2008 specification. This paper deals with the bearing testing results by manufacturer and research of the basic and modified rating life of bearings, the winning of new types of bearings, in accordance with the relevant specifications.

Keywords: bearings, modified reference rating life, testing

Abstract: The implementation in the industrial practices of the accounting technologies of the ferrous powdery wastes, now stored in the regional ponds of the nearby ferrous industry, mining and energetic sectors, assure in time the repossession of this place occupied by the wastes, to the natural environment. The recovery through pelletizing of the pulverous ferrous wastes stored in the regional ponds can be significant for the environmental protection, given by the increase of recovery for pulverous wastes and reduction of depository spaces for these wastes. The economical aspect is reflected by transferring depositary expenses to other purposes. In the paper some researches and relevant results are presented, regarding the obtaining of the pellets, using wastes resulted from ferrous industry (steel dust, agglomerating–furnace dust), mining (red mud, galvanically sludge) and energetic (thermal power plant ash) sectors. In addition, in the pellets recipes, graphite is used as the reducing agent, respectively bentonite and lime are used as binders.

Keywords: pulverous wastes, pellets, environmental protection

The **ACTA TECHNICA CORVINIENSIS – Bulletin of Engineering, Tome X [2017], Fascicule 2 [April–June/2017]** includes scientific papers presented in the sections of:

» **The VI^th^ International Conference Industrial Engineering and Environmental Protection 2016 – IIZS 2016**, organized by **University of Novi Sad, Technical Faculty "Mihajlo Pupin" Zrenjanin**, in **Zrenjanin, SERBIA, October 13–14, 2016**. The current identification numbers of the selected papers are the **# 2**, **# 8**, **# 12** and **# 25**, according to the present contents list.

» **The 11th International Conference ELEKTRO 2016**, organized by **University of Žilina, Faculty of Electrical Engineering**, in **Štrbské Pleso – High Tatras**, **SLOVAKIA**, **May 16–18, 2016.** The current identification numbers of the papers are the **# 7**, **# 13** and **# 24**, according to the present contents list.

» **The International Conference Management of Technology – Step to Sustainable Production (MOTSP 2016)**, organized by the **Faculty of Mechanical Engineering and Naval Architecture**, **Croatian Association for PLM** and the **University of North**, in **Porec/Parenzo, Istria, CROATIA, June 01–03, 2016.** The current identification number of the papers are the **# 1**, **# 3**, **# 9**, **# 11**, **# 15** and **# 20**, according to the present contents list.

» **The 3rd International Scientific Conference on Mechanical Engineering Technologies and Applications (COMETa 2016)**, organized by the **Faculty of Mechanical Engineering, University of East Sarajevo**, in **Jahorina, Republic of Srpska, BOSNIA & HERZEGOVINA, December 7–9, 2016.** The current identification number of the papers are the **# 4**, **# 16**, **# 18** and **# 22**, according to the present contents list.

Also, the **ACTA TECHNICA CORVINIENSIS – Bulletin of Engineering, Tome X [2017], Fascicule 2 [April–June/2017]**, includes original papers submitted to the Editorial Board, directly by authors or by the regional collaborators of the Journal.

ISSN:2067-3809

We are very pleased to inform that our international and interdisciplinary journal **ACTA TECHNICA CORVINIENSIS ■ Bulletin of Engineering** completed its nine years of publication successfully [**issues of years 2008 – 2016, Tome I–IX**].

In a very short period it has acquired global presence and scholars from all over the world have taken it with great enthusiasm.

Every year, in four online issues (**fascicules 1 – 4**), **ACTA TECHNICA CORVINIENSIS ■ Bulletin of Engineering [e-ISSN: 2067-3809]** publishes a series of reviews covering the most exciting and developing fields of science and technology. Each issue contains papers reviewed by international researchers who are experts in their fields. The result is a journal that gives the scientists and engineers the opportunity to keep informed of all the current developments in their own, and related, areas of research, ensuring the new ideas across an increasingly the interdisciplinary field.

Now, when will celebrate the tenth years anniversary of **ACTA TECHNICA CORVINIENSIS ■ Bulletin of Engineering**, we are extremely grateful and heartily acknowledge the kind of support and encouragement from all contributors and all collaborators!

On behalf of the Editorial Board and Scientific Committees of **ACTA TECHNICA CORVINIENSIS ■ Bulletin of Engineering**, we would like to thank the many people who helped make this journal successful. We thank all authors who submitted their work to **ACTA TECHNICA CORVINIENSIS ■ Bulletin of Engineering**.

ACTA Technica CORVINIENSIS
BULLETIN OF ENGINEERING

ACTA TECHNICA CORVINIENSIS – BULLETIN OF ENGINEERING. Fascicule 1 [JANUARY-MARCH]
ACTA TECHNICA CORVINIENSIS – BULLETIN OF ENGINEERING. Fascicule 2 [APRIL-JUNE]
ACTA TECHNICA CORVINIENSIS – BULLETIN OF ENGINEERING. Fascicule 3 [JULY-SEPTEMBER]
ACTA TECHNICA CORVINIENSIS – BULLETIN OF ENGINEERING. Fascicule 4 [OCTOBER-DECEMBER]

ACTA TECHNICA CORVINIENSIS
– Bulletin of Engineering
Tome X [2017]
Fascicule 2 [April – June]
ISSN: 2067 – 3809

[1.]Peter ZAHN, [2.]Michael NEUBAUER, [3.]Armin LECHLER

DIFFERENT APPROACHES TO IMPROVE THE DYNAMIC BEHAVIOR OF MACHINE TOOL FEED DRIVES

[1-3.]University of Stuttgart, Institute for Control Engineering of Machine Tools and Manufacturing Units (ISW), Seidenstraße 36, Stuttgart, GERMANY

Abstract: To increase productivity and efficiency of industrial machine tools, one important aspect is the dynamic behavior of their feed drives. At the Institute for Control Engineering of Machine Tools and Manufacturing Units (ISW) of the University of Stuttgart, various approaches, based on constructive methods, control engineering or additional actuators were examined, which can influence the dynamic behavior in a positive way. In this paper, exemplary solutions are presented with their benefits and drawbacks to provide an overview on the currently ongoing research work. For validation and illustration of the different principles, simulative and experimental results are presented.
Keywords: machine tool feed drives, control, dynamic behavior

INTRODUCTION AND MOTIVATION

Feed drives in machine tools are needed to perform a relative movement between workpiece and tool as defined in a NC program. Nowadays, electromechanical servo drives are typically used for this purpose, which are configured either as direct drive or used with additional mechanical gear elements such as *ball screw drives* (see [1] as an overview).

Primary goals of dimensioning and control of feed drives are on the one hand the exact tracing of a given target contour with low latency. On the other hand, static and dynamic disturbances, for example process forces, shall be optimally compensated. The dynamic behavior not only influences machining accuracy and manufacturing time, it also has an impact on wear and damages of machine and tool.

For the feed drive system, which consists of mechanical, drive and control components these targets lead to two basic properties: high accuracy and good dynamic behavior, guaranteed under all predictable operating states. In the following text, an overview of different cross-domain approaches is given, which target on improvements in the dynamic behavior of feed drives. So they can help to expand the area of application or enhance the performance of machine tools.

The presented technologies for improved dynamical behavior can be subdivided into three main categories which are shown in Table 1. The following chapters show examples currently under research with their advantages and drawbacks, marked as advantageous (+), neutral (o) or unfavorable (-).

Table 1 – Comparison of different approaches for improved dynamics

	Constructio n-based	Control-based	Actuator-based
Effort/costs	-	+	o
Robustness	+	o	+
Upgrade capability	-	+	o
System Complexity	+	-	-

CONSTRUCTION-BASED APPROACHES

Construction-based approaches to achieve optimal dynamical behavior can be seen as the classical method. Here, the increased stiffness of all components which are involved in the feed motion is essential. However, a simple oversizing of those components is counterproductive regarding requirements like mass, material and cost reduction. For that reason, two detailed solutions are presented which offer significant improvement potential with moderate expenses.

Constant-level preload force in ball screw drives

Ball screw drives are one typical kind of components in machine tools to provide linear motion. Circulating rolling elements between a threaded spindle and nut transfer forces under rolling friction which leads to an efficient transmission from rotary to linear motion.

Typically preloaded double nuts are used to achieve a high stiffness and avoid backlash.
To provide the needed stiffness and guarantee the rolling contact under all operating conditions, it is important to choose an adequate preload. Simultaneous, the preload shall be chosen as small as possible to reduce friction induced heat generation and component wear. Furthermore, the reduction of the preload force over the lifetime of a ball screw drive due to wear has to be compensated by an initial oversizing.
To cope with these restrictions and achieve an optimal sized preload force over the lifetime, a novel adjustment mechanism is currently under research. It uses a spring-loaded, self-retaining adjustment wedge between both involved nuts as shown in Figure 1. The increased distance between the nuts result in a higher preload force without the need of an external active actuator. Because of the self-retention of the adjustment element, the preload force is only adapted as far as the preload is too small for a reliable operation.
As a result, the ball screw drive autonomously keeps an adequate preload force and ensures a constant stiffness and load capacity over the whole life cycle.

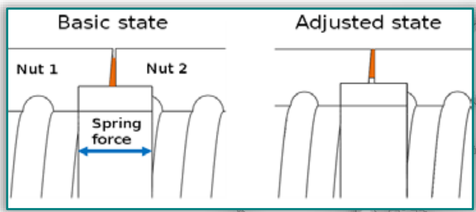

Figure 1 – Function principle of the self-adjusting ball screw double nut

Compliant bearing arrangement in feed drives

The first natural frequency of a feed drive is typically an axial vibration in feed direction and determined by the mechanical construction. This parameter limits the achievable control parameters of the drive so it is preferable to have the first natural frequency at a rather high value with moderate amplitude exaltation.
One construction-based method to deal with this limitation and increase the drive dynamics is an axial compliant bearing arrangement for the ball screw spindle which is enhanced by a strong axial damping element as specified in [2]. With an adequate sizing of the spring stiffness relative to the damping coefficient, the first natural frequency can be shifted significantly to a higher level while simultaneously reducing its amplitude. Figure 2 shows an appropriate frequency response of such a feed drive. The behavior of a typical conventional design with fixed bearing and its visible resonance exaltation is depicted in red. Shown in blue is a feed drive with compliant bearing and reduced exaltation as well as in green with optimal bearing and damping which results in a nearly flat amplitude curve. Based on this behavior, the amplification factor k_V of the position controller can be increased significantly, resulting in enhanced bandwidth of the feed drive.
Crucial for an effective application is certainly a damper with a sufficient high damping coefficient and also a high bandwidth. This aspect is currently a technical limitation of the method.

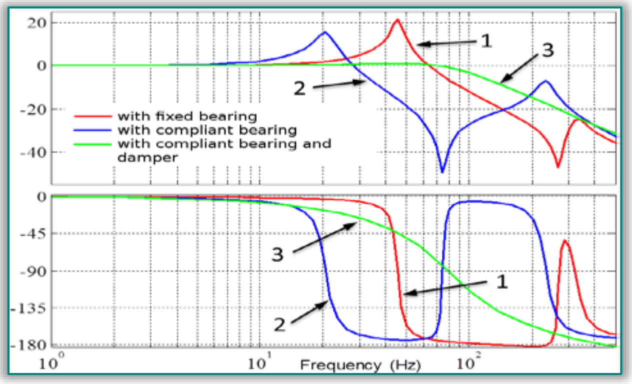

Figure 2 – Simulation-based comparison for a conventional feed drive (red) and optimal sized compliance and damping (green) [2]

CONTROL-BASED APPROACHES

In the field of the control theory, extended structures of the classical cascade control promise an improved dynamic behavior especially for high-dynamic drives. One important factor here is the availability of a linear position sensor on the output side which enables drive-based vibration damping. With the use of novel highly performant controller platforms, the parallel computation of individual system models, the feed-back of additional state variables (like acceleration) for the compensation of non-linear behavior or generally minimizing dead time become practicable. In the following section, two exemplary methods to increase the bandwidth are shown, which are currently under research.

Velocity control for minor gear ratio

To achieve high rapid traverse velocities in feed drives, increasingly smaller gear ratios are chosen in combination with low-inertia, high-dynamic motors. This however also reduces the ratio between the motor and the table related moment of inertia, resulting in a challenge for optimizing the parameters of the controller cascade.
One possible solution is to extend the controller cascade as shown in [3] and depicted in Figure 3. Here, a weakly parameterized rotation speed controller (which is closed with the actual motor speed) is strongly damping the mechanics in the area of the first natural frequency.
An additional linear velocity control loop (shown in red), based on a table-mounted position sensor compensates the damping and raises the phase response in the critical area. As a result, the amplification factor k_V of the position controller can be increased by a factor of two depending on the inertia ratio while maintaining comparable stability and robustness.

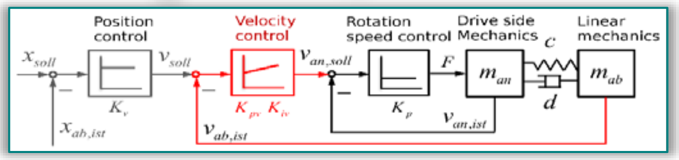

Figure 3 – Extended control loop for high dynamic drives [3]

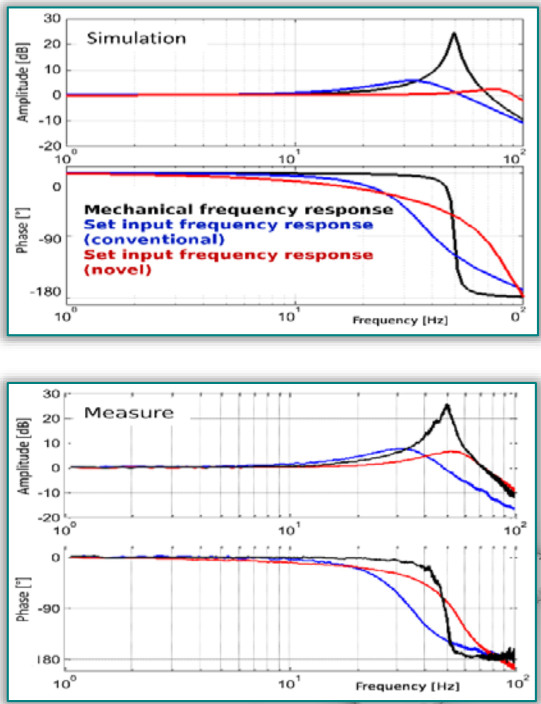

Figure 4 – Comparison of frequency response (conventional to novel method) [3]

Figure 4 shows the corresponding frequency responses for mechanics (black) and set input for a conventional cascade controller (blue) and the novel, extended cascade (red). The plots are compared between simulation (left) and measurement (right). The higher bandwidth of the novel method and the correspondence between simulation and measurement is clearly visible.

Increased current control bandwidth by sliding mode control

Typically, the bandwidth of the current control with its small electrical time constant is much higher compared to the behavior of the mechanical components, so the current control is not limiting the overall performance of a feed drive. However, there are applications where a high dynamic torque control is demanded, for example to compensate high frequency process forces. One possible controller variant, which increases the bandwidth of the current control is the *direct sliding mode current control* as presented in [4].

The essential characteristic of this method is a modulation technique that minimizes switching processes in the power electronics which reduce bandwidth and energy efficiency. Figure 5 shows a measured comparison between a conventional current controller (red) and a direct sliding mode controller (blue), where the increased bandwidth can be seen from the frequency response.

Important aspects in realizing this controller are an adequate platform for high frequent computations and a current measurement system with sufficient bandwidth.

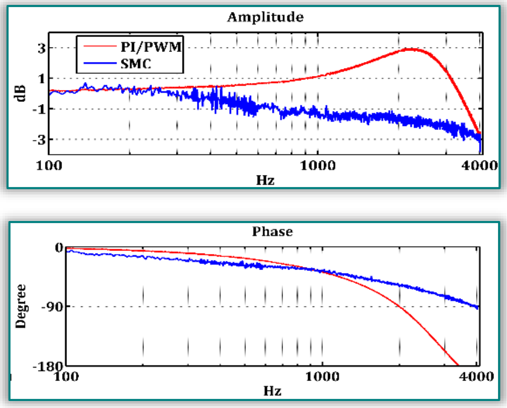

Figure 5 – Comparison of current control bandwidth for conventional (PI/PWM) method and direct sliding mode control (SMC) [4]

ACTUATOR-BASED APPROACHES

Actuator-based approaches for improved dynamic behavior typically request the installation of additional components which can be retrofitted. As a result, they provide new degrees of freedom due to their direct physical influence on the dynamic behavior of the mechanics. One challenge remains the implementation of the needed control logic, especially in commercial drive systems without open interfaces.

Semi-active damping

One exemplary application of an actuator-based approach is the semi-active damping of feed drives as shown in [5]. An additional mechanical friction-based damping actuator is used to reduce the amplitude exaltation at the first natural frequency by directed brake intervention. Subsequently, the choice of the controller parameter is less limited by the mechanics and the overall behavior can be improved.

The damping actuator is triggered in dependence of the difference between motor and linear velocity, so that the damping force is applied only when the table of the feed drive is overshooting. Figure 6 shows the needed extension of the controller cascade for this concept.

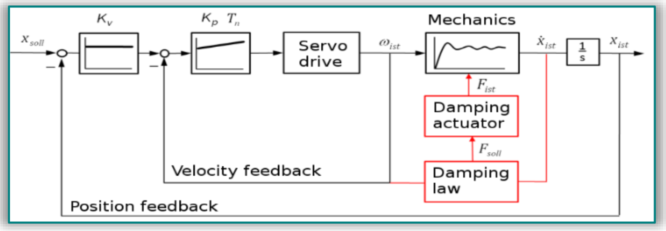

Figure 6 – Extended drive controller with semi-active damping [5]

The provided friction force, which acts between the linear bearing and the table, withdraws vibration energy from the feed drive. Due to the appropriate and short activation of only a few milliseconds, the normal operation is not influenced by the damping force.

Figure 7 shows the effect of the semi-active damping for a position setpoint and a disturbance force step. It is remarkable, that the setpoint step can tracked with significant less deviation and also position errors due to external forces are reduced. As a result, the amplification factor k_V of the position controller can be increased.

This approach creates some extra effort regarding mechanics, control and energy consumption, but the increased drive bandwidth overweigh this drawback.

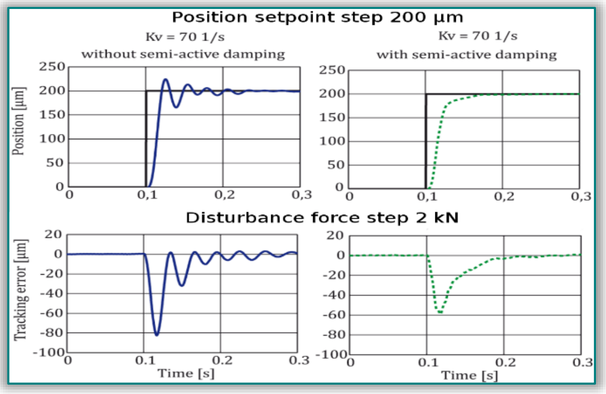

Figure 7 – Improvement potential for position and disturbance step [5]

Adaptive friction in glide bearings

The absolute value of the mechanical friction occurring in linear guides and bearings of a feed drive can also be seen as a damping effect that influences the choice of the maximum controller parameters. Nevertheless, the relationship between this friction force and the speed is non-linear and typically described by a *Stribeck curve.* Moreover, the excessive amount of static friction at low speeds leads to positioning errors.

At the ISW, a novel concept for glide bearing was developed, which uses a piezoactuator to induce ultrasonic vibrations on the contact areas as described in [6]. Depending on the chosen amplitude and frequency of the superimposed vibration, the friction characteristics can be linearized over the complete velocity range. This also improves the positioning accuracy in the field of precision manufacturing processes. By a variation of the ultrasonic vibration, also the damping in the guiding system can be adapted for different operating conditions.

For the implementation of this approach, novel guiding elements are needed which include the piezoactuators. Furthermore, it is necessary to integrate logic and power electronics in the machine if the friction coefficient shall be adapted appropriate to individual process phases.

CONCLUSION AND OUTLOOK

In the previous chapters, different approaches to improve the dynamical behavior of feed drives were presented with their characteristics. They can also be differentiated regarding the needed effort for their implementation, requiring additional hardware or specialized control structures. Construction and actuator-based methods are beneficial regarding robustness, because they are less prone to parameter errors.

Another important criteria regarding the use of such techniques is the availability of adequate open and performant platforms for the implementation of the algorithms. The conducted research has especially identified FPGA-based platforms like [7] as beneficial for such implementations.

Substantial scope of further research projects is currently the transfer of the presented concepts on rotary axis like they are often used in the context of industrial robots. Here, new processes and industrial applications can be exploited with the better dynamic behavior.

Acknowledgement: The authors would like to thank the Deutsche Forschungsgemeinschaft (DFG) for the funding of the research work, especially within the grants VE454/13-2 and LE2904/6-1.

Note: This paper is based on the paper presented at The International Conference Management of Technology – Step to Sustainable Production (MOTSP 2016), organized by the Faculty of Mechanical Engineering and Naval Architecture, Croatian Association for PLM and the University of North, in Porec/Parenzo, Istria, CROATIA, June 01–03, 2016.

References

[1] Altintas, Y. et al.: Machine tool feed drives, CIRP Annals - Manufacturing Technology, 60(2011), 779-796.
[2] Pritschow, G. et al.: Ball screw drives with enhanced bandwidth by modification of the axial bearing, CIRP Annals - Manufacturing Technology, 62(2013)1, 383-386.
[3] Sun, Z. et al.: Bandbreite des Vorschubsystems erhöhen, MM Maschinenmarkt, (2015)43, 46-49.
[4] Laptev, I. et al.: Direct sliding mode current control of feed drives, CIRP Annals - Manufacturing Technology, 64(2015)1, 373-376.
[5] Frey, S.: Verbesserung des dynamischen Verhaltens von Vorschubantrieben durch semiaktive Dämpfung, Fraunhofer IRB Verlag, Stuttgart, 2013.
[6] Engel, T. et al.: Adaptive Friction Bearing for Reduction of Stick-Slip Effects, Advanced Material Research, 1018(2014), 351-356.
[7] Frick, F. et al.: Modular Design Approach for Model-Based Drive Control Systems on Reconfigurable Logic, Applied Mechanics and Materials, 704(2014), 380-384.

ACTA TECHNICA CORVINIENSIS
– Bulletin of Engineering
Tome X [2017]
Fascicule 2 [April – June]
ISSN: 2067 – 3809

[1.]Istvan KUCORA, [2.]Ljiljana RADOVANOVIC, [3.]James G. SPEIHT, [4.]Borivoje SIKIC, [5.]Zeljko BURSAC

ETHYLENE PYROLYSIS FURNACE TUBE DAMAGE INSPECTION

[1.] Stock Company for Production of Petrochemicals, Raw Materials and Chemicals „HIP-Petrohemija“ Pančevo- under Restructuring, Pančevo, SERBIA
[2.] University of Novi Sad, Technical faculty Mihajlo Pupin, Zrenjanin, SERBIA
[3.] CD&W Inc., Laramie, Wyoming 82070, USA
[4.] Army Republic of Serbia, SERBIA
[5.] The Serbian Academic Center, Novi Sad, SERBIA

Abstract: This aim of this study is to identify failure mechanism of ethylene pyrolysis furnace tube after five year of operation. The tubes were manufactured from centrifugally cast heat resistant steel HK 40. Failure analysis of the radiant tubes was performed by careful visual inspection of the failed tubes, scanning electron microscopy observation of crack region samples, hardness and micro-hardness measurements. Selected specimens were prepared from the four samples, measurements was carried out at inner, middle and outer sides of the samples. The experimental results showed that the mode of tube failure was a combination of high temperature carburization attack and creep damage leading to intergranular cracking. Maximum hardness is associated with internally carburized zone where the amount of carbides is maximum in this region. The hardness of the radiant tubes decreases as the distance moves from the inner surface to the middle section. The metallurgical background of the combined action of carburization and creep ductility exhaustion have been investigated and are explained. Pyrolysis tube failures can be prevented by a combination of proper furnace operation, materials choice, regular inspections and good design.
Keywords: ethylene pyrolysis; furnace; tube; damage; inspection

INTRODUCTION

Ethylene is a key product in the petrochemical industry, and it is produced by the thermal cracking of complex hydrocarbons in pyrolysis furnaces. The furnace coils are formed from the tubes by welding. The tubes used in thermal cracking furnaces in an ethylene manufacturing process are usually made of HP and HK grades of heat resistant stainless steel. These alloys exhibit excellent properties in terms of oxidation resistance, carburization resistance, high temperature creep and thermal expansion. These tubes are exposed to high temperature (approximately 1100 °C and internal pressure of about 1 bar). Normal service life of these coiled tubes is approximately 100.000 h, but does depends on the service condition and could vary from 30.000 to 180.000 h [4].

Ethylene pyrolysis furnace tubes which are made of high Cr-Ni alloys often become difficult to weld after few years in service due to carburization and creep damage. The presence of carburization, often attempted to detect by magnetic permeability, can escape detection due to high Cr-Ni content of the alloy. Based on optical microstructural analysis and supported by scanning electron microscopy, this paper establishes that carburized material becomes difficult to weld due to carburized internal layers of the tube and cause hot shortness. To provide a practical way out for ethylene furnace operators, a solution annealing heat treatment is recommended to have a successful weld.

Pyrolysis coils in ethylene cracking furnaces (Fig. 1) are exposed to very severe conditions, e. g. high temperatures up to 1150 °C, severe start/stop and decoke cycles, oxidizing and nitriding flue gases at the outside and carburizing atmospheres at the tube inside surface. Therefore, high-alloyed centrifugal cast Ni-Cr-Fe alloys with adequate high temperature corrosion resistance, good high temperature strength, good machinability and weldability (even after years of service) are required.

Radiant coils have a limited life and failure is caused by a variety of factors, many being related to furnace operation. However, each pyrolysis plant experiences specific operational conditions and operational philosophies. Therefore, each plant has typical causes for radiant coil failure and it is of importance for operators to analyze and to understand the typical failure mechanisms. This will enable them to consider the material grades, which would be best suited for those particular conditions and also to keep failures within limits by proper furnace operation.

Damages of the furnace coils may be produced by creep, carburization, thermal shocks and accidental overheating [9]. Any failure in these tubes results in shut-down of the cracking furnaces and wasting both cost and time. Replacement of these coils is expensive and difficult. Carburization and creep are the main causes of failure in the heat resistant tubes of ethylene cracking furnaces, leading to a decrease in ductility and embrittlement of the cracking tubes.

The radiant coil assembly (figure 1) of the ethylene furnace was investigated at Stock Company for Production of Petrochemicals, Raw Materials and Chemicals „HIP-Petrohemija" Pančevo – Republic of Serbia. The furnace tubes were fabricated from HK40 steel casting with an internal diameter of 63.5 mm and wall thickness of 16 mm. A section of failed tube was analyzed to determine the cause of failure.

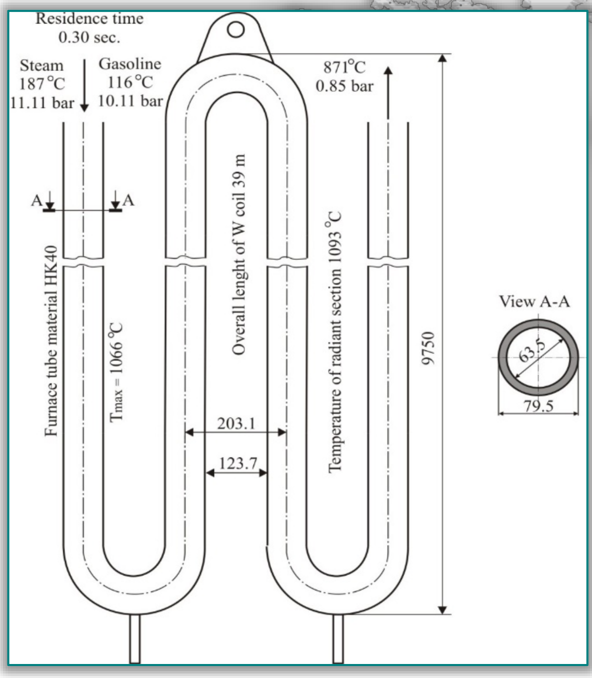

Figure 1. The radiant coil assembly

It is the purpose of this paper to investigate the main failure mechanisms for tubes and outlet parts of pyrolysis furnace coils. In most cases there is a combination of factors which ultimately lead to the failure, e.g. carburization and creep ductility exhaustion. This results in bulging, bending and vocalization of the tubes. Also, brittle fracture during furnace trips can result in large, longitudinal cracks on many tubes in the furnace.

MATERIAL OF FURNACE TUBE

The radiant coils used in our cracking furnace are made by centrifugal casting process. They have appropriate ductility and weldability in as-cast conditions, and lose their ductility and weldability after being used in service. As normally produced, the HK alloy type is stable austenitic over its entire temperature range of application. The austenitic matrix in this kind of high-temperature alloy provides a great mechanical resistance at high temperatures.

Extended exposure at the normal operating temperature of 1093°C have three detrimental effects in these microstructures: grain boundary voids and cracking of the protective oxide scale due to creep, carburization attack and the evolution of intermetallic compounds [1]. All these reduce both mechanical strength and ductility during service life.

Chemical composition and mechanical properties of the steel are presented in tables 1 and 2, respectively [Kubota Metal Corporation].

Table.1. Chemical composition of HK40 (wt%)

Comp.	C	Mn	Si	Cr	Ni	P	S
Min. %	0.35	0.4	0.5	23	19	-	-
Max. %	0.45	1.5	1.5	27	22	0.03	0.03

Table. 2. Mechanical properties of HK40

Mechanical properties		Centrifugal castings at Temperature [^{0}C]					Static castings
		21	760	870	980	1090	21[°C]
U.T.S. Rm	[MPa]	579	262	165	103	38	324
Y.S. Rm	[MPa]	303	165	110	62	34	310
El.	%	20	13	16	42	55	17

CARBURIZATION

During service, hard deposits of carbon (coke) build up on the inner wall of the tube, reducing heat transfer and restricting the flow of the hydrocarbon feedstock which requires that the furnace must be periodically taken off-line and "decoked" by burning out the accumulated carbon. Carburization is the carbon enrichment and carbide formation in the tube material under influence of the presence of carbonaceous gases and high temperatures. This accelerates carbon diffusion in tube material, especially during the decoking period. Carburized material in the inner wall of the radiant tube has a higher thermal expansion coefficient and tends to increase in volume and place stresses on the tube. These thermal stresses make the tube more susceptible to creep failure [9].

The deposition of the coke at high temperature is generally inhibited by the presence of a chromium oxide (Cr_2O_3) layer on the inner surface of the tube. When this film in present carbon diffusion into the tube is retarded. However, during decoking, the tube may be subjected to severe thermal shock that results in removal of the chromium oxide layer, so the carburization attack is increased [10]. Because of exposure of tube at elevated temperature, carbon diffusion could promote formation of continuous and/or separated carbides in grain boundary and matrix [1, 10,]. These carbides decrease the creep resistance and ductility at high temperature. Figure 2. Pyrolysis furnace radiant zone - consequence of a high creep rate Metal dusting is a catastrophic form of carburization that can result in rapid metal wastage in both ferritic and austenitic alloys. This damage mechanism typically has the appearance of localized pitting, or grooving, along the inner walls of pipe and tubes [10].

The ethylene cracking reaction releases free carbon that can deposit on tube surfaces accelerating carbon diffusion and hence carburization in tube material [8].One of the main problems with pyrolysis furnaces is carbon deposition on inner wall of the tubes and creation of a porous layer of coke. Coke formed in the pyrolysis furnace tubes is classified as catalytic and pyrolytic. Adherent coke can have two detrimental effects. First, it acts as a thermal insulator which requires a higher tube wall temperature in order to maintain the same gas temperature. Secondly, it accelerates carburization attack of the tube material.

Carburization leads to the formation of metal carbides in the grains and grain boundaries that consequently reduce the mechanical properties, creep resistance, service life time and weldability of the tubes. The non-magnetic (austenitic) microstructure of these tubes becomes ferromagnetic due to carburization reaction.

Coke is normally removed using decoking technique which consists of shutting off the hydrocarbon feed and passing a mixture of air and steam through the coil. During decoking cycles because of sapling the oxide scale, carburization was accelerated to inner surface that results in an increase of inner surface hardness with respect to outer. Tubes can be subjected to a severe thermal shock where the temperature is increased above normal leading to creep which results in sagging of the tubes. In practice, the need for decoking is dictated by the process parameters particularly gas temperature, flow rates and conversion ratio [4].

CREEP

Creep is the primary cause of the furnace tube damage. It usually initiates within the tube wall some two-thirds of the way through from the outer surface, making it impossible to detect by in situ metallography [7]. This is opposite to boiler super heaters and headers where creep damage initiates at the outside surfaces, making it much easier to detect.

Creep elongation (also called stretching) occurs because of creep by the self-weight of the tube and the coke layer present in the tube and is influenced by temperature, the load carrying cross section of the tube, and the material used. A consequence of a high creep rate is the need to shut down the furnace and to shorten the coils (some end-users have lowered to bottom floor). Failures can occur if tubes are not shortened before they reached the heater floor (figure 2). The coils are warped and bowed, resulting in higher tube stresses and creep rates.

Figure 2. Pyrolysis furnace radiant zone – consequence of a high creep rate

LIFE ASSETMENT

Predicting the life of furnace tubes has long been a problem for petrochemical and refinery industry. Even though failure of heater tubes is not a major safety issue, the prediction of remaining life is important because of cost savings resulting from the optimization of process parameters or reduction of inspection frequency and avoidance of unscheduled outages.

INSPECTION

The tube coils should be inspected closely for bulging, cracking, bowing, sagging, splitting, scaling, corrosion, and deposits from fuel gas. Fittings may show signs of damage, distortion or corrosion.

In order to investigate the mechanical properties, tensile, hardness and micro hardness tests were performed. Microstructures were characterized by using optical microscopy and scanning electron microscopy (SEM). Examinations are focused on three regions, namely inner surface marked I, middle section (region II) and outer surface (region III).

SAMPLES PREPARING

Samples (figure 3) were machined from the as-received tube section for evaluation, one unused piece, one used but not cracked piece (one year in use), one piece showing sagging and different degrees of cracking (five year in use) and one piece which was not sagged but contained cracks (five year in use) at the inner surface that did not penetrate the entire thickness. Cutting was performed by using a precision sectioning machine with direct water-cooling of the specimen.

Figure 3. As received samples

The specimens were ground with SiC papers of the grades 180, 220, 320, 500, 1000 down to grit 2400 (Struers Standard 43-GB-1984, DIN69176, Part 1,2,4) with a pressure of 70-80 N and water as a lubricant. Polishing was done on nylon cloth with 0.3-lm alumina paste. Then, the specimens were etched in Kalling's etching reagent (1.5g $CuCl_2$ in 33ml H_2O, 34ml ethanol and 33ml HCl) to determine the size and location of precipitates in the matrix. For more investigation, the specimens were electrolytically etched with KOH solution.

HARDNESS AND MICRO HARDNESS TESTS

Brinell hardness measurements (HB 5/750/20) were performed on the tube wall cross section to evaluate mechanical strength and to determine a possible carburization /decarburization. The hardness of unused, unfailed and damaged tubes is presented in table 3. It is found that the longer service time results in the higher hardness value which can be attributed to the formation of metallic carbides due to carbon diffusion into the matrix of material at elevated temperature.

Table 3. Brinell hardness of analyzed samples

Sample	Time in use	[$HB_{5/750/20}$] Inner surface	Middle section	Outer surface	Average
1	new	186	185	186	186
2	1 year	191	187	188	188
3	5 year	258	237	223	239
4	5 year	284	261	248	264

Micro hardness measurements were performed by Vickers method applying a load of 25g ($HV_{0,\ 025}$) for hardness determination of the particular micro constituents. Measurements were carried out at inner, middle and outer sides of the samples. In the as-cast condition (tube never used in service), the micro hardness of the austenite at the inner tube surface was measured to be HV 246 (average of three readings).

Microhardness measurements showed a significant increase in the hardness at the tube's internal surfaces (table 4). The hardness decreases as the distance from the tube's internal surface is increased, suggesting a decrease in the carburization density.

Table 4.Micro hardness of analyzed samples

Sample	Location	[$HV_{0.025}$] Inner surface	Middle section	Outer surface	Average
1	grain boundary	250	242	247	246
	grain	102	96	98	98
2	grain boundary	267	246	250	254
	grain	149	97	101	115
3	grain boundary	362	308	269	313
	grain	202	176	106	161
4	grain boundary	401	340	297	346
	grain	224	192	147	187

MICROSTRUCTURE

Microstructure of the samples from the tubes analyzed by optical microscope and scanning electron microscope. The microstructure of as-cast HK40 alloy consists of an FCC gamma matrix and a cellular structure, which involves $M_{23}C_6$ carbides on the dendrite boundaries (Figure 4).

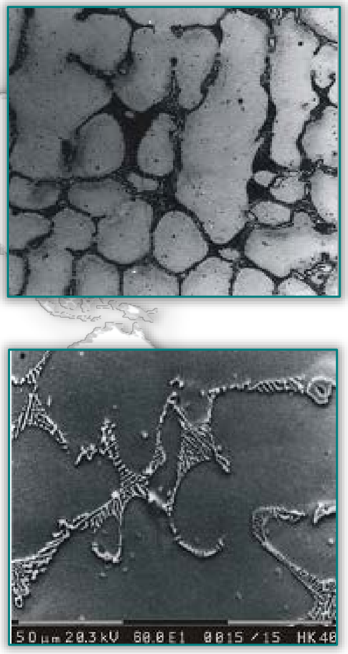

a)

b)

Figure 4. As-cast structure of the alloy HK40,
a.) optical - x 150, b.) sem - x 600

The sample 2 material that presumably had been exposed to less severe service conditions displayed only coarse $M_{23}C_6$ type carbides. In sample 3 and 4, $M_{23}C_6$ eutectoid carbides of the as-cast condition were observed to have coarsened and transformed into M_7C_3 carbides with a heavily faulted structure. This carbide transition was observed to have occurred via an in-situ mechanism and also resulted in γ precipitation in M_7C_3. The crack in sample 3 and 4 was visible to the unaided eye, and its propagation appeared to be associated with the carburization and oxidation phenomena. It is evident that the cracks are propagated along the grain boundaries of the austenite grains (Figure 5). This structure was altered in all of three samples due to prolonged exposure to high temperatures, and it was observed that a continuous network of coarse carbides decorated the dendrite boundaries. Across the used tube wall, the materials were observed to have formed three distinct zones with different microstructures: the zones beneath the inner and outer surfaces and the region in between. The microstructure of this centrifugally cast tubular material consist of dendrite grains aligned in the direction of tube diameter and a protective oxide scale is usually present on the inner and outer surfaces.

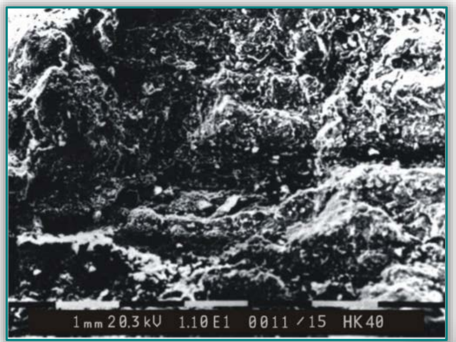

a)

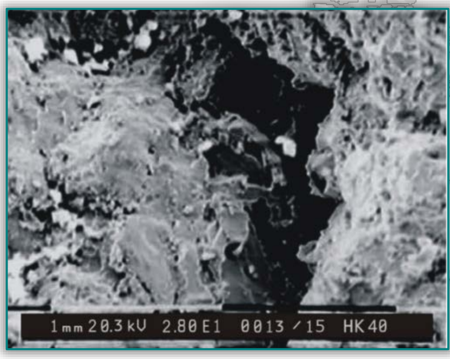

b)

Figure 5. SEM images of sample 3 - a.) Surfaces with crack extended along dendrite grain boundaries – intergranularly, b.) Area with the presence of secondary cracks

The results of the fractured surface analysis presented in figure 5 could be used for explanation of the fracture initiation and propagation mechanisms. The fracture was initiated on oxidation/corrosion products from the inner side of the tube wall. The crack propagates intercrystally, i.e. along the grain boundaries of fine dendrites. Secondary cracks were also identified.

In sample 3, the volume percent of carbides varied across the tube cross-section (fig. 6), gradually increasing from the outer to the inner surface, being 36.2% and 44.7%, respectively. Sample 3 also contained, unlike sample 2, circular intra granular carbides in addition to a macrocrack.

Sample 3, which had been removed from the same furnace as sample 4, showed more severe microstructural degradation to approximately Stage IV in the model of Petkovic-Luton and Ramanarayanan [5].

In both samples, the carbides appeared to have coarsened and become continuous along the grain boundaries during service. This was more pronounced in Sample 3, suggesting that it had experienced more carburization than Sample 4.

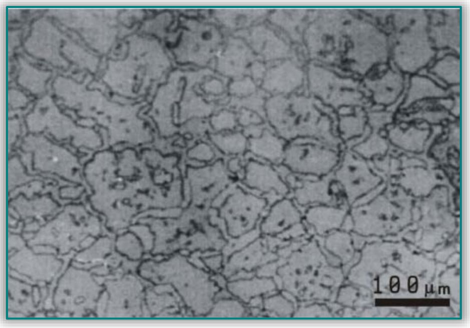

a)

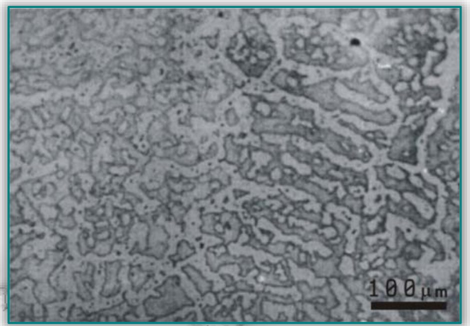

b)

Figure 6. Light micrographs from areas beneath: (a) the inner and (b) the outer surfaces of sample B.

CONCLUSION

In this study, ethylene pyrolysis furnace tube damage inspection was performed. The experimental results showed that the mode of tube failure was a combination of high temperature carburization attack and creep damage leading to intergranular cracking. Analyzed cracks in the failed tubes have their origin in the inner side of the tube walls, and propagating across their thickness.

Brinell hardness measurements were performed on the tube wall cross section to evaluate mechanical strength and to determine a possible carburization/ decarburization. This maximum hardness is associated with internally carburized zone where the amount of carbides is maximum in this region. The hardness of the radiant tubes decreases as the distance moves from the inner surface to the middle section.

To avoid such degradation it is necessary to check the operation and decoking temperature and to ensure that the temperature is less than the design temperature. All heater tubes should be inspected, preferably early in life, to establish base-line conditions for tube diameter, wall-thickness, microstructure, and metal hardness.

Acknowledgements

This paper is the result of the research within the project TR 34028, which is financially supported by the Ministry of Education and Science of Serbia, PD TE — KO Kostolac and Messer Tehnogas.

Note

This paper is based on the paper presented at The VIth International Conference Industrial Engineering and Environmental Protection 2016 – IIZS 2016, organized by University of Novi Sad, Technical Faculty "Mihajlo Pupin" Zrenjanin, in Zrenjanin, SERBIA, October 13–14, 2016, referred here as [11].

References

[1] Al-Meshari, A., Al-Rabie, M., Al-Dajane, M., Failure Analysis of Furnace Tube, J Fail. Anal. and Preven.13:282–291 (2013)
[2] Goswami, A., Kumar, S.,Failure of pyrolysis coils coated with anti-coking film in an ethylene cracking plant, Engineering Failure Analysis 39:181–187 (2014)
[3] Guan K, Xu H, Wang Z., Analysis of failed ethylene cracking tubes, Eng Fail Anal 12:420–431 (2005)
[4] May I.L., Silveira, T.L., Vianna, C.H., Criteria for the evaluation of damage and remaining life in reformer furnace tubes, Int. J. Press. Ves. Pip. 66:233–241 (1996)
[5] Petkovic-Luton, R., Ramanarayanan, T.,Mixed oxidant attack of high temperature alloys in carbon- and oxygen containing environments, Oxidation of Metals, 34:381 (1990)
[6] Saeed Reza Allahkaram, Sadegh Borjali, Hamed Khosravi, Investigation of weldability and property changes of high pressure heat-resistant cast stainless steel tubes used in pyrolysis furnaces after a five-year service, Materials and Design 33:476–484 (2012)
[7] Tari, V., Najafizadeh A., Aghaei M.H., Mazloumi, M.A., Failure analysis of ethylene cracking tube, J Fail. Anal. Prev. 9:316–322 (2009)
[8] Ul-Hamid A., Tawancy H.M., Mohammed A.-R.I., AbbasN.M., Failure analysis of furnace radiant tubes exposed to excessive temperature, Eng. Fail. Anal. 13:1005–1021 (2006)
[9] Jacoby, D., and Gommans, R. Typical Failures in Pyrolysis Coils for Ethylene Cracking. Materials and Corrosion, 54(11): 881-887 (2003).
[10] Guttmann, V., and Burgel, R. Corrosion and Mechanical Stress at High Temperatures. Applied Science Publishers, Ltd. London, United Kingdom (1980).
[11] Kucora, I., Radovanovic, L., Speiht, J.G., Sikic, B., Bursac, Z., Ethylene pyrolysis furnace tube damage inspection, The VIth International Conference Industrial Engineering and Environmental Protection 2016 – IIZS 2016, Zrenjanin, Serbia, (2016)

ISSN:2067-3809

ACTA TECHNICA CORVINIENSIS
– Bulletin of Engineering
Tome X [2017]
Fascicule 2 [April – June]
ISSN: 2067 – 3809

[1.]Jyh-Chyang RENN, [2.]Wen-Jen HSU, [3.]Yun-Ruei LI

DEVELOPMENT OF HYDROSTATIC BEARING WITH SPOOL-TYPE RESTRICTOR FOR LARGE SINGLE COLUMN VERTICAL LATHE

[1-3.] National Yunlin University of Science and Technology, Faculty of Mechanical Engineering, 123 University Road, Section 3, Douliou, TAIWAN

Abstract: In this paper, a hydrostatic bearing with novel single-acting spool-type pressure feedback restrictor for large single column vertical lathe is developed. Due to the increasing demands of larger dimension, heavier load and higher precision for current and future machine tools, the development of hydrostatic bearing has become a more and more important issue over the past decades. Nowadays, the most commonly used pressure feedback restrictor for hydrostatic bearings installed in a large single column vertical lathe is membrane type, in which a thin and flexible metal sheet serves as the key component to meter the hydraulic oil flow precisely. However, the membrane-type restrictor is not quite suitable for extremely heavy load. Therefore, an alternative to design the hydrostatic bearing using spool-type restrictor is presented in this paper. Generally speaking, spool-type restrictor is easier to manufacture and has the advantage of lower cost than the membrane-type restrictor. It is thus expected that the developed spool-type restrictor can support much heavier load in machine tools than the membrane type. There are two significant features regarding this novel design. The first one is the introduced orifice restrictor which avoids effectively the influence of possible oil temperature variation. The second feature is the design of two adjustable hand wheels that are built into the valve body to widen the application range. Finally, a prototype of a single-unit hydrostatic bearing is successfully implemented and the experimental results prove the validity of the hydrostatic bearing with the proposed spool-type restrictor.
Keywords: hydrostatic bearing, pressure feedback restrictor, spool-type, single column vertical lathe

INTRODUCTION

Generally speaking, the trend of new generation machine tools is towards larger dimension, heavier load and higher precision. Among many different key components for current and future machine tools, the bearing is believed to play the most important role. Compared to traditional ball bearing, the advantages of aerostatic and hydrostatic bearing are non-contact, low friction and wear, low heat generation, etc. However, aerostatic bearing is only suitable for light load manufacturing.

For machine tools with large dimension and heavy load, like the large single column vertical lathe studied in this paper, the development of hydrostatic bearing becomes an inevitable task. Figure 1 shows the scheme of a large single column vertical lathe. The diameter of the rotary table may vary from 6 m to 10 m [1]. To support this very heavy rotary table, several hydrostatic bearings under the rotary table are utilized. In addition, these hydrostatic bearings are placed symmetrically about the center of rotation.

Nowadays, the most commonly used pressure feedback restrictor for hydrostatic bearings installed in a large single column vertical lathe is membrane type, in which a thin and flexible metal sheet serves as the key component to meter the hydraulic oil flow precisely as shown in Figure 2 [2-6, 11].

However, the membrane-type pressure feedback restrictor is not quite suitable for extremely heavy load. In addition, the membrane itself suffers from the fatigue problem [7, 10, 11]. Therefore, an alternative to design the pressure feedback restrictor for hydrostatic bearing using spool type is presented in this paper. Some previous reports [7, 8 and 10] indicated that disadvantages like the complex structure and difficult adjustment of the spool-type restrictor are inevitable. However, such a spool-type design is still believed to be a promising technique because the manufacturing of spool-type restrictor is basically easier than that of the above-mentioned membrane-type restrictor. In addition, there are many world-wide international or local famous companies that can manufacture different kinds of reliable spool-type hydraulic valves with excellent reputation.

Therefore, it is believed that the spool-type restrictor is a better choice when designing hydrostatic bearings for the large single column vertical lathe. In the following, the design concept of hydrostatic bearing with single-acting spool-type pressure feedback restrictor is illustrated.

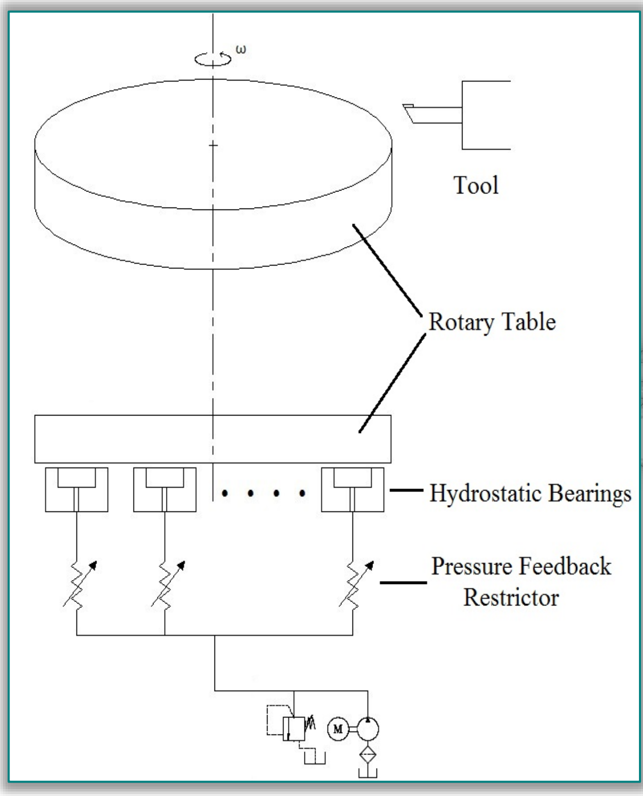

Figure 1 – Scheme of a large single column vertical lathe

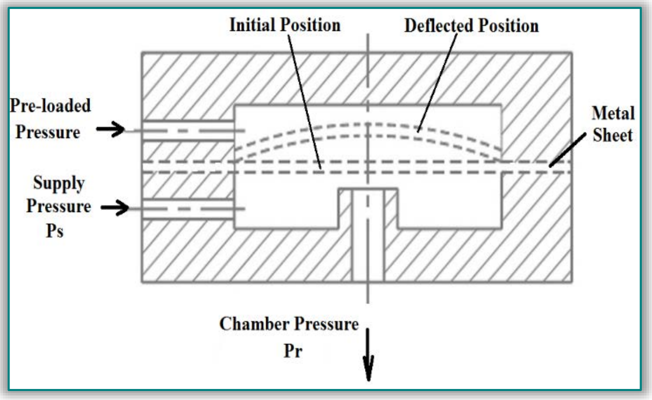

Figure 2 – Scheme of membrane-type pressure feedback restrictor

DESIGN OF HYDROSTATIC BEARING WITH SPOOL-TYPE PRESSURE FEEDBACK RESTRICTOR

Figure 3 shows the scheme of the developed hydrostatic bearing with novel spool-type pressure feedback restrictor. The operational principle is briefly described as follows. The initial opening allows basic flow rate of hydraulic oil through the orifice to the chamber to maintain a constant thickness of oil film between the circular pad and platform. It is worth mentioning that the circular pad is also called the hydrostatic bearing in some literatures. However, if some external disturbance load is imposed to the platform as shown in Figure 3, the thickness of oil film decreases and the chamber pressure, Pr, increases. In addition, if the chamber pressure exceeds some specific value defined by the spring, then the orifice opening will become larger due to the chamber pressure feedback. In details, the feedback chamber pressure acts on the right end of the spool and moves the spool to the left. This results in more hydraulic oil flowing to the chamber of the circular pad. Consequently, the chamber pressure increases trying to overcome the external disturbance load and enlarge the gap to maintain a constant thickness of oil film between the circular pad and platform.

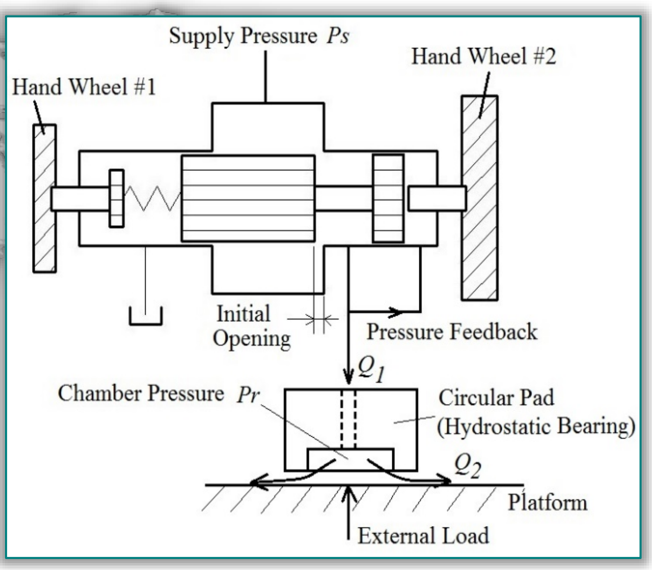

Figure 3 – Scheme of the hydrostatic bearing with novel spool-type pressure feedback restrictor

From Figure 3, it can also be observed that the proposed structure is active closed-loop pressure control scheme. However, no electric pressure sensor is necessary since the feedback pressure is directly connected to the right end of the spool. Hence, there are two significant features regarding this novel design. The first one is the introduced orifice-type restrictor which avoids effectively the influence of possible oil temperature variation. This can easily be proved by the following flow-rate equation through an orifice. Obviously, from Eq. 1, the flow-rate is independent of the oil viscosity and hence the temperature variation.

$$Q = C_f \cdot \pi \cdot d \cdot x\sqrt{\frac{2(Ps-Pr)}{\rho}} \quad (1)$$

where C_f - flow coefficient, d - diameter of the spool, x - opening of the orifice, Ps - upstream supply pressure, Pr - downstream chamber pressure.

The second feature is the design of two adjustable hand wheels that are built into the valve body to widen the application range. The handwheel#1 adjusts the pre-compression of the spring and set the effective working range of chamber pressure feedback. Since the chamber pressure is directly proportional to the external disturbance load, the handwheel#1 can then be adjusted to meet the actual external load condition accordingly. On the other hand, the handwheel#2 is used to regulate the initial opening of the orifice since the hydraulic oil must always flow into the chamber of the circular pad to set up the initial load capacity before the real operation. It is worth mentioning that circular pad is actually the hydrostatic bearing.

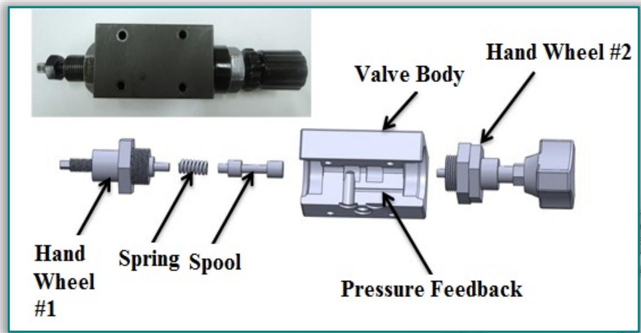

Figure 4 – Real picture and all parts of the restrictor

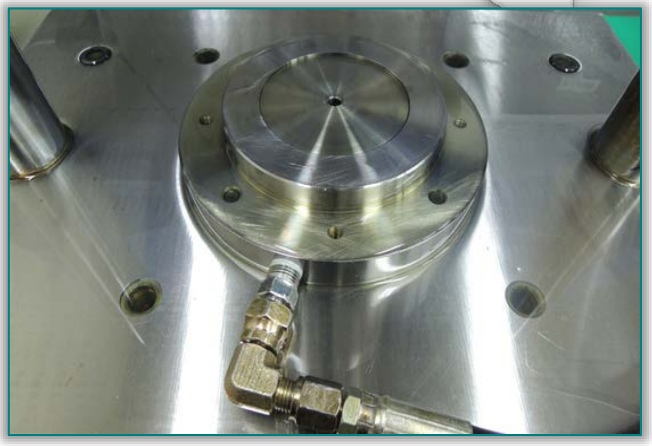

Figure 5 – Real picture of the circular pad (hydrostatic bearing)

Thus, the chamber pressure gradient formula can be described by Eq. 2. Obviously, from Eq. 2, the initial flow-rate through the orifice, Q_1, is necessary for the build-up of the chamber pressure and maintaining a definite oil-film thickness between the circular pad and platform. Finally, the real picture together with all parts of the developed spool-type pressure feedback restrictor is depicted in Figure 4. In addition, the real picture of the circular pad (hydrostatic bearing) is shown in Figure 5.

$$\frac{dP_r}{dt} = \frac{\beta_e}{V_e}\sum(Q_1 - Q_2) \quad (2)$$

where Pr - chamber pressure, β_e - bulk modulus of hydraulic oil, V_e - effective chamber volume, Q_1 - in-flow rate into the chamber, Q_2 - out-flow rate from the chamber.

EXPERIMENTAL TEST RIG

To evaluate the performance of the developed single-unit hydrostatic bearing with spool-type pressure feedback restrictor, a test bench is designed and constructed. Figure 6 shows the circuit diagram and real picture of the test bench. There are two power units in this test bench. The upper power unit is utilized to produce various external disturbance loads.

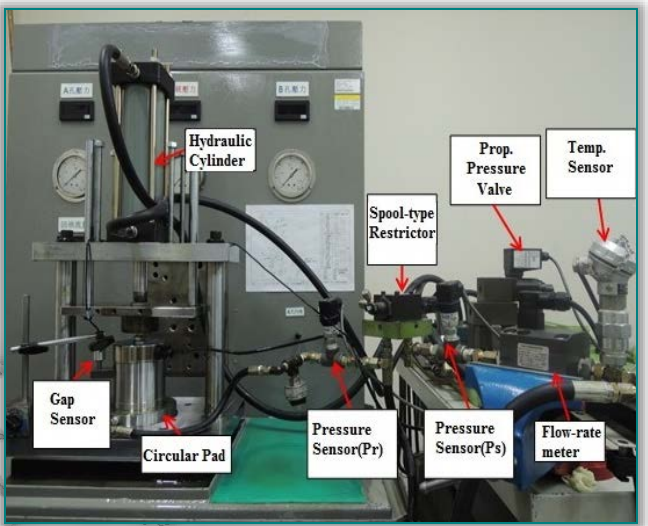

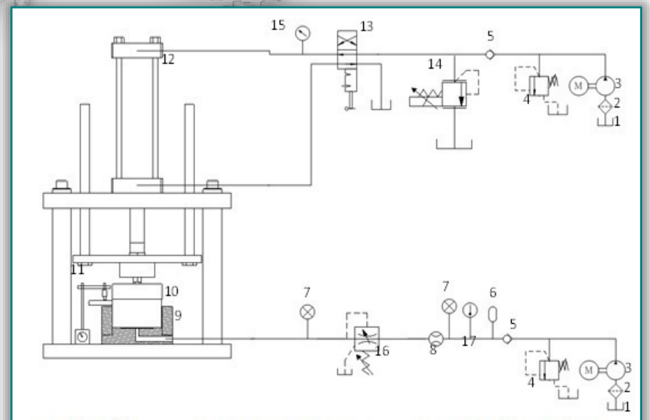

Figure 6 – Circuit diagram and real picture of the test bench

The key component is the proportional pressure valve (#14) which controls the load pressure precisely and is used to simulate various external disturbance loads acting on the circular pad (#9) through the hydraulic cylinder (#12). The adjustable range for the external disturbance load from 0 to 2000 Kgf or 20000 N is available in this test bench. On the other hand, the lower power unit is specifically used for the hydrostatic bearing.

To compensate the oil film variation caused by the external disturbance load, the developed spool-type pressure feedback restrictor (#16) is connected to the circular pad. The pressurized hydraulic oil supplied by the pump (#1) flows through the restrictor and enters the circular pad. It establishes a thin oil film between the circular pad and load cell (#10). Consequently, the load cell and cylinder rod (#12) are lifted up and floats above the circular pad.

By applying different external disturbance loads through the hydraulic cylinder, the oil-film thickness changes accordingly. In this case, the proposed spool-type pressure feedback restrictor is expected to play an important role to maintain a constant thickness of oil film. The relief valve (#4) is set at 30 bar and the maximal flow-rate output of the pump (#1) is 10 L/min.

EXPERIMENTAL RESULTS AND DISCUSSION

The performances of the developed single-unit hydrostatic bearing with spool-type pressure feedback restrictor can be evaluated in two ways. The first way is the static performance test. The external disturbance load acting on the load cell is increased slowly from 350 to 1850 Kgf by electrically controlling the proportional pressure valve.

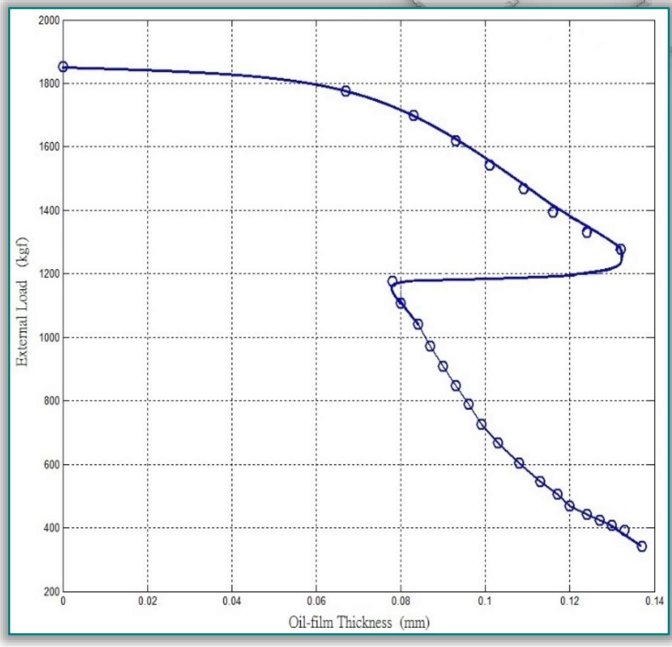

Figure 7 – Static performance test results of developed hydrostatic bearing with spool-type pressure feedback restrictor

At the beginning operating point of 350 Kgf, the external load is smallest which results in a largest oil-film thickness of 0.137 mm as shown in Figure 7. However, the oil-film thickness will decrease when the external load is further increased. In addition, if the external load exceeds a specific limit of 1200 Kgf, the oil-film thickness increases rapidly due to the operation of the spool-type pressure feedback restrictor. This increased oil-film thickness prevents the real contact between the load cell and circular pad. It is worth mentioning that this limit depends actually on the pre-compression of the spring, the spring constant as well as the friction force between the spool and valve body.

In other words, this limit can be adjusted according to the real operation condition. Figure 8 shows the static performance comparisons between the hydrostatic bearing with and without spool-type pressure feedback restrictor. It is clear that the static performance of hydrostatic bearing without any restrictor is worse than that with restrictor. Its oil-film thickness decreases monotonically as the external load is increased continuously.

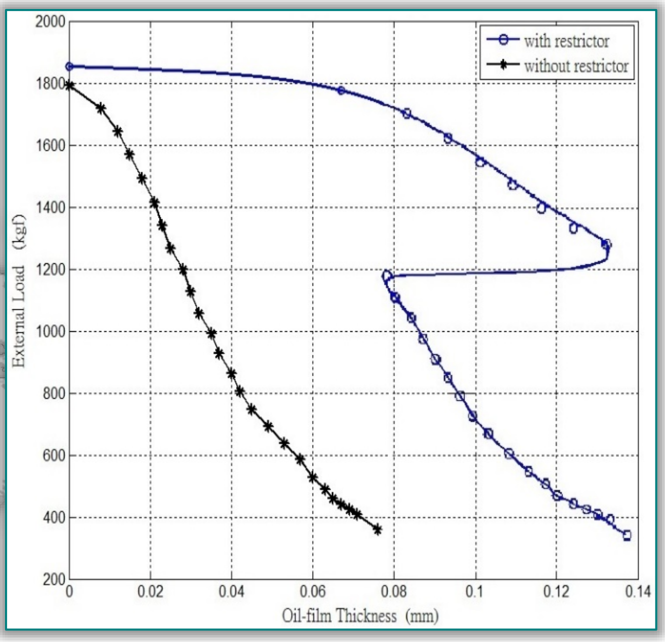

Figure 8 – Static performance comparisons between hydrostatic bearing with and without restrictor

The second means to evaluate the performance of the developed single-unit hydrostatic bearing with spool-type pressure feedback restrictor is the dynamic test. In the dynamic test, a square wave representing the external disturbance load from 350 to 1400 Kgf is produced by sending an equivalent electric signal to the proportional pressure valve. The frequency of the square wave is set to be 0.1 Hz. The experimental result of oil-film thickness for hydrostatic bearing without any restrictor is shown in Figure 9.

Obviously, the oil-film thickness seems to be an inverse square wave approximately in response to the square wave input of external load. In other words, the oil-film thickness cannot be kept a constant and the smallest thickness is around 0.07 mm which may cause the real contact and undesirable wear between the load cell and circular pad. On the other hand, the experimental result of oil-film thickness for hydrostatic bearing with the developed spool-type pressure feedback restrictor is shown in Figure 10.

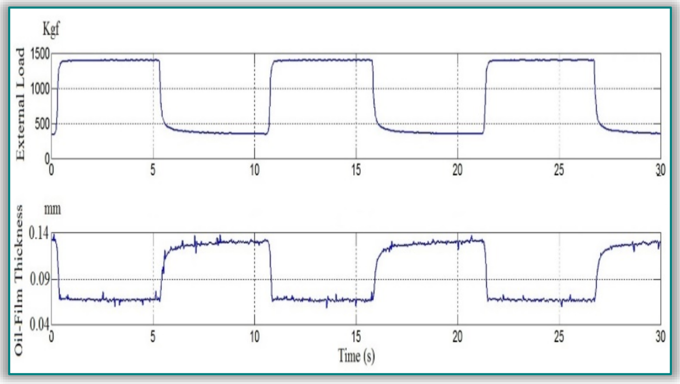

Figure 9 – Experimental results of hydrostatic bearing without restrictor

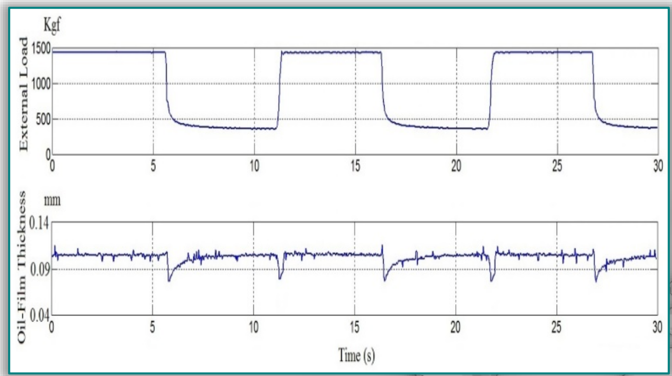

Figure 10 – Experimental results of hydrostatic bearing with restrictor

It can be observed that the oil-film thickness is nearly a constant valve regardless of the square wave input of external disturbance load from 350 to 1400 Kgf. Therefore, the real contact and undesirable wear between the load cell and circular pad can be avoided. This is exactly the principle function for a hydrostatic bearing.

CONCLUSIONS

In this paper, a single-unit hydrostatic bearing with spool-type pressure feedback restrictor for a large single column vertical lathe is successfully developed and implemented. Besides, four conclusions may be drawn from this research.

1. The successful development of hydrostatic bearing with spool-type restrictor is verified by both the static and dynamic tests. And the results are satisfactory.
2. In addition to the large single column vertical lathe, the proposed hydrostatic bearing together with spool-type restrictor is also suitable for other machine-tool applications with heavier load, like the surface grinding machine, etc.
3. One most innovative design revealed in this paper is the design of two built-in hand wheels to adjust the application range. In addition, such a design also overcomes the fault of difficult adjustment in some conventional spool-type restrictors mentioned in previous reports [7, 8 and 10].
4. The range of applied external disturbance load for the developed prototype is recommended to be from 1300 to 1500 Kgf. Within this range, the hydrostatic bearing possesses highest stiffness and the corresponding oil film thickness can be maintained at a nearly constant value. On the other hand, this operational range can also be adjusted by the hand wheel #1 shown in Fig. 3.

Acknowledgment

The financial support of the Ministry of Science and Technology under grant number MOST-103-2221-E-224-047 is greatly appreciated.

Note

This paper is based on the paper presented at The International Conference Management of Technology – Step to Sustainable Production (MOTSP 2016), organized by the Faculty of Mechanical Engineering and Naval Architecture, Croatian Association for PLM and the University of North, in Porec/Parenzo, Istria, CROATIA, June 01–03, 2016.

References

[1] Catalogue of Pietro Carnaghi SPA, www.pietrocarnaghi.com/en/20/ay.html, 2015.
[2] Wang, C., Cusano, C.: Dynamic Characteristics of Externally Pressurized Double Pad Circular Thrust Bearing with Membrane Restrictors, Transactions of ASME, Journal of Tribology, 113(1991), 158-165, 1991.
[3] Sharma, S. C., Sinhasan R., Jain, S. C.: Performance Characteristics of Multi-recess Hydrostatic/Hybrid Flexible Journal Bearing with Membrane Type Variable-Flow Restrictor as Compensating Elements, Wear, 152(1992), 279-300.
[4] Brecher, C., Baum, C., Winterschladen M., Wenzel, C.: Simulation of Dynamic Effects on Hydrostatic Bearing and Membrane Restrictors, Production Engineering, 2007.
[5] Kang, Y., Shen, P. C., Chang, Y. P., Lee, H. H., Chiang, C. P.: Modified Predictions of Restriction Coefficient and Flow Resistance for Membrane-Tape Restrictors in Hydrostatic Bearing by using Regression, Tribology International, 40(2007), 1369-1380.
[6] Kang, Y., Shen, P. C., Chang, Y. P., Lee, H. H.: Modified Determination of Fluid Resistance for Membrane-Type Restrictor, Industrial Lubrication & Tribology, 59(2007)3, 123-131.
[7] Rippel, H. C.: Design of Hydrostatic Bearings: Part1-Basic Concepts and Pad Design, Machine Design, 1963, 108-117.
[8] O'Donoghue, J. P., Rowe, W. B.: Hydrostatic Bearing Design, Tribology International, 2(1969)1, 25-71.

[9] Chena, D., Fan, J., Zhang, F.: Dynamic and Static Characteristics of a Hydrostatic Spindle For Machine Tools, Journal of Manufacturing Systems, 31(2012), 26-33.
[10] Rowe, W.: Hydrostatic, Aerostatic and Hybrid Bearing Design, Elsevier, 2012.
[11] Sawano, H., Nakamura, Y., Yoshioka H., Shinno, H.: High Performance Hydrostatic Bearing Using Variable Inherent Restrictor with a Thin Metal Plate, Precision Engineering, 41(2015), 78-85.

ISSN:2067-3809

ACTA TECHNICA CORVINIENSIS
– Bulletin of Engineering
Tome X [2017]
Fascicule 2 [April – June]
ISSN: 2067 – 3809

[1.]Milija KRAIŠNIK, [2.]Milan ŠLJIVIĆ, [3.]Jovica ILIĆ, [4.]Jelica ANIĆ

COMPRESSIVE PROPERTIES OF COMMONLY USED POLYMERS IN ADDITIVE MANUFACTURING PROCESSES

[1,4.]Faculty of Mechanical Engineering, East Sarajevo, BOSNIA & HERZEGOVINA
[2,3.]Faculty of Mechanical Engineering, Banja Luka, BOSNIA & HERZEGOVINA

Abstract: Production methods based on additive manufacturing technologies represent a powerful approach to the rapid and efficient production of complex prototypes and functional parts from different materials. This paper presents the procedure of development and production of a holder using a fusing deposition modeling process. Since compression is the dominant load on the holder in exploitation, mechanical testing was carried out and the results obtained can contribute to adequate material selection.
Keywords: Additive manufacturing, mechanical properties, polymers: ABS plus, ABS, PLA

INTRODUCTION

Modern, unconventional production processes are mainly used today for fabrication of prototypes and functional elements of extremely complex geometric configurations. Their implementation is based on the principle of joining material layer by layer in order to obtain a physical model that is identical to the virtual model, without using the tools and accessories. This production concept is known as Additive Manufacturing – AM in scientific and professional community. In the last thirty years, a number of procedures of additive manufacturing has been developed and successfully applied, whose main features are reported in [1-3].

In general, for the realization of any AM process the following are needed: material, energy and a CAD model. Taking into account quality and functionality of the obtained product, the correct choice of materials to be used for the fabrication is of great importance. Therefore, it is necessary to know the mechanical properties because they enable a preliminary assessment of the behavior of materials during exploitation.

The paper [4] presents the results related to the tensile strength of test samples produced by using different additive processes. Also, the same paper reports recommendations for the selection of AM procedure depending on the required strength of the product. Results from the study [5] clearly show that the mechanical properties of the 3D-printed polyether-ether-ketone (PEEK) sample were superior to the 3D-printed pattern of the ABS polymer. Fragassa and Minak in the work [6] announced the results of the mechanical properties of four photopolymer resins known under their commercial names as FullCure720, PA, MK3 and VeroBlu. On the basis of various mechanical tests similarities and differences were found in the behavior of materials in quasi-static loads. Influence of processing conditions on the tensile strength of 3D-printed models has been published in [7].

Previous studies of mechanical properties have been done regardless of the fact that manufacturers of material must provide information related to the physical and mechanical properties. However, as stated in [6], secondary experimental verification is required in terms of the increased reliability of the final components, which are obtained by using innovative and insufficiently known technologies.

Since polymeric materials are predominantly used in the AM procedures today, the paper presents the results of experimental research related to characterization of compressive properties of the three most commonly used polymers: Polylactic Acid – PLA, Acrylonitrile Butadiene Styrene - ABS and an enhanced version of ABSplus. Also, the paper presents the development and production of functional parts of the tested polymers using the AM process which is based on the technology of material extrusion.

THE PROCESS OF MATERIAL EXTRUSION

Material extrusion is an additive manufacturing process for fabrication of prototypes and final parts based on the principle shown in Figure 1.

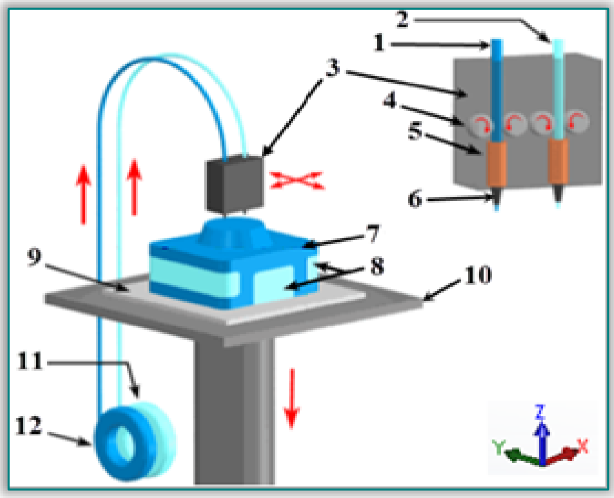

Figure 1. Schematic view of material extrusion process: 1-Build material filament, 2-Support material filament, 3-Extrusion head, 4-Drive wheels, 5-Liquifiers, 6-Extrusion nozzles, 7-Part, 8-Part supports, 9-Foam base, 10-Build platform, 11-Support material spool, 12-Build material spool [8]

The material in the form of a wire is fed into the nozzle around which electrical resistant heaters are located. Due to the heating and maintaining the temperature above the melting point, the material in viscous state is applied to the platform in the form of layers, wherein it rapidly solidifies. When a layer has been formed, the platform lowers, and the nozzle starts making the next layer. The thickness of the layer and vertical accuracy depend on the diameter of the nozzle opening. Various types of materials are used including ABS plastics, polyamides, polycarbonates, polyethylene and polypropylene.

EXPERIMENTAL RESEARCH

Experimental research consists of two parts. The first part refers to the development and fabrication of functional parts (the holder) and test samples for mechanical tests using material extrusion, and the second part is focused on the characterization of the compressive properties of used materials.

Additive manufacturing of the holder using material extrusion

Fabrication of the holder from the tested polymer was performed in the Laboratory for Technology of Plasticity at the Faculty of Mechanical Engineering in Banja Luka. In order to do so, 3D Printers Dimension Elite (left on Figure 2) and LeapFrog Creatr XL (right on Figure 2) were used. The physical model was based on material extrusion technology.

Figure 2. 3D printers: Dimension Elite (left) and LeapFrog Creatr XL (right)

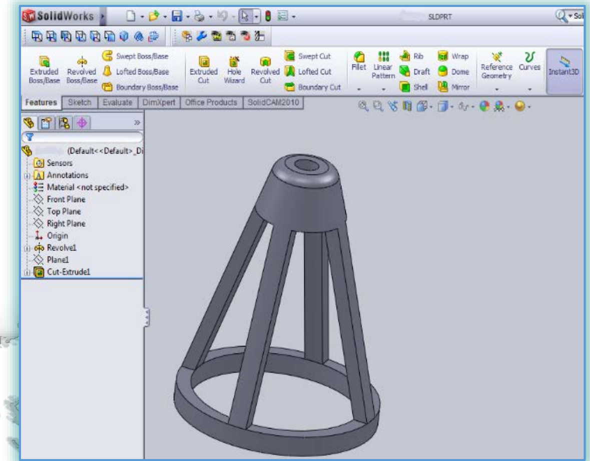

Figure 3. Holder design in SolidWorks software

The development of functional parts using material extrusion technology consisted of the following procedures:

- Product design in a CAD software package,
- Conversion of CAD models in STL format recognized by 3D printers,
- Transfer of STL files to the computer that controls the three-dimensional printer,
- Processing of STL files within the CatalystEX and Simplify3D in which all the parameters for the required model are set and adjusted,
- Creating a three-dimensional model using additive technology,
- Further processing of created prototypes and
- Post-processing techniques.

The above procedure was applied in its entirety for the development of the holder. The holder was designed in SolidWorks software package, Figure 3. After transferring STL files to a computer that controls the operation of the 3D printer and loading the generated model, the adjustment of operating parameters within the CatalystEX and Simplify3D software package, Figure 4, was performed.

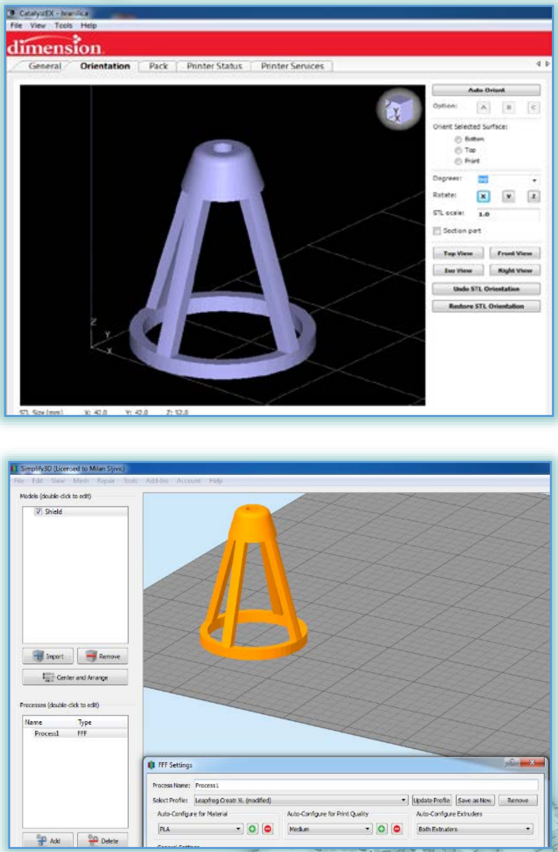

Figure 4. Preprocessing and adjusting operating parameters in software packages: a) CatalystEX i b) Simplify 3D

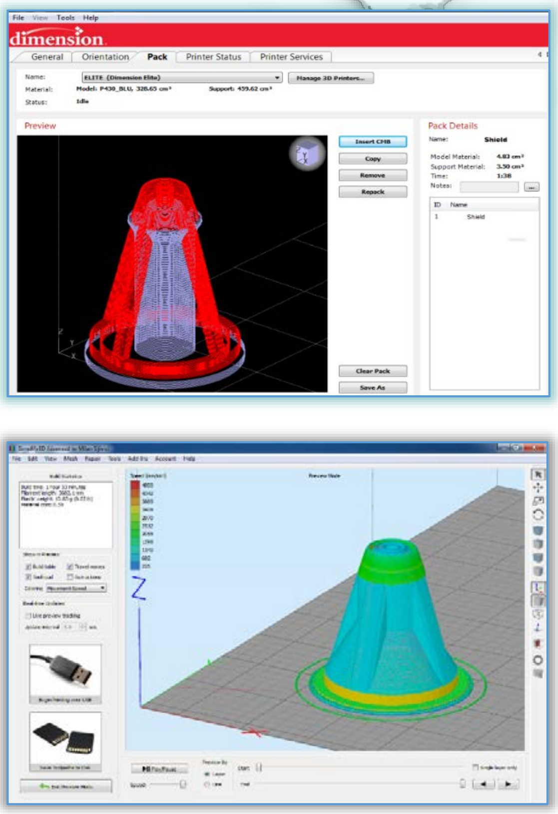

Figure 5. Positioning of a model on the printing platform and preparation of the 3D printing process of a holder in software packages: a) CatalystEX (Dimension Elite) and b) Simplify3D (LeapFrog 3D štampač)

The selection of the model orientation and the best position, processing of support and layers, as well as the arrangement of the model on the 3D printer platform are shown in Figure 5. Figure 6 shows a finished, i.e. printed element.

In the process of additive manufacturing of holders from the ABSplus polymer the Dimension Elite 3D Printer by manufacturer Stratasys from the United States has been used. The fact that the manufacturer patented the ABSplus polymer represents a limiting factor in terms of application of other types of 3D printers.

The making of holders from ABS and PLA polymers was carried out on the LeapFrog Creatr XL 3D printer. In this case a broader range of materials can be used because by using universal software different process parameters can be defined, such as the temperature of the nozzle, the speed of 3D printing, platform temperature, etc. The final result is the optimization of the additive manufacturing process of functional parts, depending on the material being used.

The parameters of holder fabrication on different 3D printers are shown in Table 1.

Table 1. The parameters of holder fabrication

Parameter	3D Printer	
	Dimension Elite	LeapFrog
Production time	98 minutes	113 minutes
Volume of the base material	4.83 cm^3	10.83 g
Volume of the support material	3.50 cm^3	4.65 g
Material price	7.46 €	5.43 €

Figure 6. The holders produced using additive manufacturing technology

The holders produced using additive manufacturing technology are shown in Figure 6.

Compressive testing

Experimental research of compressive properties was carried out on cylindrical polymer samples of original dimensions D_0 = 10 mm and H_0 = 20 mm, Figure 6.3. All samples were built on Dimension Elite and LeapFrog 3D printers in the Laboratory for Technology of Plasticity at the Faculty of Mechanical Engineering Banja Luka. Compressive testing of material was performed at the Laboratory for Welding and Material Testing at the

Faculty of Mechanical Engineering in East Sarajevo. The samples were deformed by using the universal testing machine "Shimnadzu", type AGS-20 kN NXD (Figure 7), and Trapezium X software was used for processing and graphical display of compression test results.

Figure 7. Testing machine with compressive module

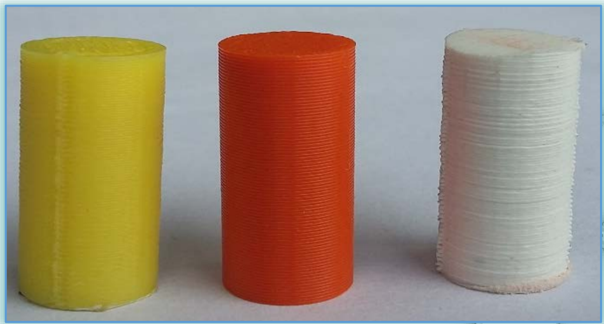

Figure 8. Samples for compressive testing:
a) ABS, b) ABSplus, c) PLA

a)

b)

c)

Figure 9. The appearance of samples after testing:
a) ABS, b) ABSplus, c) PLA

The total of 15 samples were used for compressive tests, wherein the characterization of the particular polymer was based on the results of five individual tests. A set of undeformed samples and those after testing is shown in Figures 8 and 9, respectively.

Typical behavior of the ABS, PLA and ABSplus polymer in compression for one of the five test samples is presented in Figure 10 (a), (b) and (c). The diagrams of Engineering stress (σ) / Engineering strain (ε) were automatically generated in the course of tests. In doing so, data relating to the initial tube size and test conditions were used.

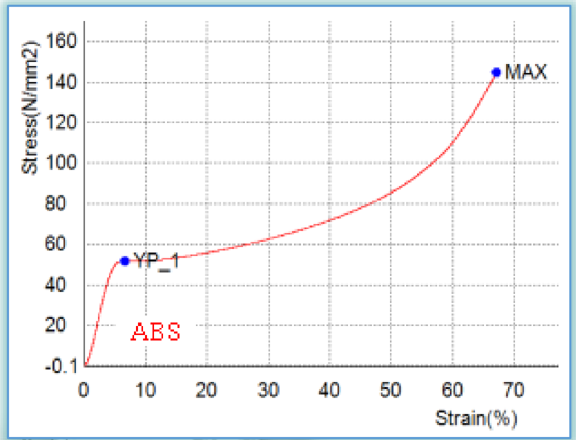

a)

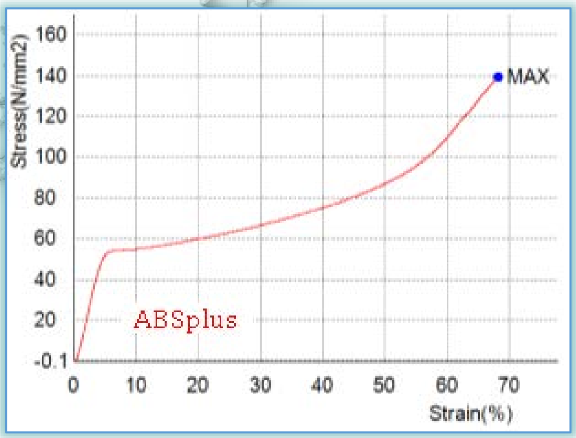

b)

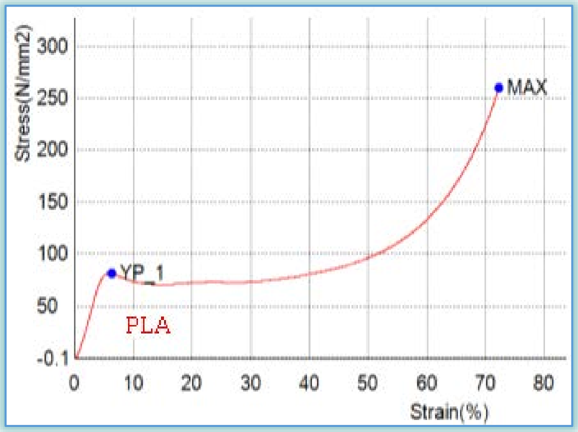

c)

Figure 10. The curves σ-ε in compressive testing of different materials

The compression of all samples was conducted at the 5 mm/min speed of deformation. The mean values of yield stress R_{PT}, compressive strength r_{pM}, the maximum relative deformation ε_M and modulus of elasticity E_P were determined based on the results of five tests for the ABS and ABSplus polymer.

In compressive testing the PLA polymer demonstrated high plastic properties and because there were not any cracks it was not possible to determine the compressive strength. Therefore, only yield stress and R_{PT} and compaction module E_P were determined for this polymer. Comparative presentation of the results is given in Table 2.

Table 2. Mean values of compressive properties

Material	Yield stress R_{PT} [N/mm²]	Compressive strength R_{pM} [N/mm²]	Max. strain ε_M [%]	Modulus of elasticity E_P [GPa]
ABS	50,74	144,27	68,38	1,52
ABSplus	54,76	142,85	69,08	1,64
PLA	86,54	---	---	2,20

The analysis of the results

Analysis of fabrication of functional parts showed strong influence of material and 3D printer type on product quality. The best holder quality was achieved on the Dimension Elite – Stratasys professional printer using ABSplus polymers. Therefore, it is recommended to use the mentioned printer for the fabrication of finished parts, but in this case higher production costs must be taken into account.

The flows of curves σ-ε and the numerical values in Table 2 show that during mechanical compressive testing, ABSplus and ABS polymers behave similarly. The PLA polymer showed the greatest resistance to the turn to a plastic area. Numerically speaking, samples from the PLA polymer have 70% higher yield strength in comparison to the ABS polymer, or by 58% compared to the ABSplus polymer. However, after moving to the plastic area, the PLA polymer samples acted as perfectly plastic material in the initial stages of deformation, with no indications of strain hardening. However, with increasing level of deformation, especially for $\varepsilon > 50\%$, there was a pronounced strain hardening, which was still not enough to determine the compressive strength of the PLA polymers, because even with high loads there were no cracks on the free surface of samples.

CONCLUSIONS

The process of Additive Manufacturing based on material extrusion technology is suitable for the fabrication of functional components, but the quality and the production costs depend on the type of material and the type of the 3D printer being used.

Overall results of mechanical compressive tests showed that the PLA polymer has the highest yield strength, but its ductile properties are significantly variable and depend on the level of deformation. The resistance and ductility properties of ABSplus and ABS polymers are quite similar.

As the results presented in this study may contribute to the adequate selection of polymer materials for additive manufacturing processes, the following recommendations can be generally given:

- Due to the reduced toughness at higher levels of plastic deformation, PLA polymers are to be preferably used for parts which are mainly axially loaded;
- ABSplus and ABS polymers are advantageous for producing parts that work in varying operating conditions due to which complex stress states occur.

Acknowledgment

The results presented in this paper are part of the research activities within the Tempus project WIMB: 543898 – TEMPUS – 1 – 2013 – 1 – ES – JPHES, whose implementation is financed by the European Union.

Note

This paper is based on the paper presented at The 3rd International Scientific Conference on Mechanical Engineering Technologies and Applications (COMETa 2016), organized by the Faculty of Mechanical Engineering, University of East Sarajevo, in Jahorina, Republic of Srpska, BOSNIA & HERZEGOVINA, December 7–9, 2016.

References

[1] Plančak, M. (2004). Brza izrada prototipova, modela i alata, Fakultet Tehničkih Nauka, Novi Sad

[2] Šljivić, M. (2007). Tehnologija brze izrade prototipskih proizvoda i alata, Mašinski Fakultet, Banja Luka

[3] Šercer, M., Godec, D., Pilipović, A. (2012) Aditivne tehnologije za mala i srednje velika preduzeća, Fakultet strojarstva i brodogradnje, Zagreb

[4] Tiro, D., Brdarević, S. (2015). Komparativna analiza zatezne čvrstoće tri postupka brze izrade prototipova, 9th Research/Expert Conference with International Participations "QUALITY 2015", Neum, B&H, str. 189-194,

[5] Wenzheng, W., Peng, G., Guiwei, L., Di Zhao., Haibo, Z., Ji Zhao (2015) Influence of Layer Thickness and Raster Angle on the Mechanical Properties of 3D-Printed PEEK and a Comparative Mechanical Study between PEEK and ABS, Materials 2015, 8,; doi:10.3390/ma8095271, p.p. 5834-5846

[6] Fragassa, C., Minak, G. (2008). Standard characterization for mechanical properties of photopolymer resins for rapid prototyping, 1st Symposium on Multidisciplinary Studies of Design in Mechanical Engineering, Bertinoro, Italy

[7] Galeta, T., Kladaric, I., Karakas, M. (2013). Influence of processing factors on the tensile strength of 3D-printed models, Materiali in tehnologije / Materials and technology 47, UDK 621.7:004.896, ISSN 1580-2949, p.p. 781-788.
[8] Tiro, D., Denjo, D. (2015). Comparative analysis of dimensional accuracy for Z-corp, RTV and Cube 3D rapid prototyping processes, 19th International Research/Expert Conference "Trends in the Development of Machinery and Associated Technology" TMT 2015, Barcelona, Spain, p.p. 65-68.

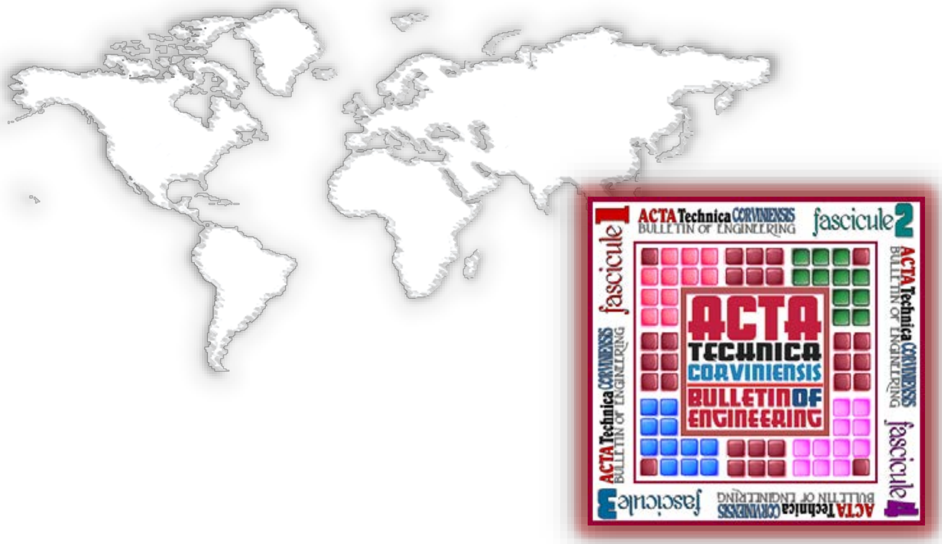

ISSN:2067-3809

ACTA TECHNICA CORVINIENSIS
– Bulletin of Engineering
Tome X [2017]
Fascicule 2 [April – June]
ISSN: 2067 – 3809

[1.]Levente TÓTH

RESOLUTION LIMIT OF SMALL IMAGE SENSORS SIZE

[1.] Doctoral School on Safety and Security Sciences, Obuda University, Budapest, HUNGARY

Abstract: Safety video surveillance systems have been relying on the technological achievements and developments of the consumer market in a number of respects from the very beginning. It is no different in the case of Ultra HD (4K). Although in spite of the fact that the market penetration of the ultra-high definition Broadcast technology is considerably slower than previously predicted, 4K-resolution slowly but surely infiltrates into the domain of video surveillance systems. More and more manufacturers include Ultra HD cameras in their portfolios. The question, however, is rather simple: is this sector really prepared to implement this technology? Does higher resolution actually provide more information? Have all the opportunities provided by full HD been fully exploited, or is there still room for improvement in this area?
Keywords: UHD, 4K, resolution, diffraction, limit of resolution

INTRODUCTION

We experience technological races in various fields of life. Be it the motor industry or the mobile phone market, we see more and more new technological developments in the given field. Manufacturers bid against one another to gain the largest possible market share, using various marketing tools. A pixel war is ongoing on the mobile front, while in television technology we have hardly been introduced to the 4K resolution when an advanced version of 8K was already displayed in exhibitions.

This trend did not leave the field of video surveillance systems untouched, either. More and more manufacturers include cameras with resolution exceeding Full HD in their portfolio. Many people think that the larger the number of pixels, the better the image quality and thereby the more details visible in the picture.

A declared objective of this article is to highlight that image quality does not only depend on the resolution of the imaging sensor. We have reached a level where we need to take into account such physical limitations that directly work against a more detailed image display.

CHANGES IN MARKET TRENDS IN THE LAST FEW YEARS

The statistics of camera sales in Hungary for Bosch, leading manufacturer in surveillance video systems, provides a good description of the technological advancements in this field.

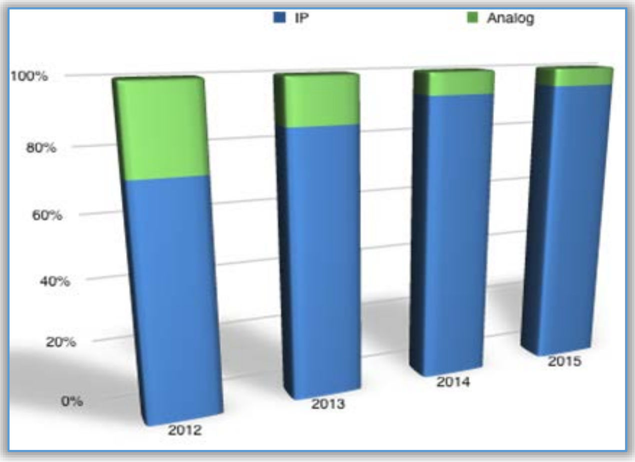

Figure 1: Statistics of Bosch camera sales in Hungary (source: own editing)

Analog camera sales keep shrinking, while sales of IP cameras are increasing at the same rate.[1] A further breakdown of sales statistics for HD and higher resolution cameras show that sales are more and more relevant for larger resolution equipment [1]. The higher the resolution of the camera we choose, the higher the chance that under some circumstances we will run into resolution limits.

[1] According to data by Attila Bárány, Head of Marketing at Bosch

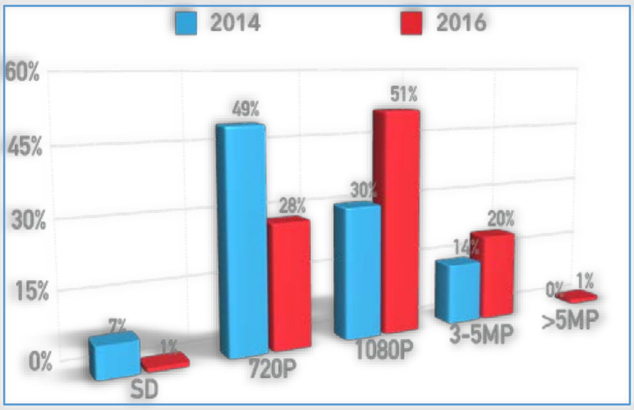

Figure 2: Camera sales according to resolution between 2014 and 2016 (source: own editing)

DIFFRACTION LIMIT

Diffraction as physical phenomenon is mostly relevant in wave optics. Projecting parallel light rays, incoming at a perpendicular angle, through a slit the size of which corresponds to the wave length of the light shows that light waves can reach areas of the receiving screen that are optically shaded if we assume a straight line of light propagation.

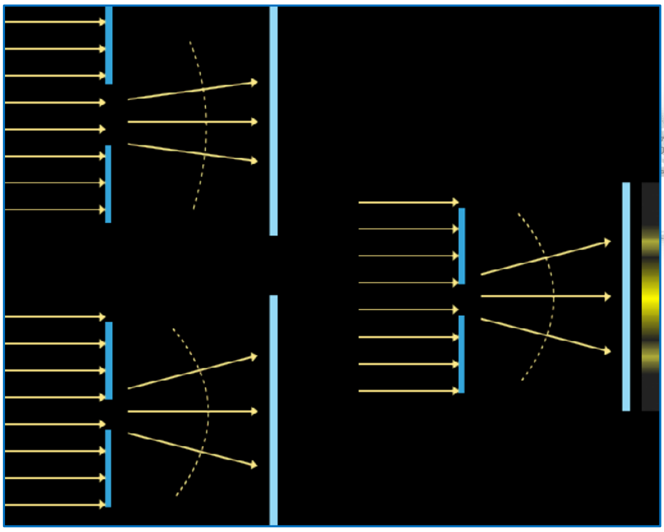

Figure 3: Correlation between diffraction and slit (source: own editing)

According to the Huygens-Fresnel principle, [2, pp. 413-414] elemental waves interfere in various ranges of the wave space, meaning that they either weaken or strengthen each other. This diffraction pattern is clearly visible in the receiving screen. The most intensive line of light is in line with the middle of the slit, and it gradually fades to the right and left up to the point of extinction. In case we consider the slit to be one-dimensional, the most intensive spot of light will be in the intersection of the screen and the line perpendicular to the screen, going through the middle of the slit. The intensity then decreases in both positive and negative directions until extinction. From here, we again see increasingly bright lanes, which again starts to fade after it reaches its maximum, until the second point of extinction (Figure 3, right side). The value of diffraction is proportional to the wavelength of the light, and inversely proportional to the size of the slit (Figure 3, left side).

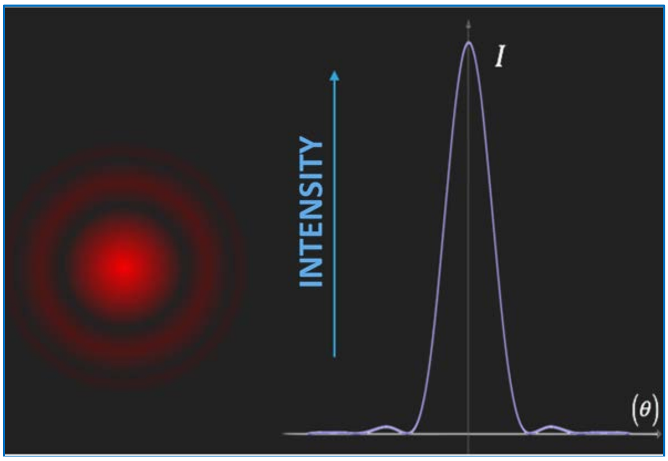

Figure 4: Airy disk and intensity function (source: own editing)

Through a round slit, light beams emanating from a single point will display as concentric, gradually fading circles with alternating brighter and darker light rings. The image thus produced is called the Airy[2] disk. (Figure 4). The intensity function beside the disk clearly shows that the second maximum value following the first, main minimum is only a fraction (1.75%) of the main maximum. Subsequent maximum values keep decreasing. The third maximum value is only 0.42% of the main maximum (these circles will only be visible with a very powerful light source).

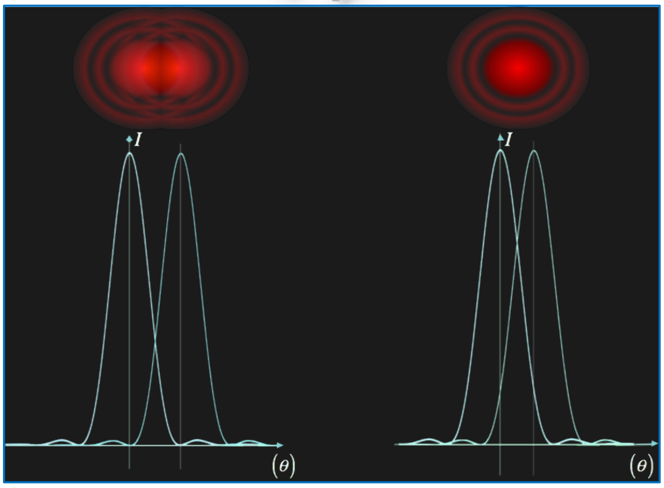

Figure 5: Rayleigh criterion (source: own editing)

When testing the resolution limit of an imaging equipment, an important concept id the Rayleigh[3] criterion. Let us examine the images displayed though a small round opening of two incoherent light disks that

[2] Sir George Biddell Airy (1801–1892) mathematician and astronomer

[3] Lord Rayleigh (1842-1919) physicist

are far from each other as compared to their diameters. Due to the diffraction, the displayed image of the two pointlike light sources will be an Airy disk.

In case the distance between the two pointlike light sources are comparable to the size of the slit, the image will be blurred and we will not be able to tell them apart [3, p. 149]. According to the Rayleigh criterion, the two pointlike spots will be just barely differentiated if on the displayed image the maximum of one Airy disk falls on the first minimum of the other Airy disk (Figure 5).

In order to calculate the first minimum of the Airy disk intensity function, we need to be able to compile the function itself. Assessing the resolution limits in an optical system [4, p. 117], and omitting a full mathematical deduction, for the direction corresponding to the first minimum of the function, the following relation can be stated:

$$\theta_0 = \arcsin\left(1{,}22\frac{\lambda}{D}\right) \quad (2.1)$$

where D is the diameter of the round aperture, and λ is the light's wave length. Consequently, the two points that are in α elongation from each other can be differentiated if:

$$\alpha \geq \theta_0 = 1{,}22\frac{\lambda}{D} \quad (2.2)$$

Since angles are very small in such close proximity of points, it will not be greatly misleading to state that:

$$\sin\theta_0 = \tan\theta_0 = \frac{r}{f} \quad (2.3)$$

where r is the radius of the first minimum circle, while f is the focal distance of the optic system (camera lens). Since the slit of a lens is (N),

$$N = \frac{f}{D} \quad (2.4)$$

where *D* in this case is the slit of the incoming pupil of the camera lens, thereby using this information as well as the equations 2.1 and 2.3, we can determine the radius of the first minimum of the Airy disk corresponding to various apertures:

$$r = 1{,}22 \cdot \lambda \cdot N \quad (2.5)$$

As per equation 2.5, the size of the Airy disk is proportional to the wavelength and the size of the aperture. At an aperture of F8.0, and taking the wavelength of green light (520 mm), the diameter of the Airy disk is

$$2r = 2{,}44 \cdot 5{,}2 \cdot 10^{-7} \cdot 8 = 10{,}15\ [\mu m] \quad (2.6)$$

The maximum aperture can be as high as F64 in some automatic iris lenses, which means an eight times larger Airy disk as compared to the result of equation 2.6.

CORRELATION BETWEEN DIFFRACTION BARRIER AND PIXEL SIZE

As technology in manufacturing develops, the elemental pixel size in CCD[4] and CMOS[5] image receivers keep decreasing. In the past twenty years or so, the elemental pixel size has shrunk to less than 1/100, while surface sensitivity per unit (mV/μm²) has increased in the same ratio. This is due to technological inventions such as OCML, OCCF and the tungsten shield, which has a 20-40% lower reflection than the previously used aluminium layer [5, pp. 27-30].

While the spectacular shrinking of mobile phones poses a certain expectation towards camera and lens manufacturers, this would not be a demand in video surveillance. Still, the size reduction for image receivers and lenses is ongoing. Image sensors used today with a resolution of 5 MP or higher mostly have a size of 1/1.8" (7.17 mm x 5.32 mm), or maybe 1/1.7" (7.6 mm · 5.7 mm) in better cases. On the contrary, the format for DSLR cameras keeps getting larger in parallel with resolution. The Canon PowerShot G1 X Mark II type DSLR camera has a nearly 13 megapixel (MP) image receiver with a size of 1.5"-os (18.7 mm x 14 mm) [6]. This is a 6.8 times larger surface than that of the 1/1.8" format.

When we compare the CMOS sensors of a Sony IMX185LQJ type Full HD [7] and a IMX226CQJ type 4K [8], we see that the elemental pixel size in the smaller resolution equipment is 3.75 μm x 3.75 μm, while the same value for 4K is 1.85 μm X 1.85 μm. since we are talking of small sizes, the difference does not seem large. Calculating, however, the surface size of the elemental pixel, the result for the former is 14.06(25) μm², while for the high-resolution latter equipment is barely its quarter at 3.42(25) μm².

Putting aside the Bayer filter used in the colour camera, and the fact that the colour information for these image receivers is compiled from 3 elemental pixels and these are not closely connected to each other, let us examine the effect of the Airy disk, caused by diffraction, on imaging.

Figure 6 shows that in case of low resolution, the Airy disk covers exactly one full pixel. Assuming an identical aperture, the light beam emanating from one point is spread over several pixels in a high-resolution equipment. This means that pixels close to each other will display identical information. In image receiving units with different sizes, the aperture value to limit maximum resolution will be different. Generally, we can state that at identical image sensory formats, higher-resolution elements will experience a deterioration in resolution at higher aperture values.

---

[4] Charged Couple Device

[5] Complementary Metal-Oxide Semiconductor

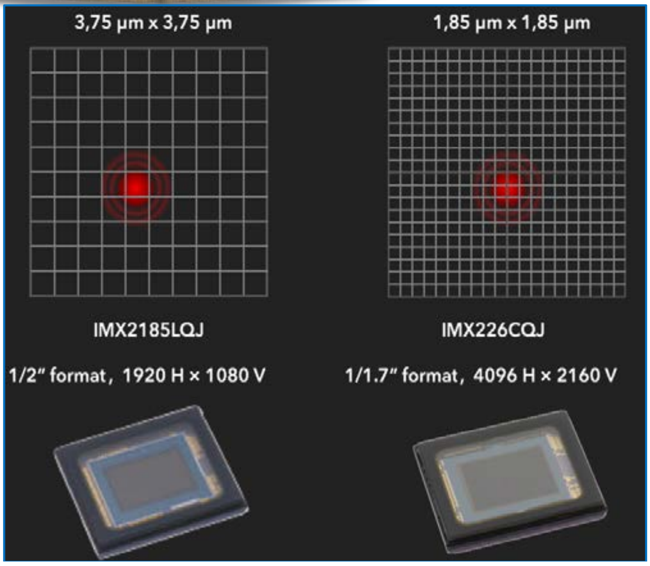

Figure 6: The influence of diffraction under high and low resolution (source: own editing)

CORRELATION OF SENSITIVITY AND PIXEL SIZE

Increasing the resolution of image receivers correlates with yet another issue, which is the decrease in sensitivity. It is easy to see that under identical lighting condition, a smaller elemental pixel size will receive a lower number of photons during a given time unit than a larger one. Consequently, the sensitivity and dynamic range of the equipment is worse. A lower number of received photons, assuming an identical quantum efficiency (QE) will result in less electrons. This decreased charge will in turn we comparable with the decoder noise and dark current noise produced by the image receiver. These together will also have a negative effect on resolution. [9, pp. 35-36]

The increases signal-noise relationship may result in further problems in image processing, transfer and storage as well. Processing a noisy image by software is more difficult, for example in motion detection the number of false alarms may increase, or contrarily: raising the threshold value may reduce the identification of real motion. Higher noise will also cause worse performance in compression, which in turn leads to a larger bandwidth for transferring and an increase in storage space demand.

TEST RESULTS

All of the above suggest that the physical limitations we have mentioned will considerably reduce image quality. I have verified the validity of theoretical calculations by measurements. When creating the appropriate test environment, I paid attention to Section 5.3 of the upcoming IEC 62676-5 standard, which provides a detailed prescription for the type of the test image, as well as the relative positioning of the camera, the illumination and the light meter. The test chart used for measurements is ISO 12233, as recommended in the standards.

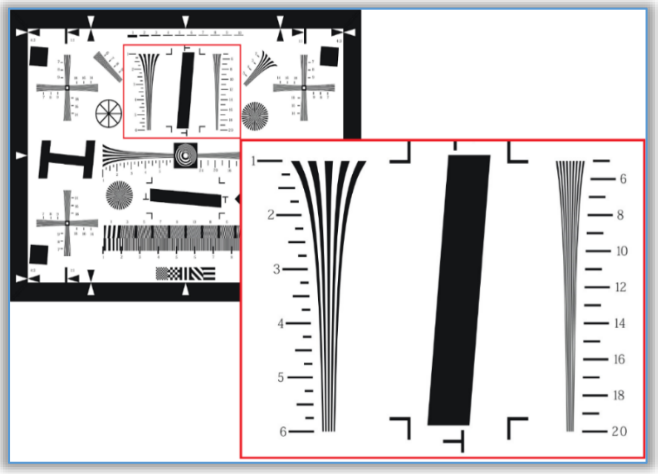

Figure 7: ISO 12233 test chart and enlarged wedge pattern (source: own editing)

The wedge pattern in the middle-top section of the test chart provides guidance for assessing horizontal resolution. The point where the increasingly frequent black and white lines can no longer be told apart (they merge) is called the camera's resolution limit. The corresponding line pair/millimetre (lp/mm) value can be read from the scale. To avoid any imprecisions of the reading, I have determined the resolution by using the Olympus HYRes 3.1 software.

When selecting cameras with differing resolutions, I aimed to choose from more or less the same (premium) category by leading manufacturers. The types I have examined according to resolution are: 2 MP (Full HD), 3 MP, 5 MP (3K) and 8 MP (4K). Manufacturers of the cameras tested are: Axis, Bosch, Hikvision and Samsung[6].

It is important to note that resolution was greatly influenced by the resolution limit of the lenses. Therefore, when selecting test camera lens, I took into consideration the manufacturers' recommendations, and I used the same 3 MP lens for both the 2 MP and 3 MP cameras.

The purpose of the testing was to determine how the richness in detail is influenced by various illumination values in cameras with varying resolutions.

Image 6 shows the results at an average lighting environment of 200 lx. At this lighting, the image quality corresponds with the resolution of the cameras.

Reducing the environmental illumination to 5 lux resulted in a drastic deterioration of resolution in 8 MP and 5 MP cameras. The reduction is 43% and 41%, respectively. The deterioration in resolution for equipment with a lower number of pixels is only 13% and 20% (Figure 7).

[6] Since this test does not aim at ranking the cameras, these measurement values intentionally do not include the type and manufacturer; the list is in alphabetical order, and does not in any way correspond to the rank of the test images.

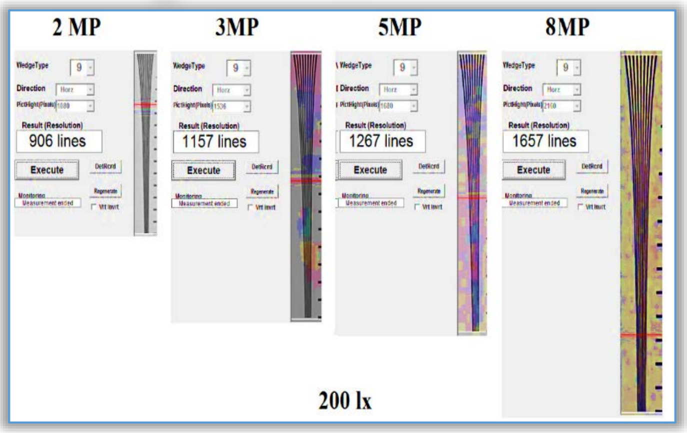

Figure 8: Resolution comparison at 200 lx environmental illumination (source: own editing)

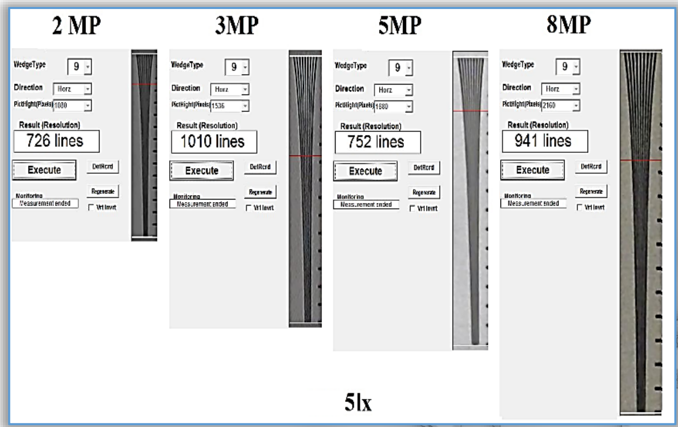

Figure 9: Resolution comparison at 5 lx environmental illumination (source: own editing)

Further reducing illumination resulted in further deterioration in resolution. 5 MP and 8 MP cameras both suffered a 54% reduction in resolution. The same value for the 3 MP equipment was only 18%. The resolution of the 5 MP camera at this level of lighting nearly equalled that of the Full HD equipment, while the 4K camera with the highest resolution produced a result lower than the 3 MP camera.

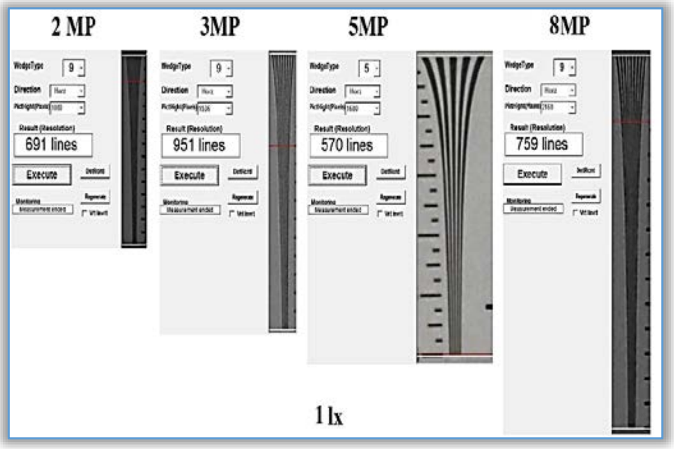

Figure 10: Resolution comparison at 1 lx environmental illumination (source: own editing)

The above measurements were conducted indoors with an artificial (2,700 K colour temperature) light source. However, to assess the influence of the diffraction barrier, I needed an environmental illumination of several thousands of lux, therefore further testing took place outdoors on a sunny late spring morning (on 20 May) at 11 a.m. The results in case of the 4K camera have verified my expectations: the equipment's resolution deteriorated by 41%, and the measured value was close to the resolution of a Full HD camera. Diffraction did not cause a decrease in resolution for the 5 MP, 3 MP and 2 MP cameras (Figure 11). For the latter two cameras this is acceptable, but the case of the 5 MP camera requires some explanation. The aperture for the lens used in this machine varied between F1.8 and F8. At an aperture of F8, no considerable diffraction effect can be measured in this 1/1.8" image receiver.

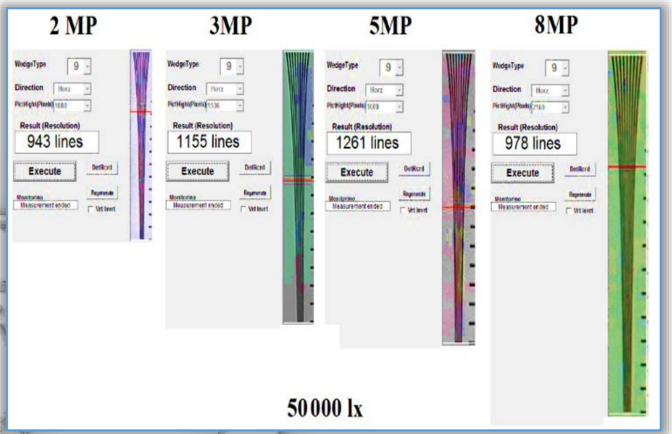

Figure 11: Resolution comparison at 50.000 lx environmental illumination (source: own editing)

CONCLUSIONS

Due to the development of manufacturing technologies, the size of CCD and CMOS image sensors have been decreasing in video surveillance cameras. Concurrently, there is a race of sorts between the manufacturers the produce cameras with ever-increasing resolution, and as statistic show, sales have moved in this direction as well. The consequence of the decrease in format and increase in resolution is that pixel element size is shrinking. This results in unwanted outcomes that counteract against producing images that are rich in detail and have a large resolution. The resolution of cameras with 4K or more pixels shrunk to a format of 1/1.7" will have both bottom and top limits regarding lighting environment. In poor illumination the signal-noise ratio deteriorates, and with it the resolution. The efficiency of compression for a noisy image is worse, thereby the image requires a larger bandwidth at transmission and more space for storage. In case of outdoors application, when in summer the illumination can reach up to100.000 lx, the diffraction caused by the contracting compartment of the automatic iris lens will result in poorer resolution. In the two extremes, the deterioration in quality can be so bad that even a good Full HD camera could produce an image that has less noisy and more details.

The above analysis does not mean that 4K cameras with such a small format are useless. At stable and sufficient illumination (ranging from a few hundred to a few thousand lux), it is recommended to trust the camera's auto shutter function to deal with brightness control, and use a manual aperture lens instead. The aperture should be at its maximum, although this may result in a decrease of depth of field. Under more extreme environmental lighting, the camera's auto shutter function will not be able to handle the huge light range. In this case, we should choose a lens where the aperture will not exceed F8, and use a supplementary light source in dusk. If worse comes to worst, we may also consider using several smaller resolution cameras.

Bibliography

[1.] Honovich, J. IPVM, http://ipvm.com/reports/resolution-stats-2016, downloaded: 2016.10.31.
[2.] Wolf, E. és Born, M.: Priciples of Optics, Cambridge, Cambridge University Press, 1999.
[3.] Sanjay M. W. és Dilip A. D.: Essentials of Physics, Delhi, PHI Learning Private Limited, 2013.
[4.] Raghuvanshi, G.: Engineering Physics, New-Delhi, PHI Learning Private Limmited, 2010.
[5.] Suzuki, T.: Challenges of image-sensor development, San Francisco, IEEE, 2010.
[6.] Canon, Compact Digital Cameras, http://www.canon-europe.com/for_home/product_finder/cameras/digital_camera/powershot/powershot_g1x_mark_ii/ -specification, 2016
[7.] Sony, New Product Information, http://www.sony.net/Products/SC-HP/new_pro/september_2013/imx185lqj_e.html, 2016
[8.] Sony, New Product Information, http://www.sony.net/Products/SC-HP/new_pro/february_2014/imx226_e.html, 2016
[9.] Janesick, J. R.: Scientific Charge-coupled Devices, Bellingham, SPIE, 2001.

ISSN:2067-3809

ACTA TECHNICA CORVINIENSIS
– Bulletin of Engineering
Tome X [2017]
Fascicule 2 [April – June]
ISSN: 2067 – 3809

[1.]Zoran PANDILOV, [2.] Aleksandar NAUMOV

BENEFITS OF APPLICATION OF CAD/CAM SYSTEMS IN METAL PROCESSING COMPANIES

[1.]Institute of Production Engineering and Management, Faculty of Mechanical Engineering, SS. Cyril and Methodius University Skopje, MACEDONIA,
[2.]Brako Veles, Rashtanski pat b.b., Veles, MACEDONIA

Abstract: The main goal of the research presented in this paper is to show the benefits that companies from the metal processing industry gain from the implementation of CAD/CAM technology in all segments of the product life cycle, from design to production of final product. Analyzing the production processes in metal processing companies and the global market requirements, in order to stay competitive on the market, the implementation and using of the flexible automation and CAD/CAM technology in the companies in all steps of the product life cycle is necessary. The crucial benefits of using the CAD/CAM technology in the metal processing companies are increased productivity of the engineers-designers, increased production productivity, high and repeatable quality and high production flexibility.
Keywords: CAD/CAM technology, Computer Aided Design (CAD), Computer Aided Manufacturing (CAM), metal processing industry, product life cycle, selecting of CAD/CAM systems

INTRODUCTION

The companies of the metal processing industry today are facing with very big challenges, as a result of the tremendous competition on global level. High quality, low price and short delivery times are the elements that the company should realize in order to stay competitive on the market. In one word, the companies have to orientate into the borders of so-called "Iron triangle", presented on Figure 1 [1].

Figure 1. "Iron triangle" [1]

On other side, the dynamic of product changes and improvements desired by the market, needs high flexibility of the company in all steps in the product life cycle, from design to production of final product.

High product quality and high productivity, the companies can achieve with application of automation in the production process. In order to enable desired changes, flexibility in the designing and production process, the implementation and using of the flexible automation and CAD/CAM technology in all steps of the product life cycle is necessary.

In practice, the CAD/CAM technology is used for creating technical drawings, making drafts, geometric modeling of parts and assemblies that actually present digital representation of the designed products, geometric model analysis, creating technical documentation, programming CNC (Computer Numerical Controlled) production equipment, production process, quality control, packaging, etc.

Implementation of CAD/CAM technology in metal processing companies includes choosing of the right combination of CAD/CAM system (software, hardware and production equipment), purchasing the system and staff education. Which type of CAD and CAM tools will be used, depends of the product type, prescribed production technology, desired quantities, desired quality level and quality repetition requirements and desired design and production flexibility. The benefits that the metal processing companies gain from the implementation of CAD/CAM technology in the design and production processes, as well as, the approaches in choosing the right CAD/CAM system, are presented in this paper. The presented results are based on practical experience from the metal processing companies.

POSITION OF THE CAD/CAM TECHNO-LOGY IN THE PRODUCT LIFE CYCLE

The Figure 2 [2], [7] presents the position of the CAD/CAM technology in the typical life cycle of one product from the metal processing industry. The typical product life cycle contains two main processes:

» The design process
» The manufacturing process

In general, the typical life cycle starts with idea for development of a new or redesigned existing product, mainly as result of market research (for new products) or market feedback (for existing product). All necessary information about the product (design and functionality requirements, quality level, desired production quantity, very often the price level, etc.) are collected and analyzed in order to define the final concept of the product that will pass through all steps in the designing and manufacturing process.

CAD (Computer Aided Design) is part of the designing process, which is based on creating geometric model of the product that presents a digital representation of the designed product. In this process, except the visualization of the product, the CAD tools are used for additional activities with the geometric model, like different types of strength analyzes, simulation of the product functionality and at the end, as output from the designing process, preparation of technical documentation and generating necessary files as DXF, STEP, IGES or other files, that could be used in the process of manufacturing, if is necessary.

CAM (Computer Aided Manufacturing) is a part of the manufacturing process. Input in this process are the technical documentation, the geometric model and the created files in the design process. The largest influence of the CAM technology in the production process is in preparation of the production (mainly in the process of CNC based equipment programming) and in the direct process of production, where CNC based production equipment is used.

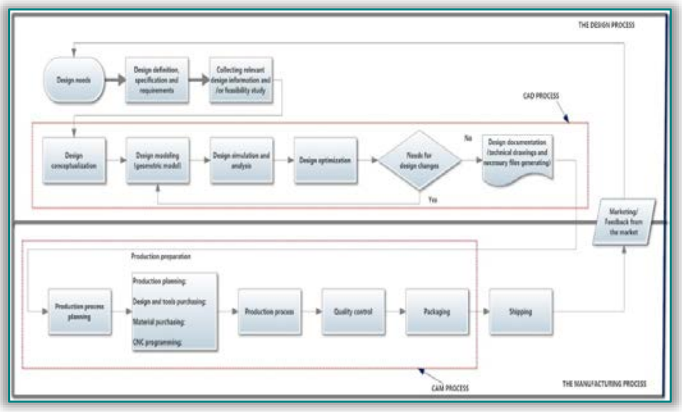

Figure 1. Typical product life cycle [2]

(COMPUTER-AIDED DESIGN) AND BENEFITS FROM IT`S IMPLEMENTATION

CAD (Computer Aided Design) can be defined as a product design by application of hardware (computer) and graphical software, that supports and improve the designing process in all its stages, from conceptualization to final documentation [9], [13]. The base of CAD is creating visual and digital interpretation of the product, represented by geometric model [4].

Today many different companies are present on the world market, that offer CAD applications, which includes different modules for designing and analyzing of the models, manipulation with the models and generating the necessary documentation [11]. From the wide range of applications on the market, the most used in the metal processing industry are CATIA and SolidWorks from Dassault System Company, AutoCad and Inventor from Autodesk, NX Unigraphis and SolidEdge from Siemens, etc.

All this applications include wide range of modules for different activities with the geometric model of the designed product, as modules for strength analysis, motion simulation, thermal and fluid flow simulation and analysis, etc. [9].

Nowadays, it is impossible company from the metal processing industry to be competitive on the market, without using CAD application in the design process. We can mention the general benefits that the companies gain with implementation of CAD system, compared with non using of CAD system. The major benefits are mentioned bellow [13]:

» Increased productivity of the engineers-designers;
» Increased quality of the product design;
» Unification of the design standards;
» Data base creation;
» Determination of the product quality and functionality early in the construction stage;
» Decreasing or completely elimination of the prototyping needs;
» Uniquely designation of the parts names;
» Elimination of the irregularities that can be issued by manual making of the drawings;
» Fast and simple way for model corrections;
» The engineers-designers become free from routine activities. That enables them to be more concentrated on creative activities;
» Design process starts directly with 3D (three dimensional) modeling;
» Easy file exchanges (communication) between different CAD applications using standard files – translators as IGES, STEP, ACIS, DXF, etc.;
» Geometric model can be used for different analysis and CNC programming directly.

For the purposes of this paper, in order to present the influence of using CAD application in the design process on the designer's productivity, two different approaches in designing with CAD application, are compared for the same product. Namely, the design process for one product group from the metal processing industry, fork extensions for fork lift (Figure 3), that contains 200 different dimensions (variants), cross sections and lengths from the same design, is analyzed. All dimensions that define the cross sections and the lengths of the variants, are closely connected with the dimensions of the parent fork on which the product is mounted, with exactly defined equations according ISO 13284-2003.

Figure 2. Fork extensions for fork lift – 3D model

For this purpose, the designing process is done by using SolidWorks software, as CAD application. The both analyzed approaches in the design process, are:

» Designing each variant separately;
» Designing, using parameter modeling with design tables.

In the first approach, all variants (cross sections and lengths) are designed separately with changing of each dimension that defines the product for each variant.

In the second approach, design table is created, in which all relations between the products dimensions and parent fork dimensions are defined, and each variant is designed only with changing of the parent fork dimensions. The only activity that designer should do is to fill the measures for the parent fork (Figure 4). The dimensions of the fork extension are calculated automatic using the defined equations, and all dimensions are applied on the 3D model.

For the both approaches, the times necessary for design process are measured and estimated per unit of variant. The results are presented in Table 1.

Analysing the results in the table, we can see that the first approach doesn't include any lead time for preparation of the designing of variants, which make it much more productive approach in designing of few variants. But designing of bigger number of variants, according the results in the Table 1, takes much less time using design tables, because the time estimated per unit of variant is few times less than the first approach.

Namely, the productivity of the designers using the second approach is 32/8.9=3.56 times bigger.

Saving time of 32-8.9=23.1 minutes per variant, for 200 variants is 77 hours in total, which equals to two work weeks of the designers.

Finally, we can summarize that different approaches in designing process, using different tools available in the CAD applications, can increase the designer's productivity several times.

Table 1. Measured times of the both approaches for designing product from (Figure 3), [10]

Design steps	Design each variant separately: Time per variant (min)	Design using design table: Total time (min)	Design using design table: Time (min) / variant for 200 variants
Creating 3D model	20		
Creating 2D drawing	10		
Creating DXF files	2		2
Creating 3D model and design table		360	1,8
Initial creating 2D drawing		20	0,1
Creating 3D model using design table for each variant			3
Creating 2D drawing using design table for each variant			2
Total time per variant (min)	32		8,9

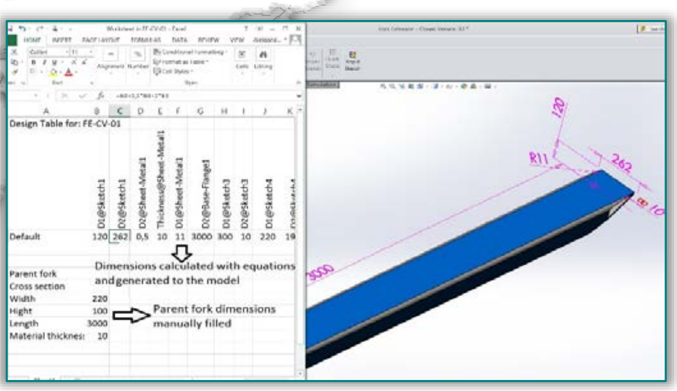

Figure 3. Modeling with design table

CAM (computer-aided manufacturing) and benefits from it`s implementation

CAM (Computer Aided Manufacturing) can be defined as application of computer technology in the process of production, using Computer Numerical Controlled machines (CNC machines) and software applications, nearly in all steps in the production process [9].

Implementation of CAM technology in the production process is one of the key factors for the companies from the metal processing industry to stay competitive on the market [4].

Today, almost all technological process that are part of the metal processing industry, are covered by CAM and CNC technology. Milling, cutting, bending, drilling, turning, painting, etc., as basic technological processes in metal processing industry are completely covered with flexible automation, with using CNC machines and adequate software applications (CAM tools) for programming of the machines.

Of course, the conventional approach in above mentioned technological processes using conventional production equipment is still present in metal processing industry. CAM supported and the conventional technological process have their own advantages and disadvantages. The general comparison, between CAM supported and conventional approach in metal processing technological processes are presented in Table 2.

The general benefits that the companies gain from the implementation of CAM technology in the production process, are:

» High productivity;
» High flexibility in the production process;
» High quality and repeatability of the quality;
» Less influence of the operators on the product quality;
» Elimination of technological errors during the programming of the equipment;
» Less scrap (For the cutting technology)

Table 2. CAM supported vs conventional technological processes

Criteria	CAM	Conventional
Flexibility	+	+
Productivity	+	-
Desired operator knowledge for the technological process	+	-
Influence of the operator on the product quality	+	-
Product quality	+	-
Quality repetition	+	-
Programming engineer engagement	-	+
Costs per hour	-	+
Maintenance costs	-	+
Production preparation time	-	+
Scrap (for cutting machines)	+	-

For purposes of this paper, in order to present the influence of the implementation of CAM technology on the productivity of production process in metal processing industry, two major technological process are analysed, milling and welding. For the both approaches, preparation and production times, for milling same part using CAM technology and conventional milling technology and welding of same product using robot welding station and manual welding, are measured. The results are estimated per unit of product and analysed.

A. Milling process

Milling process is analysed for metal part, shown on (Figure 5). Material of 407cm^3 is removed from the processed part with simple milling in lines, using the same milling tools on CNC milling centre and conventional milling machine and using optimal available milling parameters (number of revolutions, feeds and cutting depts.) on the both machines. CNC milling is done on CNC vertical milling centre with FANUC 0i-M controller. Programming is done using CamWorks software application.

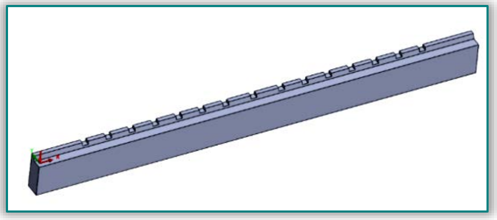

Figure 4. Milled metal part – 3D model

The conventional milling is done using conventional vertical milling machine.

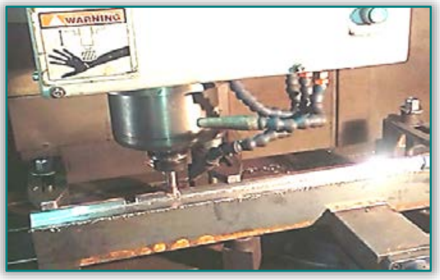

Figure 5. Milling process on CNC milling center

The time for production preparation and production time are measured and estimated per piece for the both approaches and they are presented in Table 3.

The time for production preparation and production time are measured and estimated per piece for the both approaches and they are presented in Table 3.

Analysing the measured times, we can see that time for production preparation of the CNC milling centre is longer than preparation of the conventional milling machine, but the production time is smaller. For the current case, CNC milling as approach is 1.56 times or 56% more productive approach than the milling on conventional machine.

Increasing of the product quantity, decreases the preparation time per piece, and even for 10 pieces, the CNC technology is almost 3 times more productive approach. Additional increasing of the quantity (up to 100 or 1000 pieces), decrease the preparation time to minimal amount. The influence on the total production time, comparing with the direct production (milling) time, is minor and each quantity increasing, gives smaller and smaller rise of productivity. For example, for 10 pieces, the CNC technology is 2.9 times more productive than conventional milling, and for 1000 pieces, it is 3.27 times more productive, or for increasing the quantity 100 times, the productivity is increased only 12.7%.

Of course, these numbers represent only the current case. This analysis gives results that are different from case to case, but they present real and clear picture, how the implementation of CAM technology in metal processing industry influence on the productivity of the milling technology.

Table 3. Measured processes time for milling part form (Figure 5) using CNC milling centre and conventional milling machine [10]

	Approach	For 1 piece Preparation time (min)	For 1 piece Production time (min)	For 1 piece Total (min)	For 10 pieces Preparation time (min)	For 10 pieces Total (min)
1	Milling on conventional milling machine	70	360	430	7	367
2	Milling on CNC milling center	165	110	275	16,5	126,5
3	Productivity of CNC milling VS conventional milling			1,56		2,90

	Approach	For 100 pieces Preparation time (min)	For 100 pieces Total (min)	For 1000 pieces Preparation time (min)	For 1000 pieces Total (min)
1	Milling on conventional milling machine	0,7	361	0,07	360
2	Milling on CNC milling center	1,65	112	0,165	110
3	Productivity of CNC milling VS conventional milling		3,23		3,27

On Figure 7 is presented diagram of the measured times for the milling process that refers to Table 3.

Analysing the measured times, we can see that time for production preparation of the CNC milling centre is longer than preparation of the conventional milling machine, but the production time is smaller. For the current case, CNC milling as approach is 1.56 times or 56% more productive approach than the milling on conventional machine.

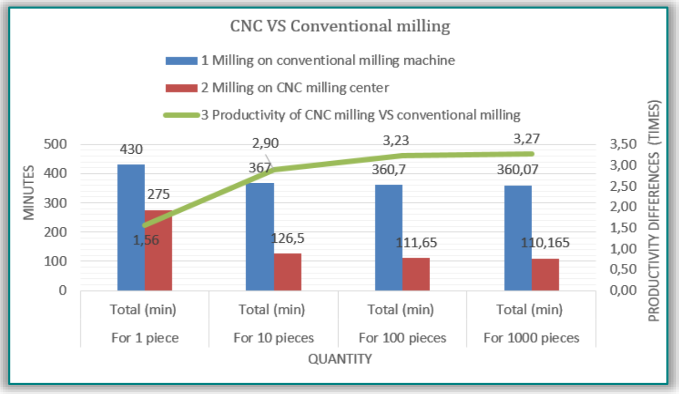

Figure 6. Diagram presentation of Table 3

Increasing of the product quantity, decreases the preparation time per piece, and even for 10 pieces, the CNC technology is almost 3 times more productive approach. Additional increasing of the quantity (up to 100 or 1000 pieces), decrease the preparation time to minimal amount. The influence on the total production time, comparing with the direct production (milling) time, is minor and each quantity increasing, gives smaller and smaller rise of productivity. For example, for 10 pieces, the CNC technology is 2.9 times more productive than conventional milling, and for 1000 pieces, it is 3.27 times more productive, or for increasing the quantity 100 times, the productivity is increased only 12.7%.

Of course, these numbers represent only the current case. This analysis gives results that are different from case to case, but they present real and clear picture, how the implementation of CAM technology in metal processing industry influence on the productivity of the milling technology.

B. Welding process

Welding process is analysed for metal assembly, shown on (Figure 8)

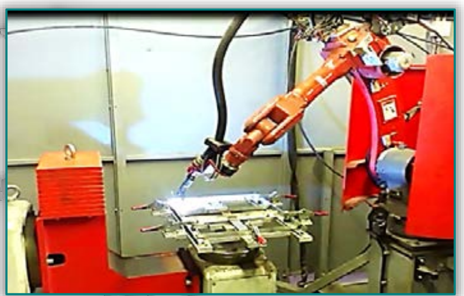

Figure 7. Welding on robot welding station

The welded part has 860mm weld length in total, and the same welding parameters (current, voltage and welding speed) are used for the manual welding and the welding using the robot welding station. For this purpose, PANASONIC robot welding station is used. For programming the robot welding station on-line method “Point to point” is used [7]. The time for welding preparation and welding process time is measured and estimated per piece for the both approaches. They are presented in Table 4.

On Figure 9 is presented diagram of the measured times for the welding process that refers to Table 4.

Analyzing the measured times from Table 4, we can see that the welding time on the welding station is less than the time necessary for manual welding, but the time necessary for programming of the robot welding station is significantly longer, that makes using of robot welding station for one piece, less productive and wrong choice. Even for 10 pieces, the total time for welding of robot welding station, estimated per piece, is longer than manual welding. According the diagram (Figure 9), the total time for robot welding approach will be on same level with the manual welding on quantity of around 50-60 pieces.

Table 4. Measured welding time for assembly from (Fig.8) using robot welding station and manual welding [10]

	Approach	For 1 piece			For 10 pieces	
		Preparation time (min)	Welding time (min)	Total (min)	Preparation time (min)	Total (min)
1	Manual welding	0	11,3	11,3	0	11,3
2	Robot welding	420	3,6	423,6	42	45,6
3	Productivity of robot welding vs manual welding (times)			0,03		0,25

	Approach	For 100 pieces		For 1000 pieces	
		Preparation time (min)	Total (min)	Preparation time (min)	Total (min)
1	Manual welding	0	11,3	0	11,3
2	Robot welding	4,2	7,8	0,42	4,02
3	Productivity of robot welding vs manual welding (times)		1,45		2,81

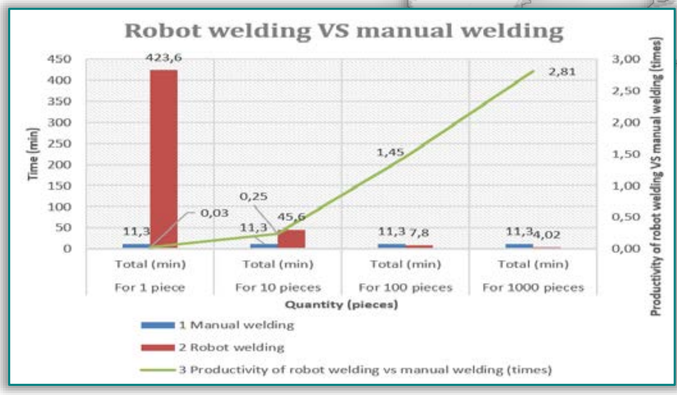

Figure 8. Diagram presentation of Table 4

Keeping in mind the fact that robot welding technology is much more expensive than manual welding, using of robot welding station could be right approach on quantity of more than 100 pieces, where the productivity of the robot welding station is 45% higher than the manual welding.

The additional quantity increasing of up to 1000 pieces, results with 2.8 times higher productivity of the robot welding station, compared with the manual welding.

According the results, we can summarize that if the preparation time for the robot welding process is longer (if the assembly on which is performed welding is more complex, the programming time is longer), the quantity that make this approach more productive is bigger.

Of course, these numbers represent only the current case, and this analysis gives different results from case to case. But nevertheless they present real and clear picture how the implementation of the flexible automation in metal processing industry influence on the productivity of the welding technology.

C. Influence of the CAM technology in material saving (Scrap decreasing)

In general, as a start of direct process of production in metal processing industries, the first action on the raw material is preparation of parts, using different technological processes for plates cutting (plasma cutting, laser cutting, gas or water jet cutting), tubes, bars and profile cutting (conventional or CNC controlled sawing), etc.

This step in the production process is directly connected with the material utilization and influence on the scrap quantity, especially for plates cutting. Using conventional cutting equipment, that is limited to cutting of straight line contours, enable big influence of the operator's skills on the material utilization. Namely, the plan for nesting of the desired parts on the raw material (the plate) is done by the operator, which in case of wide range of different part dimensions, is not always able to make the right nesting of the part, that leads to smaller material utilization (bigger quantity of scrap).

Implementation of CAM technology, mainly in the process of cutting complex contour shapes, supported with the market available nesting software applications, has improved the utilization of the row material, on the way that computer technology and software applications are used for complex calculations that make the nesting of the parts on the plates. The nesting applications have opportunities to generate NC code that is used for the CNC cutting machine as well. So the combination of the software application and CNC machine, forms the CAM system, which improves the productivity and quality of the cutting technology and the material utilization.

For purposes of this paper, in order to present the influence of the CAM technology on the raw material utilization, the case of conventional cutting using conventional shearing machine and the case of using CNC controlled plasma cutting machine for the same part specification, are analysed.

In the first case, the material nesting is done by the operator, and in the second case, it is used the nesting software ProNest (Figure10). For the second case, it is also analysed the material utilization, using different optimization levels in order to present the influence of the optimization level on the material utilization [10]. In all cases standard dimension of the raw material is used, mild steel plate 6mm thickness, 1500x6000mm plate dimensions, quality S355J2.

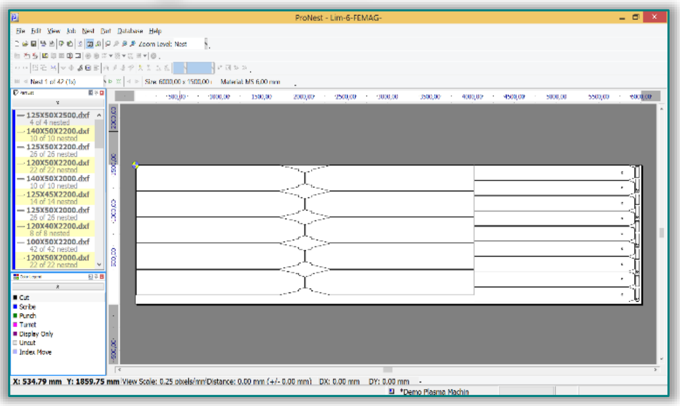

Figure 9. Nesting with ProNest application

The highest level of optimization requires larger computer capacities, which influences of the time necessary for nesting procedure, but results with higher material utilizations, Lower optimization level, requires lower computer capacities, takes less nesting time, but results with lower utilization. Which optimization level will be used, depends of the utilization criteria, the programmer`s experience and available computer capacities. On (Figure 11) is presented the material utilization using ProNest application, with higher optimization level and on (Figure12) is presented the material utilization using ProNest application, with lower optimization level. [10]

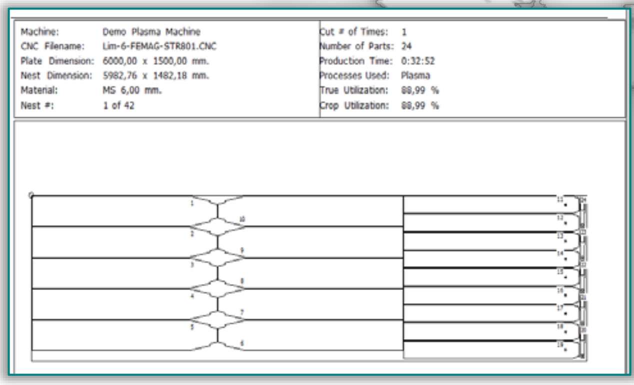

Figure 10. Material utilization with higher level optimization

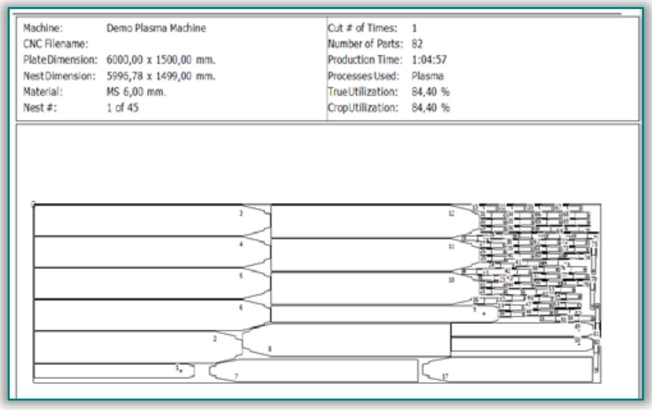

Figure 11. Material utilization with lower level optimization

The measured average utilization done by the operator for the same part specification is approximately 77%. The results are presented in Table 5.

Table 5. Material utilization for different nesting approaches

Nesting approach	Utilization
Utilization by operator	77%
Nesting with ProNest lower optimization level	84,4%
Nesting with ProNest higher optimization level	88,9%

According the results from Table 5, application of CAM tools can increase the utilization of the material from 7% to 10%, depends of the nested parts shapes and dimensions. Using different optimization levels, results with few percentage better material utilization.

We should mention, that manual cutting on conventional sawing machine, needs additional rework on the parts, which results with additional costs.

For illustration, one mid-size metal processing company that process annual quantity of 500 to 1000 tons raw material, with 10% material saves (50 to 100 tons saves), depends of the current material prices, the investment for CAM system in the process of cutting plates, can be returned in few years.

We can summarize that implementation of CAM technology in the process of material cutting, can save around 10% of the raw material, increases the productivity few times and enables cutting of complex contour shapes.

SELECTION OF CAD/CAM SYSTEM

Nowadays, on the market exist wide range of CAD/CAM systems and CNC production equipment that can be implemented almost in each technological process from the metal processing industry.

The companies from the metal processing industry sometimes have a doubt to choose CAD/CAM technology or to choose conventional approach in their processes, mainly in the production process because, as it is already mentioned, today the designing process is almost impossible without application of CAD system in the company.

D. Criteria for selecting CAD/CAM system

Which CAD/CAM system will be chosen by the company, depends on many factors, but in general, the company prescribes some criteria that the system has to fulfil in order to be adopted as best choice for the current needs of the company. There are many criteria, but in general can be classified in two bigger groups [3]:

» Exploitation criteria
» Economical-strategic criteria

The exploitation criteria, refers to the characteristic of the CAD/CAM system, which are directly connected with its usage in the practice. Some more important exploitation criteria are given below:

» Easy for use and learning;
» Compatibility with the existing company equipment;
» Effectiveness and efficiency;
» Available support, service and training;
» Upgrade possibilities;

- Available literature, manuals and handbooks.

As economical-strategic criteria we can mention the following:

- Company needs and strategies;
- Price;
- Total investment costs.

The priority level for each of above mentioned criteria, is defined by the company and it is part of its strategy. The most important during decision making is the right analysis of the company needs and adequate defining of the criteria priority. In practice, the process of analysis and making decision is time consuming, depends from case to case, and can lasts from few months to one year or more.

E. Productivity and cost effective analysis

Keeping in mind all advantages of the CAD/CAM systems and CNC technology, the decision, CAD/CAM or conventional approach in the production process, mainly depends on the volume of the production series. To determine which approach is better choice, it is necessary to analyse the both approaches from the aspect of productivity and cost effectiveness.

In general, CAM and CNC technology is much more productive, compared with the conventional technology, but the preparation for the production process takes much more time. Therefore, the production time and the preparation time estimated per piece have to be considered in order to make decision, which should be more productive. The total production time for the both approaches has to be compared, so the following equation can be used:

$$\frac{T_{pzc}}{n} + T_{prc} < \frac{T_{pzk}}{n} + T_{prk} \qquad (1)$$

where T_{pzc} is preparation time for the CAM based technological process, T_{prc} is production time of the CAM based technological process, T_{pzk} is preparation time for the conventional technological process, T_{prk} is production time of the conventional technological process and n is number of pieces form the production series. Hence, the minimal quantity of pieces in the production series that makes application of CAM systems and CNC technology more productive than the conventional approach, can be calculated as:

$$n_{min} > \frac{T_{pzc} - T_{pzk}}{T_{prk} - T_{prc}} \qquad (2)$$

But, in the decision making process, which approach is better choice, the CAD/CAM systems and CNC technology or the conventional production technology, one of the biggest disadvantages of the CAD/CAM technology, the costs for implementation and the running costs, have to be considered. Namely, the CAD/CAM systems and CNC based production equipment has higher costs per working hour, and depending on the analyzed production technology, can be even several times more expensive. Therefore, the productivity analysis is always connected with the costs analysis for the technological process. Each company has internal cost politic and calculated costs per working hour for each production equipment. The calculated costs per working hour for each production equipment include the following: costs for purchasing and implementation of the CAD/CAM system and CNC production equipment, costs for equipment amortization, labour costs, tooling costs, maintenance costs, staff education costs, etc.

Hence, considering the costs per working hour, the minimal quantity of pieces in the production series that makes application of CAM systems and CNC technology cheaper solution than the conventional approach, can be calculated as:

$$n_{min} > \frac{T_{pzc} * C_{tc} - T_{pzk} * C_{tk}}{T_{prk} * C_{tk} - T_{prc} * C_{tc}} \qquad (3)$$

where C_{tc} is the cost per working hour for the CAD/CAM system and CNC based production equipment, and C_{tk} is the cost per working hour for conventional production process.

The analysis of the productivity and the costs for both approaches in the production process, can help the company to decide – CAD/CAM system or conventional approach. Sometimes, the companies can chose CAD/CAM technology, even the costs are higher, if the productivity is decision criteria number one. At the end, the decision is part of the company strategy politic, which defines what are the priority criteria in decision making (productivity, costs, quality, etc.).

CONCLUSION

Implementation of the CAD/CAM technology in all steps of the product life cycle in the metal processing industry, from design to production, enable the companies to stay competitive and to response on the market requirements.

Analyzing the comparison between using CAD/CAM systems and conventional approach for the production technology processes, we can conclude that CAD/CAM systems have more advantages than the conventional approaches, especially in cases of higher volume of production series. Higher quality and quality repetition, higher flexibility, higher designers productivity, higher design quality, higher production productivity that can be bigger several times, saving material more than 10%, etc., are the key benefits that the companies gain from the implementation of the CAD/CAM technology and CNC based production equipment.

The analysis of the minimal volume of the production series, from aspect of productivity and economical aspects as basic criteria, helps the company to make decision which approach is more effective. Of course, the final decision needs more complex analysis, in which the companies prescribe the criteria list, and select the priority which the CAD/CAM systems have to fulfill.

References

[1] Radhakrishnan P., Subramanyan S., Raju V.: CAD/CAM/CIM, (third edition), New age International (P) Limited, Publishers, 2008
[2] Zeid I., Mastering CAD/CAM, the MGraw Hill Companies, 2004
[3] Mercer T., CAD/CAM selection for small manufacturing companies, University of Wisconsin, May 2004
[4] Rao Posinasetti N., CAD/CAM: Principles and Applications, Tata McGraw- Hill Education, 2004
[5] Groover M., CAD/CAM: Computer-Aided Design and Manufacturing, Pearson Education, 2006
[6] Lee K., Principles of CAD/CAM/CAE, Addison-Wesley, 1999
[7] Alavala R. C., CAD/CAM: Concepts and Applications, PHI Learning Pvt. Ltd., 2009
[8] Haider F., CAD/CAM and Automation, Publisher, NiraliPrakashan, 2008
[9] Elanchezhain C., Selwyn T. S., G.Shamnmuga Sundar G. S.: Computer Aided Manufacturing (2nd Edition), Laxmi Publication d (P) LTD, New Delhi, 2007
[10] Naumov A.: Application of integrated CAD/CAM systems in development and manufacturing of new products in the metal industry, Mechanical Faculty at "Ss. Cyril and Methodius" University-Skopje, Master thesis, 2014
[11] Boboulos A. M.: CAD/CAM & Rapid prototyping Application Evaluation, Ventus Publishing ApS, Ph.D. Thesis, 2010
[12] Hou M.: CAD/CAM Integration Based on Machining Features for Prismatic Parts, Faculty of the Graduate School of the University of Kansas, Ph.D. Thesis, 2008
[13] Narayan K. L., Rao K. M., M.M.M Sarcar: Computer aided design and manufacturing, prentice-Hall of India Private Limited, New Delhi, 2008
[14] S. Kant Vajpayee S. K.: Principles of Computer-integrated manufacturing, PHI Learning PVT. LTD New Delhi, 2009
[15] Sharma V.: Fundamentals of Computer-integrated manufacturing (2nd Edition), International Book House PVT Ltd., 2013
[16] Smid P.: CNC Programming Handbook, Industrial Press Inc., U.S, 2008

ISSN:2067-3809

We are very pleased to inform that our international and interdisciplinary journal **ACTA TECHNICA CORVINIENSIS ■ Bulletin of Engineering** completed its nine years of publication successfully [**issues of years 2008 – 2016, Tome I–IX**].

In a very short period it has acquired global presence and scholars from all over the world have taken it with great enthusiasm.

Every year, in four online issues (**fascicules 1 – 4**), **ACTA TECHNICA CORVINIENSIS ■ Bulletin of Engineering [e-ISSN: 2067-3809]** publishes a series of reviews covering the most exciting and developing fields of science and technology. Each issue contains papers reviewed by international researchers who are experts in their fields. The result is a journal that gives the scientists and engineers the opportunity to keep informed of all the current developments in their own, and related, areas of research, ensuring the new ideas across an increasingly the interdisciplinary field.

Now, when will celebrate the tenth years anniversary of **ACTA TECHNICA CORVINIENSIS ■ Bulletin of Engineering**, we are extremely grateful and heartily acknowledge the kind of support and encouragement from all contributors and all collaborators!

On behalf of the Editorial Board and Scientific Committees of **ACTA TECHNICA CORVINIENSIS ■ Bulletin of Engineering**, we would like to thank the many people who helped make this journal successful. We thank all authors who submitted their work to **ACTA TECHNICA CORVINIENSIS ■ Bulletin of Engineering**.

ACTA TECHNICA CORVINIENSIS
– Bulletin of Engineering
Tome X [2017]
Fascicule 2 [April – June]
ISSN: 2067 – 3809

[1.]Martin BERETA, [2.]Eva BALCOVÁ, [3.]Ladislav JANOUŠEK, [4.]Ján BARABÁŠ

LOW FREQUENCY ELECTROMAGNETIC FIELD EFFECTS ON GROWTH DYNAMICS OF YEAST CELLS

[1-3.]Department of Electromagnetic and Biomedical Engineering, Faculty of Electrical Engineering, University of Žilina, Univerzitná 1, 010 26 Žilina, SLOVAKIA
[4.]University Science Park of the University of Žilina, Univerzitná 1, 010 26 Žilina, SLOVAKIA

Abstract: The paper deals with low frequency electromagnetic field effects on growth dynamics of yeast cells Saccharomyces cerevisiae. The current state of the research of electromagnetic field interactions with biological systems is briefly introduced. Several experiments are carried out in order to investigate influence of specifically adjusted artificial low frequency electromagnetic field on Saccharomyces cerevisiae growth dynamics. The experimental apparatus, materials, conditions and evaluation methods are described in the paper. The presented results indicate the differences in growth dynamics between cells exposed to magnetic field and the unexposed ones.
Keywords: electromagnetic field, yeast cells, exposed sample, control sample

INTRODUCTION

The influence of low-frequency electromagnetic field (LF EMF) on living organisms is widely discussed issue both in scientific area and in public. The interest in this topic has increased due to the rapidly extending daily use of electronic devices and generally increasing rate of human exposure to electromagnetic radiation from various artificial sources. There are numerous experimental studies investigating electromagnetic field (EMF) effects on living cells, tissues or on human health in general. Since number of studies [1-7] showed the potential connection between LF EMF exposure and cancer or other diseases, the interest in research of EMF interaction with biological systems has grown. Numerous works focusing on experiments with living cells showed the differences in the proliferation process between cells exposed to electromagnetic field and control (non-exposed) cells [8-14]. Other works investigate the animal behavior under the exposition of EMF [15] or possibility of genotoxic effect of EMF exposure [16]. The results of these works are often non-consistent and as Buchachenko [17] stated, the biological electromagnetic effects sometimes seem to be irreproducible and contradictory.

Besides experimental investigation, many authors tried to propose physical mechanism of biological LF EMF impact. One of the first suggested physical mechanisms was ion cyclotron resonance model (ICR) firstly proposed by Liboff [18]. ICR holds that the physiological activity of some important ions can be altered when the frequency of applied time-varying magnetic field is equal to the frequency of ion motion in static magnetic field (cyclotron frequency). The same assumptions are used in the ion parametric resonance (IPR) model [19, 20], but the interpretation of ion behavior is different. Ion in IPR model is represented by a harmonic oscillator and applied combined magnetic field should affect its oscillations. Both resonance models have been criticized due to several physical imperfections [21, 22], particularly due to the problem of thermal noise. Despite the lack of satisfactory physical explanation, there remains an impressive body of experimental evidence that can be taken as an empirical basis for ICR and IPR hypotheses [8-13]. The most accepted mechanism of biological EMF effects in recent years is the radical pair mechanism [23-26]. In this mechanism, it is proposed that magnetic field could affect the reactivity of biological radicals and alter their final concentration in biological milieu. Several authors [27, 28] expect that the final concentration of radicals could be changed in the range of 2 up to 40%, when the magnetic field is applied. Since radicals have an important role in biology it could lead to significant consequences for biochemical reactions in organisms.

Although an extensive theoretical and experimental research has been carried out, the unambiguous explanation of electromagnetic field influence on living structures is still lacking. Many open questions in this research field can be answered only by great amount of repetitively obtained experimental results. Results of experiments showing LF EMF effects on growth curve of cells *Saccharomyces cerevisiae* are presented in this paper. The growth curve of yeast cells is generally composed of five basic phases [29]. When the cells are inoculated into cultivation medium, they adapt to the medium (lag phase). The lag phase is followed by the exponential phase. The cells consume fermentable sugar, *e.g.* glucose, and the biomass concentration increases exponentially. When the glucose in medium is being limited, the diauxic phase occurs and the metabolism is shifted from anaerobic to aerobic pathway. In the post-diauxic phase the cells consume ethanol and other products of fermentation. Once these energy sources are exhausted, the cells enter the stationary phase and the maximal biomass concentration is reached. The representative growth curve of cells can be seen in the Figure 1.

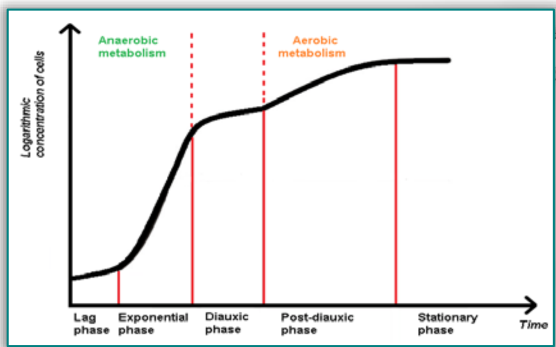

Figure 1. Representative growth curve of yeast cells (adopted from [29] and modified)

MATERIALS AND METHODS

The paper concentrates on experimental investigation of specific artificial LF EMF on growth dynamics of yeast cells. The cells are precultivated before the experiments. Two samples with the same initial concentration of cells are then used for experiments. One is exposed with artificial LF EMF of specific parameters, the other is shielded from the LF EMF. Details of experiments are described in details in this section.

A. Experimental Protocol

Yeast culture is stored in a refrigerator at 4°C. Yeasts are inoculated into glass Erlenmeyer flask (100 ml) with 10 ml of YPD medium (1% (w/v) yeast extract, 2% (w/v) peptone, 2% (w/v) D-glucose in distilled water) and cultivated for 16 hours at 25°C on an orbital shaker at 180 rpm. Cell concentration in culture medium is counting after cultivation by using counting chamber (Neubauer) and microscope (Primovert, Carl Zeiss Microscopy, LLC). The same volume of culture medium with cells is transferred into two Erlenmeyer flasks (100 ml) with 30 ml of fresh YPD in order to ensure the same initial concentration of cells in two experimental samples.

Parallel measurements of cell concentration are performed. One sample is exposed to magnetic field generated by coil (exposed sample) and one sample is shielded from the magnetic field (control sample). Concentration of cells from both samples is measured every two hours during 8 hours. The samples are cultivated at 25°C and are bubbled by air in order to ensure oxygen intake and to avoid sedimentation of cells.

B. Measurement Equipment

Measurements take place in double-chamber incubator in which Erlenmeyer flasks with cell cultures are placed. The previously designed and fabricated exposure coil is used as a source of low frequency magnetic field. The homogeneity in exposure area achieves ~90%. Schematic drawing of the measurement system can be seen in the Figure 2, and photography in the Figure 3.

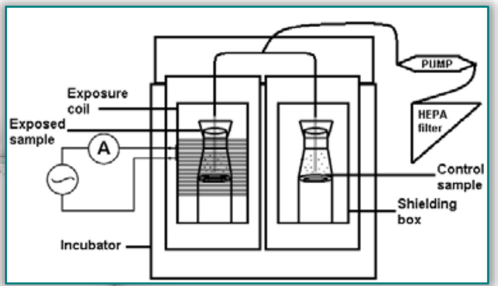

Figure 2. Measurement system schematic

Figure 3. Measurement system photo

C. Experimental Conditions

Experimental conditions are set up based on the previous results of authors [8, 30]. These conditions arose from assumptions of the ion parametric resonance model [20] and observed different growth areas of cell cultures between exposed and control samples by specific ratios of frequencies and magnetic flux density of applied magnetic field. The harmonic driving signal with frequency 1600 Hz is generated by a signal generator (Agilent E4436B, Agilent Technologies, Inc.) and amplified by a linear amplifier (Hubert A1110-05, Dr. Hubert GmbH). Magnetic flux density within the exposed volume varies spatially between 2.2 and 2.3 mT.

RESULTS AND DISCUSSION

To investigate the LF EMF influence on growth dynamics of yeast cells, the concentrations of cells are measured and growth curves are then constructed. The ratios of cell concentrations of exposed to control samples during the experiments are calculated and discussed.

Five experiments with the same exposure conditions are performed. The concentrations of both control and exposed samples of Saccharomyces cerevisiae are measured and analyzed. The growth curves presented in the Figure 4 are constructed from average values of cell concentrations, measured at selected time points (0 h, 2 h, 4 h, 6 h, 8 h) during five experiments. The error bars represent standard deviation of the measured cell concentrations. The ratios of cell concentration in exposed sample (c_{exp}) to cell concentration in control sample ($c_{control}$) can be seen in the Table 1. The bar graph in the Figure 5 shows the ratios of exposed to control cells at the end of each experiment.

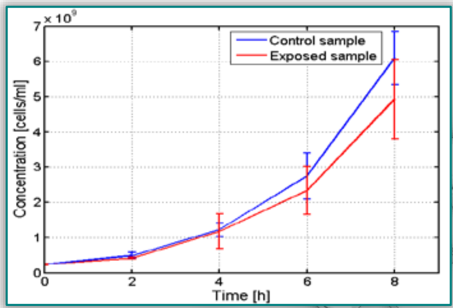

Figure 4. Growth curves of control and exposed sample

Table 1. Ratios of cell concentrations during measurements

	Ratios $c_{exp}/c_{control}$ in selected time points				
Measurement No.	0 h	2 h	4 h	6 h	8 h
1	1.0	0.83	1.66	0.93	0.75
2	1.0	0.80	0.67	0.83	0.92
3	1.0	0.73	0.85	0.62	1.01
4	1.0	0.96	0.88	0.74	0.52
5	1.0	0.94	0.77	1.18	0.87

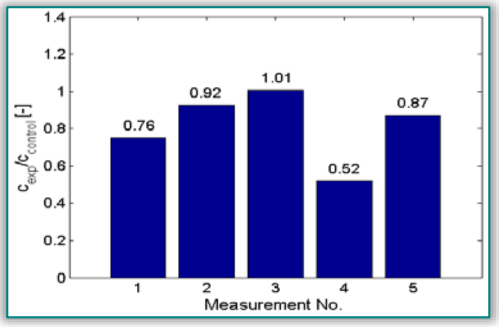

Figure 5. Ratios of cell concetrations in exposed sample to control sample at the and of each experiment

The dynamics of cell growth between exposed and control sample is slightly different. The increase of cell concentration in control sample is faster compared to the exposed sample. The final concentration of cells in exposed and control sample would very likely reach the same values, due to the identical initial conditions for cells. Since the difference of concentrations in exposed and control sample increases with time, it is probable that the control sample enters the stationary phase earlier than the exposed sample. This fact would imply slower growth dynamics of cells in exposed sample. One could then assume that the EMF in these experimental conditions has an inhibitory effect on cell proliferation processes. The ratios of concentrations of exposed to control sample presented in the Tab. 1 and Figure 5 are in most of cases lower than 1.0. It is in accordance with the previous assumption about an inhibitory effect of EMF. On the other hand it is necessary to notice very high standard deviations of measured cell concentrations (Figure 4). To eliminate this imperfection and to be able to state any satisfactory conclusion about the biological LF EMF impact, additional experiments with the same exposure conditions are needed to be performed. Furthermore it would be beneficial to evaluate several extra parameters characterizing growth dynamics of cell culture, such as absorbance, dissolved oxygen concentration, etc. Nevertheless, these preliminary results like the recent experimental studies realized at our department [8, 30] indicate the detectable interaction of electromagnetic field in low frequency range with living structures.

CONCLUSION

The presented paper dealt with low frequency electromagnetic field influence on growth dynamics of *Saccharomyces cerevisiae* cells. The preliminary results indicated, that LF EMF affect the cell proliferation processes. The obtained results implied the differences in growth dynamics of cells exposed to time-varying magnetic field (1600 Hz, ~2.3 mT) compared to control cells. The growth curves and ratios of exposed to control samples implied the inhibitory effect of EMF on cell growth. It is necessary to realize additional experiments with the same conditions and to perform proper statistical evaluation in order to state some unambiguous conclusion of the LF EMF influence on growth dynamics of cells.

Acknowledgment: This work was supported by project: ITMS: 26210120021, co-funded from EU sources and European Regional Development Fund. The work was also supported by project: University Science Park of the University of Žilina (ITMS: 26220220184) supported by the Research & Development Operational Program funded by the European Regional Development Fund.

Note: This paper is based on the paper presented at The 11th International Conference ELEKTRO 2016, organized by University of Žilina, Faculty of Electrical Engineering, in Štrbské Pleso – High Tatras, SLOVAKIA, May 16–18, 2016.

References

[1] M. Röösli, et al. "Leukaemia, brain tumours and exposure to extremely low frequency magnetic fields: cohort study of Swiss railway employees," Occup. Environ. Med., vol. 64, pp. 553-559, 2007.

[2] Z. Davanipour, E. Sobel, “Long-term exposure to magnetic fields and the risks of Alzheimer’s disease and breast cancer: Further biological research” Pathophysiology, vol. 16, pp. 149-156, 2009.
[3] L. Kheifets, et al., “A pooled analysis to extremely low-frequency magnetic fields and childhood brain tumors” Am. J. Epidemiol., vol. 172, pp. 752-761, 2010.
[4] T. Koeman, et al., “Occupational extremely low-frequency magnetic field exposure and selected cancer outcomes in a prospective Dutch cohort” Cancer Causes Control, vol. 25, pp. 203-214, 2014.
[5] L. Zhao, et al., “Magnetic fields exposure and childhood leukemia risk: A meta-analysis based on 11,699 cases and 13,194 controls,” Leukemia Research, vol. 38, pp. 269-274. 2014.
[6] M. Mattsson, M. Simkó, “Is there relation between extremely low frequency magnetic field exposure, inflammation and neurodegenerative diseases? A review of in vivo and in vitro experimental evidence,” Toxicology, vol. 301, pp. 1-12, 2012.
[7] F. I. Wolf, et al. “50-Hz extremely low frequency electromagnetic fields enhance cell proliferation and DNA damage: Possible involvement of a redox mechanism” Biochimica et Biophysica Acta, vol. 1743, pp. 120-129, 2005.
[8] J. Barabáš, R. Radil, I. Malíková, “Modification of S.cerevisiae growth dynamics using low frequency electromagnetic fields in the 1-2 kHz Range,” BioMed Research International, vol. 2015, 5 p.
[9] A.R. Liboff, “The ion cyclotron resonance hypothesis,” Bioengineering and Biophysical Aspects of Electromagnetic Fields, 3rd Ed., CRC Press, Boca Raton, Fla, USA, 2007.
[10] Y.A. Rochev, A.A. Narimanov, E.A. Sosunov, A.N. Kozlov, “Effects of weak magnetic field on the rate of cell proliferation in cell culture,” Studia Biophysica, vol. 135, pp. 93-98, 1990.
[11] A.R. Liboff, R.J. Rozek, M.L. Sherman, B.R. McLeod, S.D. Smith, “$_{45}Ca^{2+}$ resonance in human lymphocytes,” J. of Bioelectricity, vol. 6, pp. 99-102, 1987.
[12] M.G. Yost, R.P. Liburdy, “Time-varying and static magnetic fields act in combination to alter calcium signal transduction in the lymphocyte,” FEBS Letters, vol. 296, pp. 117-122, 1992.
[13] L.A. Coulton, A.T. Barker, “Magnetic fields and intracellular calcium: effects on lymphocytes exposed to conditions for cyclotron resonance,” Physics in Medicine and Biology, vol. 38, pp. 347-360, 1993.
[14] H. Ch. Lee, et al., “Effect of extremely low frequency magnetic fields on cell proliferation and gene expression,” Bioelectromagnetics, vol. 36, pp. 506-516, 2015
[15] F.S. Prato, “Non-thermal extremely low frequency magnetic field effects on opioid related behaviors: snails to humans, mechanisms to therapy,” Bioelectromagnetics, vol. 36, pp. 333-348, 2015. .
[16] M. J. Crumpton, A. R. Collins, “Are environmental electromagnetic fields genotoxic,” DNA Repair, vol. 3, pp. 1385-1387, 2004.
[17] A. Buchachenko, “Why magnetic and electromagnetic effects in biology are irreproducible and contradictory?” Bioelectromagnetics, vol. 37, pp. 1-13, 2016.
[18] A. R. Liboff, “Geomagnetic cyclotron resonance in living cells,” J. of Biological physics, vol. 13, pp. 99-102, 1985.
[19] V.V. Lednev, “Possible mechanism for the influence of weak magnetic fields on biological systems,” Bioelectromagnetics, vol. 12, pp. 71-75, 1991.
[20] N.A. Belova, V.A. Panchelyuga, “Lednev’s model: theory and experiment,” Biophysics, vol. 55, pp. 661–674. 2010.
[21] R. K. Adair, “Criticism of Lednev´s Mechanism for the influence of weak magnetic fields on biological Systems,” Bioelectromagnetics, vol. 13, pp. 231-235, 1992.
[22] R.K. Adair, “A physical analysis of the ion parametric resonance model,” Bioelectromagnetics, vol. 19, pp. 181-191, 1998.
[23] U. E. Steiner, T. Ulrich, “Magnetic field effects in chemical kinetics and related phenomena” Chemical Reviews, vol. 89, pp. 51-147, 1989.
[24] C. R. Timmel, U. Till, B. Brocklehurst, K.A. Mclauchlan, P.J.Hore, “Effects of weak magnetic fields on free radical recombination reactions,” Molecular Physics, vol. 95, pp. 71-89, 1998.
[25] J.R. Woodward, “Radical pairs in solution,” Progress in Reaction Kinetics and Mechanism, vol. 27, pp. 165 – 207, 2002.
[26] F.S. Barnes, B. Greenebaum, “The effects of weak magnetic fields on radical pairs,” Bioelectromagnetics, Vol. 36, pp. 45-54, 2015.
[27] R.J. Usselman, I. Hill, D.J. Singel, C.F. Martino, “Spin biochemistry modulates reactive oxygen species production by radio frequency magnetic fields,” PLoS ONE 9(3): e93065, 2014.
[28] M. Simkó, “Cell type specific redox status is responsible for diverse electromagnetic field effects,” Current Medicinal Chemistry, vol. 14, pp. 1141 – 1152, 2007.
[29] E. Swinnen et al, “Rim15 and the crossroads of nutrient signalling pathways in Saccharomyces cerevisiae,” Cell Division, vol. 1:3, 2006.
[30] R. Radil, J. Barabáš, “Investigation of low frequency electromagnetic field influence on cell proliferation process,” ELEKTRO 2012: proceedings, p. 456-459, IEEE 2012.

ACTA TECHNICA CORVINIENSIS
– Bulletin of Engineering
Tome X [2017]
Fascicule 2 [April – June]
ISSN: 2067 – 3809

[1.]Jovan PAVLOVIĆ, [2.]Dragoslav JANOŠEVIĆ, [3.]Vesna JOVANOVIĆ

OPTIMIZATION OF DRIVE MECHANISM OF MOBILE MACHINES MANIPULATOR USING TRIBOLOGICAL CRITERIA

[1-3.] University of Niš, Faculty of Mechanical Engineering, Niš, SERBIA

Abstract: In paper is defined the optimization tribological criteria of the manipulators crank driving mechanisms of mobile machines. Criteria indicator is mechanical efficiency of driving mechanisms, which reflects the tribological loss power of machines driving system due to friction between the elements of kinematic pairs (joints) manipulator's driving mechanisms.
Keywords: driving mechanisms, optimization

INTRODUCTION

Manipulators of mobile machines (Figure 1) represent multisegment kinematic chains with segments, in the form of lever, which are connected rotary or translational joints of the first class. The last segment in the kinematic chain of manipulators are different tools by which perform the basic functions of the machine. Drive mechanisms of manipulator built kinematic pairs of manipulators who connected with hydrostatic actuators (hydro cylinders and hydro motors).

Most common mechanisms of manipulator of mobile machines are kinematic pairs, with relatively mobile L_i (Figure 1) and fixed segment L_{i-1}, and with two-way hydrocylinder c_i which is directly linked for segments of the kinematic pairs of mechanisms. With their transfer function, the drive mechanism of manipulator, input hydrostatic parameters of forces (flow and pressure) machine drive system, are transformed into outputs parameters of mechanical power in the form of angular velocity ω_i (Figure 1) and the required driving moment M_{pi} with which the mobile segment L_i becomes executive segment of the mechanisms with rotating motion.

The total transfer function mechanism depends on transformation and transmission parameters. Transformation parameters of the mechanism are diameter of the piston and diameter of the piston rod hydro cylinder. Transmission parameters of the mechanism are: initial and final kinematic length of the hydro cylinder and position coordinates of the center of joints in which the hydro cylinder linked for segments of the kinematic pairs of mechanisms.

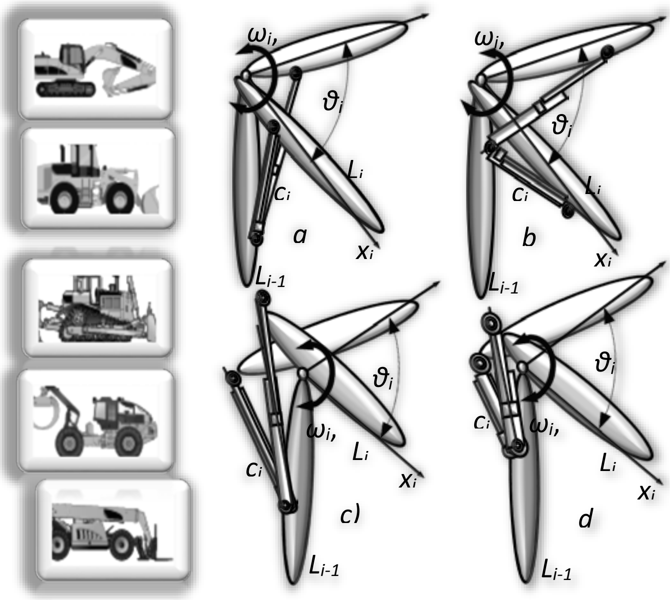

Figure 1. Possible variant solutions of the drives manipulators mobile machines

CRITERIAS OF OPTIMIZATION

The procedures synthesis the mechanisms of manipulators show that for the same given input hydrostatic parameters forces can define more variant solutions of mechanisms which have the same output parameters but different transformation and transmission parameters of their structural material.

For example, the same range angle θ_{io} (Figure 1) motion and drive moment M_{pi} executive segment of the mechanism can be achieved with the same transformation parameters (hydro cylinder same size) but different transmission parameters (Figure 1 a,b,c), where, in principle, an executive segment of the mechanism may be in the form of single arm lever (Figure 1 a,b) or the two-arm lever (Figure 1 a,b). Besides, variant solutions of mechanisms are possible with lower transformation and higher transmission parameters (Figure 1c) and vice versa, with more transformational and less transmission parameters (Figure 1d).

For selection the optimal solution driving mechanisms of mobile machines manipulators, from set of possible variant solutions, set up the basic objective function:

max . performance - min . power of machine, expressed the following criteria optimization [2][3]:

- $K_1=\max(F_m)$ - criterion of maximal functional dependence of all of the driving mechanisms manipulators, which expresses efficiency of machine functions through estimate harmonious mutual activities possible drive moments of mechanisms at negotiation the external loading of manipulator in the in the whole working area of machine,
- $K_2=\max(\eta_m)$ - tribological criteria defined on the basis of mechanical degree of usefulness drive mechanisms ηm, which reflects the tribological loss of power driving system machine because of friction between the elements of kinematic pairs (joints) of driving mechanisms manipulators,
- $K_3=\max(m_i)$ - the criteria of minimum mass mi segments of kinematic pairs driving mechanisms of manipulators expressed by general conditions factor of nominal mass, which is defined according to the criteria stress state segments of mechanisms,
- $K_4=\max(m_{ci})$ - criteria of minimum mass mci actuator (hydrocylinder) driving mechanisms of manipulators,
- $K_5=\max(m_{si})$ - criteria of minimum mass msi segments of kinematic pairs (joints) driving mechanisms of manipulators.

TRIBOLOGICAL CRITERIA

The primary function of the machine following, among others, are and tribological appearances - friction and wear between the elements of kinematic pairs - joints, of kinematic chain of machine. The consequences of tribological appearances are loss of effective power of driving mechanisms and reducing the lifetime of elements of kinematic pairs.

Generally, friction is defined as resistance to relative motion between two surfaces in contact. During the manipulation task of machine comes to explicit relative motion of elements of manipulator's kinematic pairs and under the loading. From these reasons, setting up tribological criteria of optimal determining the parameters of driving mechanisms manipulators based on the loss of energy due to frictional resistance in the joints of mechanisms. For determining tribological criteria of optimization, first are defined the general tribological factors and then is analyzed the impact of parameters of driving mechanisms on their size.

Tribological factors

According to the general tribological settings, the joints of manipulator's driving mechanisms make tribomechanical subsystems, which parameters of structure transform the function parameters in the effective parameters of driving mechanisms with the occurrence of energy loss and materials expressed by tribological parameters.

Parameters of joint function of machine's manipulator are: range δ_{ij} and relative motion velocity ω_i and loading F_{ri}, M_{ri} elements of the joint. Range and relative motion velocity elements of joints repre-sent the kinematic values determined with manipulation task. Loading elements of joint O_i (Figure 2a,b) are determines with fictive interruption of manipulator's kinematic chain in same joint, and reduction at the center of the joint of all external resistance W, M_w and internal (inertial and gravitational) loadings F_{ju}, M_{ju} separated part of the chain j>i, including force F_{ci} and moment M_{pi} of drive ci (hydro cylinder) of joint [4]:

$$\vec{F}_{ri} = \vec{F}_{ci} + \vec{W} + \sum_{j=i}^{n} \vec{F}_{ju} \quad (1)$$

$$\vec{M}_{ri} = \vec{M}_{pi} + \vec{M}_{w} + \left[\vec{r}_{w} - \vec{r}_{i}, \vec{W}\right] + \sum_{j}^{n} M_{ju} + \sum_{j=i}^{n}\left[\vec{r}_{tj} - \vec{r}_{i}, \vec{F}_{ju}\right] \quad (2)$$

Loading elements of the joint can be decomposing (Figure 2v) on the components collinear and normal to the axis e_i of the joint:

$$\vec{F}_{ri} = \vec{F}_{ni} + \vec{F}_{zi} \quad (3)$$

$$\vec{M}_{ri} = \vec{M}_{ni} \quad (4)$$

During the manipulative task drive moment of mechanism M_{pi} (Figure 2c) overcoming the moment's components of loading collinear with the axis of the joint e_i, so that, according to the equation 2, the resulting moment for axis of the joint is: $M_{zi}=0$.

Other components the joint loading F_{ni}, F_{zi}, M_{ni} strained the construction of the joint, but particular cause friction between its of elements.

For the plane configuration of manipulator's driving mechanism, according to equation 3, only the normal force F_{ni} that burdens the joint, depends among other loading and from reduced force F_{ci} of drive (hydro cylinder), apropos of parameters of driving mechanism.

On the other loadings of the joint F_{zi}, M_{ni}, parameters of driving mechanism have no effect because the reduced force of drive operates in a plane of manipulator normally on the axis of the joint. Therefore, from loading of the joint, as one of tribological criteria factors of optimization of manipulator's driving mechanisms, taking only the normal force F_{ni}. This force is besides being burdening the construction of the joint causes and friction between its relatively movable elements.

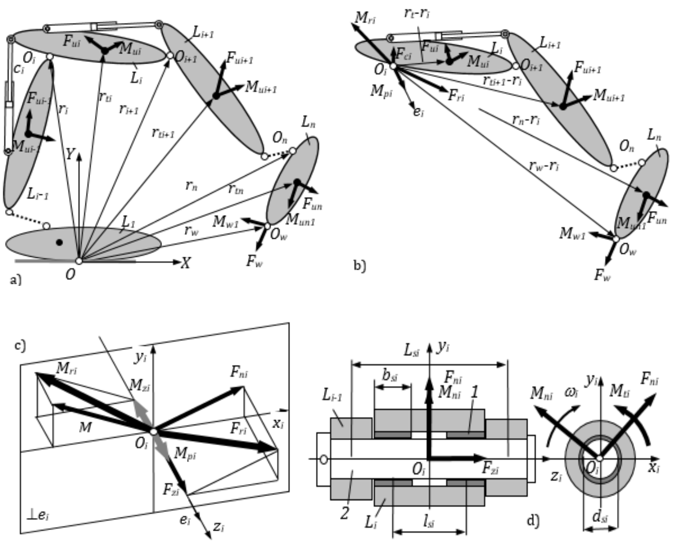

Figure 2. Tribological criteria of driving mechanisms optimization - Loading analysis of the joint kinematic pair of mechanism

ANALYSIS

How much are the impact parameters of driving mechanisms on the joints of loading show the following analysis. Observing are two comparative mechanisms, one with smaller transformational (smaller diameter piston D_1 and connecting rod d_1 of hydro cylinder c_1) (Figure 3a) and larger transmission parameter (larger connection length r_1) and second with larger transformational ($D_2>D_1, d_2>d_1$, of hydro cylinder c_2) but smaller transmission ($r_2<r_1$) parameters (Figure 3b).

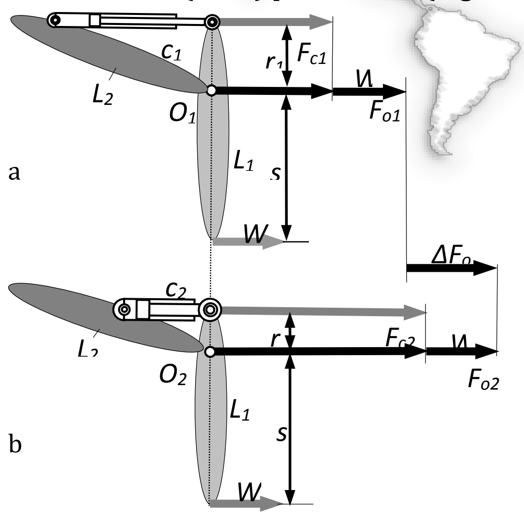

Figure 3. Comparative analysis of loading of the joint mechanism

Mechanisms have the same overall transfer function of drive moment and executive segments with the same kinematic lengths s on which ends act the same vector of external loading W. Because the simpler analysis are considered the position of mechanisms when the directions of activities forces in the hydro cylinders parallel to the directions of the resistance movement forces. With the introduced assumptions, forces in the hydro cylinders of mechanisms have value (Figure 3):

$$F_{c1} = \frac{W \cdot s}{r_1} \qquad (5)$$

$$F_{c2} = \frac{W \cdot s}{r_2} \qquad (6)$$

Forces F_{o1} and F_{o2} in the joints kinematic pairs of mechanisms are:

$$F_{o1} = F_{c1} + W = W(\frac{s}{r_1} + 1) \qquad (7)$$

$$F_{o2} = F_{c2} + W = W(\frac{s}{r_2} + 1) \qquad (8)$$

The difference of forces ΔFo in the joints exists and is:

$$\Delta F_o = F_{o2} - F_{o1} = W \cdot s(\frac{1}{r_2} - \frac{1}{r_1}) \;\forall\; r_2 < r_1 \Rightarrow \Delta F_o > 0 \qquad (9)$$

Obtained results of performed analysis shows that variant solutions of driving mechanisms with smaller transformational, and larger transmission parameters, have smaller loading of the joint elements, and vice versa.

Structure parameters of the joint define: shape, macro and micro geometry and material elements of joint, as an agency and method for lubrication of the joint. Elements of rotating joins, fifth class of manipulator's driving mechanisms, are performed in the form of one pair of sliding sleeve 1 (Figure 2g) embedded in the hub of a relatively movable segment L_i and bolt 2 linked to a relatively fixed segment L_{i-1} of kinematic pair.

Macro-geometry was determined basic dimensions of the joint: diameter of bolt (shaft) d_{si}, width of sliding sleeve b_{si}, diameter of hubs D_{si}, range of sleeve l_{si} and range of hubs L_{si}.

Micro-geometry refers to the quality of surfaces and type of overlap elements of the joint. As an indicator of parameters impact of driving mechanisms on the structural parameters of the joint is determined based on loading and mechanical characteristics the elements of joint, shaft diameter (bolt) of joint:

$$d_{si} = \max \begin{cases} (F_{nmi} / 2 \cdot e_{si} \cdot p_{sm})^{1/2} \\ (2 \cdot F_{nmi} / \pi \cdot \tau_{sm})^{1/2} \\ [8 \cdot F_{nmi}(L_{si} - l_{si}) / \pi \cdot \sigma_{sm}]^{1/3} \end{cases} \qquad (10)$$

where: F_{nmi} - maximum value of force which burdens the elements of joint, acting normal to the axis of joint, e_{si} - ratio of width sliding sleeve l_{si} and shaft diameter d_{si} of joint (Figure 2g), $p_{sm}, \tau_{sm}, \sigma_{sm}$ - allowed stresses of the surface pressure, shearing and bending the elements of joint.

Equation 10 shows that for the same materials of elements of joints, variant solutions of driving mechanisms with smaller transformational and larger transmission parameters have, due to smaller loading, smaller sizes elements of joints, and vice versa.

Tribological parameters of joint are related to friction and wear between elements of joint. The consequence of friction between elements of joint of driving mechanisms is the loss of energy during its transfer with occurrence of the thermal loading of joint. Due to wear caused the loss of materials and changes microgeometry elements of the joint.

According to the function parameters and structure of the joint, tribological parameters are:

a) Moment Mti of friction between elements of joint:

$$M_{ti} = -\text{sign}(\omega_i)\frac{d_{si}}{2}\mu_{tz}\cdot F_{ni} \qquad (11)$$

b) Power Nti lost due to frictional resistance between elements of joint:

$$N_{ti} = M_{ti}\cdot\omega_i \qquad (12)$$

where: ω_i – angular velocity of executive segment of mechanism, μ_{tz} - coefficient of friction between the sliding elements of the joint.

The last two equations show that, for the same material of elements of the joints p_{sm} and same lubrication conditions μ_{tz}, variant solutions of driving mechanisms with smaller transformational but larger transmission parameters have less power losses due to the occurrence of frictional resistance between of elements of the joints and vice versa.

CRITERIA OF OPTIMIZATION

Based on the above performed analysis sets up tribological criteria of the optimal determining parameters of machine manipulator's driving mechanisms with the aim that power loss due to frictional resistance between the mechanism's elements of joint would be minimal:

$$K_2 = \min\left(\sum_i^n N_{ti}\right) \qquad (13)$$

where: n - number of manipulator's driving mechanisms.

As a relative indicator kr2 of tribological criteria of optimization takes are mechanical efficiency η_m of driving mechanisms for the certain position of the manipulator:

$$k_{r2} = \eta_m = \prod_i^n \frac{N_i}{N_i + N_{ti}} = \prod_i^n \frac{M_{pi}}{M_{pi} + M_{ti}} \qquad (14)$$

where: N_i, M_{pi} – power, apropos driving moment, of mechanism without friction in the joints [5].

CONCLUSIONS

Defined tribological criteria shows that the syntheses of driving mechanisms crank manipulators of mobile machines should aim choosing smaller transformation and larger transmission parameters of mechanisms. Because with smaller forces of hydro cylinders and larger connection lengths - which hydro cylinder binds to segments of the mechanism, it provides less loading of joint mechanism for the same external loading. Lower loading of joints mechanisms cause less frictional resistance and wear between the elements of joints which increases the total mechanical efficiency and lifetime of the mechanism.

Acknowledgment

This paper is financially supported by the Ministry of Education and Science of Republic of Serbia, Project No. 35049. This support is gratefully acknowledged.

Note

This paper is based on the paper presented at The VIth International Conference Industrial Engineering and Environmental Protection 2016 – IIZS 2016, organized by University of Novi Sad, Technical Faculty "Mihajlo Pupin" Zrenjanin, in Zrenjanin, SERBIA, October 13–14, 2016.

References

[1.] Janošević, D., Jovanović. V., Synthesis of Drive Mechanism in Hydrulic Excavator (In Serbian: Sinteza pogonskih mehanizama hidrauličkih bagera), University of Niš, Faculty of Mechanical Engineering,Serbia, Niš, 2016.

[2.] Janošević, D., Optimal synthesis of Drive Mechanism in Hydrulic Excavator, (In Serbian: Optimalna sinteza pogonskih mehanizama hidrauličkih bagera), PhD thesis, University of Niš, Faculty of Mechanical Engineering, Serbia, Niš, 1997.

[3.] Janošević, D., Pavlović, J., Jovanović, V., Milić, P., Kinematic and Dynamic Simulation of the Wheel Loaders with the Z-bar Working Mechanism, IMK-14 – Research & Development in Heavy Machinery 20(2), pp. 39-46, 2014.

[4.] Tamminena, J., Sandstroma, C.E., Andersson, P., Influence Of Load On The Tribological Conditions In Piston Ring And Cylinder Liner Contacts In A Medium-Speed Diesel Engine", Tribology International 39(12), pp. 1643-1652, 2006.

[5.] Pavlović, J, Janošević, D., Jovanović, V., Tribological Criteria of Efficiency Evaluation in Work of Loader Manipulato, 17th Symposium on Thermal Science and Engineering of Serbia, University of Niš, Faculty of Mechanical Engineering in Niš,Serbia, ISBN 978-86-6055-076-9, October 20–23, 2015., pp.879-884.

ISSN:2067-3809

ACTA TECHNICA CORVINIENSIS
– Bulletin of Engineering
Tome X [2017]
Fascicule 2 [April – June]
ISSN: 2067 – 3809

[1.]Yung-Cheng WANG, [2.]Bean-Yin LEE, [1.]Chih-Hao HUANG, [3.]Chi-Hsiang CHEN

DEVELOPMENT OF THE AXIAL PRECISION INSPECTION SYSTEM FOR SPINDLES IN TOOL GRINDERS

[1.]National Yunlin University of Science and Technology Department of Mechanical Engineering, TAIWAN
[2.]National Formosa University Department of Mechanical and Computer-Aided Engineering, TAIWAN
[3.]TOP WORK Industry Co., Ltd and Department of Technology, TAIWAN

Abstract: Because of the rapid development of precision machinery, the demands on the dimensional precision of cutting tools have much increased. In the investigation, a rotary axis measurement system with laser diodes and Position Sensitive Device (PSD) has been proposed. The parallel deviation between the spindle axis and correlated linear axis of the machine can be measured by the developed system. With the aid of this system, error of the rotation axis during installation or operation can be reduced Measurement results of the spindle axis with Y-axis have demonstrated that horizontal angle error is 5.557 arc-seconds and the vertical angle error comes to -19.961 arc-seconds.
Keywords: tool grinder, linear axis, rotation axis, parallel error

INTRODUCTION

In comparison with other machine tools, the tool grinder is more complex and requires higher precision and reliability. The grinding of a tool grinder is performed by the wheel spindle and tool-holder axis. Details regarding the tool design and grinding method can be found in [1-3]. Hence the installation of rotation axis will determine the grinding precision and the inspection of the rotation axis is the key factor. Currently dial gauges inspection with master gauges is employed for the measurement such that error of the master gauge will affect the measurement results and the correction for machines is not ideal. That will lead to the incorrect geometrical dimensions during the grinding of tools.

Castro [4] estimated the error analysis method for the rotation axis of machine tool with aid of laser interferometer, i.e. with HP laser interferometer and a laser diode module for inspecting the rotation error of a lathe where the standard reflector sphere was hold on the rotating body and actuation error of the standard reflector sphere was measured by Laser beam combined with a convergent lens. The speed data of the spindle were acquired by Laser diode system. The results indicated that during the increment of the spindle speed the radial error the rotation axis decreased from 1.49μm to1.08μm and the axial error increased from 0.30μm to 0.87μm.

Prashanth [5] proposed that the radial error of machining with the high-speed spindle was able to be detected by Doppler axial measurements method. By the mutually perpendicular laser beam to irradiate on the sphere and infrared sensor to capture the rotation angle of the spindle, the measured data after analysis revealed that the spindle will generate axial and radial error as the speed increased.

Wen-Yuh Jywe [6] developed an optical measuring device for detecting rotary axis error by a master gauges set up in the rotation axis of machine tool and a mirror fixed on the top of master gauge. With the reflection principles of optics, the displacement and angular error of rotation axis can be measured by the laser beams and the corresponding detectors.

In this study, the laser beam has been arranged on the rotation axis and laser optical axis can be regarded as the rotary axis by the optimal adjustments of the fixture. With the integration of PSD and LabVIEW software, the parallelism inspection system for the rotary axis of the spindle can be developed and the parallelism error of the spindle axis will be improved.

FUNDAMENTAL THEORY

Errors of rotation axis

With the development of multi-axis machine tool, the error of rotation axis must be considered, because this error will affect the whole accuracy of the machine. The error inspection items of conventional rotation axis include radial error, axial error, tilt error and positioning error, according to the specification ISO230-7 case C-axis, as shown in Figure 1.

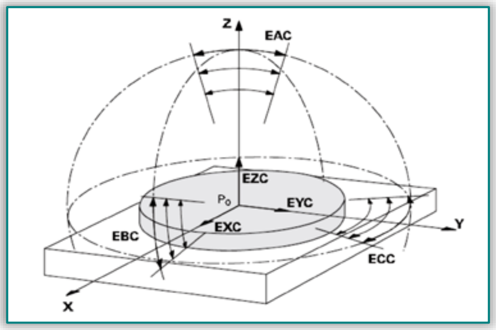

Figure 1 – Scheme of errors in C rotation axis [4]

In the experimental tool grinder, spindle has been installed on the linear axis (Y-axis). The tool grinding wheel is fixed on the spindle shown in Figure 2.

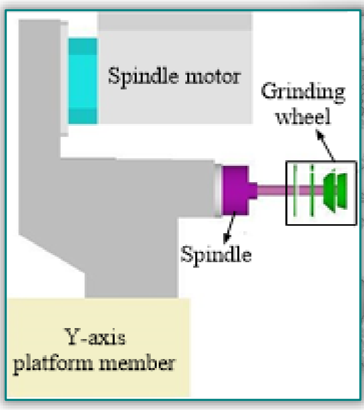

Figure 2 – Wheel installed on spindle

If there is the tilt error in the spindle, the error EAB and the ECB in the spindle and the wheel will appear. That will directly result in the grinding position deviation of the wheel such that the machining precision will be reduced, as shown in Figure 3 and Figure 4.

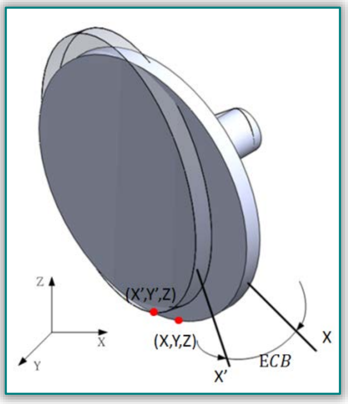

Figure 3 – ECB error

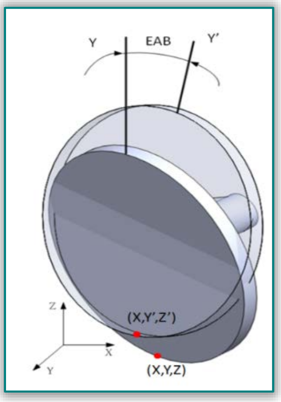

Figure 4 – EAB error

Position sensitive device

Position Sensitive Device (PSD) is based on the photoelectric effect to detect the position drift on a linear axis or a plane. It is a new type of semiconductor position sensitive detector, in addition to the photodiode array and positioning performance of the CCD, but also with the features of high sensitivity, high resolution, fast response and the uncomplicated circuit configuration. In this investigation, two-dimensional PSD has been employed to measure the displacements by detecting the position change of the laser beam installed on the rotation axis when the dynamic rotation took place.

Operational amplifier

Operational Amplifier (OPA) serves as a high-gain voltage amplifier with DC-coupled differential input and single-ended output. Generally it is used for addition and subtraction and other analog arithmetic circuit by an operational amplifier and its output will be connected to its inverted input terminal and a negative feedback configuration can be formed. In this study, the combination of an operational amplifier has been employed by an operational amplifier circuit and serves as the offset signal of the amplifying medium PSD, as shown in Figure 5.

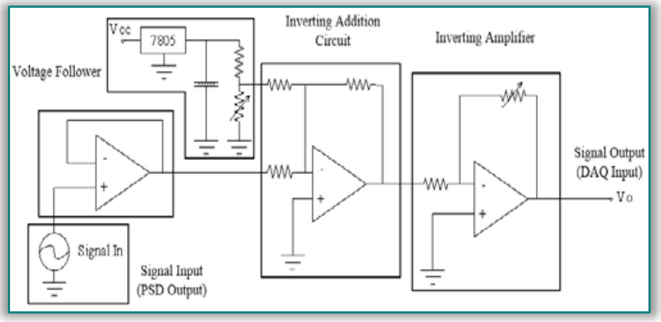

Figure 5 – Circuit of signal amplification

CONSTRUCTION OF SYSTEM

The spindle has been installed the parallel movement of the linear axis (Y-axis), as shown in Figure 2.This research is used parallelism measurement system for the spindle axis, the parallelism measurement system for the spindle axis will directly impact the geometry error of the tool. This research used the laser characteristics of the higher scheduling and collimated, and used the PSD to measurement the distance of the linear axis (Y-axis) to measure the angle error. The angle error can be summarized as shown in Figure 6.

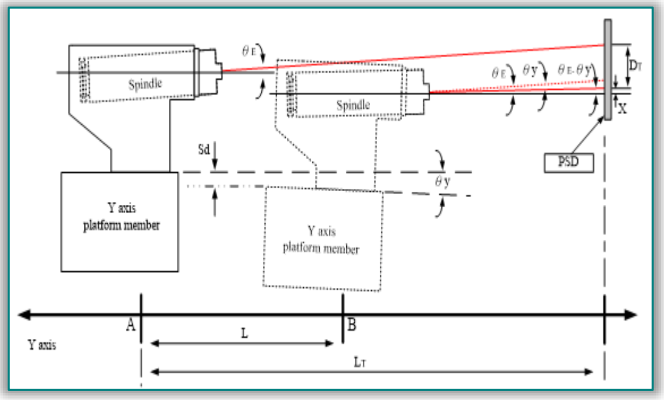

Figure 6 – Angle error analysis (The mechanical side view - vertical error)

The core of all the questions was spindle assembling precision, hence the measurement rotation axis system was used laser diode module, and PSD was installed the laser beam front end, the PSD measurement system can be explained by the parallel angle of the spindle axis and the Y-axis. Trigonometric functions of error angle can be expressed as follows:

$$\tan\theta_E = \frac{D_T+X}{L_T} \Rightarrow X = L_T \times \tan\theta_E - D_T \quad (1)$$

where θ_E is the parallel angle of the spindle axis and the Y-axis, L_T is the distance between the leaser source and the PSD, D_T is the PSD traveling distance, X is the PSD measured displacement to calculate θ_E formula.

The Y-axis platform member from point A to point B, hence the Y-axis assembling precision will directly impact the PSD measurement results. Trigonometric functions of error angle can be expressed as follows:

$$\tan(\theta_E - \theta_y) = \frac{Sd+X}{L_T - L} \Rightarrow \left(\frac{\tan\theta_E - \tan\theta_y}{1+\tan\theta_E \times \tan\theta_y}\right) = \frac{Sd+X}{L_T - L} \quad (2)$$

Where θ_y is the Y-axis pitch angle or yaw angle, Sd is the Y-axis horizontal straightness and the vertical straightness, L is the Y-axis traveling distance.

The PSD measure displacement (X) of the continuity equation can be expressed as follows:

$$\left(\frac{\tan\theta_E - \tan\theta_y}{1+\tan\theta_E \times \tan\theta_y}\right) = \frac{Sd+L_T \times \tan\theta_E - D_T}{L_T - L} \quad (3)$$

Expansion formula (3) can be expressed as follows:

$$\left(L_T \times \tan\theta_y \times (\tan\theta_E)^2\right) + \left(L-(D_T\text{-}Sd) \times \tan\theta_y\right) \times \tan\theta_E + (L_T\text{-}L) \times \tan\theta_y - D_T + Sd = 0 \quad (4)$$

The parallel angle of the spindle axis and the Y-axis are solved used quadratic equation. The error angle can be expressed as follows:

$$\tan\theta_E = \frac{-B \pm \sqrt{B^2 - 4AC}}{2A} \quad (5)$$

The parallel angle of the spindle axis and the Y-axis (θ_E) are solved used A、B and C.

$$A = L_T \times \tan\theta_y$$
$$B = L - (D_T\text{-}Sd) \times \tan\theta_y \quad (6)$$
$$C = (L_T - L) \times \tan\theta_y - D_T + Sd$$

Fixture design

Details of the fixture for Laser beam include a laser diode module and the adjustment of the angle and position, the structure shown in Figure 7.

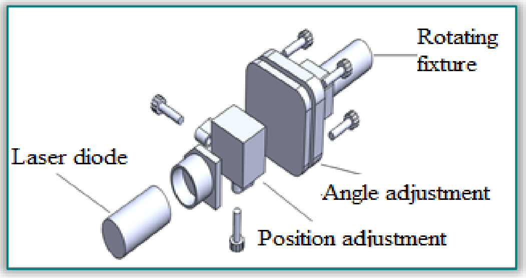

Figure 7 – Fixture construction of laser beam

Because the laser diode module arranged on the rotation axis will create angle α and displacement S shown in Figure 8, the arrangement error α (shown in Figure 9) can be determined with the position change induced by the arrangement. And the error can be eliminated by adjusting the angle and the position of the fixture.

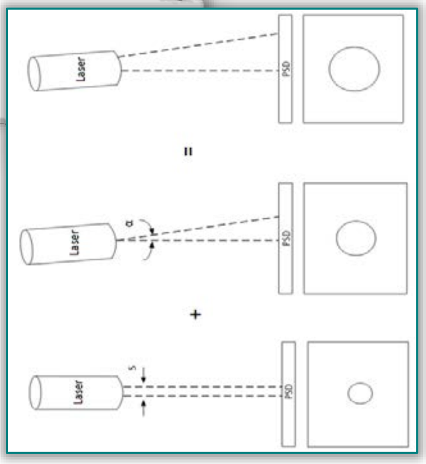

Figure 8 – Install error of the fixture

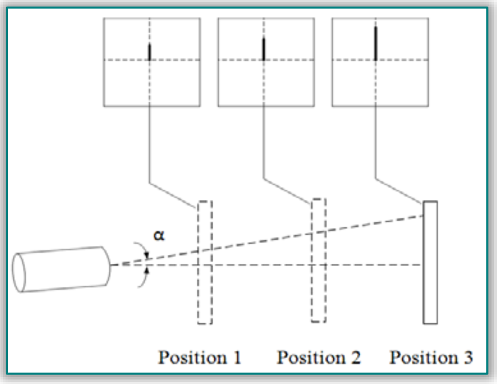

Figure 9 – PSD single change cause by arrangement error of laser beam

The position sensor fixtures will hold a PSD and is installed on the precision platform, the structure shown in Figure 10.

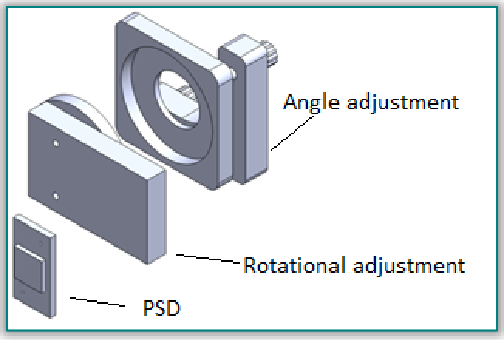

Figure 10 – The fixture structure of the position sensor

PSD fixture must be orthogonal with laser beam, because installation will develop the angle αi and angle βi, shown in Figure 11.The quadrature error can be eliminated by adjusting the angle and rotation of the fixture.

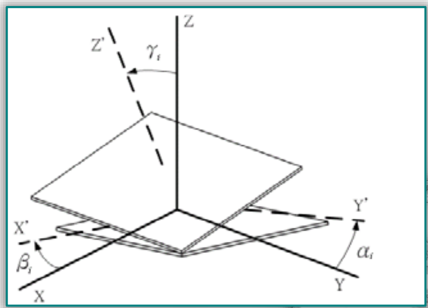

Figure 11 – Arrangement errors of the fixture for the position sensor

Development of measurement program

The LabVIEW software was used to develop the parallelism inspection system for the rotary axis of the spindle, the PSD to receiving laser beam and the light spot centroid position converted into a voltage value, use DAQ signal acquisition card, a voltage signal acquisition to computer to calculates and stores data, its signal the processing flow shown in Figure 12.

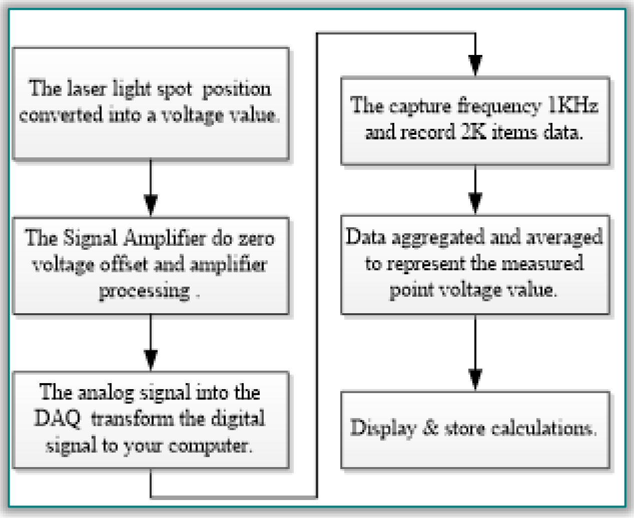

Figure 12 – Signal processing of PSD

Systematic measurement

After system correction, inspection parallelism error between laser source and Y-axis, spindle rotation to each 30 point measurement, and moving the Y-axis machine position from 0mm to -200mm position to observe the PSD measured value, calculate the parallelism error between laser source and Y-axis.The measurement process shown in Figure 13.

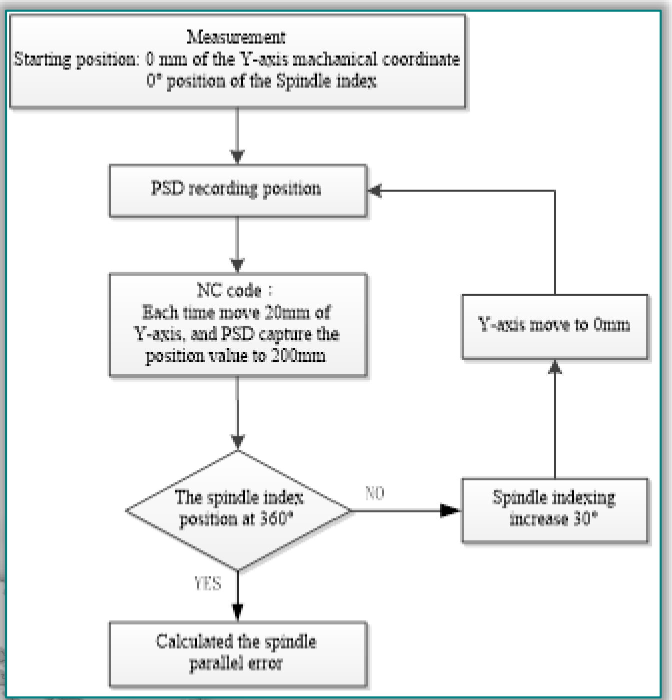

Figure 13 – Measurement processes for parallelism of Spindle

RESULTS AND DISCUSSION

By adjustment fixture of laser beam and PSD, angle and displacement offset can be regulated. If laser beam is coincident with the spindle axis, the measurement data result from the conical geometry of laser beam and the corresponding position coordinates of Y-axis which will form a circular cross, as shown in Figure 14.

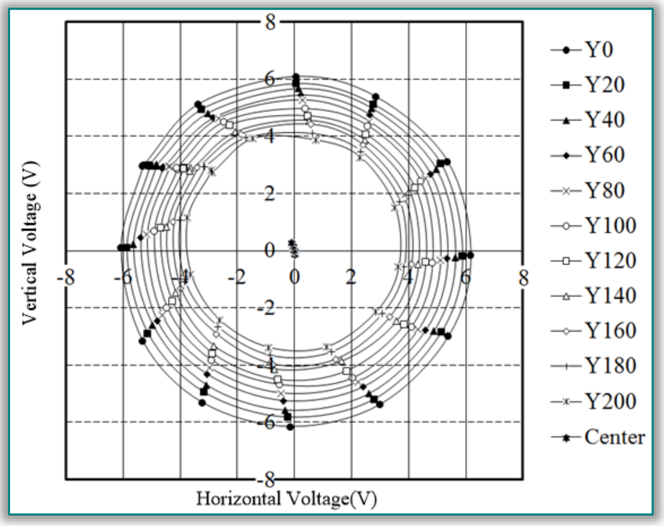

Figure 14 – Measurement results of the PSD

The application of Renishaw laser interferometer will perform measurements of angle error and straightness errors in the Y-axis. After error compensation, the displacement of the spindle axis is expressed as Figure 15.

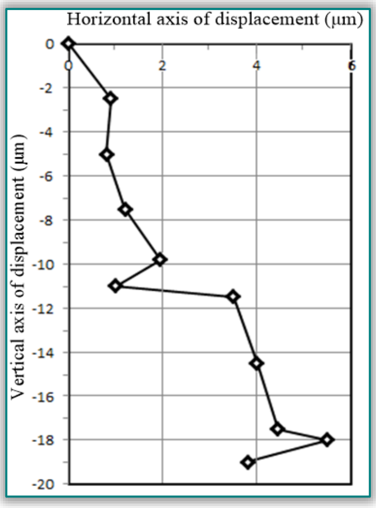

Figure 15 – Displacement of the spindle axis

Measurement results

By the measured data of the axis displacement in horizontal and vertical direction and position coordinates of each point in Y-axis, the horizontal and vertical error curve can be described. With the fitting equations, angle errors can be calculated as shown in Figure 16 and Figure 17, Table 1. It reveals that the average value of horizontal angle is 5.557 arc-seconds and that of vertical angle -19.961 arc-seconds, while measurements have been repeated 10 times.

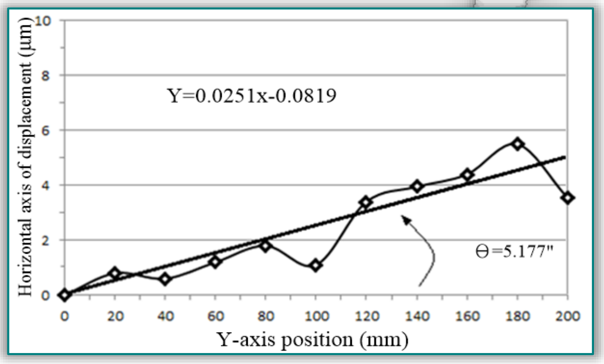

Figure 16 – Error curve of Horizontal position

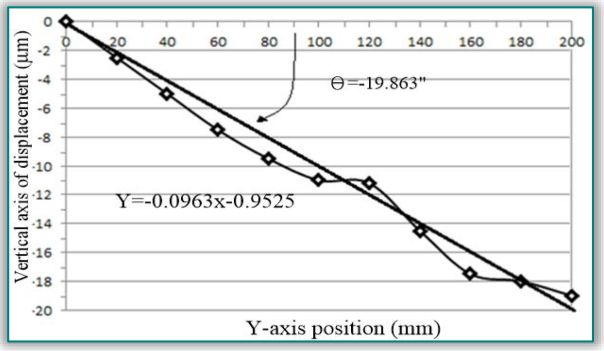

Figure 17 – Error curve of Vertical position

Table 1 – Measurement results

NO.	Horizontal angle (arc-seconds)	Vertical angle (arc-seconds)
1	5.177	-19.863
2	5.878	-20.379
3	5.094	-20.317
4	5.981	-20.007
5	5.734	-20.193
6	5.647	-19.716
7	5.358	-19.161
8	5.552	-20.644
9	5.896	-20.281
10	5.252	-19.039
Average value	5.557	-19.961
Standard deviation	0.322	0.526

Validation results

Measurement results resulting from the parallelism measurement system of spindle axis and the master gauges have been shown in Table 2.

Table 2 – Parallelism verification of the spindle axis

Angle error / System	Horizontal angle (arc-seconds)	Vertical angle (arc-seconds)
Master gauges	5.761	-4.839
Laser system	5.557	-19.961

The error of the horizontal angle of master gauge is 5.761 arc-second that of the vertical angle 4.839 arc-second. Experimental analysis demonstrated that the straightness error of master gauges is 5μm and roundness error 6μm. The total resultant error will contribute to 11μm. In measuring range of 160mm, the angle error of master gauges is 14.184 '' and the measurement results is close to result measured by this system 15.122"as shown in Figure 18.

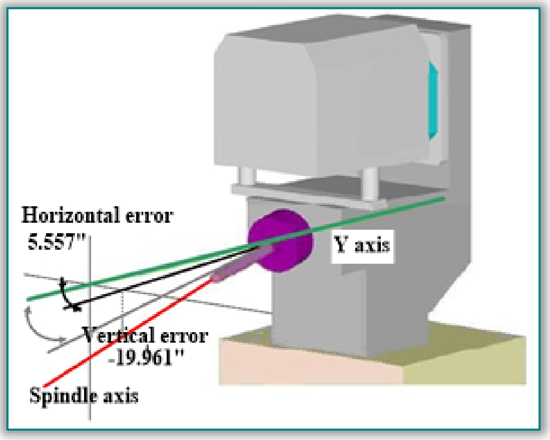

Figure 18 – Parallel state of spindle axis

Horizontal angle is adjustable by fixing screw during assembling procedure and hence the error can be corrected as shown in Figure 19. The error of vertical angle can be compensated by scraping technology. Therefore an error measurement result of the vertical angle is larger and parallelism between the spindle axis and Y-axis of the machine can be realized by the measurement results.

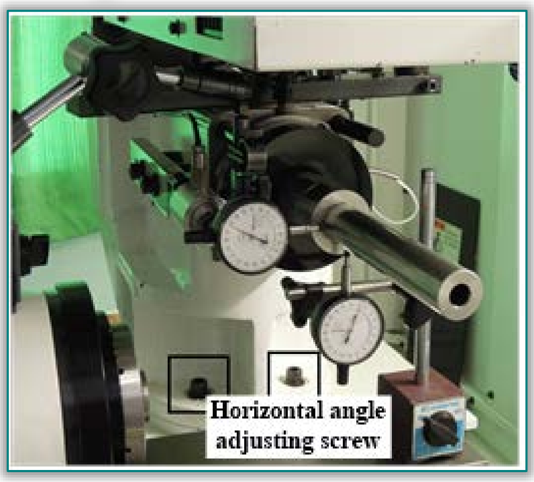

Figure 19 – Adjustment screw
for horizontal angles of Spindle

CONCLUSION

This research of parallelism measurement system for the spindle axis can be summarized by two points:

- The horizontal angle deviation between the spindle axis and Y-axis is 5.557 arc-seconds, the vertical angle deviation -19.961 arc-seconds.
- This difference between the system and master gauge value is 15.122”. Because the master gauges exists the error of 14.184"at length 160mm, this difference subtracts the error of master gauge is only 0.938".
- It reveals that the use of the laser beam visualizing the linear axis integrated with PSD is available for error measurements of parallel axis.

Note

This paper is based on the paper presented at The International Conference Management of Technology – Step to Sustainable Production (MOTSP 2016), organized by the Faculty of Mechanical Engineering and Naval Architecture, Croatian Association for PLM and the University of North, in Porec/Parenzo, Istria, CROATIA, June 01–03, 2016.

References

[1] Chen, J. Y., Lin, B. Y., Chen C. H.: Planning and analysis of grinding processes for end mills of cemented tungsten carbide, Journal of Materials Processing Technology, 201(2007), 618-622.
[2] Chen, J. Y., Lin, W. Y. Lee, B. Y., Chen C. H.: Development of database and searching system for tool grinding, Journal of Achievements in Materials and Manufacturing Engineering, 26(2008)2, 159-162.
[3] Chen, J. Y., Lu, H. S., Lee, B. Y., Chen C. H.: Design and implementation of cutting tools search system, Journal of Achievements in Materials and Manufacturing Engineering, 30(2008)1, 95-102.
[4] Castro, H. F. F.: A Method for Evaluating Spindle Rotation Errors of Machine Tools Using a Laser Interferometer, Salvador, 2008, 526-537.
[5] Prashanth Anandan, K., Burak Ozdoganlar, O.: An LDV-Based Methodology for Measuring Axial and Radial Error Motions when Using Miniature Ultra-High-Speed (UHS) Micromachining Spindles, Precision Engineering, 37(2013)1, 172–186.
[6] Jywe W. Y.: An optical rotation axis error measuring device, Intellectual Property Office, Taiwan, 33(2006)2, I247095.
[7] ISO230-7 Test code for machine tools —Part 7: Geometric accuracy of axes of rotation.

ISSN:2067-3809

ACTA TECHNICA CORVINIENSIS
– Bulletin of Engineering
Tome X [2017]
Fascicule 2 [April – June]
ISSN: 2067 – 3809

[1.]M.G. SOBAMOWO, [2.]A. T. AKINSHILO

DEVELOPMENT OF AN IMPROVED COMPUTER-AIDED ANALYSIS FOR THE THERMAL AND MECHANICAL DESIGN OF SHELL AND TUBE HEAT EXCHANGERS

[1-2.]Department of Mechanical Engineering, University of Lagos, Akoka, Lagos, NIGERIA

Abstract: The last past few decades have witnessed a considerable number of different attempts to design the Shell-and-tube heat exchangers have been developed. However, most of these designs focused on the thermal analysis of the heat exchanger without much consideration of the effects of the mechanical parts of the systems. Moreover, such complete designs have never been an easy "straight forward" task since it involves a lot of mathematical models, which are not easily and directly related to each other. A consequence of this is that, at the present time, there is no assurance of complete design of the equipment, but with the aid of Computer Aided Design which takes both Thermal and Mechanical design of the E type shell of the equipment into a deep consideration. Therefore this project aims at presenting a complete design with effective considerations of welding and analysis of stress of Shell-and-tube heat exchangers for different types of passes, flows, shapes and working fluids using Computer-Aided design with the aid of Visual Basic.Net. The computer-aided analysis and theoretical analysis are in agreement. It can be said that the developed computer program has some advantages to its credit which includes less skill requirement, high precision and accuracy of the design. It must be mentioned that the computer program can accept a design that satisfies the temperature correction factor, fouling factor, pressure drop and velocity of the fluid on both tube and shell side without investigating other options that may be more better, since the design parameters are been supplied. This programme will serve as a handy tool for designers who want to simulate various working process, conditions parameters and shape geometry.
Keywords: Shell and tube heat Exchanger, thermal and mechanical design

INTRODUCTION

The shell and tube heat exchangers are the most versatile type of heat exchangers. It provides relatively large ratios of heat transfer area to volume and weight and can be easily maintained. They offer great flexibility to meet any service requirement. Shell and tube heat exchangers are designed for high pressure relative to the environment and high pressure differences between the fluid streams. They find useful applications in process industries, in conventional and nuclear power station and are also used in air conditioning and refrigeration system.

These heat exchangers are capable of handling a quite high load at moderate size with good thermal and hydraulic efficiency in the moderate range of industrial applications. Consequently, this type of heat exchangers occupied a large area of research and investigation to establish the more easily and efficient procedure of design with optimization in its characteristics and cost. Lord et al. [1] pointed out the important of design details. These design considerations include pressure drop, mean temperature difference, types of flow, fluid properties, location, tube size and arrangement, flow-induced vibration, baffles in the shell, flow distribution and bypass prevention. Madson [2] designed Heat Exchangers for liquids in Laminar Flow. Butterworth [3] outlined a general procedure for the design of shell and tube heat exchangers where the overall heat transfer coefficient varies along the heat exchanger. Also, few years later, the same author presented a detailed procedure for the calculation of equation [4]. In another paper, Bell [5] submitted a procedure for the global thermal and hydraulic design of the shell and tube bundle heat exchanger. There is no available complete approach for the thermal-hydraulic design of the shell and tube heat exchanger where enhanced surfaces are used in the open literature. However, there are comprehensive correlations for the prediction of the heat transfer coefficient on finned tube surface. For predicting heat exchanger performances, it is necessary to calculate the overall heat transfer coefficient, and pressure drop for both fluids in tube and shell side. Fluid flow in the tube side is relatively simple. Many correlations for calculating heat transfer coefficients and pressure drops in the tube side are available, including Colburn correlation and Dittus-Boelter correlation [6] for obtaining heat transfer coefficients, and plain tube pressure drop method [18] for calculating pressure drop. However, fluid flow in the shell-side is more complex. Bell-Delaware method [7] can be used for calculating heat transfer coefficients and pressure drop. Furthermore, developed Delaware method [8] and Chart method [9] are proposed for heat transfer coefficients, while for pressure drop using simplified Delaware method [10]. Although these methods had been claimed to be effective for calculating shell-side heat transfer coefficients and pressure drops, they always give significantly different results in most cases. Leong [11] developed a shell and tube heat exchanger design software for education applications which is suitable for teaching the thermal and hydraulic design of shell and tube heat exchangers to senior undergraduate student in mechanical and chemical engineering and train new graduate engineers in thermal design. In the recent past, some experts studied on the design, performance analysis and simulation studies on heat exchangers. Mohammed [12] investigated experimentally and theoretically the thermal-hydraulic designs of shell and tube heat exchanger using the step by step technique for a single tube pass. Ramanathan [13] presented a novel technique to design shell and tube heat exchangers based on the cell method. This technique defines a cell to comprise of only one tube row. Adelaja [14] developed a computer-aided analysis of the thermal and mechanical design of the shell and tube heat exchanger. The developed Heat Exchanger Simulator software was done in order to complement the teaching of the thermal and mechanical properties of the shell and tube heat exchangers, bringing to the student knowledge of the applications of these exchangers. Although, in the earlier work, Mukhareej [15] also presented work on effective design of shell and tube heat exchanger, most of these designs approaches in the literatures are focused on the thermal-hydraulic analysis of the heat exchanger without much consideration of mechanical design of the systems. Moreover, such complete designs (with effective considerations of welding and analysis of stress in the equipment) have never been an easy “straight forward” task since it involves a lot of mathematical models, which are not easily and directly related to each other. Therefore there is no assurance of complete design of the equipment. Therefore, this work presents a complete design (Thermal, hydraulic and Mechanical design with effective considerations of welding and analysis of stress in the equipment) of Shell-and-tube heat exchangers of different types of passes , E type shell, and working fluids with the aid of Visual Basic.Net computational tool.

DESCRIPTION OF SHELL AND TUBE HEAT EXCHANGER

The principal components of the shell and tube heat exchangers are: shell, shell cover, tubes, channel, channel cover, tube sheet, baffles and nozzles. Others include tie rods, spacer, pass partition plates, impingement plates and longitudinal baffles, sealing strips, support and foundation.

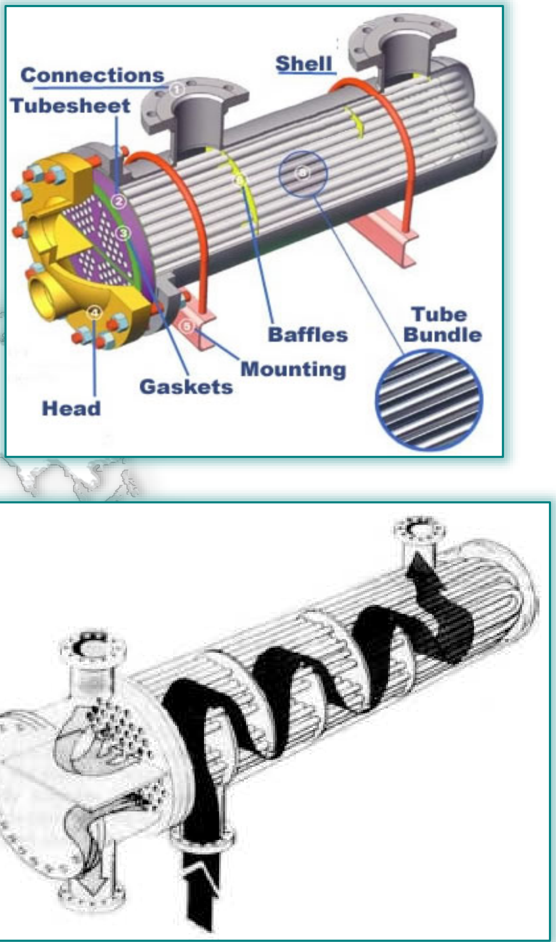

Figure 1. Conceptual diagram and fluid flow pattern of a Shell and Tube heat exchanger [22]

The basic sizes of shell available include 8, 10, 12 inches, we find 2 inches of increment step start from 13 to 25 inches. From 25 to 39 inches, there is a 2-inches increment and from 39 to 72 inches we find 3-inches increment in shell tube size. Basically during service the heat exchanger may function as single phase (such as cooling or heating of a liquid or gas) or two phase such as vaporization or condensing or a combination of several services. The tube side design includes the tube layout and the tube pitch. There are four tube layout patterns which include the triangular 30°, rotated triangular pattern 90°, square pattern 90°, and rotated square 45°. A rotated triangular pattern accommodates more tubes than a square or rotated square pattern. Furthermore a triangular pattern produces more turbulence and a high heat transfer coefficient.

However a typical tube pitch is 1.25 times the tube outer diameter and does not permit mechanical cleaning of the tube since access is not available. Consequently a triangular layout is limited to cleaning of shell side service. For services that require mechanical cleaning on the shell side square pattern must be used. The tube pitch defined as the shortest distance between adjacent tubes for a triangular pattern TEMA (Tubular Exchangers Manufacturers Association) specifies a minimum tube pitch of 1.25 times the tube outer diameter while for square pattern TEMA recommends a minimum clearing lane of 4 inches between adjacent tubes. Shell configuration patterns as classified by TEMA is based on the shell side fluid flow and there are E, F, G, H, J, K and X.

DESCRIPTION OF THE COMPUTER PROGRAMME

The graphic user interface developed for the thermal, hydraulic and mechanical design of the shell and tube heat exchanger using Visual Basic.Net computational tool is designed and primarily developed for the simulation of industrial operating conditions, for simulating practical application of shell and heat exchangers. Also for enhancing the understanding of functional operation of the equipment by beginner due to it step by step guide of algorithm. The computational programme compatible with any Microsoft Windows-based Personal Computer of at least a 4MB of RAM and 7MB of free hard disk space.

COMPONENTS OF THE SOFTWARE

The computational programme consists of four modules which are the thermal section and mechanical section, design section and the help section as shown in the figures (2-5) below.

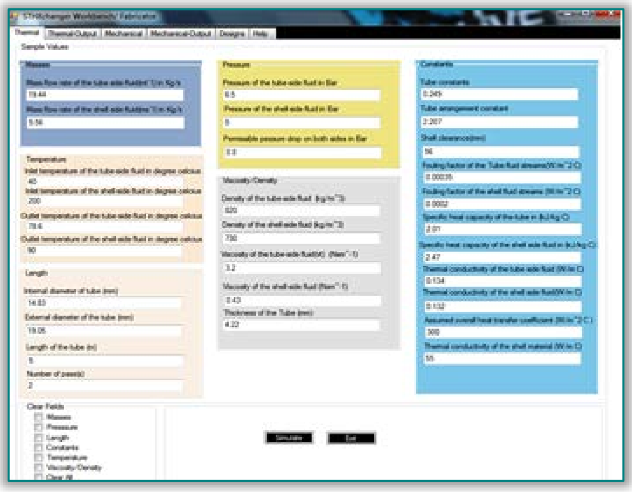

Figure 2. Input for the Thermal- Hydraulic Design

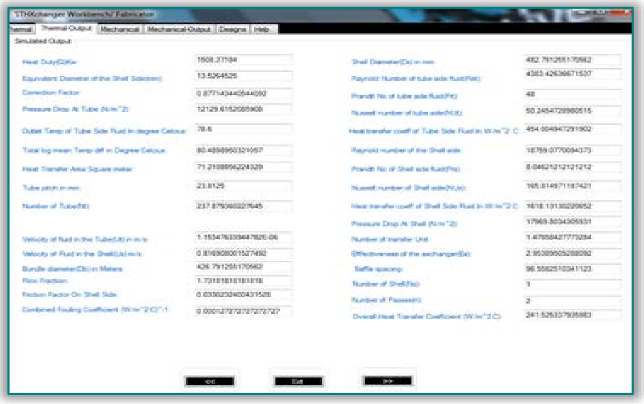

Figure 3. Output for the thermal hydraulic design

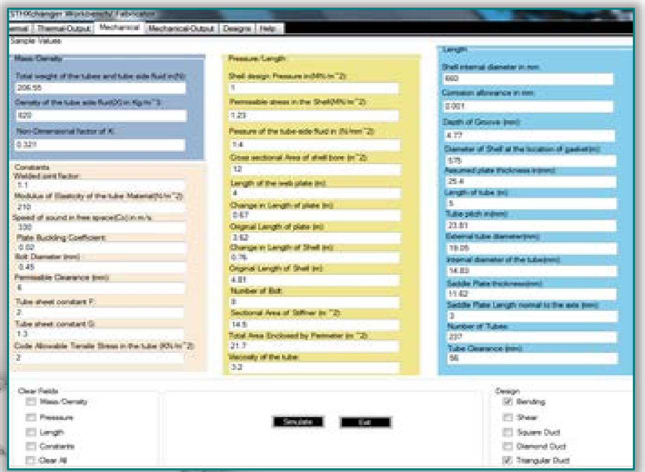

Figure 4. Inputs for Mechanical Design

Figure 5. Output for Mechanical Design

The thermal design provides detail of the heat duty, velocity of the fluid in tube and shell, heat transfer area square meter, number of tube, tube pitch, pressure drop at tube and shell side, shell equivalent diameter, correction factor, outlet temperature of the tube side fluid, bundle diameter, flow fraction, friction factor on shell side, combined fouling coefficient, shell diameter, Reynolds number on tube and shell side, Prandtl number on tube and shell side, Nusselt Number on tube and shell side, baffle spacing, number of shell and overall heat transfer coefficient, heat transfer coefficient on the tube and shell side fluid, effectiveness of the exchanger, total log mean temperature difference.

The mechanical design of the exchangers involves the determination of the thickness of the shell, channel, shell cover, tube plate, floating head cover, nominal diameter of bolt, radial stress in tube, numbers of bolt required, number of web plate, maximum permissible stress of the tube plate, baffle spacing, critical velocity of the tube side fluid, speed of sound perpendicular to axis, natural frequency of the tube, buckling load under comprehensive load, sound induced velocity, critical buckling stress for plate, effective saddle width, critical velocity of flow of pipe buckling a complete design is relevant for both the optimisation of the fluid flow process of the shell and tube heat exchanger as well as the cost optimization during construction and maintenance. The computational tool for the computer aided analysis is tested to evaluate its performance using the physical properties of crude oil and kerosene, standard parameters from Mechanical Engineers handbook were supplied to test the mechanical designed and the results are shown.

CONCLUSION

In this work, a complete design with effective considerations of welding and analysis of stress of Shell-and-tube heat exchangers for different types of passes, flows, shapes and working fluids using Computer-Aided design with the aid of Visual Basic.Net has been presented. Since the computer aided analysis and theoretical analysis are in agreement, it can be said that the computer program has some advantages to its credit which includes less skill requirement, high precision and accuracy of the design. It must be mentioned that the computer program can accept a design that satisfies the temperature correction factor, fouling factor, pressure drop and velocity of the fluid on both tube and shell side without investigating other options that may be more better, since the design parameters are been supplied. This programme will serve as a handy tool for designers who want to simulate various working process, conditions parameters and shape geometry.

References

[1.] Lord R.C., Minto P.E., Slusser R.P. Design of Heat Exchanger, Mcgraw Hill, New York, 1970.
[2.] Madson N., Design of Heat Exchanger for Liquid Laminar Flow, University of Rhode Island, 1974.
[3.] Butterworth, D. A Calculation Method For Shell And Tube Heat Exchanger in Which The Overall Coefficient Varies Along The Length", Conference on Advances in Thermal And Mechanical Design of Shell And Tube Heat Exchangers, 1973.
[4.] Butterworth, D. and Cousins, L. B. "Use of Computer Programs in Heat Exchangers Design", Chemical Engineering, McGraw-Hill, 1979.
[5.] Bell K. J. "Preliminary Design of Shell and Tube Heat Exchanger", Heat Exchange Thermal-Hydraulic Fundamentals and Design, McGraw-Hill., New York. 1980.
[6.] Bhatti, M. S., and Shah R.K. Turbulent and transition convective heat transfer in ducts, Handbook of Single-Phase Convective Heat Transfer, Wiley, New York, 1987.
[7.] Taborek, J., Shell and tube heat exchangers, Heat Exchanger Design Handbook, Hemisphere Publishing Corp., New York, 1988.
[8.] Gnielinski, A., Zukauskas A. andSkrinska A., Banks of plain and finned tubes, in Heat Exchanger Design Handbook, Hemisphere Publishing Corp., New York, Vol. 2, 1988.
[9.] Ayub Z. H. A new chart method for evaluating single-phase shell side heat transfer coefficient in a single segmental shell and tube heat exchanger. Applied Thermal Engineering, vol. 25, pp. 2412-2420, 2005.
[10.] Kern, D. Q. and Kraus A.D. Extended Surface Heat Transfer, McGraw-Hill, New York, 1972.
[11.] Leong K.C. and Toh K.C. Shell and tube heat exchanger design Software for educational applications, International Journal of Engineering, vol. 14, No. 3, p. 217-224, 1998.
[12.] Mohammed A. G. "Experimental And Theoretical Studies of Shell And Tube Heat Exchanger Using Step By Step Method", M.Sc. Thesis, Mech. Eng. Dept., Al-Mustansiriy Univ., Baghdad, Iraq, 2005.
[13.] Ramanathan V.G., Ketan A.N., and Nayak A. A novel way to design shell-and-tube heat exchangers based on the cell method, 2009.
[14.] Adelaja A.O., Ojolo S.J. and Sobamowo M.G., "Computer Aided Analysis of Thermal and Mechanical Design of Shell and Tube Heat Exchanger" Advanced Materials Research, vol 367, pp.731-737, 2012.
[15.] Mukharej R. Effectively Design Shell and tube Heat exchangers, Chemical Engineering Progress, 1998.

ISSN:2067-3809

ACTA TECHNICA CORVINIENSIS
– Bulletin of Engineering
Tome X [2017]
Fascicule 2 [April – June]
ISSN: 2067 – 3809

[1.]Hugo ZUPAN, [2.]Mihael DEBEVEC, [3.]Niko HERAKOVIC

INVENTORIES IN THE WAREHOUSE - MONITORING, ANALYSES AND OPTIMIZATION WITH SIMULATION

[1-3.]Laboratory for Handling, Assembly and Pneumatics, Faculty of Mechanical Engineering, University of Ljubljana, Askerceva 6, SI-1000 Ljubljana, SLOVENIA

Abstract: This paper presents a simulation model through which the inventories in the warehouse can easily be followed and the appropriate value of the minimum stocks determined. The simulation model of the warehouse is based on the discrete events and built in the software package Tecnomatix Plant Simulation. A reasonable approach how to treat inventories of the existing situation as well as the inventories movement in the warehouse through its analysis is presented. In the article the analyses are carried out on the basis of the results of simulation suggestions and a new methodology is proposed together with guidelines for improving the material flow in the production and warehouse process.
Keywords: discrete event simulation, stock optimization, inventory tracking, minimum stocks, digital warehouse

INTRODUCTION

At a time of rising costs, time pressures in production and globalization in general, logistics is one of the key factors for the success of the company [1]. If the company wants to stay competitive it must continuously increase its efficiency on all fields of manufacturing – also in a warehouse [2].

Achieving optimal inventories is one of the fundamental problems of storage. All inventory optimization approaches are not effective. For this reason, it is necessary to choose proven optimization approach, such as upfront simulation of storage [3].

Today the simulation is becoming an increasingly useful tool in production. Its key advantage is that it does not consume materials, energy and resources, but only the data. Thus, variants production and storage processes tested in advance and we are looking for the optimum solution [4, 5, 6, 7, 8, 9].

A computer simulation can provide us with a comprehensive selection of analyses tools, such as bottleneck analysis, statistics and graphs through which different scenarios in warehouses are evaluated.

STARTING POINTS AND RESEARCH OBJECTIVES

In the initial stage we set some guidelines for the development of the model of a warehouse for cases where the company does not have a comprehensive database of stored pieces. The ultimate goal of the research is to establish the correct minimum values of stock and to reduce inventories in the warehouse.

The essential parts of the research are:
- a computer model development of a virtual warehouse,
- monitoring of the pieces' movement in a warehouse,
- analyses of the flow and
- optimization by using new methodologies.

Analyses of the obtained results from the simulation allow us to better understand the unwinding of transactions of stored pieces in the production process.

When developing a computer model, the characteristics and limitations of the actual warehouse are considered and once the model is made, the simulation is used as a tool to monitor the status for each stored piece / end product / tool in the warehouse using tables and graphs. The model is designed specifically to subscriber, since proposals may be implemented in the optimization of a real warehouse.

The procedure is the following: after completing the analyses the optimization of the inventories in the warehouse is made by means of indicators (discussed in the chapter 4.1) and in particular with the reduction of current stock using the new proposed methodology (discussed in chapter 4.3).

The model has also been tested in the real company and in the initial stage the guidelines for making a macro system and roughly enumerated characteristics of storage have been set.

Together with the company we have decided that we would observe only the movement of component parts of different product codes (CP), which are permanently in stock and are located in the warehouse of parts. Company CP movements for all product codes in the warehouse is defined as 6 different transactions between the individual locations (Figure 1), which are identified by the following codes:

- ¤ 01: the receipt of CP in acquiring warehouse, which then go to the warehouse,
- ¤ 02: complaints go directly to the CP storage,
- ¤ 10: The return of CP from the production back to the warehouse,
- ¤ 12: CP sales from the warehouse through retail,
- ¤ 13: CP emitting from the warehouse into production
- ¤ 14: CP that come in acquiring warehouse in the review and then goes directly into production.

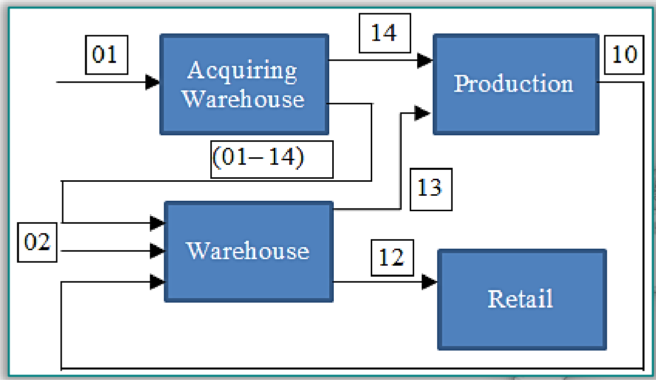

Figure 1 – Transactions between the individual locations

WAREHOUSE MODEL

Building of the warehouse model was carried out in two basic steps:

- ¤ the development of logical warehouse model, and
- ¤ the building of the computer model.

Logical warehouse model

In this step, the objective of using simulation is to collect data on inventories of CP's for all product codes, which are permanently in stock. For this purpose the model of a virtual warehouse was developed, which is set on the basis of the actual warehouse (Figure 2).

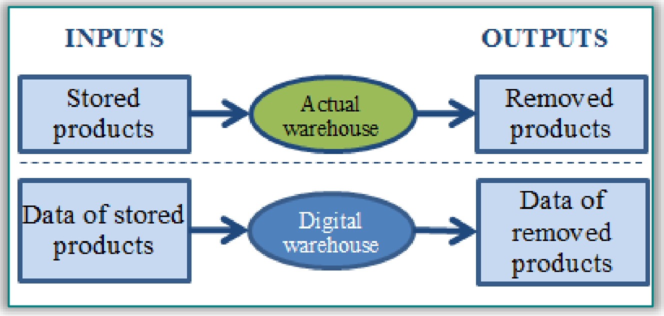

Figure 2 – The basic principle of the virtual warehouse

Computer model

The simulation model (Figure 3) of a workshop was built in the Plant Simulation software package. The simple logical dependences of the production processes in the model are denoted by standard built-in objects, and the complex logical dependences are denoted with methods or libraries in the programming language SimTalk [10, 11, 12].

The developed simulation model consists of 40 standard objects of the software package and more than 300 lines of logical dependences written in SimTalk.

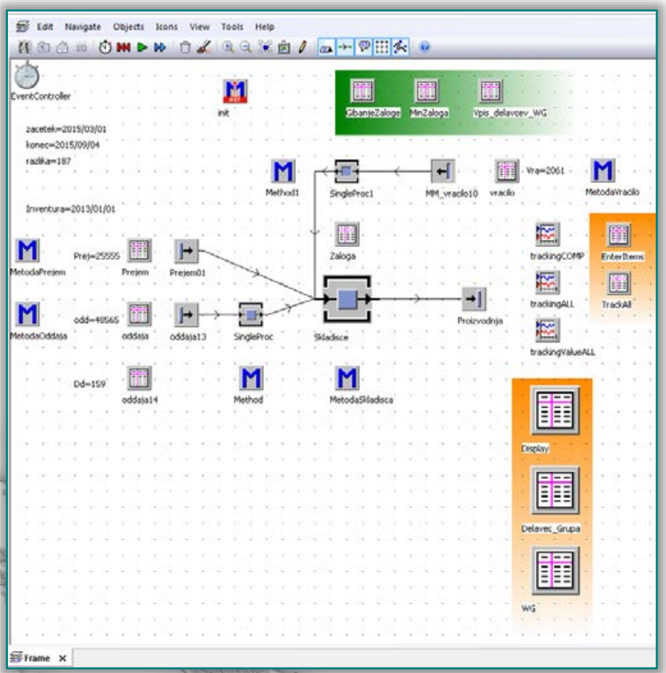

Figure 3 – Computer – digital warehouse model (simulation model)

The input data for the simulation were obtained directly from an Excel table, which is obtained from the integral information system of the company.

ANALYSES OF WAREHOUSE MODEL OF ALL COMPONENT PARTS

When analyzing the warehouse different indicators and guidelines set by mutual agreement with the company were used. The main purpose of the analyses is to obtain appropriate guidelines on which inventories in the warehouse can be reduced, and thus the value of the invested capital in stocks.

After the successful implementation of simulation the following data is obtained:

- ¤ Output table and
- ¤ Graphs to track individual component and a graph of the combined stocks.

Output table

Output data structure obtains two groups of data:

- ¤ output data from the simulation, which also include the input data of simulation, which were obtained from the database of the company and

¤ data which were collected through the analyses of the output data from the simulation.

Output data of the simulation

Output table of material flow from the simulation obtains categories as presented in Table 1. The output data from the simulation are complemented with categories, which are necessary for analysing the flow of items in the warehouse.

Table 1 – Table structure of the material flow of simulations

Colum name	Description
ID	serial number of the record
Code of product	Code of CP
SAP	SAP code of CP
Title	Description of CP
Supplier	Supplier of CP
Current state [-]	the current state of stocks
Current minimal stock [-]	set point of minimum stocks
usage [-]	consumption of pieces in the observed period of the simulation
Min [-]	the minimum number of pieces in the warehouse during the observation period of the simulation
Max [-]	the maximum number of pieces in the warehouse during the observation period of the simulation
Average [-]	the average number of pieces in the warehouse during the observation period of the simulation
Average value [€]	the average value of pieces in the warehouse during the observation period of the simulation
Max value [€]	maximum value of pieces in the warehouse during the observation period of the simulation
Max - Min [-]	the difference between the number of pieces max and min in the warehouse during the observation period of the simulation
Min – Current minimal stock [-]	the difference between the number of pieces and current minimal stock in the warehouse during the observation period of the simulation
Delivery time [days]	delivery time for an item (in days)
Item price [€]	Item price
Consumption from the warehouse [-]	consumption of pieces from the warehouse during the observation period of the simulation

Collected data from analyses

Completed list of indicators and guidelines of material flow simulations for the analyses, set together with the company, is listed below:

¤ *Indicator fz:* An indicator of the relative size of inventory in the warehouse for product.

¤ *Indicator fdp:* Indicator of overstock value in the warehouse for product.

¤ *NEW min:* The proposed new minimum stock.

¤ *Adj NEW min:* The proposed new minimum stock.

¤ *min – NEW_min:* The difference between the current and the adjusted minimum stock.

¤ *Curr value min:* Value in € of the current minimum stocks.

¤ *New value min:* The value in € of NEW minimum stocks: the average daily consumption from store.

¤ *Avg consum:* The average daily consumption from store.

¤ *Min avg:* Minimum stock according to the average consumption.

In the simulation we also used a new method for calculating the new minimum stock, which is explained in section 4.3.

Graph for tracking of the separate component and of all components

A stock in the warehouse (printouts in the form of graphs) can be monitored for a specific component or for all components in the warehouse.

Graph for tracking of each component part

Graph plots how stocks of component part in warehouse evolved (Figure 4). The graph plots the value of inventory only for those CP which we want. For each selected CP it also plots its current value of the minimum stock.

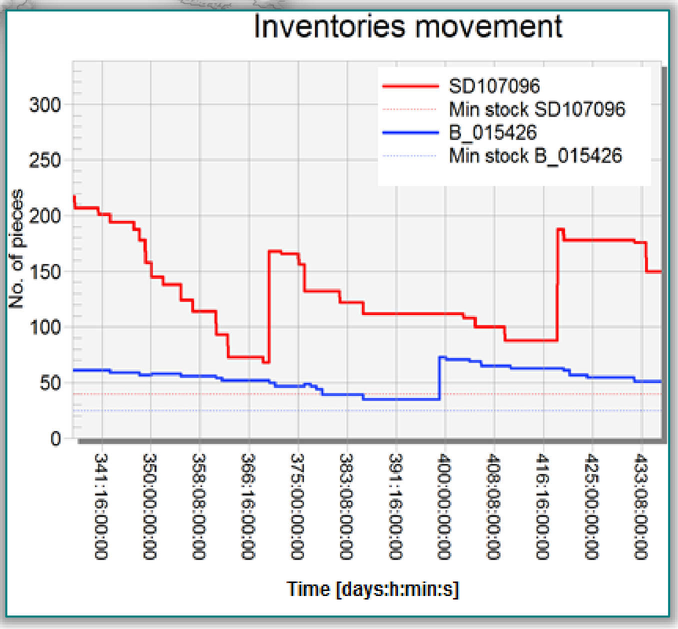

Figure 4 – Graph of inventory movement for separate CP

Graph for tracking sum of all component parts

Graf plots the sum of all pieces in the warehouse, the average value of the stock pieces and a minimum total stock of pieces in the observation time (Figure 5).

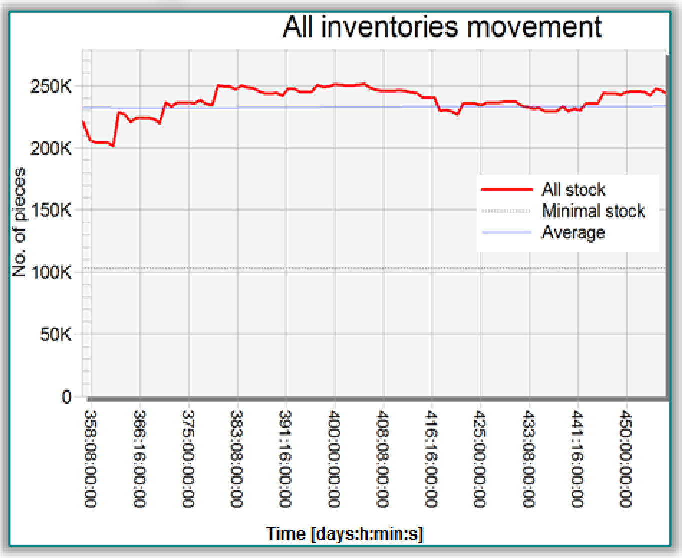

Figure 5 – Graph of all inventories movement for CPs which are permanently in stock

The proposed new minimum stocks methodology determination

The results of the new minimum stocks suggest three different values for each component part:

1) The minimal stock according to average consumption is calculated with Equation (1) to get new minimum stock of the average consumption:

$$\text{Min avg}\,[-] = \text{Avg C}[-]\cdot\text{DT [days]} \qquad (1)$$

where: Avg C [-] – the average daily consumption from store [-], DT [days] – delivery time of CP [days]

2) Through the Equation (2) we propose a new methodology for calculating the minimum stocks, which is calculated through simulation by and represents recommended new minimal value for each CP depending on the observation period. The methodology takes into account the average of the average consumption in time and the delivery time:

$$\text{NEW min}\,[-] = \text{avg}_{\text{avg}}[-]\cdot\text{DT[days]} \qquad (2)$$

$$\text{avg}_{\text{avg}}[-] = \frac{1}{n}\sum_{i=1}^{n}\left(\frac{\text{UsaUN }[-]}{\text{ND [days]}}\right)_i \qquad (3)$$

where: n – the number of transactions items in the observed period [-], UsaUN [-] – the sum of used items until the observed time [-], ND[days] – the number of days until the observed time [days]

Through the Equation (4) we propose improved new methodology for calculating the specific minimum stocks for component parts with non-periodical consumption. The equation (4) gives adjusted new minimum stock for each CP depending on the observation period.

$$\text{adj NEW min}[-] = \text{avg}_{\text{avg1}}[-]\cdot\text{DT[days]} \qquad (4)$$

$$\text{avg}_{\text{avg1}}[-] = \frac{\text{avg}_{\text{avg}}[-]+\text{AvgC }[-]}{2} \qquad (5)$$

The proposed value of the minimal stock according to equation (4) allows better offset data which had big variations and uneven periodicals transactions in the past.

Discussion of new methodology

Equation (1) calculates new minimum stock of the average value during the observation period. Equation (2) proposes completely new methodology for the determination of minimum stocks.

The proposed method according to Equation (2) was tested in the actual company and its practical utility was proven. The differences between both equations occur when CP does not have steady consumption. Equation (4) calculates an interim value of the variables between Equations (1) and (2). It gives offset value of those CP that had large deviations and irregular periodicity.

Findings of proposed new minimal stocks

The simulation results provide three different proposed new minimal number of component parts for each product code. The differences between the values of the calculations for Equations (1) and (2) are minimal.

The number of all component parts of new stock for approx. 1900 different product codes is according to Equation (2) totally 22000. According to Equation (1) this number is slightly lower.

The purpose of the new methodology (Equation (2)) is not to get the lower number of component parts than we get with the Equation (1), but to obtain the number of component parts of all product codes that more accurately covers the evenness of the consumption from the warehouse.

After implementing the new methodology into the company, it has been tested for the minimal stocks value, calculated with Equation (2) and Equation (4), for few CP. After 6 month of testing the proposed methodology has been proved as a reliable and more appropriate one as the methodology, described by the Equation (1).

CONCLUSIONS

By analyzing the data from the warehouse we wanted to understand the characteristics of the behavior of the warehouse system. Analyses provided very useful information in solving the problem, because one can see exactly what data is most critical and needs immediate attention.

The results of the analysis of the warehouse give us an advice how to set new minimal stocks values. Analyses of the company showed that during the period of approximately 1.5 years the 350 CPs of different product did not change and they were only lying in the warehouse.

The analyses also showed that it is reasonable to reduce the minimum stocks value from current 100000 pieces to about 22000 pieces, when the production is increased and to around 12000 pieces when the production is decreased.

The main objective of the simulation was to optimize stock levels and activities in purchasing. From the graphs for each CP the purchasing mistakes that had occurred in the past can be observed and may be avoided in the future. Also graph of total stocks value is a good indication of general warehouse state. The value in this graph should be as low as possible, because it means less capital tied up in the warehouse and consequently less costs.

Because the minimal stocks values depend on the production volume, the company is running the simulation every few months and always adjusting the minimal stock values for each CP. By doing this, they are keeping the individual optimal values for each CP.

In the future work we will focus to implement this idea into place buffers in production processes.

Note

This paper is based on the paper presented at The International Conference Management of Technology – Step to Sustainable Production (MOTSP 2016), organized by the Faculty of Mechanical Engineering and Naval Architecture, Croatian Association for PLM and the University of North, in Porec/Parenzo, Istria, CROATIA, June 01–03, 2016.

References

[1] AUTOMATICA Accompanying Program: Smart factory, 6th international Trade Fair for Automation and Mechatronics, Munich, 3 – 6 June 2014.
[2] Hicks, B. J.: Lean information management: understanding and eliminating waste, International Journal Of Information Management, 27(2007)4, 233-249.
[3] Debevec, M., Simic, M., Herakovic, N.: Virtual factory as an advanced approach for production process optimization, International journal of simulation modelling, 13(2014)1, 66-78.
[4] Ayadi, M., Costa Affonso, R., Cheutet, V., Masmoudi, F., Riviere, A., Haddar, M.: Conceptual Model for Management of Digital Factory Simulation Information, International Journal of Simulation Modelling, 12(2013)2, 107-119.
[5] Cigolini, R., Pero, M., Rossi, T., Sianesi, A.: Linking supply chain configuration to supply chain performance, Simulation Modelling Practice and Theory, Department of Management, Economics and Industrial Engineering (DIG), Politecnico di Milano, Italy, 2013.
[6] Herakovic, N., Metlikovic, P, Debevec, M.: Motivational Lean Game to Support Decision between Push and Pull Production Strategy, International Journal of Simulation Modelling, 13(2014)4, 391-526.
[7] Kocisko, M., Novak-Marcincin, J., Baron, P., Dobransky, J.: Utilization of progressive simulation software for optimization of production systems in the area of small and medium companies, Technical Gazette, 19(2012)4, 983-986.
[8] Wenzel, S., Jessen, U., Bernhard, J.: Classification and conventions structure the handling of models within the Digital Factory, Computers in Industry, 56(2005)4, 334-346.
[9] Eskandari, H., Rahaee, M.A., Memarpour, M., Hasannayebi E. and Malek, S.A.: Evaluation of different berthing scenarios in Shahid Rajaee container terminal using discrete-event simulation, in Winter Simulation Conference (WSC), 2013.
[10] eM-Plant Objects Manual, Tecnomatix Technologies GmbH & Co. KG., 1998.
[11] eM-Plant Reference Manual,Tecnomatix Technologies GmbH & Co. KG., 1998.
[12] Bangsow, S. Tecnomatix Plant Simulation, Modeling and Programming by Means of Examples, Springer, 2015.

ISSN:2067-3809

We are very pleased to inform that our international and interdisciplinary journal **ACTA TECHNICA CORVINIENSIS ■ Bulletin of Engineering** completed its nine years of publication successfully [**issues of years 2008 – 2016, Tome I–IX**].

In a very short period it has acquired global presence and scholars from all over the world have taken it with great enthusiasm.

Every year, in four online issues (**fascicules 1 – 4**), **ACTA TECHNICA CORVINIENSIS ■ Bulletin of Engineering [e-ISSN: 2067-3809]** publishes a series of reviews covering the most exciting and developing fields of science and technology. Each issue contains papers reviewed by international researchers who are experts in their fields. The result is a journal that gives the scientists and engineers the opportunity to keep informed of all the current developments in their own, and related, areas of research, ensuring the new ideas across an increasingly the interdisciplinary field.

Now, when will celebrate the tenth years anniversary of **ACTA TECHNICA CORVINIENSIS ■ Bulletin of Engineering**, we are extremely grateful and heartily acknowledge the kind of support and encouragement from all contributors and all collaborators!

On behalf of the Editorial Board and Scientific Committees of **ACTA TECHNICA CORVINIENSIS ■ Bulletin of Engineering**, we would like to thank the many people who helped make this journal successful. We thank all authors who submitted their work to **ACTA TECHNICA CORVINIENSIS ■ Bulletin of Engineering**.

ACTA TECHNICA CORVINIENSIS
– Bulletin of Engineering
Tome X [2017]
Fascicule 2 [April – June]
ISSN: 2067 – 3809

[1.]Goran JANAĆKOVIĆ, [2.]Jasmina RADOSAVLJEVIĆ, [3.]Dejan VASOVIĆ,
[4.]Jelena MALENOVIĆ-NIKOLIĆ, [5.]Ana VUKADINOVIĆ

THE INTEGRATED SAFETY PERFORMANCE MODEL BASED ON SAFETY INDICATORS AND SAFETY LIFECYCLE

[1-5.]University of Niš, Faculty of Occupational Safety, Niš, SERBIA

Abstract: Systems approach in safety is applied during the analysis of complex safety systems and identification of key performance indicators. The integration of the safety system is necessary to enable efficient use of safety resources, and to take into consideration all technical, human and organizational aspects of safety. Safety lifecycle is an engineering process designed to optimize safety system and increase the level of safety. The main advantage of applying this model in real systems is increasing the effectiveness of the protection of employees and goods and the efficiency of safety resource use. In this paper, we describe the model for safety performance assessment of integrated safety systems, based on selected safety indicators and safety lifecycle.
Keywords: safety, safety performance, safety indicators, safety lifecycle, integrated safety system

INTRODUCTION

Safety system is a complex combination of resources (people, materials, equipment, hardware and software components, data, information, knowledge, services) integrated with the aim to fulfill the specific needs related to the protection of human, material and immaterial goods. The system is human-made system, physical according to the form of existence, dynamic and open according to the relationship with the environment. Its main task is to achieve optimal conditions in working and living environment, which leads to: the effective discharge of duties in an appropriate work environment in which employees are protected from the harmful effects that can lead to injuries, occupational diseases or deaths; minimal impact of work processes on the environment from the point of pollutant emission, waste generation and use of non-renewable resources; taking into account the potential risk of natural disasters and catastrophes.

The essence of a successful safety system is to focus on the causes of adverse events, to prevent their occurrence, or to reduce to reduce negative effects of their appearance if they cannot be avoided. The safety system, its elements and interaction with the environment are presented in Figure 1.

Many economic and social factors can influence decisions on safety, such as maintenance of devices and equipment and the implementation of certain measures.

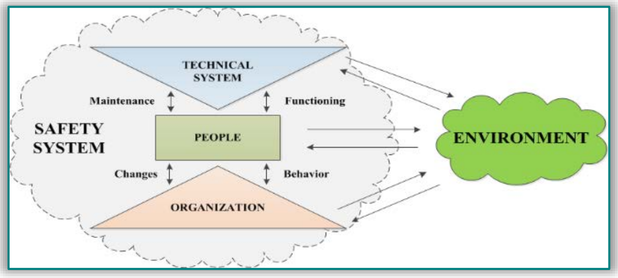

Figure 1. Safety system as an open system, and its environment

Therefore, the basic elements of the safety system are: technical and technological system, people (employees and employers), organizations and environment with which the system interacts (Figure 1). Technical-technological system requires proper maintenance during the functioning. An organizational change and organizational safety culture influence the behavior of employees. The environment affects the safety system by certain norms and standards that must be applied in the safety system.

MATERIAL AND METHODS

Safety indicators

The level of safety is described by a set of indicators. These indicators describe the safety outcomes and some safety activities carried out with the aim of increasing the level of protection and education of employees, and preventing adverse events. A lot of indicators are used to describe the level of safety, general or special for a particular industry. These indicators describe human aspects in safety (e.g. human activities, human errors, etc.), technical aspects (e.g. system malfunctions, reliability, availability, maintenance, etc.), and organizational aspects (e.g. hierarchy of decision making in safety, organizational procedures, safety reporting, etc.). Also, there is also a significant impact of the environment in the form of standards that apply in a particular industry (e.g. ISO, OHSAS, ANSI, IEC or HACCP standards, etc.), that are in [1] included as environmental (external) indicators.

According to [1], the following factors are taken into consideration: technical factor, human factor, organizational factor, and environmental (external) factor. The most important indicators for every factor are presented in Table 1. Some other interesting indicators can be found in [2-5].

Table 1. Safety factors and indicators

The factor	The indicators	Type
Technical	The number of safety levels	Activity
	The number of failures of technical safety systems	Outcome
	The number of accidents	Outcome
	The intensity of maintenance	Activity
	Maintenance costs	Outcome
Human	The rate of injuries	Outcome
	An index of skills of employees	Activity
	The degree of compliance with operating procedures	Activity
	Employee satisfaction index	Activity
	The number of errors and omissions	Activity
Organizational	The efficiency of safety resource management	Activity
	The share of jobs with higher risk	Activity
	The number of controls of workplace safety in practice	Activity
	The annual average number of hours of employee training	Activity
	The number of guidelines for occupational health and safety	Activity
External	The level of safety technologies	Activity
	The level of implementation of legislation	Activity
	The number of implemented voluntary standards	Activity
	The number of available databases on accidents	Activity
	The amount of available funds	Outcome

Safety indicators by themselves, whether they describe safety activities, or safety outcomes, are not sufficient to improve the safety system or the level of safety. One of the solutions to increase the efficiency of the safety system is the integration of the system.

The integration of safety systems increases the efficiency of safety resources consumption, and reduces cost and risks. The integrated safety system is important in organizations to efficiently use safety resources [6].

Lifecycle of integrated safety systems

The purpose of integrated safety system is to integrate technical systems with human resources, and to enable documented risk management. Integrated safety system conceptually means that safety is not treated as an independent entity, neither its technological nor human and organizational aspects. It requires a slightly different approach for safety interpretation, starting with the identification of activities and defining the concept of the system, its implementation or adaptation of the existing system, the continuous maintenance, improvement and development of the system.

To be able to achieve better efficiency of safety resources consumption and the highest possible level of safety, safety lifecycle was introduced. As safety system is usually treated as a complex socio-technical system, only its technical part was initially analyzed and described by means of safety lifecycle [7-11]. Safety lifecycle is and engineering process designed for systematic specification, development and optimization of a safety system. The most prominent standards that include description of safety lifecycle are IEC 61508, IEC 61511, ANSI/ISA S84 and EN 50126 [7-10].

Initially, it was applied for technical part of safety system. The lifecycle also includes the effects of the environment where this system is functioning, organizational structure that defines work activities, as well as people that perform certain activity, at least in the context of the operation and maintenance of safety instrument systems. Safety lifecycle of integrated safety system is presented in Figure 2.

The lifecycle starts with identification of goals and purpose of the system, and definition of concepts and the scope of the system. Identification of potential risks is the most important phase during the creation of safety system. The risks, cost and social responsibility are defined as the most important criteria for definition of integrated safety system [1].

Selection of key safety indicators

Analysis of the effectiveness of the safety system is based on several criteria. Multidisciplinary and interdisciplinary character of safety requires that more people participate in design, implementation, analysis and improvement of the safety system.

These processes are based on the analysis of multiple criteria (attributes or indicators), so it is natural to employ methods of multi-criteria (multi-attribute) analysis. Among others, the analytic hierarchy process (AHP) and its fuzzy extension, fuzzy analytic hierarchy process (FAHP) are applied for occupational safety decision-making problems and for determining priorities of criteria and indicators in occupational safety systems.

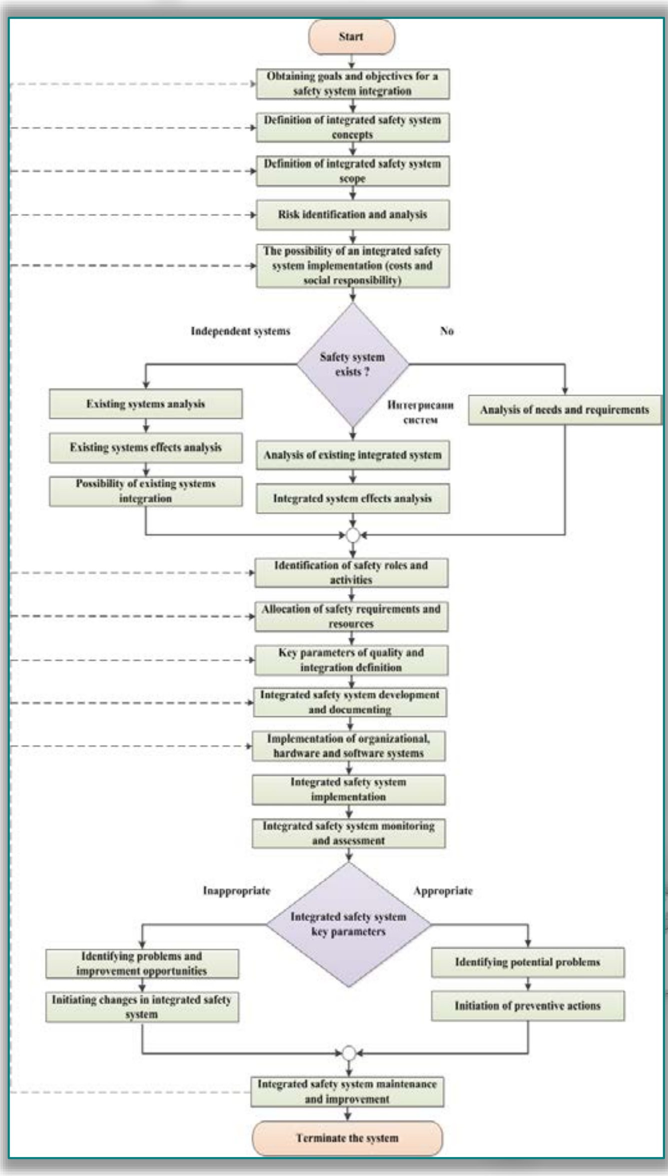

Figure 2. Safety lifecycle of integrated safety systems with safety performance assessment

It is recommended that the number of indicators is limited, so that each of the indicators could have a sufficient impact on the efficiency and effectiveness of a safety system. In [1], proposed number of key performance indicators is 20, or 5 indicators for each factor. In some situations, "less is more". The complexity of the safety system sometimes requires a larger number of monitoring indicators than proposed, or an update of the number and types of indicators that are taken into consideration when deciding on the safety system.

It is recommended that the participation of a larger number of experts in the selection of indicators. Recommended minimum number of experts is 5, to cover all social, technical and organizational aspects of a safety system.

Method of selection of appropriate indicators for evaluating the integrated system of protection under the protection of the life cycle takes place in two steps:

1. Selection of key indicators using the experts' ranking, where experts rank n indicators, assigning them ranks from 1 to n;
2. The ranking of key indicators using a method of multi-criteria analysis, by comparing the selected key indicators in pairs, or by using some other methods of identification of weights of indicators.

Table 2 shows some specific methods that can be used during the ranking of key safety indicators.

Table 2. Multi-criteria methods

Category	Weighting methods
Unique synthesizing criteria	Analytic hierarchy process (AHP), Data envelopment analysis, Fuzzy Analytic hierarchy process (fuzzy AHP), Grey relational analysis, Multi-attribute value theory (MAVT), Multi-attribute utility theory (MAUT), The Technique for Order of Preference by Similarity to Ideal Solution (TOPSIS), Utility theory additive (UTA)
Outranking	Elimination and Choice Expressing Reality (ELECTRE), Preference ranking organization method for enrichment evaluation (PROMETHEE), Organization, Rangement Et Synthese De Donnes Relationnelles (ORESTE)

In [1], it is proposed the method for selection and ranking of occupational safety indicators based on the expert evaluation method and the fuzzy analytic hierarchy process (fuzzy AHP). Also, group decision-making based on aggregation of individual judgments or individual ranks is recommended.

DISCUSSION

Safety system is a complex system that needs an engineering approach for specification, development, assessment and optimization, and continuous improvement. The main goal of the improvement process is increasing the level of safety, reducing the number of accidents, occupational injuries and illnesses related to work, and at the same time using effectively all available safety resources.

Based on the described algorithm, the existing safety systems in organization are analyzed. They can be modified, and included as parts of integrated safety system. Based on defined requirements, new roles, models of management and control, and phases are identified. More precise definition of roles, processes and safety activities simplifies implementation of organizational mechanisms and safety instrumented systems, with improved safety requirements allocation and connection with unique work processes.

Detailed development and documentation of integrated safety system becomes the most important, and also definition of key performance indicators of quality of safety system, as well as the quality indicators of the process of integration. The next step is implementation of integrated safety system. The application of the system is connected with the adequate monitoring and assessment of the system, identification and benchmarking of key performance indicators.

Inappropriate values of key performance indicators of the system affect the occurrence of adverse effects. Identification of these problems can initiate improvement and changes in the system. Even when key parameters of the system are appropriate, some leading indicators can be used for identification of potential problems and for initiating preventive activities [12]. This double confirmation mechanism is the most important in maintenance and continuous improvement of integrated safety system.

Based on identified problems, expanding the scope and purpose of the system is initiated, additional concepts are defined, and scope of the system is expanded.

Further, the possibility of realization of a modified system is assessed, the analysis of the effects of the existing system is applied, and new roles and / or phase are introduced. Also, it can be proposed the introduction of new hardware and software solutions, allocated new requests for protection and defined additional key parameters of safety and integration quality.

The ranking of key safety performance indicators is based on the AHP or fuzzy AHP method. It can be also done by applying the other methods, such as interval-based AHP method, TOPSIS, VIKOR, ELECTRE, PROMETHEE, or the combination of several methods (e.g. AHP and goal programming, or AHP and TOPSIS).

CONCLUSIONS

Industrial development has demanded changes in the safety approach, is caused by a sudden increase in risk and the number of accidents. Thus, safety approach was changed in accordance with technological challenges, to enable use of new approaches and methods of risk management. Incremental development of safety is not enough good, because it is necessary to solve certain problems immediately, regardless of the lack of prior experience on them, with a broad understanding of the potential causes and methods of prevention of adverse events.

In this paper, the integrated safety performance model based on safety indicators and safety lifecycle is presented. It is based on systems analysis and continuous improvement of integrated safety system, monitoring of key performance indicators values (leading and lagging safety indicators). Safety indicators are not enough to make adequate decisions. Some decision-making procedures and methods, based on multiple available criteria, are needed.

The main problems in safety management are limited safety resources and the existence of multiple independent systems responsible for the quality and variety of forms of safety and security (occupational safety, fire protection, environmental protection, and safety instrumented systems). A lack of coordination between these independent systems leads to inefficient use of resources, and inadequate data exchange to ignore certain potential causes of adverse events. The problem can be eliminated by applying the systems approach supported by safety lifecycle and safety benchmarking based on indirect and direct safety performance indicators, as described in presented model.

Acknowledgment: The research is a part of the projects III 44006 and III 42006, under the auspices of the Ministry of Education and Science, Republic of Serbia.

Note: This paper is based on the paper presented at The VIth International Conference Industrial Engineering and Environmental Protection 2016 – IIZS 2016, organized by University of Novi Sad, Technical Faculty "Mihajlo Pupin" Zrenjanin, in Zrenjanin, SERBIA, October 13–14, 2016.

References

[1] Janaćković, G., Savić, S., Stanković, M., Selection and ranking of occupational safety indicators based on fuzzy AHP: Case study in road construction companies, S.A. Journal of Industrial Engineering, Vol. 24, No. 3, pp. 175-189, 2013.

[2] Grabowsky, M., Ayyalasomayajula, P., Merrick, J., Harrald, J.R., Roberts, K., Leading indicators of safety in virtual organizations, Safety Science, Vol. 45, pp. 1013-1043, 2007.

[3] Louvar, J., Guidance for safety performance indicators, Process Safety Progress, Vol. 29, pp. 387–388, 2010.

[4] Øien, K., Utne, I., Herrera, I., Building safety indicators: Part 1 – theoretical foundation, Safety Science, Vol. 49, pp. 148–161, 2010.

[5] Kongsvik, T., Almklov, P., Fenstad, J., Organizational safety indicators: Some conceptual considerations and a supplementary qualitative approach, Safety Science, Vol. 48, pp. 1402-1411, 2010.

[6] Janaćković, G., Factors influencing efficient integration of safety systems, V. Conf. Human and Social Sciences at the Common Conference, Slovakia, pp.13-17, 2013.

[7] IEC 61508, Functional Safety of Electrical/Electronic/Programmable Electronic Safety-Related Systems, Geneva: International Electro technical Commission, 1998.

[8] IEC 61511, Functional safety - safety instrumented systems for the process industry, Geneva: International Electro technical Commission, 2003.

[9] ANSI/ISA S84.01, Application of Safety Instrumented Systems to the Process Industries, Int Society for Measurement & Control, Research Triangle Park, NC, 1996.

[10] EN 50126, Railway applications: The specification and demonstration of reliability, availability, maintainability and safety (RAMS) for railway applications, 1999.

[11] Janaćković, G., Savić, S., Stanković, M., Safety Lifecycle and risk assessment, In Proc. Of the 1st International Conference Life Cycle Engineering and Management ICDQM-2010, Belgrade, Serbia, pp. 255-261, 2010.

[12] Janaćković, G., Savić, S., Stanković, M., Multi-criteria decision analysis in occupational safety management systems, Safety Engineering, Vol. 1, No. 1, pp. 17-23, 2011.

ACTA TECHNICA CORVINIENSIS
– Bulletin of Engineering
Tome X [2017]
Fascicule 2 [April – June]
ISSN: 2067 – 3809

[1.]Marián HRUBOŠ, [2.]Dušan NEMEC, [3.]Rastislav PIRNÍK, [4.]Aleš JANOTA, [5.]Emília BUBENÍKOVÁ, [6.]Peter NAGY

MOBILE TWO-DIMENSIONAL LASER SCANNER USED FOR CLASSIFICATION OF OBJECTS IN THE URBAN AREA

[1-6.]Department of Control and Information Systems, Faculty of Electrical Engineering, University of Žilina, Žilina, SLOVAKIA

Abstract: The paper deals with classification of objects in the urban area, particularly road surface, facades of buildings and pole-like objects. The attention is paid to processing of three-dimensional models generated and reconstructed on the base of two-dimensional mobile laser scanning. There are different methods available to classify scanned objects; however, various shortcomings and limitations are usually identified in relation to their practical usage. Most classification methods applied to the three-dimensional models are based on range data processing. We present our three-stage classification algorithm that has been proposed and implemented with motivation to explore how range and reflectivity data could be used separately or in fusion to classify certain objects. The paper shows results of practical experiments based on real data recordings and proving usability of the proposed algorithm.
Keywords: Laser, scanning, 3D model, algorithm, classification

INTRODUCTION

Generation and reconstruction of three-dimensional (3D) models is a hot research topic in many application areas. Data collection is the first and most important step in every approach since improper selection of the measurement method can impair the whole process or make it quite impossible due to unrealizable requirements (e.g. accuracy, distance). The ideas presented in this paper are based on data collected by mobile two-dimensional (2D) laser scanning in the form of point clouds that contain information about positions of scanned points; however, nothing is known about which of the points represent and belong to particular objects. Therefore various classification approaches are being proposed and tested. Membership of the same object may be expressed in different ways, e.g. by adding a color aspect, unique signs or through points separation into the specific file. Our intention has been to propose, implement and test classification algorithms capable of identifying and extracting road infrastructure objects such as road surface, trees like objects and facades of buildings. The class of potential applications where 3D models might be used is quite wide – from a transport domain (autonomous steering, intelligent transport systems, navigation, etc.) to visualization of various environments like factories, office buildings, airport areas, critical infrastructures, etc.

State-of-Art Survey

Generation and reconstruction of 3D models of various scenes from point clouds has made a considerable progress in the recent decade. Unlike terrestrial laser scanning (characterized by high accuracy and a static way of measurement) and airborne laser scanning (characterized by a mobile way of measurement and ability to scan large land areas but with lower accuracy), the mobile laser scanning process proposes dynamic measurements with average accuracy. Differences among existing solutions result from different models uses. 2D laser scanners are usually based on a time-of-fly measurement method. The important factor influencing total velocity of mobile measurement system movements is scanning frequency and a total number of implemented scanners. Measurement systems usually combine equipment for dynamic collection of information with positioning systems. Combination of laser scanners and cameras is often motivated by intention to get as true representation of the scene as possible. An example of low-cost and portable solution to road mapping with removable sensors can be found in [1]. Combining information from a camera, scanner, digital maps and data characterizing vehicle dynamics may ensure selection of lines and road shaping (curving) [2]. The approach [3] brings laser-based detection of road edges while search for the lines is based on camera image processing. Laser scanners are also very often combined with the Global Positioning System (GPS), Inertial Navigation System (INS) and/or other devices recording moved distances (e.g. odometers). A state of the system may be estimated from measurements containing accidental errors with the help of a Kalman filter [4]. Combination of the 2D laser scanner and the GPS is also employed in accurate navigation tasks in urban environments where the satellite signal may temporarily be lost due to high buildings [5]. A 2D laser scanner, GPS-based positioning and the INS may be operated together to monitor vehicle movements and subsequently re-construct its trajectory [6]. If synchronization of multiple autonomously working devices is needed, time stamps are added to any information coming from each device [7]. Our attention is paid to classification of selected objects of the road infrastructure such as road surface, facades of buildings, pole-like objects and vegetation. Most existing approaches have the same initial step: a physical location of used components and configuration. In [8] data about movement of the mobile platform are provided by the odometer. The segmentation algorithm utilizes knowledge of properties of objects found in the scene like horizontal character of road surface, vertical character of facades of buildings or a variable shape of tree-tops and bushes (classified as scattered points). One of the very important factors used in classification may be reflectivity [9], with success rate about 95% cases. A special problem seems to be classification of pole-like objects, especially trees. An approach integrating classification data from multi-spectral image and a point cloud may use a normalized Digital Surface Model [10]. High vegetation could be detected using air-borne laser scanning [11]. Object surface properties are also considered when using a scanner with continuous waveform modulation [12]. The approach [13] consists of three steps: trees detection, simplification of a point cloud and trees modeling. Determination of height and diameter of trees may apply physical and statistic functions and data from air-borne laser scanning [14]. Extraction of pole-like objects from laser scanning data is a mature task. The method [15] is applicable only to vertical objects without an additional structure - traffic signs and trees are unrecognizable. The approach [16] proposes 4 steps to recognize objects in urban environment: localization, segmentation, extraction of contour and clusters classification, together with several alternative procedures considered for each step. Declared detection accuracy is about 65%. The algorithm [17], successful in 77% cases, expects capture of at least three parts (ovals) belonging to a detected object. Recognition of pole-like objects based on Laplace smoothing may have detection success 64% cases [18]. The approach [19], also consisting of four phases (segmentation, multiple filtering, implementation of the 2D closed circle algorithm and the classification itself), is successful in 70-79% of cases depending on a kind of detected objects. Similar methods calculating with radius of points in profiles may be found in [20]. Information about position of scanned points for classification of 'basic' objects [21] may be sufficient if fundamental object features are considered, e.g. horizontal character of road surface. A bigger problem usually comes with classification of smaller objects situated close to a road in surrounding environments (traffic signs, street lamps, billboards, tree trunks, etc.). There is no 'absolutely' reliable method for classification of pole-like objects. Every approach has its specific limitations and needs certain improvements. Table 1 shows some of typical limitations for selected methods classifying pole-like objects.

Table 1. Limits of selected methods classifying pole-like objects

Method	Limitations	Detection
[15]	Focused on rods only without associated structure	unknown
[16]	Does not work reliably if different types of objects are to be detected	65%
[17]	Requires a scanning trace in a point cloud	77%
[18]	Requires correctly segmented points	64%
[20]	Requires more than one method and needs additional information for points classification	unknown
[22]	Does not work well for thick objects such as trees	82%

The Measurement Platform

Data processed in our research have been collected by the mobile measurement platform self-developed at the home university. It is equipped with two 2D Sick laser range scanners operating at the wavelength 905 nm. One of them is the Sick LD-OEM 1000 type, which generates data processed by the proposed classification algorithm. It features a 360° field-of-view, max. adjustable angular resolution is 0.125 and a head rotational frequency is 5 Hz up to 15 Hz selectable in 1 Hz steps. For verification of measurement principles the scanning frequency is sufficient; however, for practical commercial scanning tasks a faster 2D scanner should be employed. Accuracy of the 3D model depends on precise localization of the mobile platform. It is ensured by the NOVATEL SPAN-CPT equipment, combining data from the GPS with data from the INS. Data are recorded by the server FUJITSU Primergy RX300 with 6.4TB memory capacity. Since most sensors installed at the mobile measurement platform communicate via Ethernet, the powerful CISCO switch is also needed. Visual information is obtained via 6 IP cameras that cover the whole range of the profile scanned by laser scanners. The whole system is powered by a gas generator and the backup source UPS Eaton

2200. Since all mentioned devices work autonomously and without synchronization, a special approach to data processing is needed to enable data collection and fusion. The concept is depicted in Figure 1. A point cloud is processed off-line in a personal computer due to high demands on computing power. The chosen coordinate system respects default setting of axes Z (up), Y (forward) and X (left side in relation to Y). To calculate position of a point in the coordinate system it is necessary to extract: an initial angle of scanning, final angle of scanning, angle resolution and a distance of the point measured (calculated) by the laser scanner. Individual packets are stored together with time data on packet receipt/sending; CPU time is used as a reference time. The procedure applied for data processing according to the block diagram in Fig. 1 is summarized in Figure 2 together with steps needed for data visualization.

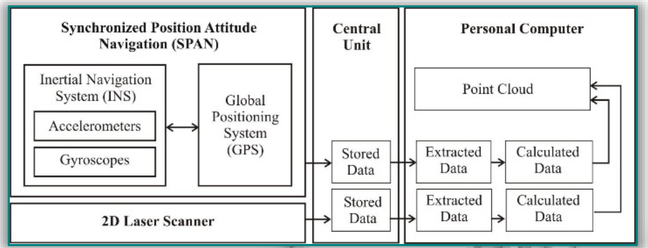

Figure 1. The block diagram of the mobile measurement platform

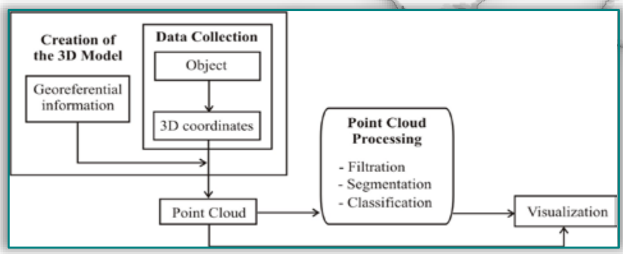

Figure 2. The principal scheme of data processing.

At the beginning raw data are available representing the measured reality. Within the following steps some operations are needed to:

- Remove unnecessary or faulty data;
- Distribute points into groups based on their membership to the same objects;
- Classify objects on the base of their position in the space (according to spatial coordinates);
- Interpret a point cloud in a graphical form.

THE CLASSIFICATION ALGORITHM

Mobile laser scanning achieves average accuracy if compared with methods of air-borne and terrestrial laser scanning. Differences exist in a way of points processing. A point cloud may be processed as a whole or in parts. The minimum item to be processed is one scanned profile or its quadrant. Sequential processing of the profile (one after another) is more advantageous since one may use information about position of points in the profile which may be unworkable in processing of a final point cloud. In some cases it may be profitable to combine or entirely substitute information about coordinates of each scanned point with information about intensity of reflected laser beam (reflectivity). There are multiple factors that influence the final reflectivity values: distance, incidence angle, structure of the surface, color, atmospheric conditions, etc. All these individual factors act at the same time but definition of their mutual dependency is rather difficult or impossible. Therefore, for practical reasons we have decided to apply only those of them whose effects were proved to be unambiguous enough and whose occurrence may be assumed, tested and understood for constant levels of other effects. Getting a value of reflectivity of the particular point while effects of other factors are ignored is for the classification purpose meaningless. Thanks to information about position of each scanned point attenuation caused by distance can be corrected and theoretically one could assume what an incidence angle is. Unfortunately, information about other factors such as object color and/or surface structure is not available despite it may significantly change the final value of reflectivity. Therefore it has no sense to observe reflectivity values only in one scanned profile. Our experiments showed us that a series of consecutive values of reflectivity obtained within several adjacent profiles can provide an added value. Thus our classification method uses intensity of reflected laser beam as additional source of information. Certain types of objects are classified sequentially, with the objects being represented by the most points first. The final algorithm we have created and present in this paper has three stages as shown in Figure 3.

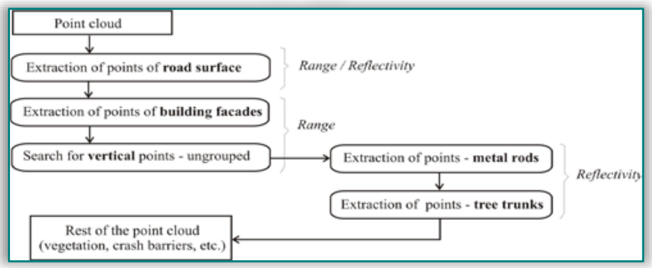

Figure 3. A concept of the three-stage classification algorithm

The principle applied in every stage results from the idea that the points that have already been processed and assigned to a certain object are not used any more. They are removed and saved to a separate file. This step brings a significant decrease of further demands on computing power and processing time. The method processes measured points in one profile after another but in several cases more profiles are being processed at once.

Road Surface

Generally, road surface could be identified based on range data, i.e. data representing measured distance from a laser head to scanned points. Unlike most other objects, road surface has typically a horizontal character.

This fact might be applied to histogram of the scanned profile where Y-axis represents frequency (number of occurrences) of the points. The spike part of the histogram then corresponds to amount of points lying in the plane representing road surface. Then one may segment all the points that are adjacent to the spike of the histogram. However, this approach fails at the moment when road surface is not spatially bounded (by road curbs, ditches, etc.) and smoothly goes to a lawn, pavement or parking area as shown in Figure 4. In those cases road edges create only slight surface irregularities (1-2 cm) which are hardly recognizable by the time-of-flight method.

Figure 4. Undistinguished spatial ends of road surface in the point cloud and the real scene (taken from a different view).

Measured points do not clearly indicate where the end of road surface is and where the parking area starts. Unlike range data processing, changes in surface material, its structure and/or color may result in changes of surface reflectivity. Considering this principle we have designed a method for extraction and classification of points belonging to road surface. When recording data the scanner head is located approximately 1.2 m above road surface. It is reasonable to take location of road surface points into considerations before reflectivity analysis is performed. The only relevant and meaningful sectors are quadrants I and IV. Processing of data from other quadrants would uselessly load the computing power. The same structure of surface will be manifested by expected reflectivity values (Figures 5 and 6). Any change of reflectivity will bring change of span and measured values.

Contrast between dark road surface and white reflex color may be used to detect an edge of the road or to extract points of horizontal traffic markings (Figure 7). Significantly visible line at the road border is easy detectable within one profile representation - see it in the marked area of Figure 8. Our classification algorithm preferably uses reflectivity values. If no striking change of line representation is detected, the way of classification is as follows (Figure 9).

Processing of points located in the quadrant I:

» The initial value (for normal incidence of the beam) and other values are used to calculate an average value of reflectivity;
» We observe an increment of the value of reflectivity for gradual increase of angle of the scanner head. Thus information about consecutive points is available;
» Change of the road surface structure is characterized by changes of reflectivity values of the whole group of points. In that place a limit angle is being determined;
» Points being below the limit angle are grouped to the 'road object' and removed, others will be kept for further processing.

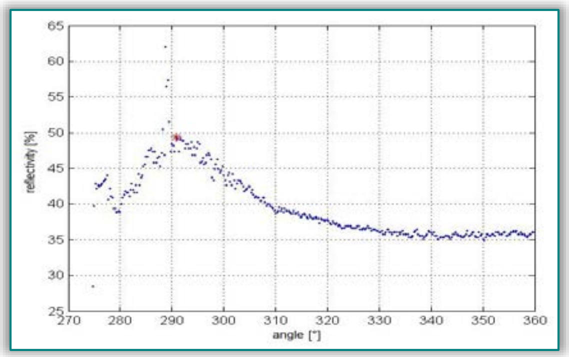

Figure 5. Reflectivity values measured in the quadrant I.

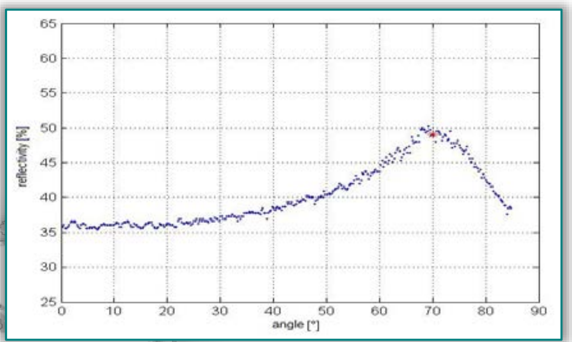

Figure 6. Reflectivity values measured in the quadrant IV.

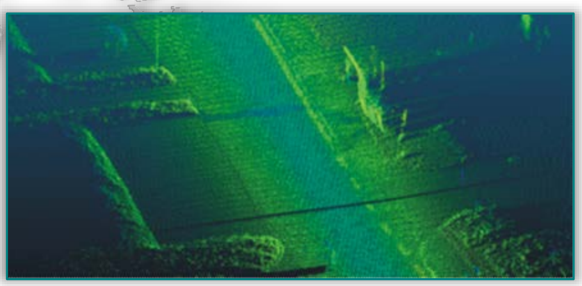

Figure 7. A point cloud with color-distinguished reflectivity.

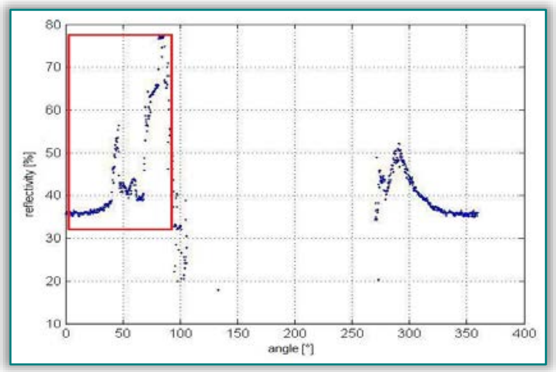

Figure 8. Reflectivity values in the profile

Processing of points located in the quadrant IV: unlike the procedure applied in the quadrant I, points with the greater angle are extracted as road surface points, others will be processed in next steps of the classification algorithm. Finally, all points belonging to road surface are removed and extracted to a separate file.

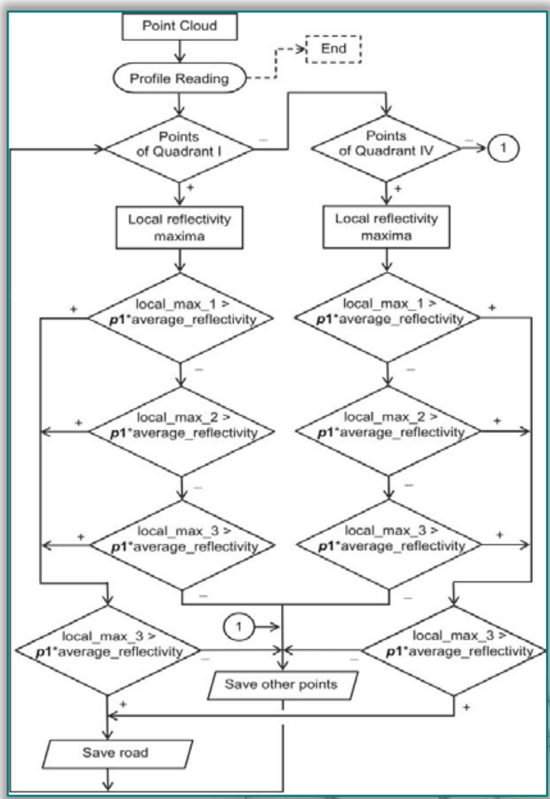

Figure 9. Algorithm for extraction of points representing road surface

Facades of Buildings

In the analyzed environment we may find a lot of vertical objects such as facades of buildings, lamp poles, vertical traffic signs or tree trunks. Facades of buildings have typically greater surface in Z-axis. We propose creation of the histogram that shows frequency of X-coordinates in the given profile (Figures 10 and 11). Vertical objects have typically a lot of values contained in a short interval. To avoid extraction of points belonging to different objects, it is necessary to consider several consecutive profiles.

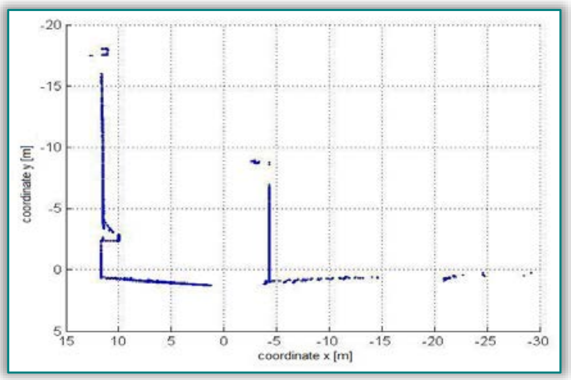

Figure 10. 2D-view at 5 scanned profiles of the building surface.

Classification of facades is based on range data since facades are very often rugged, with a various structure and different colors. Thus reflectivity is very accidental and does not create any assumable structures.

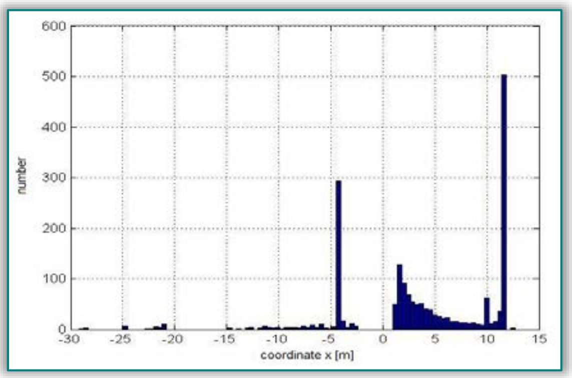

Figure 11. The histogram of coordinates occurrence.

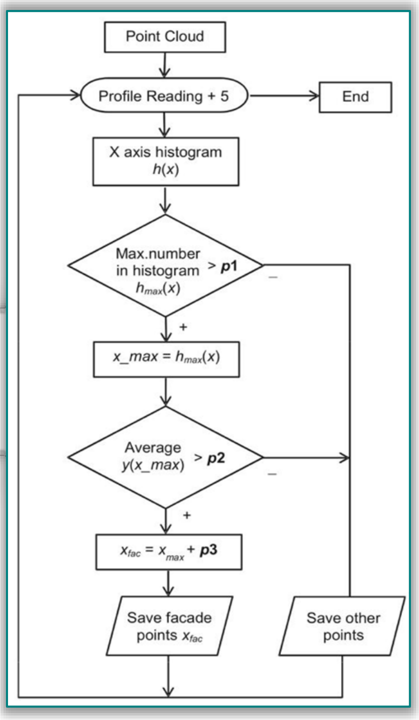

Figure 12. Algorithm for extraction of building facades

The proposed classification procedure (Figure 12) consists of several steps:

- » Creation of the histogram of X-coordinates and determination of the coordinate having the maximum number of points;
- » If the maximum number corresponds to the minimum required value of the number p1, the average value Y (height) at the value X may be determined;
- » If the average value Y fulfills condition of the minimum value p2, points found inside the surrounding area defined by p3 are extracted and saved as points belonging to the building facade.

To get the best results we must define constants p1, p2 and p3 and make decision on how the histogram is to be divided (for how many values) and how many profiles should be processed together when classifying one profile. In our case all these settings have been done experimentally.

Pole-like Objects

The third stage of the proposed algorithm enables processing of the rest of points and search for pole-like objects. Figure 13 illustrates what kinds of objects may be included - tree-tops, tree trunks, a lamp, benches or car profiles. The significant landmarks are objects that probably represent the poles of street lighting and objects representing tree trunks. Considering accuracy of time-of-flight method, we are not able to rely only on range data to distinguish between tree trunks and traffic signs situated inside vegetation. Using reflectivity values, it is possible to identify objects having the same surface characteristics. Rods of traffic signs or street lamps are made of metal, with flat surface and the same structure. On the other side, structure of tree trunks is variable, containing various cracks and irregularities causing accidental reflection. Several consecutive reflectivity values do not create any dependency. To illustrate the situation Figure 13 shows two adjacent objects being close to each other (marked inside the picture). If we compare scanned profiles from the viewpoint of range data (Figures 14 and 15), there is no chance to distinguish between a tree trunk and rod.

Figure 13. Example of the point cloud after extraction of road surface and building facades

Combining information on vertical character and reflectivity of a group of points we can identify objects with the same surface structure. These most probably represent rods of traffic signs or street lamps. The same profiles processed on the base of reflectivity values (Figures 16 and 17) show that points representing rods are mutually located in a relatively narrow range of values while points representing tree trunks are distributed accidentally.

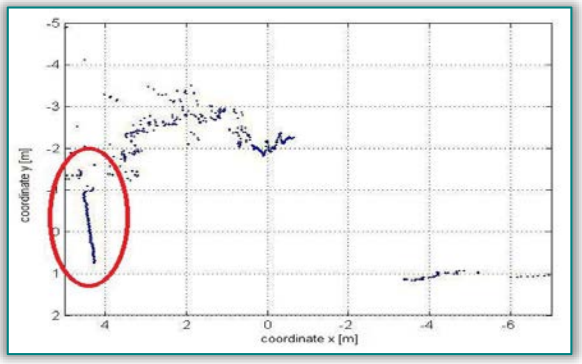

Figure 14. Scanned profiles with a marked tree-trunk

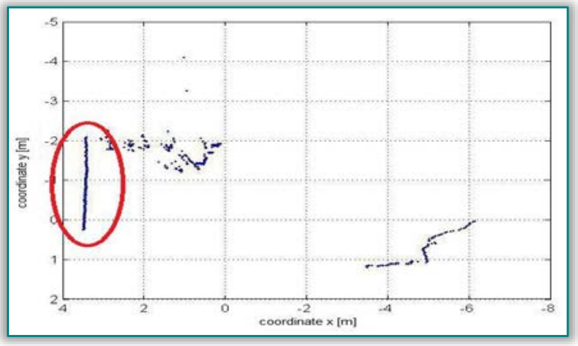

Figure 15. Scanned profiles with a marked metal rod

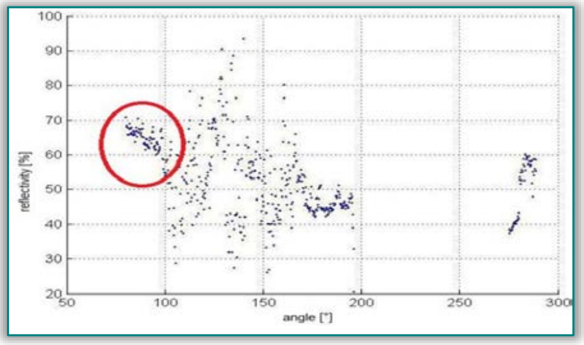

Figure 16. Reflectivity of points representing a tree trunk

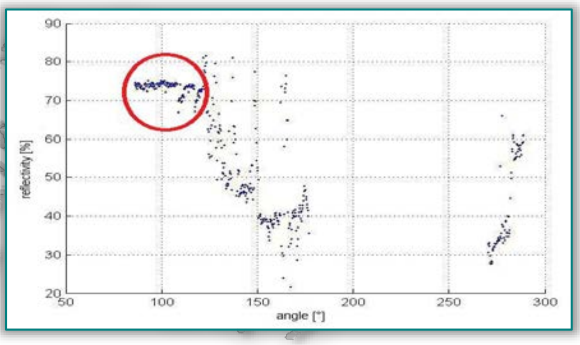

Figure 17. Reflectivity of points representing a rod

The classified tree trunk has been several times wider than the rod but considering an average distance between scanned profiles (ca 20 cm) it has been captured in one pro-file only. Based on deeper analysis of curves obtained from reflectivity measurements we have defined the basic classification between tall pole objects (poles of street lamps, poles of trolley-lines) and short ones (rods of traffic signs). A tall object is captured during one scan standardly along the whole length which gives a sufficient number of points for processing (Figures 19 and 20). Smaller and thinner objects are captured as if diagonally distributed which creates a specific shape. At the edge most of the laser beam is reflected to surrounding environment, in the middle the maximum value is obtained. This feature may be used for classification, too. Points in the profile are approximated to a curve. The result is a second-degree polynomial evaluated for the constant en-try. For a lack of sufficient data samples this approach is still under our development.

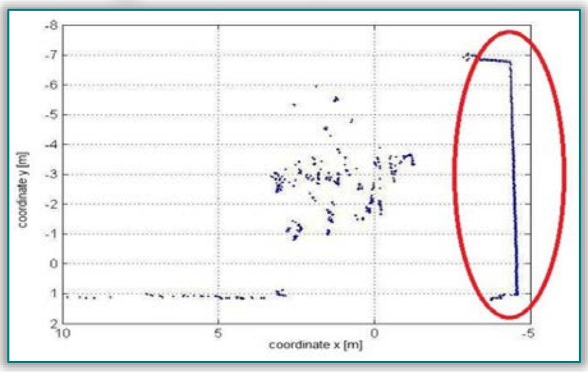

Figure 18. The profile representing grass, tree-top and a lamp

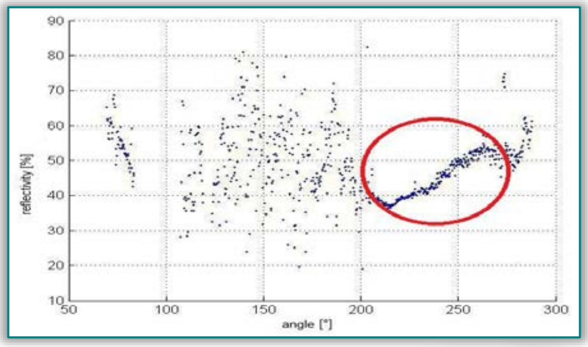

Figure 19. Reflectivity values with marked points belonging to the lamp pole

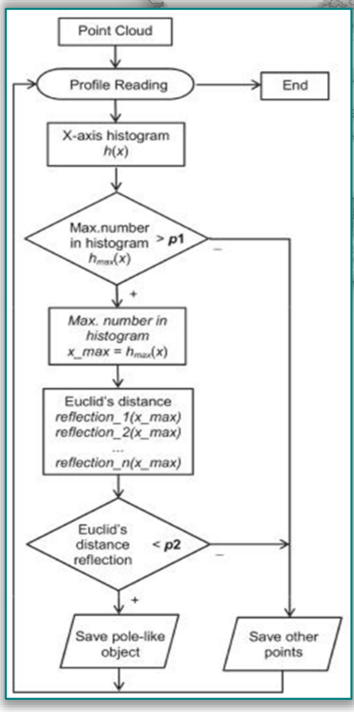

Figure 20. The procedure for extraction of pole-like objects

The classification procedure (Figure 20) is focused on taller pole-like objects:

» Creation of the histogram of X-coordinates and determination of coordinates having a maximum number of points;
» If the maximum number corresponds to the minimum required number p1, determination of the average value Y (height) for the X value;
» Gradual computation of Euclidean distance of reflectivity values expressed in dependency on the angle for vertical points;
» Classification of points having a lower mutual distance than p1 as pole objects.

Next steps focused on classification of other identifiable objects (tree-tops, bushes, vegetation) are not presented here. They may be based on analysis of range data, quadrants II and III, followed by analysis of diffuseness of reflectivity data caused by various positions of leaves. Finding clusters with expected features may result in identification of tree-tops.

CLASSIFICATION ALGORITHM TESTING

The proposed algorithms have been tested using real data obtained by the mobile measurement platform. To maximally eliminate inaccuracy of the final model classification is performed before integration of other data considering all axial inclinations and the altitude. As a representative example we can show a point cloud of a part of the university campus (Fig. 21). At the parking area we can see poles of street lamps, some parts of traffic signs and other objects (cars, waste containers). The route of the mobile platform movement is recognizable through the highest density of the scanned points. Before classification itself the points were filtered from a distance-based point of view. The higher distance of scanned points is, the higher inaccuracy occurs due to vibrations. Therefore, despite the fact that the scanner is ranged up to 200 m, all points located in a distance greater than 30 m from the scanner head have been filtered out.

Classification of Road Surface

Comparing a distance of the scanner head to road surface with distances to other objects, it is clear that just points of road surface are the most represented points in the obtained cloud. They represent more than half of all scanned points. From the quantitative point of view sequential analysis of profiles and points contained in them is most demanding computing power among all proposed sub-algorithms. The model presented here has contained fewer than 630 000 points (size of the text file 24 MB) and its processing lasted about 1 hour (DELL studio, CPU: i7 Q720 1.6 GHz, RAM 4GB, MS Windows 7). As mentioned earlier, road surface is identified through significant changes of reflectivity caused by changes of the surface structure. The first change found near road edge may be caused by presence of the white line as a part of the road traffic marking. It is detectable very well. In comparison with the black asphalt significant increase of reflectivity can be observed. If the white line is missing, surface of a different material (in our case grass and paving) causes changes of reflectivity (decrease, increase, or scattering). The edge may not be defined strictly. Sometimes places with undetectable transition may appear in the analyzed scene. Then the algorithm also classifies those points as not belonging to road surface (Fig. 22).

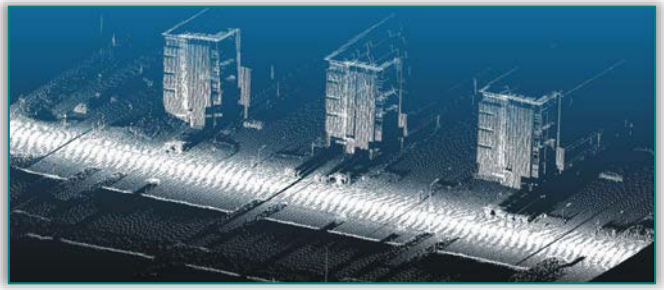

Figure 21. A cloud of non-classified filtered points.

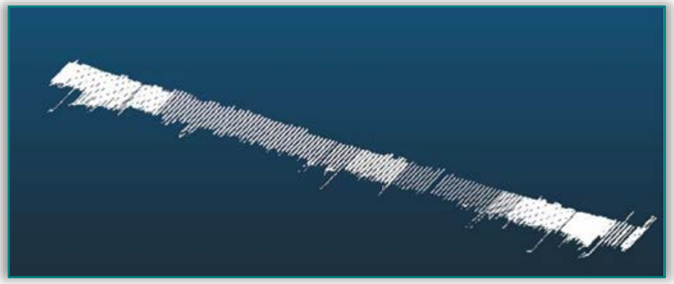

Figure 22. Extracted points representing road surface.

Classification of Building Facades

A new point cloud (Figure 23) is significantly smaller. Thanks to that its off-line processing is faster (for the given example ca 20 minutes). As described earlier, classification is based on range data processing. As far as the constants are concerned their values have been experimentally set to the following values:

» p1 - the best results have been obtained for the limit value 700 (to avoid interchange of trees and lamps);
» p2 - an average height of the object was set to 4 m (to eliminate close and densely covered objects);
» p3 - a range around the maximum X coordinate is 1 m; this value considers various juts (windows, window sills).

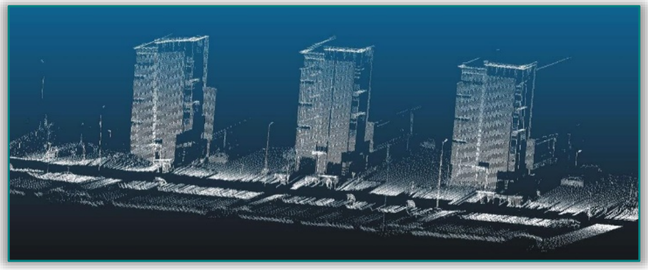

Figure 23. A cloud of points after road surface removal

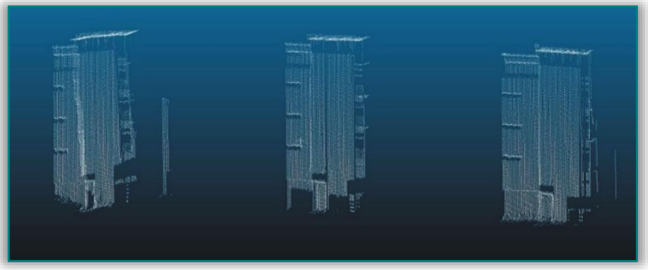

Figure 24. Extracted points representing building facades

For large and relatively flat surfaces the algorithm works reliably. Most of the points belonging to building facades is correctly identified and extracted (Figure 24). The applied approach defines one potential coordinate with facade appearance (using a group of profiles) per one profile. In the case of two buildings standing against each other only that one with a larger number of points contained in a plane would be detected. The procedure for multilevel processing has not been included yet. The points situated at edges of a detected building or outside the tolerance interval of the determined X-coordinate do not fulfill condition for assignment to building facades and will be put into the file for further processing (Figure 25).

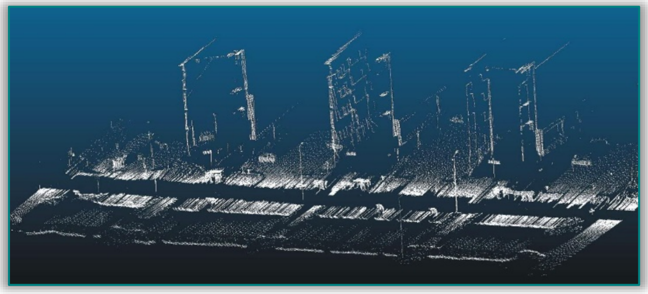

Figure 25. A cloud of points after facades extraction

Classification of Pole-like Objects

After removal of building facades the cloud contains points representing mostly smaller objects (Figure 25). Through internal setting (histogram range, Euclidean distance) the algorithm has been adapted to identify and classify taller objects that are captured in a sufficient range. Narrow rods of traffic signs have been during the test captured only partially. Therefore information about their position and reflectivity is incomplete what makes their classification under considered conditions impossible.

Close to the trajectory of the mobile laser scanner there are three poles and at the next row of parking places another two ones. Focusing on wider objects the algorithm has been able to extract three of them. Relevant points have been automatically saved to a separate file (Figure 26). Two poles situated in a distance slightly lower than 30 m have not been classified. Point coverage has not been sufficient to fulfill conditions for extraction. It results from algorithm parameters settings.

Figure 26. Extracted points representing poles of street lamps

CONCLUSIONS

The proposed classification algorithms have been developed within the research project and tested on multiple 3D models generated for different road infrastructure environments. The main advantages of the proposed approach as mentioned in the paper are preferential use of range data or reflectivity data or both for different classification tasks. The main disadvantage results from the fact that if a set of points representing the given object is not sufficient, the object is not classified. This problem is typical for classification methods based on range data processing. Static test measurements of pole-like objects provide excellent results also for smaller objects (e.g. rods of traffic signs). Problems have been identified only if surface has been damaged or color has been varying. Classification of facades works perfectly for large plane surfaces. However, rather bad results appear if the building with a complicated structure has been obliquely oriented. Our future research will be oriented to fuse point clouds with visual information - images obtained from cameras integrated in our mobile measurement platform.

Acknowledgment

This work was supported by Slovak Research and Development Agency under the project No. APVV-15-0441

Note

This paper is based on the paper presented at The 11th International Conference ELEKTRO 2016, organized by University of Žilina, Faculty of Electrical Engineering, in Štrbské Pleso – High Tatras, SLOVAKIA, May 16–18, 2016**References**

[1.] Z. Huijing, Ch. Yuzhong, S. Ryosuke, An efficient extrinsic calibration of a multiple laser scanners and cameras' sensor system on a mobile platform. In Proceedings of the IEEE Intelligent Vehicles Symposium. Istanbul (Turkey), 2007, p. 422–427.

[2.] M. Tsogas, N. Floudas, P. Lytrivis, et al. Combined lane and road attributes extraction by fusing data from digital map, laser scanner and camera. Information Fusion, 2011, vol. 12, issue 1, p. 28–36. ISSN: 1566-2535.

[3.] A. Huang, D. Moore, M. Antone, et al. Finding multiple lanes in urban road networks with vision and lidar. Auton Robot, 2009, vol. 26, issue 2-3, p. 103–122. ISSN: 0929-5593. DOI: 10.1007/s10514-009-9113-3

[4.] G. Welch, G. Bishop An introduction to the Kalman filter. 2006, TR95-041, 16 pages. [Online] Cited 2015-03-30. Available at: http://www.cs.unc.edu/welch/media/pdf/kalman intro.pdf

[5.] J. Peng, El Najjar M.E., C. Cappelle A novel geolocalisation method using GPS, 3D-GIS and laser scanner for intelligent vehicle navigation in urban area. In Proceedings of the International Conference on Advanced Robotics ICAR, Munich (Germany), 2009, p. 1–6. ISBN: 978-1-4244-4855-5.

[6.] M. Joerger, B. Pervan, Range-domain integration of GPS and laser-scanner measurements for outdoor navigation. In 19th International Technical Meeting of the Satellite Division of the Institute of Navigation (ION GNSS 2006), Fort Worth, TX (USA), 2006, p. 1115–1123.

[7.] A. Soloviev Tight coupling of GPS, laser scanner, and inertial measurements for navigation in urban environments. In Proceedings of the Position, Location and Navigation Symposium IEEE/ION, Monterey (Canada), 2008, p. 511–525, eISBN: 978-1-4244-1537-3, print ISBN: 978-1-4244-1536-6. DOI: 10.1109/PLANS.2008.4570059

[8.] I. Abuhadrous, S. Ammoun, F. Nashashibi, et al. Digitizing and 3D modeling of urban environments and roads using vehicle-borne laser scanner system. In IEEE/RSJ International Conference on Intelligent Robots and Systems (IROS 2004), 2004, vol. 1, p. 76–81. DOI: 10.1109/IROS.2004.1389332

[9.] J.X. Hang, X.G. Lin Object-based classification of urban airborne lidar point clouds with multiple echoes using svm. ISPRS Annals of the Photogrammetry, Remote Sensing and Spatial Information Sciences, 2012, vol. I-3, p. 135–140. ISSN: 1682-1750.

[10.] N. Haala, C. Brenner Extraction of buildings and trees in urban environments. ISPRS Annals of the Photogrammetry & Remote Sensing, 1999, vol. 54, no. 2-3, p. 130–137.

[11.] M. Rutzinger, N. Pfeifer Detection of high urban vegetation with airborne laser scanning data. In Proceedings of ForestSat'07, 2007, Montpelier (France), 2007, 5 p. on CD.

[12.] A.T. Darmawati Utilization of multiple echo information for classification of airborne laser scanning data. MSc Thesis, Enschede (the Netherlands): International Institute for Geo-Information Science and Earth Observation (ITC), 2008, 77 p.

[13.] M. Rutzinger, A.K. Pratihast, O.S. Elberink, et al. Detection and modelling of 3D trees from mobile laser scanning data. International Archives of Photogrammetry, Remote Sensing and Spatial Information Sciences, 2010, vol. 38, part 5, p. 520–525.

[14.] X. Yu, J. Hyyppa, M. Vastaranta, et al. Predicting individual tree attributes from airborne laser point clouds based on the random forests technique. ISPRS Journal of Photogrammetry and Remote Sensing, 2011, vol. 66, issue 1, p. 28–37. DOI: 10.1016/j.isprsjprs.2010.08.003

[15.] C. Brener Advances in GIScience. Lecture Notes in Geoinformation and Cartography (Extraction of features from mobile laser scanning data for future driver assistance system). Berlin-Heidelberg (Germany): Springer-Verlag, 2009, p. 25-42. ISBN: 978-3-642-00317-2. DOI: 10.1007/978-3-642-00318-9-2

[16.] A. Golovinski, V. Kim, T. Funkhouser Shape-based recognition of 3D point clouds in urban environment. In 12th International IEEE Conference on Computer Vision, 2009, p. 2154–2161. ISBN: 978-1-4244-4420-5. DOI: 10.1109/ICCV.2009.5459471

[17.] M. Lehtomaki, A. Jaakkola, Hyyppä, et al. Detection of vertical pole-like objects in a road environment using vehicle-based laser scanning data. Remote Sensing, 2010, vol. 2, no. 3, p. 641–664. ISSN: 2072-4292. DOI:10.3390/rs2030641

[18.] H. Yokoyama, H. Date, S. Kanai, et al. Pole-like objects recognition from mobile laser scanning data using smoothing and principal component analysis. ISPRS – International Archives of the Photogrammetry, Remote Sensing and Spatial Information Sciences, 2011, vol. XXXVIII-5/W12, p. 115–120. DOI: 10.5194/isprsarchives-XXXVIII-5-W12-115-2011

[19.] M. Vakautawale Information Extraction from Mobile Laser Scanner for Inventory Application. MSc Thesis, Enschede (the Netherlands): University of Twente Faculty of Geo-Information and Earth Observation (ITC), 2010, 63 p.

[20.] S.I. Ee-Halawany, D.D. Lichti, Detection of road poles from mobile terrestrial laser scanner point cloud. In International Workshop on Multi-Platform/Multi-Sensor Remote Sensing and Mapping (M2RSM). Xiamen (China), 2011, p. 1–6. ISBN: 978-1-4244-9402-6. DOI: 10.1109/M2RSM.2011.5697364

[21.] I. Stamos, O. Hadjiliadis, Z. Hongzhong, et al. Online algorithms for classification of urban objects in 3D point clouds. In 2nd International Conference 3D Imaging, Modeling, Processing, Visualization and Transmission (3DIMPVT). Zurich (Switzerland), 2012, p. 332–339.

[22.] S. Pu. Advances in 3D Geoinformation Systems (Automatic building modeling from terrestrial laser scanning). Berlin (Germany): Springer-Verlag, 2008, p. 147-160. ISBN: 978-3-540-72134-5. DOI: 10.1007/978-3-540-72135-2 9

ISSN:2067-3809

ACTA TECHNICA CORVINIENSIS
– Bulletin of Engineering
Tome X [2017]
Fascicule 2 [April – June]
ISSN: 2067 – 3809

[1.]Ali M. ELTAMALY, [2.]Yehia SAYED, [3.]Amer Nasr A. ELGHAFFAR

POWER FLOW CONTROL FOR DISTRIBUTION GENERATOR IN EGYPT USING FACTS DEVICES

[1.] Electrical Engineering Department, Mansoura University, Mansoura, EGYPT
[2,3.] Electrical Engineering Department, Minia University, Minia, EGYPT

Abstract: A purpose of power flow studies is to minimize the power distribution losses and the cost of power drawn from the substation, without affecting the voltage regulation. The current electrical power needs are increasing rapidly in line with technological developments. Optimal Power Flow (OPF) problem is to optimize a certain objective over power network variables under certain constraints. The variables may include real and reactive power outputs, bus voltages and angles, the objective may be the minimization of generation cost or maximization of user utilities and the constraints may be bounded on voltages or power levels, or that the line loading not exceeding thermal or stability limits. Optimal reactive power dispatch problem as a sub-problem of the Optimal Power Flow (OPF) is a very important optimization problem in power systems as proper management of reactive power injection into the power system can minimize losses in real power, voltage deviations and save voltage stability. The power system uses the simplified symbol such as a one-line diagram, per-unit system, moreover direct on various regard of alternating current power parameters, such as voltages, voltage angles, active power and reactive power. Researchers studied many different solutions have been proposed to solve the OPF problems. This paper presents a survey for Flexible Alternating Current Transmission Systems (FACTS) that can consider for OPF in power system.
Keywords: Power System, OPF, FACTS

INTRODUCTION

The current electrical power needs are increasing rapidly in line with technological developments. This electrical power needs the increase in contrast with depletion of the energy sources availability of oil and coal [1]. Optimal Power Flow (OPF) problem is to optimize a certain objective over power network variables under certain constraints. The variables may include real and reactive power outputs, bus voltages and angles, the objective may be the minimization of generation cost or maximization of user utilities and the constraints may be bounded on voltages or power levels, or that the line loading not exceeding thermal or stability limits [2].

Researchers studied many different solutions have been proposed to solve the OPF problems for examples; using advanced power converter technologies [3], a stand-alone Renewable Energy (RE) system based on Energy Storage (ES) [4], multi-objective Evolutionary Algorithm (EA) for high levels of penetration from Distributed Generations (DG) [5]. Gravitational Search Algorithm (GSA) is proposed to find the optimal solution for optimal power flow (OPF) problem in a power system [6], using the Jaya Algorithm (JA) one from methods that's used with OPF [7] and realized OPF problem by means of Particle Swarm Optimization (PSO) algorithm with consideration Static Var Compensation (SVC) system and Static Synchronous Compensator (STATCOM) [8].

OPF PHYSICAL CONSTRAINTS

OPF includes any optimization problem which seeks to optimize the operation of an electric power system (specifically, the generation and transmission of electricity) subject to the physical constraints imposed by electrical laws and engineering limits on the decision variables [9] [14]. Since power flow is considered under steady state balanced condition, a positive sequence model of the power grid is adopted for power flow solution [10].

The basic equation for power flow analysis is derived from the nodal analysis equations for the power system,

OPF constraints may be categorized into equality constraints and inequality constrain [15].
OPF formulations incorporating the AC power flow show in equations (1), (2) are both nonlinear and non-convex for N bus power system [11].

$$P_i = \sum_{j=1}^{n} |Y_{ij}||V_i||V_j| \cos(\theta_{ij} + \delta_j - \delta_i) \qquad (1)$$

$$Q_i = \sum_{j=1}^{n} |Y_{ij}||V_i||V_j| \sin(\theta_{ij} + \delta_j - \delta_i) \qquad (2)$$

FACTS SYSTEM CLASSIFIED

It is well documented that the planning and the optimum operation of an electrical system involve developing evolution scenarios of the electrical energy requirement such as installation and implementation of FACTS controllers [9].
The purpose of FACTS controllers is to facilitate the supply of loads inflexible and rapid fashion while providing optimal management of electrical networks. Voltage problems can constrain transfers and can result in more blackouts than first-swing instability, poor damping, and thermal overloads combined.
Today, heavily utilized transmission systems may require more MVAR of compensation for each MW of new load to survive single contingencies without voltage collapse. Reactive power planning and operations are very complex. Most system planners develop rules to define limits to system loading, determine constrained interface limits and demonstrate the steady state effect of system modifications.
For a variety of generation dispatches, the limiting contingency could be different and the cause of the transmission limitation could vary among voltage, dynamic stability, or thermal restrictions. Furthermore, different pricing considerations would change the magnitude and economic value of bottled energy.
Based upon each scenario, the transmission planner could propose shunt capacitors, power system stabilizers, transmission line upgrades (including phase angle regulators), FACTS controllers, or combinations of improvements.
The likelihood of each case scenario would then need to be considered to formulate a final plan [12]. The variables in power system depend on the type of busses that's simulating with FACTS devices. Each bus in power system can be classified as:

» **Load bus (P-Q bus)**

Buses without generators are defined a load busses, they generated active power P, and reactive power Q, are taken as zero. The load drawn by these buses are simulated by active power (P) also reactive power (Q) in which the negative sign contains the power flowing out of the bus. So this bus is referred to as P-Q bus [10].

» **Generator bus**

This is a sources bus that's generators are connected. The active power and voltage magnitude are specified in this bus, while the reactive power and phase angle require calculating [10]. This bus also the voltage magnitude is kept without changes by setting field current of the synchronous generator.
In another hand, if this bus has a renewable energy source as solar or wind energy, it's controlled through a prime mover while voltage is controlled through the generator excitation. By keeping input power constant through turbine governor control and fixing bus voltage by using Automatic Voltage Regulator (AVR) system. Reactive power supplied by the generator depends on the system configuration logic. By increasing the prime mover's governor set points increases the power that generator supplies to the power system [10].

» **Slack bus (Swing or reference Bus)**

This is an arbitrarily-selected bus a special generator bus serving as the reference bus for the power system. Its voltage is assumed to be fixed in both magnitude values, phase angle and simulated by per unit value ($1\angle 0^{\circ}$ Pu), in slack bus P and Q are unknown.

OPF SOFTWARE SIMULATION

OPF can be simulate by programming software as example using World Power Simulator (WPS) and power system simulator, figure (1) shows single line diagram using WPS software for simulate OPF by the values of voltage magnitude, voltage angle, active power and reactive power for a design 6 bus which depend on 14-Busses IEEE standers.

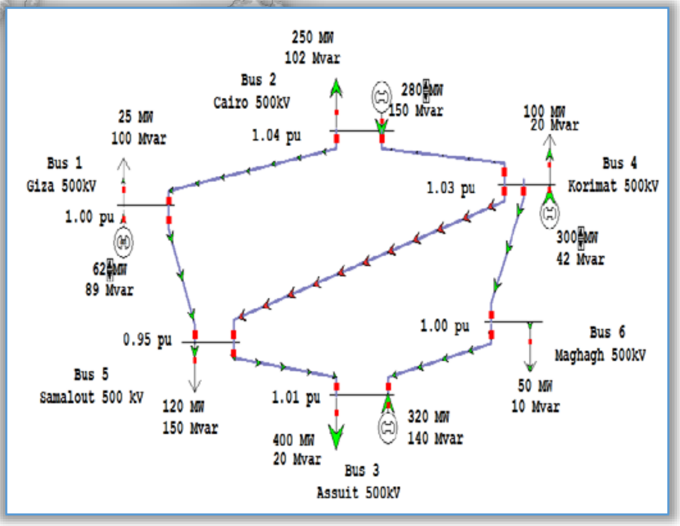

Figure 1. Single line diagram for small electrical grid OPF simulator

Table (1) shows the data for busses in the system, by start the system to simulate energizing busses its will show the optimum operation for the voltage, voltage angle, the output active power and output reactive power from generators. The results showing in table (2) and table (3).

Table (1) Data for busses in the system

Bus No.	Name of Bus	Types of Bus
Bus 1	Giza 500kV	Slack Bus
Bus 2	Cairo 500 kV	Generator Bus
Bus 3	Assuit 500kV	Generator Bus
Bus 4	Korimat 500kV	Generator Bus
Bus 5	Samalout 500 kV	Load Bus
Bus 6	Maghagha 500kV	Load Bus

Table (2) Data for Busses Loads with generator Bus

No of Bus	Name of Bus	Load - MW	Bus Load Mvar	Gen MW	Gen Mvar
Bus 1	Giza 500kV	25.0	100.00	61.72	88.87
Bus 2	Cairo 500kV	250.0	102.00	279.65	150.09
Bus 3	Assuit 500kV	400.0	20.00	320.00	140.11
Bus 4	Korimat 500kV	100.0	20.00	300.00	41.55
Bus 5	Samalout 500kV	120.0	150.00	-	-
Bus 6	Maghagha 500 kV	50	10.00	-	-

Table (3) Data for Voltage magnitude and Voltage angle

No of Bus	Name of Bus	Bus Nom kV	Bus PU Volt	Bus optimal Volt (kV)	Bus Angle (Deg)
Bus 1	Giza 500kV	500.00	1.00000	500.000	0.00
Bus 2	Cairo 500kV	500.00	1.04000	520.000	0.55
Bus 3	Assuit 500kV	500.00	1.01000	505.000	-6.47
Bus 4	Korimat 500kV	500.00	1.03000	515.000	0.89
Bus 5	Samalout 500kV	500.00	0.95363	476.815	-2.58
Bus 6	Maghagha 500 kV	500.00	1.00460	502.300	-3.79

APPLICATION TO ADD FACTS CONTROLLERS

FACTS is a transmission system which use reliable high-speed thyristor based high-speed controllable elements such as SVC, TCSC, and UPFC etc. [16]. Are designed based on state of the art developments in power semiconductor devices.

Issues include increased utilization of existing facilities such as secure system operation at higher power transfers across existing transmission lines which are limited by stability constraints, the development of control designs for FACTS devices, and determination of functional performance requirements for FACTS components [13].

The maximum benefit from a FACTS Controller is obtained when its use is coordinated with other transmission equipment. This requires that the utility applying the controller consider the information infrastructure and communications required for this coordination. It also requires decisions made with system operators about defining reference values for the FACTS Controllers and switching procedures for conventional transmission equipment (tap changing transformers, switched capacitors, etc.)

An important activity that must be part of the application is an estimate of the functional reliability of the overall system and specific analysis that shows the security of the system considering possible malfunctions of portions of the coordinated control. An important part of the application to add FACTS Controllers to a transmission system is the functional specification for the Controller.

In addition to the ratings and standards requirements there are several considerations that may be unique to FACTS Controllers [17]. These include the communication interfaces with the system, the level of automation in the substation and coordination of substation switching equipment and relays. Some utilities also standardize the symbols used to depict equipment in graphical displays and the acronyms and abbreviations used in all printed documents.

This equipment includes substation event recorders that are invaluable for both documenting the benefit of FACTS Controllers and diagnosing control and protection issues. A careful determination of how much of this equipment is to be supplied with the FACTS Controller and how much will be added by the utility greatly enhances both the acceptance and usefulness of FACTS products [12] [18].

CONCLUSION

The proposed of study OPF with FACTS by different techniques to updates and new plans level of Conventional Generation (CG). FACTS can provide control of voltage magnitude, voltage phase angle and impedance. Therefore, it can be utilized to effectively increase power transfer capability of the existing power transmission lines, and reduce operational and investment costs. In this paper shows the software method depending on IEEE-30 bus systems. FACTS devices it is clear that discussed in this paper to reduce the power losses total cost in the system. Also various FACTS controllers like STATCOM, SVC and UPFC etc.

References

[1.] Ontoseno Penangsang, Primaditya Sulistijono and Suyanto "Optimal power flow using multi-objective genetic algorithm to minimize generation emission and operational cost in micro-grid " International Journal of Smart Grid and Clean Energy, PP; 410:416, vol. 3, 2014.

[2.] K. Mani Chandy, Steven H. Low, Ufuk Topcu and Huan Xu " A Simple Optimal Power Flow Model with Energy Storage" 49th IEEE Conference on Decision and Control, December 15-17, Hilton Atlanta Hotel, Atlanta, GA, USA, 2010.

[3.] Chao-Tsung Ma and Tzung-Han Shr "Power Flow Control of Renewable Energy Based Distributed Generators Using Advanced Power Converter Technologies" Journal of Clean Energy Technologies, DOI: 10.7763, PP; 48:53, Vol. 3, No. 1, January 2015.

[4.] Kodjo Agbossou, Mohanlal Kolhe, Jean Hamelin, and Tapan K. Bose "Performance of a Stand-Alone Renewable Energy System Based on Energy Storage as Hydrogen", IEEE transactions on energy conversion, PP; 633:640, VOL. 19, 2004.

[5.] Keshav Pokharel, Maizura Mokhtar, and Joe Howe "A Multi-Objective Planning Framework for Optimal Integration of Distributed Generations" Centre for Energy and Power Management which is partly funded by BAE Systems UK.

[6.] Serhat Duman, Ugur Guvenc, Yusuf Sonmez and Nuran Yorukeren "Optimal power flow using gravitational search algorithm " elsevier journal, Energy Conversion and Management 59, PP: 86–95; 2012.

[7.] Warid Warid, Hashim Hizam, Norman Mariun and Noor Izzri Abdul-Wahab "Optimal Power Flow Using the Jaya Algorithm "mdi journal engineering, Energies, 2016.

[8.] Nanda Kumar Easwaramoorthy and R. Dhanasekaran "Solution of Optimal Power Flow Problem Incorporating Various FACTS Devices "International Journal of Computer Applications (0975 – 8887) Vol 55, 2012.

[9.] Afshin Lashkar Ara, Ahad Kazmi and Mohammad Behshad "Improving power systems operation through multi-objective optimal location of optimal unified power flow controller "Turkish Journal of Electrical Engineering & Computer Sciences, PP: 1893- 1908, 2013.

[10.] Anumaka, M. C. "Power Flow Study on Alternating Current (Ac) Power System" (IJITR) International journal of innovative technology and research, Volume No.2, P; 1068 – 1071, 2014.

[11.] Ingrida Steponavičė, Ingrida Steponavice and Steffen Rebennack "Optimal power flow: a bibliographic survey I Formulations and Deterministic Methods " Energy Systems manuscript, 2012.

[12.] IEEE Working group "Transmission System Application Requirements for FACTS Controllers" IEEE Power & Energy Society; The Institute of Electrical and Electronic Engineers, Inc, IEEE 2013.

[13.] Abdel-Moamen M. A and Narayana Prasad Padhy "Optimal Power Flow Incorporating FACTS Devices - Bibliography and Survey" IEEE-2003.

[14.] Jennifer F. Marley, Maria Vrakopoulou and Ian A. Hiskens "An AC-QP optimal power flow algorithm considering wind forecast uncertainty" Innovative Smart Grid Technologies - Asia (ISGT-Asia), IEEE 2016.

[15.] Miguel Chávez-Lugo, Claudio R. Fuerte-Esquivel and Claudio A. Cañizares "Practical Security Boundary-Constrained DC Optimal Power Flow for Electricity Markets" IEEE Transactions on Power Systems, 2016.

[16.] Sajan Varma "FACTS devices for stability enhancements" International Conference on Green Computing and Internet of Things (ICGCIoT), ISBN: 978-1-4673-7910-6, IEEE – 2015.

[17.] Ishit Shah, Neha Srivastava and Jigar Sarda " Optimal placement of multi-type facts controllers using real coded genetic algorithm" Electrical, Electronics, and Optimization Techniques (ICEEOT), International Conference on, ISBN: 978-1-4673-9939-5, IEEE-2016.

[18.] D. G. Ramey and M. Henderson "Overview of a Special Publication on Transmission System Application Requirements for FACTS Controllers" Power Engineering Society General Meeting, IEEE - 2007.

ISSN:2067-3809

ACTA TECHNICA CORVINIENSIS
– Bulletin of Engineering
Tome X [2017]
Fascicule 2 [April – June]
ISSN: 2067 – 3809

[1.] Davor ZORC

INTERNET OF THINGS (IoT) IN INDUSTRIAL ENGINEERING EDUCATION

[1.] University of Zagreb, Faculty of Mechanical Engineering and Naval Architecture, Ivana Lucica 5, Zagreb, CROATIA

Abstract: This paper presents an overview of current state of affairs in the Internet of Things (IoT) domain and briefly discusses its industrial applications. This has provided a motivation for the development of educational IoT laboratory setup based on legacy (mature) microcontroller-based control hardware, which should be easily upgraded by expanding it with a serial connection-equipped embedded network controller board such as ESP8266 module. The laboratory setup upgrade process is briefly outlined and Industrial IoT educational aspects implementable on such a platform are briefly discussed.
Keywords: Internet of Things, industrial computer control, education

INTRODUCTION

Internet of Things (IoT) is one of the latest "buzzwords" in the information and communication technology (ICT) sector, likely to exceed the impact of already well-known Cloud Computing paradigm [1]. Integration of sensors with microprocessor and wireless network adapters is hardly a new concept, but widespread availability, low prices and possibility of miniaturization lead to widespread use of such small-scale and ubiquitous systems. The goal of IoT movement is to network everything, from home appliances [2] and cars [3], to healthcare [4, 5], and smart cities and smart energy systems [3, 6, 7]. IoT prophets declare that it will be the next great industrial revolution, and that it will change everything within our lifetimes.

Similar statements have also been heard when microprocessors were first introduced. Many people did not believe that such small thing can have such profound impact. But 45 years later we can see that it was true – we have at least one microprocessor core in our pocket phone and many household appliances. So it really seems possible that IoT will change many things in our lives that we have taken for granted. Current state of the art is that IoT devices are getting increasingly smaller (possibly 1 cubic cm or less) and also cheaper. Perhaps in the future, people will have it implanted in their bodies as well [4]?

IoT may use standard Internet protocols but there are many other things to standardize (like data formats) so as to enable interoperability. Currently there is a kind of a "Standards War" with still uncertain final outcome which should establish who will be able to control this huge system. Industry consortiums are formed in order to protect their market shares, while at the same time various interest groups are also involved, such as those supporting an open system approach, which should be available to anyone. The main challenges facing the future of IoT are [2, 8, 9]:

- Privacy and security problems;
- Notable increase in electro-magnetic noise due to enormous number of such devices;
- Substantial increase in the amount of generated/stored data (so-called "data deluge").

Naturally the bulk of research efforts are aimed at solving the above problems, so that IoT devices may find their place in the future ICT infrastructure in spite of those challenges.

For more than 25 years we at the Faculty of Mechanical Engineering and Naval Architecture at the University of Zagreb teach mechanical engineering students how to control machines by means of microprocessors-based systems. In doing so we want them to have a first-hand experience using dedicated laboratory setups even at entry-level and basic courses such as "Electrical engineering basics" and with more details in specialized courses such as "Microprocessor-based control". In our current scheme, device networking is typically based on industrial protocols and computers are mostly in the form of Programmable Logic Controllers (PLCs) in the role of typical industrial hardware, which may also be equipped with Internet protocols too [10], even if those protocols would not be the best suited ones for low-level industrial control due to possible issues with the demand for simultaneous real-time operation of control algorithms.

Assuming that this new IoT paradigm is here to stay, there is no way of avoiding the introduction of those systems into the ever changing subject curriculum, for which a dedicated laboratory setup is currently being built. As a first step towards achieving this goal we have initiated the upgrade of current setups for analog, digital and PLC-based control, which has been emulated by a microcontroller system commanded via a PC terminal. The proposed upgrade consists of a wireless system on a module being able to communicate with user's smartphone, tablet or notebook computer. By using IoT technology this control could be carried out over Internet from any place worldwide, thus extending the laboratory work into the virtual domain [11]. To this end this paper presents our implementation of the aforementioned IoT system using ESP8266 chip, a System on chip with processor, network adapter and Wi-Fi link [12].

The paper is organized as follows. In chapter 2 industrial IoT is discussed in general terms in order to illustrate its applicability to industrial system supervision and control, while in chapter 3 the target ESP8266 embedded IoT system suitable for such purposes is presented. Chapter 4 is dedicated to the laboratory setups built for educational purposes, which may be suitable for the implementation of IoT concepts in automation and control. Concluding remarks are given in Chapter 5.

INDUSTRIAL IoT (IIoT)

The rise of computer-based control systems in the form of easy-to-use universal controllers started in late sixties by the advent of first PLCs (programmable logic controllers), whereas today these control platforms predominate in industrial applications, representing a well-established, standardized, reliable, easy-to-use and affordable control system solution. The main advantage of such systems is that PLC programming languages are oriented towards control-specific tasks, and are much easier to use and learn then standard higher-level computer programming languages (see e.g. [10], [18] and [19]). On the other hand, computer networks for industrial use have also progressed recently, thus resulting in several solutions that are now industry standards, while in the meantime there was also a rise of Internet use and Internet/Ethernet protocols. This technology became widely known to programmers and general public. So this notable change in the way how people exchange information and communicate had also an impact in industrial systems [20].

Moreover, today's industry along with PLC's also fields a growing number of industrial PC's and their corresponding communication protocols. Although Ethernet protocols are neither designed nor well suited for low-level control in industry (because of stringent requirements on real-time communication), the advances in microprocessor processing speed seem to compensate for that disadvantage. Finally, a range of modifications to Ethernet protocols has been introduced over the years, so now there are Ethernet variants that are able to handle real-time problems as well. This represents a fertile field for the introduction of Internet of Things (IoT) into the industrial communication environment as well. In particular, in the survey paper [15], IoT is defined as: "A dynamic global network infrastructure with self-configuring capabilities based on standard and interoperable communication protocols where physical and virtual 'Things' have identities, physical attributes, and virtual personalities and use intelligent interfaces, and are seamlessly integrated into the information network".

The Industrial Internet of Things (IIoT) [15] technology is apparently aimed towards bringing automation and control systems to new levels, so the trend of using IoT [14] technology in the industry seems to be on the rise. The term IIoT (Industrial Internet of Things) is often encountered in the manufacturing industries, referring to the industrial subset of the IoT.

IIoT in manufacturing would probably generate so much business value that it will eventually lead to the fourth industrial revolution, the so-called Industry 4.0. In particular, IoT represents the final cornerstone in the Industry 4.0 concept, the others being: (i) machine-to-machine (M2M) interfacing which enables large-scale flexible production, (ii) mobile Internet which allows for flexible data collection, (iii) Big Data and Cloud Computing which may enable the innovative concepts of industrial intelligence, and (iv) social media to promote the Industry 4.0 as a new product [21]. However, it is likely that the main beneficiaries of this new "revolution" will likely be the countries in the developed world, whose existing information infrastructure is significantly better equipped for the uptake of these propulsive technologies compared to developing countries.

So the scope of IIoT is broader then only technical aspect of it, as it includes global business plans and the way things will be manufactured in the future [17]. One of basic technologies for IoT integration within the existing infrastructure is radio-frequency identification (RFID) technology. Using RFID tags objects can be identified, tracked and monitored, and they have been used since 1980s in logistics, pharmaceutical production, retailing, and supply chain management. Another foundational technology for IoT is the wireless sensor networks (WSNs), which mainly use interconnected intelligent sensors for sensing and monitoring. With the advances in wireless communication, smartphones, and sensor network technologies, an increasing number of networked "things" or smart objects are being involved in IoT [15]. As mentioned above, so far, IoT has been gaining attraction in specific industries such as logistics/transportation, intelligent manufacturing, retailing, and pharmaceutics/healthcare. The key to the IoT success appears to be its standardization, which should provide interoperability, compatibility, reliability, and effective IoT system operation on a global scale.

In particular, IoT can be considered as a world-wide physical inter-connected network, within which "things" or smart devices can be accessed and controlled remotely. The decentralized and heterogeneous nature of IoT requires that the architecture provides efficient event-driven capability.

Thus, service-oriented architecture (SOA) is considered a suitable approach to achieve interoperability between heterogeneous devices in a multitude of ways. In order to do that a four-layered architecture is elaborated for IoT in [15], comprising the following components (i) sensor layer, (ii) network layer, (iii) service layer, and (iv) interface layer. From the viewpoint of the information network, the IoT is a complex heterogeneous network, which includes the connection between various types of smart devices through various communication technologies.

It is broadly accepted that the IoT technologies and applications are still in their infancy. There are still many research challenges for industrial use such as: technology issues, standardization requirements, security protocols, and privacy concerns. Nevertheless, IoT approach will significantly augment network traffic and data storage needs so it can be presumed that IoT will gradually be developed as those technologies evolve.

MODULE nodeMCU

Node MCU (Figure 1) is one of many solutions suitable for small-scale IoT applications [13]. It is a small and inexpensive module based on ESP8266 chip technology [12], which is basically a microcontroller connected to a Wi-Fi transmitter/receiver unit. The target microcontroller can be programmed in a familiar way, for example using Arduino's software tools and its C-like higher-level programming language [16], or by using a LUA interpreter.

The microcontroller module is connected to the PC by using the embedded USB interface which is then used for transferring the user program to the module. Besides running the user program, this embedded system runs the whole stack of Internet protocols. So, if its Internet part is configured properly, one can easily connect to the local wireless network. In this way this small-scale embedded microcontroller system can be visible to all Internet users and it can also be controlled by virtually anybody from any location (of course, password-restricted access is possible). On the user side of the communication only a suitable Internet browser is needed running on user smart device.

The embedded system can also be configured to become a Wi-Fi hotspot and can be accessed from smart phones or laptops in its vicinity. This system can but need not be connected to the global Internet.

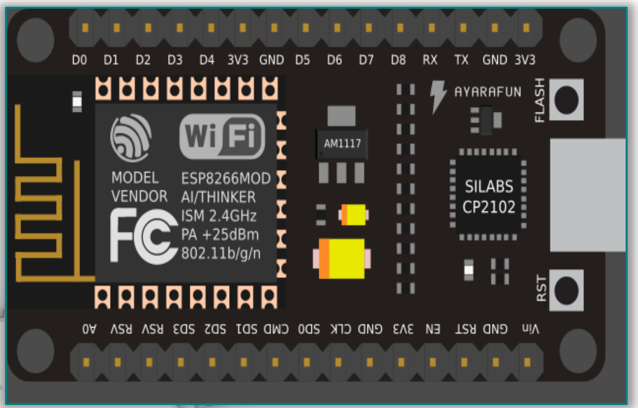

Figure 1 – Module nodeMCU printed circuit board with component layout.

LABORATORY SETUPS

The Robotics and Manufacturing Systems Automation Department at the Faculty of Mechanical and Naval Engineering, University of Zagreb, Croatia has a long standing tradition of teaching electrical and electronics engineering, automatic control, computer control, robotics and other related fields.

In particular, within the introductory electrical/ electronics engineering courses there was a need to enable undergraduate students to get first-hand experience in computer control of engineering systems in order to grasp its basic concepts. For that reason, several variants of computer-based control systems laboratory setups have been developed over the last 25 years.

Laboratory setup - version 1

First computer control laboratory setup was developed in 1993 (Figure 2), comprising of three physical systems (processes) intended to be controlled by the dedicated microcontroller:

- A model of street traffic lights (semaphores), which represents a case study in sequential control;
- A model of temperature controlled chamber, which is used to demonstrate the concepts of closed-loop control by using a simple relay feedback controller;

- A PLC application for universal digital control, which is primarily used to demonstrate the effectiveness of logic control-oriented programming languages, such as Instruction Set language.

The communication with the target controller is implemented using a serial PC interface, wherein the PC user communicates with the microcontroller by using a serial terminal program (Hyper-terminal).

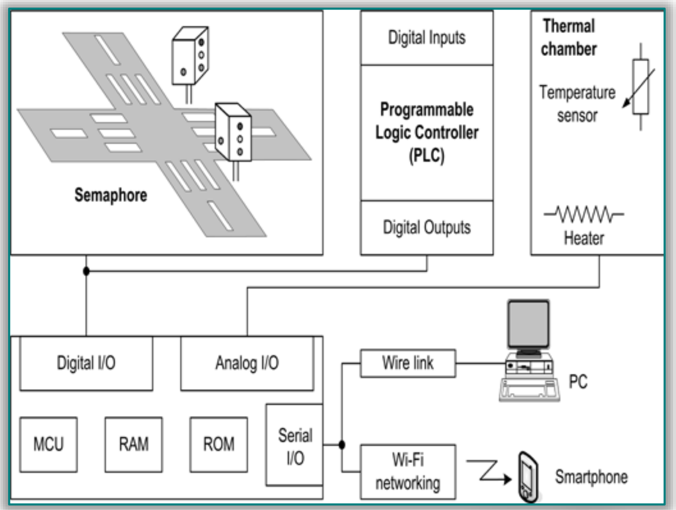

Figure 2 – Laboratory setup
for computer control education purposes.

Laboratory setup - version 2

Second version of the aforementioned laboratory exercises has been developed in 2013, and it includes a PC application for animated simulation, programming or configuration of aforementioned physical objects intended for control system testing.

The simulation and process data visualization system interfaces for the traffic lights (semaphores), PLC system emulation and thermal chamber control are shown in Figures 3 – 5, respectively.

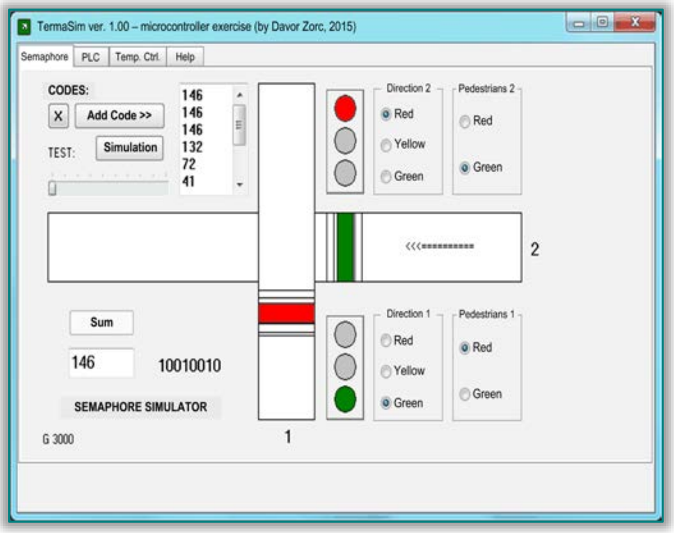

Figure 3 – Simulation of traffic lights (semaphore)
system for simple crossroads.

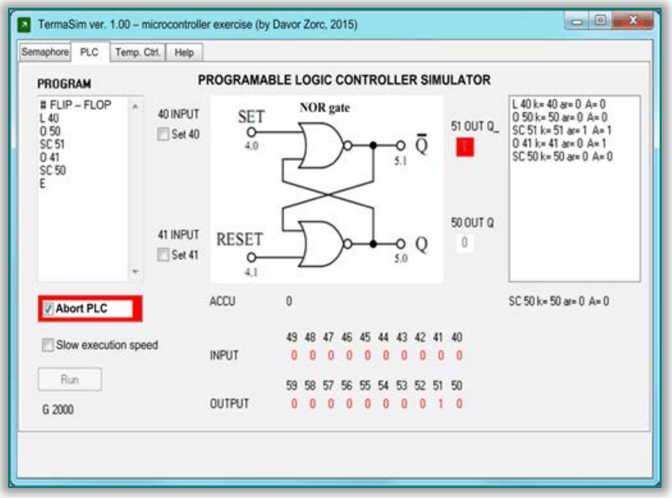

Figure 4 – Simulation of Flip-Flop operation using PLC Instruction Set language.

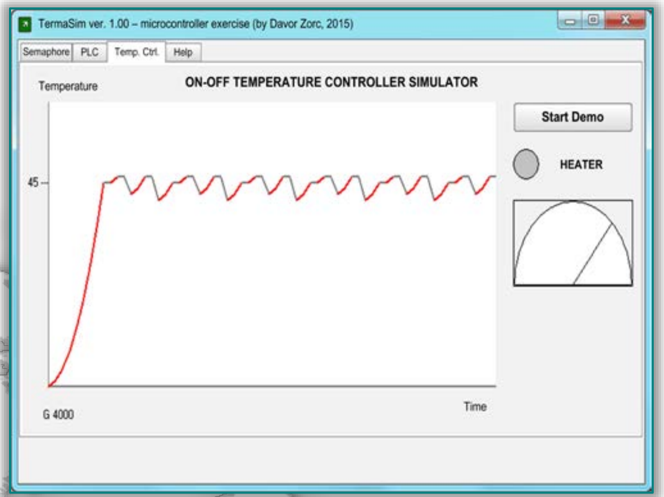

Figure 5 – Simulation of Thermal chamber On/Off (relay feedback) control.

After the functionality of the control code has been thoroughly checked within the simulation environment, the control program may then be downloaded through the serial interface onto the target microcontroller system and then run for the purpose of final control code verification.

Laboratory setup - version 3

Third version of the laboratory setup is a work in progress, which includes porting the same functionality of the version 2 setup to the Arduino/ESP8266 platform. This version does not need a PC as terminal device; on the contrary, students may program/configure different objects of control system using tablet PCs or even their own smartphones.

A tablet PC or smartphone is connected to the ESP8266 module by choosing it from the instantaneously generated list of available Wi-Fi hotspots. When connected, Internet browser can be used to monitor and manipulate control program objects.

Alternatively, ESP8266 can be configured as Telnet protocol server. In this way user interface is of the console type, but Telnet app needs to be downloaded beforehand. As this exercise is for students physically present in the laboratory, ESP8266 can be configured/programmed as intranet device, i.e. for local use only.

CONCLUSIONS

The paper has first presented an overview of Internet of Things (IoT) technologies state-of-development and potentials for its application in industrial applications in the form of Industrial Internet of Things (IIoT). This has provided an additional motivation for the inclusion of such topics in the teaching programs (curricula) dealing with electrical engineering, automation and industrial systems control-related subjects currently being taught at the University undergraduate level.

Using current embedded microcontroller technology it should be relatively straightforward to develop small-scale hardware and software applications including basic IoT functionalities, which can be easily integrated with the existing legacy hardware and control-oriented software via simple serial interface. Hence, these augmented teaching aids should be able to provide an additional benefit in the overall teaching process through the inclusion of straightforward interfacing between the user (student) and the legacy control hardware.

Since the IoT technology is still under development, it is reasonable to expect that it would gradually find its place in various industries. However, based on the current state-of-affairs in the IoT field, increased efforts are required in terms of development and implementation of suitable standards. Since reliability is crucial in industrial applications, and particularly attention needs to be devoted to communication system security, many problems already present in general Internet use may also be expected with increased uptake of IoT in industrial applications. Since security issues can be overcome, as proven by the reliability of today's Internet commerce and banking, notable attention needs to be devoted to this particular aspect of IoT, in order to facilitate successful implementation of IoT in the industry in the near future.

Acknowledgements

Technical support related to the functionality testing and initial development of Arduino/ESP8266 embedded system provided by Professor Mario Essert and Mr. Zvonko Grgec is highly appreciated, as well as the initial efforts made by Igor Ratković, mag. ing. during the development of second-generation laboratory exercises on Arduino platform.

Finally, useful discussions and technical support provided by Professor Danijel Pavković in the preparation of the final manuscript are also greatly appreciated.

Note

This paper is based on the paper presented at The International Conference Management of Technology – Step to Sustainable Production (MOTSP 2016), organized by the Faculty of Mechanical Engineering and Naval Architecture, Croatian Association for PLM and the University of North, in Porec/Parenzo, Istria, CROATIA, June 01–03, 2016.

References

[1] Want, R., Schilit, B. N., Jenson, S.: Enabling the Internet of Things, IEEE Computer Magazine, 48(2015)1, 28-35.
[2] Grau, A.: Can You Trust Your Fridge, IEEE Spectrum, 52(2015)3, 50-56.
[3] Jin, J., Gubbi, J., Marusic, S., Palaniswami, M.: An Information Framework for Creating a Smart City Through Internet of Things, IEEE Internet of Things Journal, 1(2014)2, 112-121.
[4] Jiang, Z., Abbas, H., Jang, K. J., Mangharam, R.: The Challenges of High-Confidence Medical Device Software, IEEE Computer Magazine, 49(2016)1, 34-42.
[5] Catarinucci, L., de Donno, D., Mainetti, L., Palano, L., Patrono, L., Stefanizzi, M. L., Tarricone, L.: An IoT-Aware Architecture for Smart Healthcare Systems, IEEE Internet of Things Journal, 2(2005)6, 515-526.
[6] Zanella, A., Bui, N., Castellani, A., Vangelista, L., Zorzi, M.: Internet of Things for Smart Cities, IEEE Internet of Things Journal, 1(2014)1, 22-32.
[7] Spanò, E. Niccolini, L., Di Pascoli, S., Iannacconeluca, G.: Last-Meter Smart Grid Embedded in an Internet-of-Things Platform, IEEE Transactions on Smart Grid, 6(2015)1, 468-476.
[8] Roman, R., Najera, P., Lopez, J.: Securing the Internet of Things, IEEE Computer Magazine, 44(2011)9, 51-58.
[9] Stankovic, J. A.: Research Directions for the Internet of Things, IEEE Internet of Things Journal, 1(2014)1, 3-9.
[10] Creating and using user-defined web pages on S7-1200, Siemens AG, support.industry.siemens.com/cs/document/58862931/creating-and-using-user-defined-web-pages-on-s7-1200?dti=0&lc=en-WW, 2016-02-26.
[11] Ruiz, E. S., Martin, A. P., Orduna, P., Martin, S., Gil, R, Ruiz Larrocha, E., Albert, M. J., Diaz, G., Meier, R., Castro, M.: Virtual and Remote Industrial Laboratory: Integration in Learning Management Systems, IEEE Industrial Electronics Magazine, 8(2014)4, 45-58.
[12] ESP8266EX Datasheet – version 4.3, Espressif Systems IOT Team bbs.espressif.com/, 2016-02-26.
[13] NodeMCU, en.wikipedia.org/wiki/NodeMCU, 2016-02-26.

[14] Atzori, L., Iera, A., Morabito, G.: The Internet of Things: A survey, Computer Networks, 54(2010)15, 2787-2805.
[15] Xu, L. D., He, W., Li, S.: Internet of Things in Industries: A Survey, IEEE Transactions on Industrial Informatics, 10(2014)4, 2233-2243.
[16] Arduino Website, www.arduino.cc/, 2016-05-03.
[17] Internet of Things, en.wikipedia.org/wiki/Internet_of_Things#Manufacturing, 2016-05-03.
[18] Berger, H.: Automating with SIMATIC, Publicis MCD Verlag, Munich, Germany, 2000.
[19] Bolton, W.: Instrumentation and Control Systems, Newness (imprint of Elsevier), Oxford, UK, 2004.
[20] Reynders, D., Mackay, S., Wright, E.: Practical Industrial Data Communications, Newness (imprint of Elsevier), Oxford, UK, 2005.
[21] Chen, C., Xu, L.: SAP: Enabler of Industry 4.0, Huawei Technologies Co. Ltd, 2015.

ISSN:2067-3809

ACTA TECHNICA CORVINIENSIS
– Bulletin of Engineering
Tome X [2017]
Fascicule 2 [April – June]
ISSN: 2067 – 3809

1.Aleksandar ŽIVKOVIĆ, 2.Milan ZELJKOVIĆ, 3.Miloš KNEŽEV

THERMAL MODEL OF HIGH SPEED MAIN SPINDLE

1-3.University of Novi Sad, Faculty of Technical Sciences, Novi Sad, SERBIA

Abstract: In the last period a high-speed main spindles, by modern machine tools, are used with basic goal - to increase efficiency. The prediction of thermal behavior of the spindle is essential for machining precision. The main source of heat on the spindle occurs due to friction torque on bearings with angular contact. The heat generated on the bearings transfers to the spindle and surrounding air, thus causing the thermal expansion of spindle elements. This paper presents a 3D FEM thermal model of the main spindle with hybrid angular contact ball bearings.
Keywords: angular contact ball bearings, FEM, main spindle, thermal behavior

INTRODUCTION

The development of technology in producing high speed machine tools can be observed from the area of machine tool application [1]. The behavior of machine tools while in exploitation is conditioned by the behavior of certain vital assemblies. Especially significant are the spindle units, as the principle units of machine tools, since they determine the accuracy and productivity [2]. Behavior of this assembly during exploitation is conditioned by numerous parameters which can be grouped in three groups [3]:

a) conceptual,
b) geometric, and
c) other significant parameters.

Within constructive and geometric parameters it is possible to consider an influence of spindle, drive element and bearing support. Other significant parameters are: stiffness and bearing dumping, temperature and limited speed. At high-speed spindle and bearings rotations, a high heat amount is generated, and rotate elements (spindle, inner bearing rings and other revolving assembly elements) present rotational masses in system, which demands a precise cooling adjustment, lubrication and balancing. In this paper, the finite element method is used to simulate the temperature distribution of main spindle system. This model includes the major heat sources, the heat transfer between spindle elements for a transient analysis of the thermal behavior.

THERMAL FEM MODEL OF THE HIGH SPEED MAIN SPINDLE

The solid model of main spindle is built by using Inventor and the structure such as thread hole, keyhole, chamfer, fillet and so on are simplified. This structure has no effects on the analysis result. FEM model of the spindle has been importing to ANSYS APDL. In defining the thermal model of the spindle: the spindle shaft, bearings (rings and balls), and the housing, SOLID 87 element is used. Model consists of 31295 finite elements total. The finite elements CONTA 174 and TARGET170 were used to simulate contact joints. To simulate contact joints, contact pairs have been created at the joints, and the real constant TTC has been defined, i.e. the thermal contact conductivity for each ball, as well as for each contact between the outer ring/housing and inner ring/spindle shaft. The finite element thermal model is shown as Figure 1. Some assumptions are made for the thermal analysis:

1. The spindle model is axisymmetric and assumes a uniform clearance between the outer ring and the housing around the entire perimeter.
2. The thermal resistance in the axial direction, as well as axial conduction between contact elements is not considered.
3. Friction loss of the air is smaller than other heat sources, so it is neglected.
4. The heat radiation is neglected.

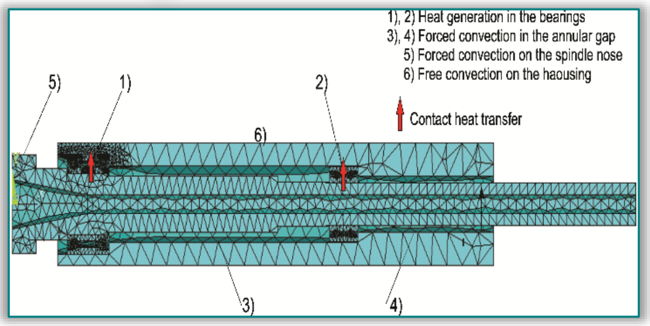

Figure 1. FEM model of the main spindle

Heat generation in the bearings

In analyzed model is assumed that the main heat sources in the assembly are bearings, because the power transmission is enabling by wheeled belt, which is setup on the spindle end, and its influence is discarded. The total frictional torque consists of torque due to applied load, torque due to viscosity of lubricant and spinning friction moment. The friction torque due to applied load and due to viscosity of lubricant at each inner and outer contact with the raceway is formulated similarly as in [4]:

$$M_{i,o(j)} = \left\{ 0.675 f_0 \left(\nu\omega_b\right)^{2/3} d_m{}^3 + f_1 \left(\frac{Q_{i,o(j)}}{Q_{i,o(\max)}} \right)^{1/3} Q_{i,o(j)} d_b \right\} \quad (1)$$

where are: f_0 - a factor depending upon the type of bearing and method of lubrication; f_1 - factor depending upon bearing design and relative load, ν -kinematic viscosity of lubricate, d_b - the diameter of the roller, Q_i and Q_o - contact loads at inner and outer raceways respectively, ω_b - angular velocity of the ball and Q_{max} - maximum contact load.

The order component of heat generation within the bearing is the spinning friction moment, which is formulated for every contact with the inner and outer raceway, based on [5]:

$$M_{S,i,o(j)} = \frac{3\mu Q_{i,o(j)} a_{i,o(j)} E'}{8} \quad (2)$$

where μ is friction coefficient and a is semi-major axis of the contact area.

The total heat generated on the inner and outer raceway can be obtained as the sum of heat generated for each ball as [6]:

$$H_{i,o(j)} = \sum_{j=1}^{Z} \omega_b M_{i,o(j)} + \sum_{j=1}^{Z} \omega_{s,i,o(j)} M_{S,i,o(j)} \quad (3)$$

Convection Boundary Condition

Heat transfer coefficient at spindle rotation, assumed that the temperature difference is minor, can be calculated from the next equation, under condition that the forced convection is considered:

$$h_v = N_u k_a / d_v \quad (4)$$

where k_a is the heat conductivity of fluids (air), N_u is Nusselt's number and d_v is the diameter of the spindle nose. In case of annular gap of the spindle, d_v changes to the size of gap $\delta_{gap.}$ The detailed determinate of the Nusselt's number is available in [6,7].

Conduction between balls and raceways

The thermal contact conductance between balls and raceways is obtained empirically in function of the rotation speed [8]:

$$h_b = \frac{Z\sqrt{14 + 2\ln\nu - 2\ln d_b}\, d_b^2}{2400} \quad (5)$$

$$\nu = \frac{n\left(d_m + d_b\right)}{19099} \quad (5a)$$

The thermal resistance is obtained as [9]:

$$R_b = \frac{d_b}{h_b A} \quad (6)$$

where A is contact area between ball and raceway.

Conduction between rings and spindle/housing

Since the ring thickness is not a section constant, the ring width can be divided into five parts based on the cross-section, as shown in Fig. 2. Heat resistance between the bearing inner ring and the spindle shaft and outer ring and the housing is determined by using the relation for cylinder heat resistance [10]:

$$R_{i,o} = \frac{\ln(R_{m(i,o)} / R_{n(i,o)})}{2\pi L_{l(i,o)} k} \quad (7)$$

where $R_{n(i,o)}$ and $R_{m(i,o)}$ are the inner and outer section radii which are observed in the inner or outer bearing ring according to Fig. 2, and $L_{l(i,o)}$ the length according to the inner and outer section (Figure 2). Heat conductivity (k) for steel is 46.6 W/m-K and it is valid for 20-200 °C [11].

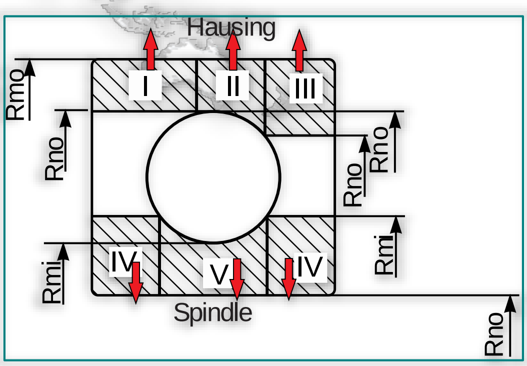

Figure 2. Conduction model of the bearing

RESULTS AND DISCUSSION

The analysis of thermal characteristics of the spindle includes stationary and non-stationary temperature change for different rotation speeds. Figure 3 predicts the temperature distribution of the spindle for rotation speed of 6000 rpm and reference temperature of 22 °C is shown.

The temperature of the front bearings is much higher than that of the rear. The maximum temperature occurs on the outer ring of the front bearing. This happens mostly because the higher generated heat and higher load occur on the front bearings. As the front bearings are very near to the top of the spindle (small length of the spindle top) heat, from the bearing in axial and radial direction, is transferred to the top of the spindle.

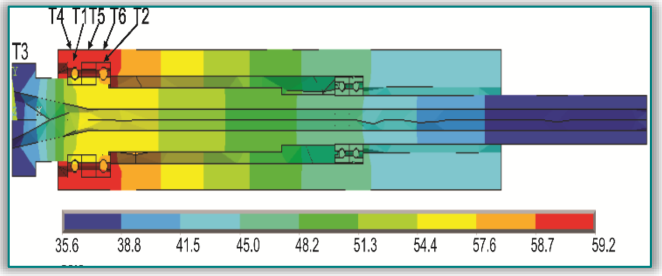

Figure 3. Temperature distribution of the spindle for 6000 rpm

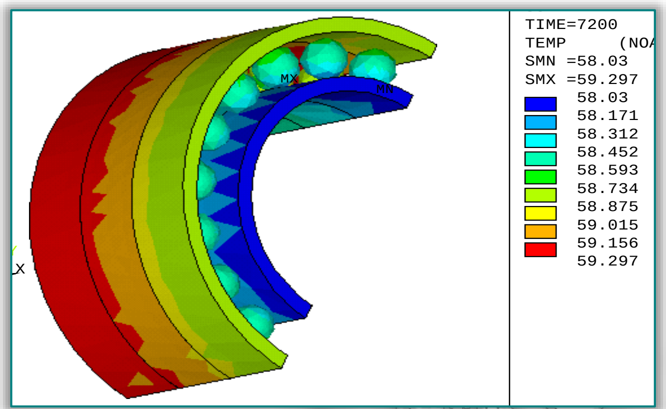

Figure 4. Temperature distribution of front bearing at 6000 rpm

Figure 5 shows the simulated temperatures on the front bearing, housing, and spindle nose during time, for characteristic points in Figure 3. Unlike the temperature of the front bearing, the temperatures in other observed places increase slowly in the initial phase and rapidly in the later phase, until they reach stationary state. Their growth in time takes longer than on the bearings. Essentially, it is important to mention that the increase of temperature for observed places follows the same trend, but in different times of reaching the stationary state.

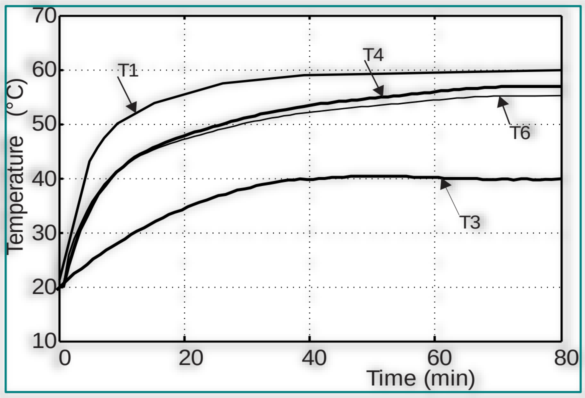

Figure 5. The temperature changes with time at the selected points for 6000 rpm

In table 1 is shows the comparison between simulation and measured temperatures difference for stationary temperature state for different rotational speed.

Table 1. Comparison of the simulated to the measured temperature

	Simulation			Experimental		
rpm	T1	T2	T3	T1	T2	T3
2000	45.2	42.6	29.4	48.1	43.2	28.2
4000	49.8	47.3	32.3	57.5	56.7	31.2
6000	59.2	59.1	35.6	67.3	63.4	32.4

The maximum difference from 2 to 10 % in stationary state, depending on the number of revolutions, is acceptable, especially since the suggested model does not consider the effects of bearing elements' change in dimensions. These changes affect the accuracy of several parameters, such as contact resistance, forced convection and generated heat in the bearing.

CONCLUSION

This paper discussed the mathematical model for predicting the spindle's temperature distribution in steady-state and non-steady-state. This model can be separated into two sub-models: the heat generated model, and the model of the spindle. In this paper, the thermal model of the spindle was created by using the finite element approach. This approach was chosen because of its major advantage, which is that heat conduction can be easily integrated with complex geometries and physical conditions, especially for any further analyses of the influence of temperature on static and dynamic behavior of the spindle. On the other hand this paper presents an analytic method for calculating the heat generated on the bearing, based on the internal distribution of load. Additionally, the simulation errors of the temperature fields are less than 10%, which in turn confirms the effectiveness of the simulated model proposed in this paper.

Acknowledgment

In this paper some results of the project: Contemporary approaches to the development of special solutions related to bearing supports in mechanical engineering and medical prosthetics – TR 35025, carried out by the Faculty of Technical Sciences, University of Novi Sad, Serbia, are presented. The project is supported by the Ministry of Science and Technological Development of the Republic of Serbia.

Note

This paper is based on the paper presented at The 3rd International Scientific Conference on Mechanical Engineering Technologies and Applications (COMETa 2016), organized by the Faculty of Mechanical Engineering, University of East Sarajevo, in Jahorina, Republic of Srpska, BOSNIA & HERZEGOVINA, December 7–9, 2016.

References

[1] Abele, E., Altintas, Y., Brecher, C. (2010). Machine tool spindle units, CIRP Annals - Manufacturing Technology, 59 (2), p.p. 781-802.
[2] Zverev, I.A., Eun, I.U., Chung, W.J., Lee, C.M. (2003). Simulation of Spindle Units Running on Rolling Bearings, International Journal of Advanced Manufacturing Technology, 21 (10-11), p.p. 889-895

[3] Zeljković, M. (1996). Sistem za automatizovano projektovanje i predikciju ponašanja sklopa glavnog vretena mašina alatki, Doktorska disertacija, Fakultet tehničkih nauka, Novi Sad.
[4] Li. H., Shin, Y.C. (2004). Integrated dynamic thermo-mechanical modeling of high-speed spindles, part 1: Model development, Journal of Manufacturing Science and Engineering, Transactions of the ASME, 126 (1), p.p. 148-158
[5] Harris, T. A., Michael., N. K. (2007). Rolling bearing analysis: Advanced Concepts of Bearing Technology, Taylor & Francis Group.
[6] Zivkovic, A. (2013). Računarska i eksperimentalna analiza ponašanja kugličnih ležaja za specijalne namene, Doktorska disertacija, Fakultet tehničkih nauka, Novi Sad.
[7] Zivkovic, A., Zeljkovic, M. Tabakovic, S., Milojevic, Z. (2015). Mathematical modeling and experimental testing of high-speed spindle behavior, International Journal of Advanced Manufacturing Technology, 77, p.p. 1071-1086
[8] Uhlmann, E., Hu, J. (2012). Thermal Modelling of a High-speed Motor Spindle, Procedia CIRP, 1 (0), p.p. 313-318.
[9] Kim, S.M., Lee, S.K. (2001). Prediction of thermo-elastic behavior in a spindle-bearing system considering bearing surroundings, International Journal of Machine Tools and Manufacture, 41 (6), p.p. 809-831
[10] Incropera, F.P., Lavine. A.S., DeWitt, D.P. (2011). Fundamentals of heat and mass transfer, John Wiley & Sons.
[11] Yovanovich, M.M. (1971). Thermal constriction resistance between contacting metallic paraboloids: Application to instrument bearings. AIAA Progress in Astronautics and Aeronautics: Heat Transfer and Spacecraft Control 24, p.p. 337-358

ISSN:2067-3809

ACTA TECHNICA CORVINIENSIS
– Bulletin of Engineering
Tome X [2017]
Fascicule 2 [April – June]
ISSN: 2067 – 3809

[1.]Marek PAVLÍK, [2.]Lukáš KRUŽELÁK, [3.]Lukáš LISOŇ, [4.]Miroslav MIKITA, [5.]Samuel BUCKO, [6.]Michal ŠPES, [7.]Michal IVANČÁK, [8.]Bystrík DOLNÍK, [9.]Ján ZBOJOVSKÝ

THE MAPPING OF ELECTROMAGNETIC FIELDS IN THE ENVIRONMENT

[1-9.] Technical University of Košice, Faculty of Electrical Engineering and Informatics, Department of Electric Power Engineering, Mäsiarska 74, 041 01 Košice, SLOVAKIA

Abstract: Today's wireless time brings some comfort, but on the other hand the impact of electromagnetic fields is serious threat to people. Many studies dealt with the effects of electromagnetic fields on living organisms, but the results are not completely clear. General and scientific public is increasingly focused on the impact of electromagnetic fields on living organisms. This is closely related limit values for parameters characterizing exposure to electromagnetic fields, depending on the frequency range, as defined by the Ministry of Health Decree 534/2007 Z.z. on the details and requirements for sources of electromagnetic radiation and exposure limits citizens to electromagnetic radiation in the environment. This contribution therefore focuses on mapping the electric and magnetic fields in the environment. The environment was selected area with a higher concentration of people in Prešov. The mapping was performed in two frequency ranges from 1 MHz to 1 GHz and 1 GHz to 2 GHz.
Keywords: electromagnetic field, electric field strength, magnetic flux density

INTRODUCTION

In the current high-growth society we are increasingly draws attention to the concept of electromagnetic field. Increasingly, the term penetrates between the general public and there is also the fact that in normal general public concerned about the possible impact of electromagnetic fields on the human body.

In the professional and scientific community, research focuses precisely on the impact of electromagnetic fields on biological effects, but research results vary widely.

Electric, magnetic and electromagnetic fields that may have adverse biological effects can be called collectively called as electrosmog. These electromagnetic fields are preferable also called as electromagnetic pollution [1] [2] [3] [4].

Slovakia Plata acts to protect the public and workers against electromagnetic fields. Both acts are in line with the recommendations of the European Union. Protection of the population in the Slovak Republic is currently provided by Ministry of Health of the Slovak Republic no. 534/2007 Coll. specifying requirements for sources of electromagnetic radiation and exposure limits citizens to electromagnetic radiation in the environment [2] [5]. Not exceeding the action values will ensure the limit values for exposure. In addition to binding legal documents, there are technical standards which are less strict and non-binding recommendations of the independent experts that are extremely severe.

HEALTH ISSUES AND RESEARCH

Since 1996, ongoing international project WHO that assessed the effect of changing static time of EM fields on human health, the environment. It was carried out by a large number of scientific laboratory studies. Some scientists these with the legal detrimental effect from exposure to low-frequency electromagnetic radiation, not their results are, however, different proven insufficient. Therefore, more attention is paid to high-frequency electromagnetic waves. Many studies have shown on the link between uses of mobile phones brain cancer. The International Commission for the Conservation Non-Ionizing Radiation (ICNIRP) warns of the possibility of developing cancer as a result of persistently high microwave radiation when using mobile phones. The World Health Organization WHO in 2011, the inclusion of electromagnetic radiation in the radio-frequency spectrum as belonging to Group 2B done from the perspective of carcinogenicity, that as a possible carcinogenic. This classification awarded by the electromagnetic radiation of radio frequencies on the basis of studies confirming the increased risk of tumor Central nervous system based on supporting nerve tissue in the brain, spinal cord between users of mobile phones [6] [7].

In 1948, American introduced study possible links between exposures microwaves, testicular degeneration, cataracts in dogs. Another study published in 1953 focused on worker's radar stations on the issues of internal bleeding, leukemia, cataracts, headaches, brain tumor to heart disease. Published studies have led to secret military research dealing with microwave effects on people and the decision to limit the permitted quantity of received microwaves. Transmitter hurts once becoming the hills above the town village, or to high masts so that the download access to do their vicinity. In today's Statistical base stations of mobile networks of other wireless equipment from us only Remote meter. However, their performance Achieve tens to hundreds of watts. Almost every television transmitter of radio is the current point in the country of which we even placed a large bounty of different antennas used for the dissemination of radio and television signals of mobile services. In close vicinity of these transmitters may even radiation Occupational exposure limits often exceeded Therefore, work on antenna systems during shutdown Perform transmitter or at reduced power. Stanislav Szmigielski over 16 years Club controlled the worker with radio devices, you'll see that those who are occupational exposure to radiofrequency microwave radiation were 14 times greater likelihood of developing chronic leukemia, 9-fold greater chance of developing acute leukemia six times higher, the probability of non-Hodgkin's lymphoma. The estimated average exposure value as were the people in the study were exposed to about 5 μW per square centimeter (50,000 mW/m^2). This level is common near a base station to the mobile networks of large television radio transmitters [6]-[8].

The incidence of cancer in the vicinity of radio transmitters has been studied in Korea. The results of various studies have shown an association between electrical magnetic polo at the potential of cancer. The authors of the study used Tajta regional ecological studies to confirm respectively refuted this association. 31 were observed in areas exposed to a low power transmitter 50kW, 11 Areas with a high transmitter output power from 100 to 1500 kW amplitude modulated areas, which corresponded to 42 radio transmitter. Cancer was confirmed in a 2 km radius of each of the transmitters, which was confirmed by the Korean Health Organization in 1995. The authors of the study evaluated the difference between the rates of cancer, leukemia, lymphoma, breast cancer, brain within 2 km from the transmitter with high power and heading 2 km of low power transmitters. It was also selected four control area were located as close as possible in areas with high power transmitters are not at least 2 km from the transmitter. The study authors found no significant differences with regard to the occurrence of cancer in the area of high-low-power transmitters. However, a significant result recorded in 11 areas with high power transmitters, where the increased incidence of leukemia in two of these areas, incidence of brain cancer in areas prospers. Further studies should help with more detailed information in the field of cancer with a radio transmitter [6] [9].

MAPPING ELECTROMAGNETIC FIELD

Precisely for the reasons described above, this paper is focused on mapping smog in the environment. The place for measuring was chosen area with an increase in population and specifically in front of the theater in Prešov. Mapping was carried out in two frequency bands. The first band was from 1 MHz to 1 GHz and a second band was from 1 GHz to 2 GHz.

Figure 1. Environment - measuring location

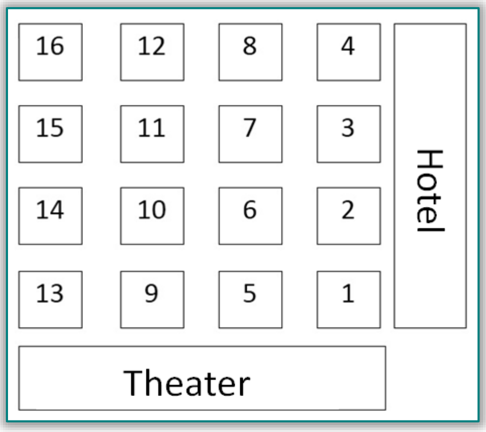

Figure 2. Grid of measurement points

The place of measurement is shown in Figure 1. The grid of measurement points is shown in Figure 2. The measurement was repeated ten times during the day, and then selected a maximum value for each measuring point.

THE RESULTS OF THE MAPPING SMOG IN THE ENVIRONMENT

The results of the mapping of the electromagnetic field can be seen in Figures 3-6. In Figure 3 you can see the map of the magnetic field H in the frequency range 1 MHz to 1 GHz, in units of mA / m. Figure 4 you can see the map of the magnetic field H in the frequency range from 1 GHz to 2 GHz in mA/m. In the Figure 5 you can see the map is the electric field E in the frequency range 1 MHz to 1 GHz in V/m. In the Figure 6 is a map shown the electric field E in the frequency range from 1 GHz to 2 GHz in V/m.

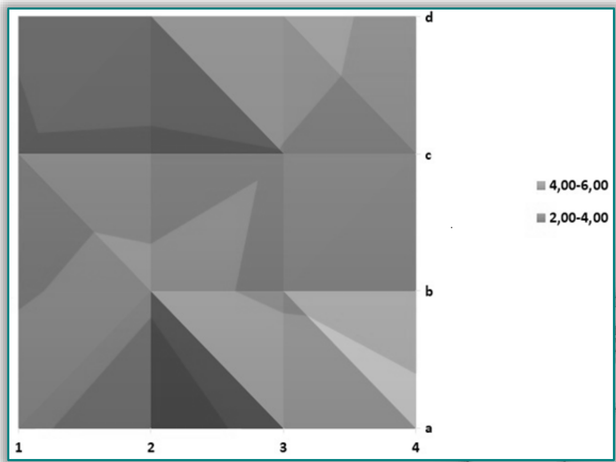

Figure 3. Magnetic field strength H
in the frequency range 1 MHz to 1 GHz in μA/m

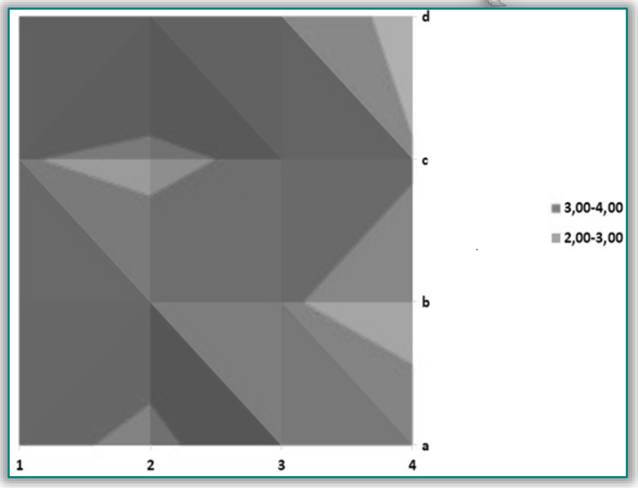

Figure 4. Magnetic field strength H
in the frequency range 1 GHz to 2 GHz in μA/m

The results shown that the higher value of the magnetic field were measured in the frequency range from 1 MHz to 1 GHz. In the case of measuring the electric field intensity were higher values also measured in the frequency range from 1 MHz to 1 GHz. Higher values in the lower frequency band were due to higher action of sources of electromagnetic radiation, especially from sources of radio waves, and also by mobile GSM devices operating in this frequency band. In the frequency range from 1 GHz to 2 GHz were measured levels of electromagnetic fields especially from mobile devices GSM1800.

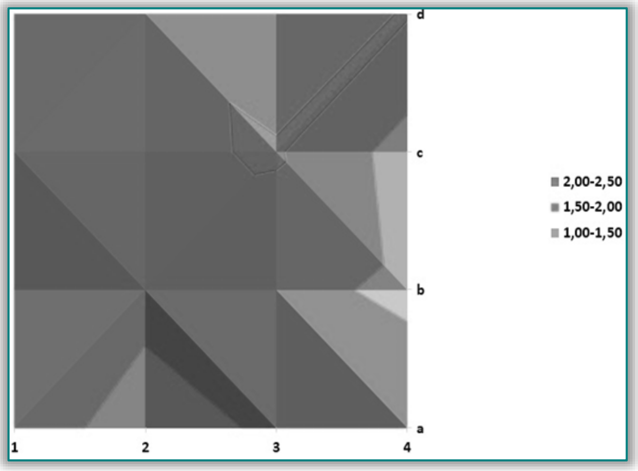

Figure 5. Electric field intensity E
in the frequency range 1 MHz to 1 GHz in mV/m

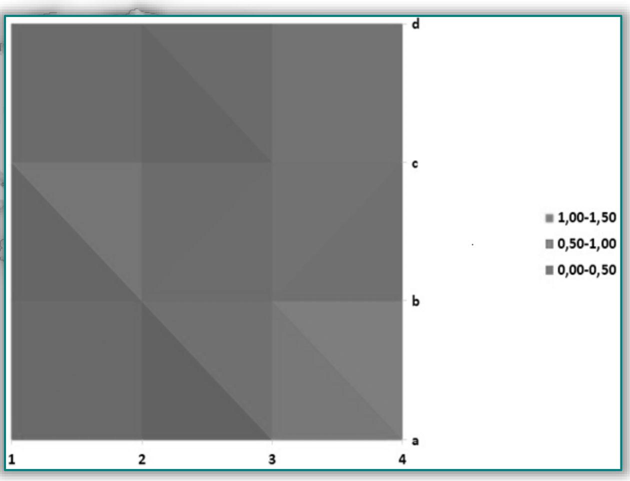

Figure 6. Electric field intensity E
in the frequency range 1 GHz to 2 GHz in mV/m

CONCLUSION

This paper was aimed at mapping the electromagnetic fields in the environment. Since almost every environment is effect by electromagnetic field. The paper focused on the environment with a higher people frequency.

From measurements it indicates the value of the electric and magnetic fields were higher in the frequency range from 1 MHz to 1 GHz than in the frequency range 1 GHz to 2 GHz, due to a greater influence of source (radio waves and mobile GSM900) just at a lower frequency range.

The measured values were compared with Ministry of Health Decree 534/2007 and at no point or value exceeded. On the contrary, they were very low.

Acknowledgement
This work was supported by the projects VEGA No.1/0132/15 and APVV-15-0438.

References

[1] Durpok, J., MORISKE, H-J. and N. Englert, "GESÜNDER WOHNEN — ABER WIE?: Praktische Tipps für den Alltag," Berlin: KOMAG mbH, 2005. [online]. [citované 2015-07-07]. Available on: < http://www.umweltbundesamt.de/sites/default/files/medien/publikation/long/2885.pdf>.
[2] Burrell, L. " What Is Electrosmog?," 2010. [online]. [citované 2015-01-21]. Available on: < http://www.electricsense.com/143/what-is-electrosmog/ >.
[3] Dujava, C. – Kolcunová, I. – Pavlík, M.: Meranie elektromagnetických polí v okolí vzdušných distribučných vedení, Elektroenergetika, Vol. 8, No. 2, 2015, ISSN: 1337-6756.
[4] Liptai, P.: Meranie elektromagnetického tienenia kombinovaného materiálu a možnosti jeho využitia. Fyzikálne faktory prostredia. Roč. 5, č. 2 (2015), s. 45-48. ISSN 1338-3922.
[5] Liptai, P.: Metodika merania a hodnotenia vysokofrekvenčných elektromagnetických polí základňových staníc mobilných operátorov v obývaných oblastiach. Ukraine – EU. Modern Technology, Business and Law. Chernihiv National University of Technology, 2016 pp. 306-309. ISBN 978-966-7496-71-5.
[6] WHO označila rádiové elektromagnetické žiarenie za možno rakovinotvorné [online Available on:http://www.dsl.sk/article.php?article=10988
[7] ICNIRP STATEMENT, On the "Guidelines for limiting exposure to time-varying electric, magnetic, and electromagnetic fields (up to 300 GHz)" [online]. Available on: http://www.icnirp.org/cms/upload/publications/ICNIRPStatementEMF.pdf
[8] ICNIRP SCI REVIEW, Mobile phones, brain tumors, and the interphone study: where are we now [online]. Available on: http://www.icnirp.org/cms/upload/publications/ICNIRPSCIreview2011.pdf
[9] Ha, M. - Lim, HJ. - Cho, SH. - Choi, HD. - Cho, KY.: Incidence of cancer in the vicinty of Korean AM radio transmitters [online]. Available on: http://www.ncbi.nlm.nih.gov/pubmed/15859510
[10] Pavlík, M. et al.: Measuring of Dependence of Shielding Effectiveness of Wet Materials on The Frequency of Electromagnetic Field in the High Frequency In: Acta Electrotechnica et Informatica. Roč. 13, č. 3 (2013), s. 12-16. - ISSN 1335-8243

ISSN:2067-3809

ACTA TECHNICA CORVINIENSIS
– Bulletin of Engineering
Tome X [2017]
Fascicule 2 [April – June]
ISSN: 2067 – 3809

[1.]Nebojša RAŠOVIĆ, [2.]Adisa VUČINA, [3.]Milenko OBAD

EXPERT SYSTEM SUPPORT IN PRODUCT DESIGN FOR ADDITIVE TECHNOLOGY AND REVERSE ENGINEERING

[1-3.]University of Mostar, Mostar, BOSNIA & HERZEGOVINA

Abstract: The design for the domain of CAD/CAM systems is a process of decision making where technical solutions have been applied in order to achieve predefined objectives. There are many factors influencing the production of a part that can affect the quality. This paper presents an expert system that provides support for the analysis of CAD model design and its transformation in order to improve production parameters. The system provides multiple analysis as the basis for proposing optimal solution of manufacturing process. Validation of results of the system model is verified through the use of reverse engineering techniques.
Keywords: CAD, expert system, additive technology, reverse engineering

INTRODUCTION

The design process requires multiple phases of the product development[1]. The new parts, configurations and assemblies are presented by some kind of rules, equations and schemes. Each one represents something new and unique [2]. Different approaches have been taken with the aim to optimize the design of a product in additive domain [3-7]. A CAD model is under consideration in terms of his basic characteristic, where weighting factors are usually applied in selection or decision making process [8-11]. Mostly, the additive methods have a common way of production, but some differences between them make great potential for manipulation of a virtual model. Expert system support for additive manufacturing is based on the series of rules which define the procedure for optimal selection of the production parameters. Also, different measuring methods have been taken with the aim to control surface quality. The case study results of this paper is verified by reverse engineering process, where scanner converts the physical object into point cloud [12]. Reverse engineering is modern technology which provides a lot of benefits and possibilities in the CAD/CAM domain [13]. Some of them are including design reconstruction with impacts on shape analysis and prototyping [14, 15], quality control and inspection on certain parts [16], request for making clone of the original model [17], remanufacture of existing parts [18], and more. Very important fact about reverse engineering process is based on effort to eliminate inaccuracy in the proposed scan algorithm [19].

THE EXPERT SYSTEM DEVELOPMENT

Selection of manufacturing parameters is one of the most important tasks which a designer has to make in additive manufacturing process. In order to choose the best for product, designer need to compare more solutions and alternatives, and then make their assessment that is followed by certain constraints. Constraints are enforced by end-use of a product, so that a designer is forced to operate always within these constraints. Build orientation and layer thickness are imposed as the primary parameters in process defining of additive manufacturing. In order to determine properly, those parameters have to be analyzed in right direction. Certain number of criteria include manufacturing time, surface roughness, process errors, geometrical complexity, assembling, functional, ergonomic and aesthetic characteristics etc. [20].

In terms of the expert system building, the first of all, it has developed a structure of the basic variables that carriers of goals and recommendations for a tasks implementation. The development environment is based on the Java platform. A knowledge that is written in a knowledge base represents fundament of the expert system. It has grouped into units that make a logical blocks. A logical blocks are specific for a some data group. A production rules are used for a procedures execution and locomotion. Variables and production rules are distributed over a logical blocks. In expert system technology, each of the expert´s rule is a heuristic. The combination of all the heuristics allows the overall decision making problem to be solved. The example of basic IT/THEN production rule applied to accuracy of additive manufacturing, has the following format:

IF: *The model surfaces need to be produced with high accuracy:*
THEN: *Layer thickness has to be minimal.*

Definition of a production rule is a simple syntax that is suitable for reading and understanding of its meaning. If condition is Boolean operator that checks truthfulness or untruthfulness of the certain case. A rules are independent facts and there are no explicit links between themselves. Manufacturing of a part carries a lot of number of various factors that must be defined in development stage. These factors are defining the overall expediency arising from a part value improvement. Relate to the previous mentioned, it has been showed the expert system rule that provides this area of the part improvement:

IF: *Select improvement direction: Value improvement guidelines*
THEN: *Performance on aspects such as capacity, power, speed or accuracy.*
Freedom from breakdown or malfunction;
Performance under varying environmental conditions.
Secure, hazard-free operation.
Simple, infrequent or no maintenance requirements.
Except for disposable products, a long lifetime which offers good value for the initial purchase price.
Little or no unpleasant or unwanted by-products, including noise and heat.

Building of knowledge base is an important step of the expert system development, besides it is necessary to achieve connection between knowledge base and work prototype together. Also, a user interface must be created as structure of a system. In that circumstances, it has provided a real contribution of a production rules. The expert system work prototype is a program that interacts with experts or novices in order to solve problems. The end user provides an interactive input by selecting one or more answers from the list or by entering data directly. The built system is running as a Java Applet, where it generates an HTML page with Applet tag. This process is running by a local Web browser. Inference engine as the expert system brain checks a control block in order to see actions taken by the end user. Logical blocks are used for instruction implementing. The crucial moments in block executing are confidence variables. A system collects the necessary information from users through static and dynamic variables, and inference engine derives all confidence and collection variables.

Testing of a system accuracy and efficiency is carried out on the steering wheel. This model in interesting from design point of view (Figure 1). Process moves through several testing stages:

- Testing and evaluating knowledge base,
- Testing action of the inference engine,
- Testing interaction and ambiguity of an user interface,
- A system validation.

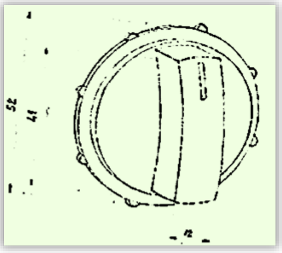

Figure 1. Sketch of the steering wheel

Note that, fulfillment of design requirements is reflected through obligatory tasks in terms of:

- Technical model requirements(Function, Form, Fit, Manufacturing Design, Assembling)
- Aesthetic model requirements (Visualization)
- Ergonomic model requirements (Ergonomic Design)

By detail analyze, there is no reason to divide model into specific zones in order to define layer thickness. For this possibility, it is not necessary to include model features, because layer thickness need to be uniform. So, model segmentation is not necessary, but individual treatment of surfaces is available. Following the system recommendations, model is viewed as integral object, where it is the most desirable to identify and highlight areas important from functional point of view. Such surfaces with a high degree of priority are reference to determine process parameters. Each of the model surfaces can be potential candidate to define process. The steering wheel has eleven candidate surfaces in total (Figure 2).

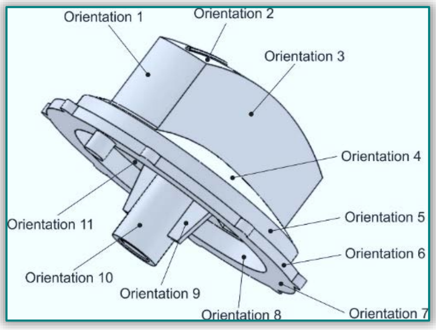

Figure 2. The surfaces as candidates to determine orientation

According to the presented rule (Figure 3), position control is achieved by confidence value definition. As evident from the rule, confidence value 30.0 is relevant mark for vertical orientation (Z axis direction), while confidence value 20.0 is not enough to be main orientation and represent horizontal orientation (X axis direction). All other marks in that diapason make a compromise between these two orientations values.

These values are results of individual treatment of a model surfaces. Also, a system recommendations are related on the layer thickness with respect to required production influential criteria. Graphical representation of the results is shown on Figure 4.

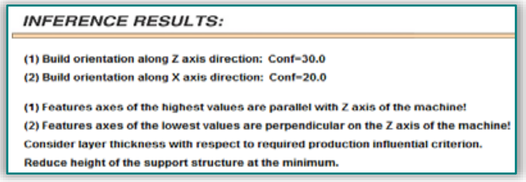
INFERENCE RESULTS:

(1) Build orientation along Z axis direction: Conf=30.0
(2) Build orientation along X axis direction: Conf=20.0

(1) Features axes of the highest values are parallel with Z axis of the machine!
(2) Features axes of the lowest values are perpendicular on the Z axis of the machine!
Consider layer thickness with respect to required production influential criterion.
Reduce height of the support structure at the minimum.

Figure 3. The inference results – analyze of geometrical complexity

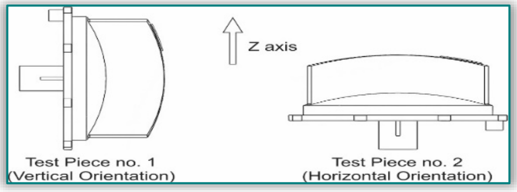

Figure 4. Graphical representation of solutions

SYSTEM VALIDATION THROUGH APLICATION OF REVERSE ENGINEERING

Quality control is a key factor in a modern approach to the process of product design. The ability to provide the geometry as it is actually designed, in its original dimensions and apply it as such is a major challenge in modern engineering. Trying to check the produced form, it's fitting and finally its function, most designers apply different measurement techniques. ATOS optical 3D scanning, based on the principle of border projection proved to be accurate in providing dimensional information in quality control and optimization and creating important measurement reports. Optical scanner delivers geometric data from an existing physical object. The obtained geometric data have been used to analyze the precision of surfaces on the model of the steering wheel of operating temperature of electrical device (Figure 4), made by recommendations of the expert system (Figure 3) by the method of 3D Print (Z450), by company ZCorp. ATOS software calculates complete polygonal grid of high-resolution area for the object by creating a smaller triangles in curved areas and larger triangles in flat areas, without decreasing the accuracy of the grid (Figure 5). The system uses a technique of the reference marking to merge data from different perspectives.

After the scanning is completed, the data supplied by the ATOS system is in arbitrary global coordinate system. To perform the comparison of scanned physical data and CAD original data, scanned data is converted into CAD data of coordinate position.

For the implementation of a detailed analysis, the scanned data is entered into the software GOM Inspect V7.5, where the alignment of compared models is done. For aligning models option prealignment was use (Figure 6). With this type of alignment, the system requires user first to define nominal point on the original CAD model, and then to select the Actual point on the scanned model.

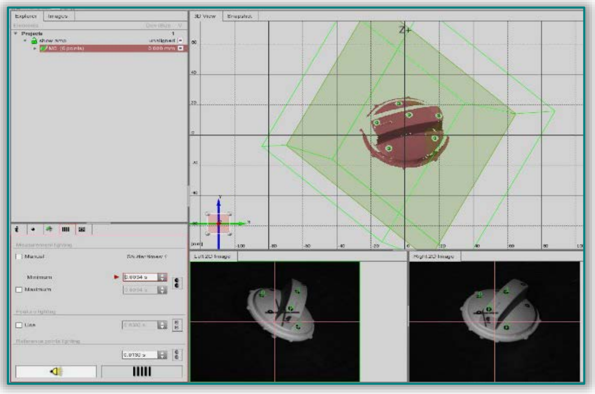

Figure 5. The scanning process of pieces that takes within the ATOS system

Based on the defined reference points, the system account the alignment for the given coordinates and proposes possible orientation of alignment. In other words, the prealignment aligns the scanned data (actual point) automatically according to the original CAD data (nominal point), regardless of the starting positions.

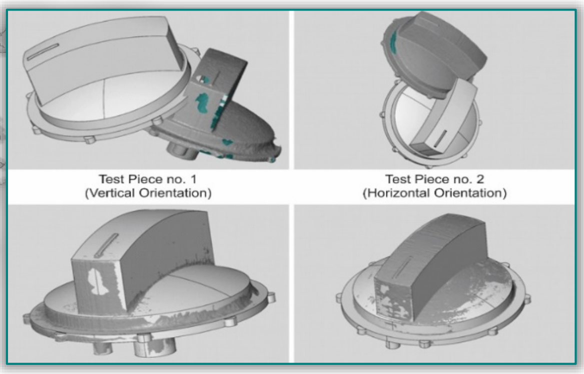

Figure 6. Alignment of objects to be compared

Figure 6 shows the alignment of scanned pieces with the original CAD model. It is immediately evident from the figure that the surfaces of the scanned pieces deviate from the original surface, i.e. the deviation at this stage is more than obvious. According to the analysis, it is concluded that the model made in the horizontal orientation has more accurate geometry than the model made in vertical direction and at this distinct degree has reduced the size of the stairs effect. In this way, the obtained results actually confirm the recommendations of an expert system in order to achieve high quality production of model surface, depending on the geometrical requirements. The process of product design shall not be retained only on the issue of the accuracy of the model, but may include an analysis of the material which is model made from. The models presented in this paper are made from ZP 150 powder. This type of powder is one of the best materials of company ZCorp., available for the use of methods of 3D printing. It provides a significant improvement compared to the previous types of powders, such as better visual impression, and of course the overall strength of the model. Therefore, it is a high performance composite material that provides very good performance for a model from which it is made.

CONCLUSION

Good design of planned product represents more than half of the successful work done. Therefore, the goal is to design a product that is simple and economical to produce. The literature states that the importance of the design process for the production is riddled with the fact that about 70% of the cost of production is determined by decisions made in the design process, while some 20% is determined by decisions made in the production process. However, successful design does not also guarantee an optimal design of a product. An important task of the design process represents a way to simultaneously reduce the cost of production and enhance the functionality and quality of product. Reducing the number of parts on the product is certainly the best opportunity for reducing production costs, because fewer parts means less wasted materials and time to develop.

Problems in the design can be reduced by using standard dimensions and shapes, because their availability and distribution contributes to the easy fitting within the functional structure. In general, the design process is a combination of a series of stages, each stage comprising a set of guidelines and recommendations in order to achieve a more optimal method of production, which ultimately improves the quality of product. Construction of the three-dimensional object at any stage of the design is of great importance especially for engineers and designers employed by the department of product development. In this way it is allowed access to various types of analysis of the model prototype, in order to ultimately conduct more effective engineering.

This way of work enables reducing the time required for product launching on the market. Therefore, the focus is on improving the part function and its task performing in assembly, but at the same time the visual impression and ergonomic design are in focus too.

According to the analysis, it is concluded that the model made in the horizontal orientation has more accurate geometry than the model made in vertical direction and at this distinct degree has reduced the size of the stairs effect. In this way, the obtained results actually confirm the recommendations of an expert system in order to achieve high quality production of model surface, depending on the geometrical requirements. The process of product design shall not be retained only on the issue of the accuracy of the model, but may include an analysis of the material which is model made from. Materials will be the subject of future research.

Note

This paper is based on the paper presented at The 3rd International Scientific Conference on Mechanical Engineering Technologies and Applications (COMETa 2016), organized by the Faculty of Mechanical Engineering, University of East Sarajevo, in Jahorina, Republic of Srpska, BOSNIA & HERZEGOVINA, December 7–9, 2016.

References

[1] Pahl, G., Beitz, W., Feldhusen, J. & Grote, K.-H., (2007) Engineering Design: A Systematic Approach: Springer.
[2] Ullman, D.G., (2010) The mechanical design process, Boston: McGraw-Hill Higher Education.
[3] Cupar, A., Pogacar, V. & Stjepanovic, Z.,(2015) Shape verification of fused deposition modelling 3D prints. International journal of information and computer science. 4: p. 1-8.
[4] Jin, G.Q., Li, W.D. & Gao, L.,(2013) An adaptive process planning approach of rapid prototyping and manufacturing. Robotics and Computer-Integrated Manufacturing. 29(1): p. 23-38.
[5] Rianmora, S. & Koomsap, P.,(2010) Recommended slicing positions for adaptive direct slicing by image processing technique. The International Journal of Advanced Manufacturing Technology. 46(9-12): p. 1021-1033.
[6] Luo, X. & Frank, M.C.,(2010) A layer thickness algorithm for additive/subtractive rapid pattern manufacturing. Rapid Prototyping Journal. 16(2): p. 100-115.
[7] Gibson, I., Rosen, D.W. & Stucker, B., (2010) Additive manufacturing technologies; rapid prototyping to direct digital manufacturing, New York: Springer.
[8] Rašović, N. & Obad, M., (2012)Adaptive slicing in 3D printing process. Proceedings of The 7th International Symposium onMachine And Industrial Design In Mechanical Engineering KOD 2012, Balatonfüred, Hungary, Faculty of Technical Sciences, Novi Sad,p. 243-246.
[9] Rašović, N., Kaljun, J., Obad, M., Novak, M. & Dolšak, B., (2012)The CAD models evaluation using weighting factors in order to optimize RPT process. Proceedings of The 10th International Conference onAdvanced Engineering, Computer Aided Design and Manufacturing CADAM 2012, Vis, Croatia, Revelin, Ičići,p. 95-98.
[10] Rašović, N., Kaljun, J. & Obad, M., (2012)Intelligent decision support system for adaptive slicing in RPT process. Annals of DAAAM for 2012 &Proceedings of The 23rd International Symposium, Zadar, Croatia, DAAAM International Vienna,p. 1095-1098.
[11] Rašović, N. & Obad, M.,(2013) Layered Manufacturing Process Supported By Expert System. Machine Design. 5(2): p. 93-98.
[12] Cekic, A., Rasovic, N., Obad, M., Kaljun, J., Dolsak, B. & Begic-Hajdarevic, D., (2016)Production of Optimized Layered Products using Intelligent Support. Proceedings of the 26th DAAAM International

Symposium, DAAAM International, Vienna, Austria,pp. 0271-0279.
[13] Vinesh Raja & Fernandes, K.J., (2008) Reverse Engineering, Springer London.
[14] Wang, J., Gu, D., Yu, Z., Tan, C. & Zhou, L.,(2012) A framework for 3D model reconstruction in reverse engineering. Computers & Industrial Engineering. 63(4): p. 1189-1200.
[15] Min, Z.,(2011) A New Approach of Composite Surface Reconstruction Based on Reverse Engineering. Procedia Engineering. 23: p. 594-599.
[16] Marciniec, A., Budzik, G., Dziubek, T. & Grzelka, M.a.,(2012) Quality control and inspection of bevel gears of the aircraft gearbox utilizing the Atos 3d Scanner. Journal of KONES. Powertrain and Transport Journal of KONES. Powertrain and Transport. 19(1): p. 261-266.
[17] Jiang, Q., Feng, X., Gong, Y., Song, L., Ran, S. & Cui, J.,(2016) Reverse modelling of natural rock joints using 3D scanning and 3D printing. Computers and Geotechnics. 73: p. 210-220.
[18] Paulic, M., Irgolic, T., Balic, J., Cus, F., Cupar, A., Brajlih, T. & Drstvensek, I.,(2014) Reverse Engineering of Parts with Optical Scanning and Additive Manufacturing. Procedia Engineering. 69: p. 795-803.
[19] Kovács, I., Várady, T. & Salvi, P.,(2015) Applying geometric constraints for perfecting CAD models in reverse engineering. Graphical Models. 82: p. 44-57.
[20] Rašović, N., (2014) Intelligent decision support in design process of products to be produced by layered manufacturing technologies. Ph.D. Thesis, University of Mostar: Mostar, BiH.

10th years ANNIVERSARY

ISSN:2067-3809

We are very pleased to inform that our international and interdisciplinary journal **ACTA TECHNICA CORVINIENSIS ■ Bulletin of Engineering** completed its nine years of publication successfully [**issues of years 2008 – 2016, Tome I–IX**].

In a very short period it has acquired global presence and scholars from all over the world have taken it with great enthusiasm.

ACTA Technica CORVINIENSIS
BULLETIN OF ENGINEERING

ACTA TECHNICA CORVINIENSIS – BULLETIN OF ENGINEERING. Fascicule 1 [JANUARY-MARCH]
ACTA TECHNICA CORVINIENSIS – BULLETIN OF ENGINEERING. Fascicule 2 [APRIL-JUNE]
ACTA TECHNICA CORVINIENSIS – BULLETIN OF ENGINEERING. Fascicule 3 [JULY-SEPTEMBER]
ACTA TECHNICA CORVINIENSIS – BULLETIN OF ENGINEERING. Fascicule 4 [OCTOBER-DECEMBER]

Every year, in four online issues (**fascicules 1 – 4**), **ACTA TECHNICA CORVINIENSIS ■ Bulletin of Engineering [e-ISSN: 2067-3809]** publishes a series of reviews covering the most exciting and developing fields of science and technology. Each issue contains papers reviewed by international researchers who are experts in their fields. The result is a journal that gives the scientists and engineers the opportunity to keep informed of all the current developments in their own, and related, areas of research, ensuring the new ideas across an increasingly the interdisciplinary field.

Now, when will celebrate the tenth years anniversary of **ACTA TECHNICA CORVINIENSIS ■ Bulletin of Engineering**, we are extremely grateful and heartily acknowledge the kind of support and encouragement from all contributors and all collaborators!

On behalf of the Editorial Board and Scientific Committees of **ACTA TECHNICA CORVINIENSIS ■ Bulletin of Engineering**, we would like to thank the many people who helped make this journal successful. We thank all authors who submitted their work to **ACTA TECHNICA CORVINIENSIS ■ Bulletin of Engineering**.

ACTA TECHNICA CORVINIENSIS
– Bulletin of Engineering
Tome X [2017]
Fascicule 2 [April – June]
ISSN: 2067 – 3809

[1.]George MATHEW, [2.]Benny JOSEPH

MICROSTRUCTURAL ANALYSIS OF FLY ASH BASED GEOPOLYMER EXPOSED TO ELEVATED TEMPERATURES

[1.] Division of Safety & Fire Engineering, School of Engineering, Cochin University of Science &Technology, Kerala State, INDIA
[2.] Department of Civil Engineering, V.K.C.E.T, Parippally, Thiruvanathapuram, Kerala State, INDIA

Abstract: Many research work related to geopolymer are being carried out in the recent years because of its better environment friendly status than ordinary Portland cement. This paper attempts to study the microstructural behaviour of fly ash based geopolymer after exposed to elevated temperatures. FTIR, XRD, TGA and SEM analysis has been carried out on geopolymer mortar/paste specimens after they were exposed to 200°C, 400°C, 600°C and 800°C. Based on the present study, the mechanism of early strength loss and the subsequent strength gain of geopolymer during temperature exposure have been established. The difference between the mass loss characteristics of geopolymer paste and OPC mortar specimen when exposed to elevated temperatures has been identified. It has also been established that, the geopolymer will have lower crack width compared to OPC specimen when they are exposed to elevated temperatures.
Keywords: Geopolymer, Fly ash, High temperature, FTIR, XRD, SEM

INTRODUCTION

Cement is the commonly used binding material in mortar and concrete. However during the production of cement almost the same mass of greenhouse gas is also released to the atmosphere [1, 2]. So an alternative material that can replace cement in concrete and mortar will reduce the generation of greenhouse gas to a great extent. One of such promising material is geopolymer.

Geopolymer (GP) is a binding material formed by alkali activation of amorphous alumina-silicate materials under warm atmosphere [3]. Even though exact reaction mechanism for the formation of geopolymer is not clearly known [4], most accepted reaction mechanism has three stages namely dissolution, hydrolysis and condensation [5-7].

The source materials (alumino-silicate) may be natural minerals, such as kaolinite, calcined kaolinite (metakaolin) and clays [5,8,9,10]. Alternatively, industry waste products such as fly ash, slag, red mud, rice-husk ash and silica fume may be used as source material for the synthesis of geopolymers [11-18].

The alkali component as an activator is a compound from the elements of first group in the periodic table. The commonly considered activators are NaOH, Na_2SO_4, water glass, Na_2CO_3, K_2CO_3, KOH, K_2SO_4 or a little amount of cement clinker and combination of alkalis [19].

Large quantity of fly ash generated in thermal power industry faces disposal issue. Only a small percentage of fly is utilized for construction purposes and remaining quantity is disposed in ash ponds or lagoons. Deposition of the fly ash in storage places can have negative influence on water and soil because of its granulometric and mineral composition as well as morphology and filtration properties [20]. Therefore use of fly ash for making geopolymer has dual benefit to atmosphere.

There are many factors which influence the mechanical properties of geopolymer concrete [3,21,22]. Microstructural analysis shows that, amorphisity and particle size of source material, Si/Al ratio etc. in geopolymer influences the mechanical properties of geopolymer concrete [23, 24, 25].

Structures are likely to expose high temperature due to accident or due to functional cause. There is much information regarding the strength loss characteristics of Portland cement concrete after exposure to high temperatures [26-31]. However only few information is available related to the engineering properties of geopolymer after exposure to elevated temperatures and particularly with respect to the microstructural aspects.

It has been reported that strength loss characteristics of fly ash based geopolymer paste, mortar and concrete after exposure to elevated temperature are different [32]. However, a clear understanding about this behaviour is possible only with a microstructural analysis. Hence present study attempts to understand some of the microstructural behaviour of geopolymer after they are exposed to elevated temperatures.

EXPERIMENTAL PROGRAM

Materials

Low calcium fly ash (ASTM Class F) obtained from a thermal power station (India) has been used for the present study. The chemical composition of fly ash is presented in Table1. The fly ash used had a specific gravity of 1.9.

Table 1. The chemical composition of fly ash

Parameter	Content % by mass)
SiO_2	59.70
Al_2O_3	28.36
Fe_2O_3+Fe_2O_4	4.57
CaO	2.10
Na_2O	0.04
MgO	0.83
Mn_2O_3	0.04
TiO_2	1.82
SO_3	0.40
Loss of ignition	1.06

A mixture of NaOH and Na_2SiO_3 solution (SiO_2= 34.64%, Na_2O=16.27%, water 49.09%) was used as alkali solution in the present investigation. NaOH pellets of 98% purity were used to make sodium hydroxide solution. The specific gravity of alkali liquid solution, having Na_2SiO_3/NaOH (molarity 10) ratio 2.5 was 1.54.

Mixture proportioning for GP specimens

Geopolymer paste or mortar was prepared for the microstructural analysis based on a mixture proportion for geopolymer concrete that gave maximum compressive strength. The mixture proportion of GP concrete which gave maximum compressive strength had aggregate content by volume (70%), the ratio of fine aggregate to total aggregate (0.35), ratio of alkali to fly ash by mass (0.55), molarity of NaOH (10), ratio of Na_2SiO_3 to NaOH (2.5) ratio of water to geopolymer solid (0.25).

Details of this study has been reported elsewhere [3].

For preparing specimens for Scanning Electron Microscope (SEM) analysis, mortar from GP concrete prepared based on the proportion as stated above was separated and used. Specimens for Fourier Transform Spectroscope (FTIR), X-ray Diffraction (XRD) analysis and Thermogravimetric (TGA) analysis were prepared with fly ash and alkali in the proportion that has been arrived in the case of GP concrete.

Casting of GP specimens

Mortar specimens of size 10 mm diameter and 10 mm thick were prepared using aluminium tubes for SEM analysis.

GP paste specimens were prepared in a small steel container for FTIR, XRD and TGA analysis.

The specimens were kept in an oven for 24 hours at 100°C for temperature curing. After temperature curing, specimens were demoulded and kept at room temperature till they were tested.

Mixture proportioning for OPC specimens

OPC mortar specimens were prepared for SEM analysis based on a mixture proportion for OPC concrete that gave almost the same compressive strength as that of GP concrete. The detail of study has been reported elsewhere [3].

For preparing specimens for Scanning Electron Microscope (SEM) analysis, mortar from OPC concrete prepared based on the proportion stated was separated and used.

Casting of OPC specimens

Mortar specimens of size 10 mm diameter and 10 mm thick were prepared using aluminium tubes for SEM analysis. After 24 hours (kept in laboratory condition), the specimens were demoulded and immersed in water till they were tested.

Heating and cooling of specimens

GP and OPC specimens (except for TGA analysis) were heated in an electric furnace to 200°C, 400°C, 600°C and 800°C. The rate of heating was kept at 5.5°C per minute. After attaining the target temperature, specimens were kept at the same temperature for 1hour to ensure that the specimens attain a uniform temperature throughout. The heated specimens were then cooled down to room temperature by air cooling.

RESULTS AND DISCUSSIONS

FTIR analysis

Figure 1 shows the comparison of FTIR spectrum of fly ash with that of GP paste at ambient temperature. FTIR spectrum of fly ash has four distinct bands identified as h, g, f and d in the figure. The wave number corresponding to 1088 cm^{-1} (d) and 460 cm^{-1} (h) represents the Si-O/Al-O stretching vibration and in plane bending vibration respectively.

The wave number 795 cm^{-1} (f) indicates the tetrahedral linkage of Si-O-Al and 553 cm^{-1}(g) indicate octahedral linkage of Al [9, 33- 35].

The peak area and peak height in the FTIR spectrum are frequently used in quantitative assessment of geopolymer reaction [Peak area]. The FTIR spectrum of geopolymer paste shows higher peaks corresponding to wave numbers 795 cm^{-1} (f), 1088 cm^{-1}(d) and 460 cm^{-1}(h) as against the FTIR of fly ash. This phenomena indicates an increase in chain length and formation of alumino-silicate compound due to polymerisation [36].

The FTIR spectra of GP paste shows an increased peak in the wave number corresponding to water molecule (3430 cm-1) when compared to fly ash. New band (1635cm-1) showing formation of water molecule is also visible in the FTIR of GP paste. These bands are due to weakly bound water molecule which were adsorbed on the surface or trapped in the large cavities between the geopolymeric products [37]. Wave number corresponding to the 1453 cm-1 (c) and 870 cm-1 (e) represent the presence of Na_2CO_3 and that might be formed due to the carbonation of unreacted sodium silicate and /or sodium hydroxide [9].

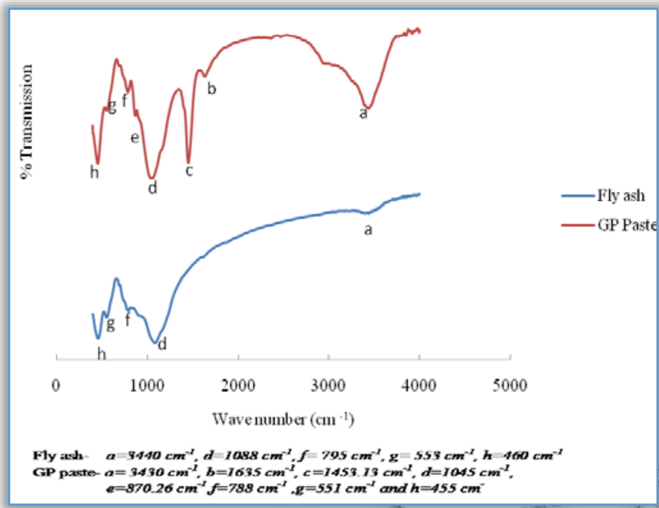

Figure 1. FTIR diagram of fly ash and geopolymer paste

The FTIR spectrum analysis of GP paste exposed to elevated temperatures is presented in Figure 2. Figure 3 shows the enlarged view of FTIR in Si-O-Si and SI-O-Al region (h to d - wave number 460 cm-1 to 1088 cm-1). Figures 2 and 3 shows a substantial reduction of the peak in Si-O-Al and Si-O-Si regions at a temperature exposure of 200°C, indicating a reduction in their bonding force and decrease in chain length [23, 38].

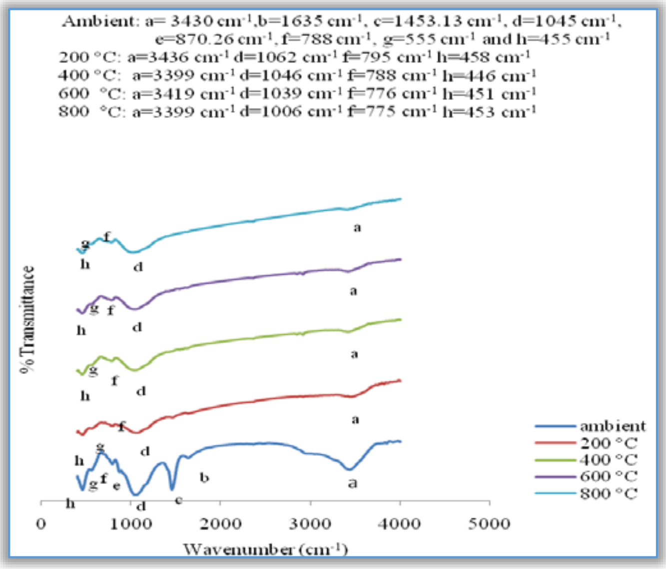

Figure 2. FTIR diagram of geopolymer paste after exposure to elevated temperatures

Figure 2 shows that, the band representing water molecule (hydroxyl groups) in GP paste (3440 cm-1) showed a marked decrease in its peak at a temperature exposure of 200°C and further increase in exposure temperature do not cause significant decrease in these peaks. This means that, most of the weakly bound water molecules that were either adsorbed on the surface or trapped in the large cavities between the geopolymeric products get expelled at about 200°C. The combined result of the above may lead to a reduced strength in GP concrete products during the initial heating process.

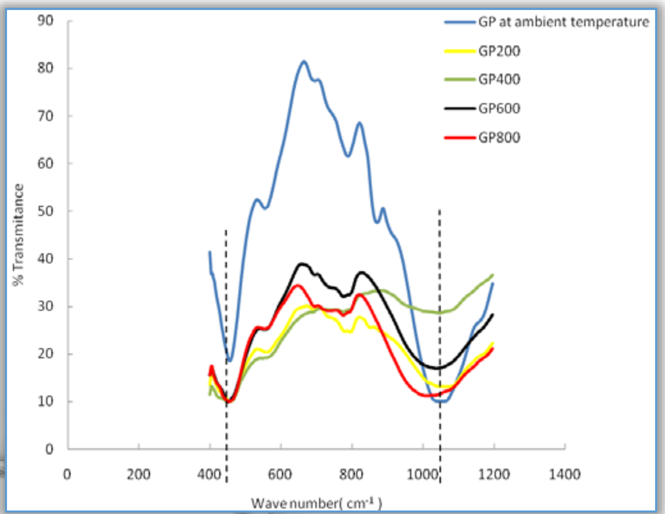

Figure 3. Enlarged view of FTIR diagram

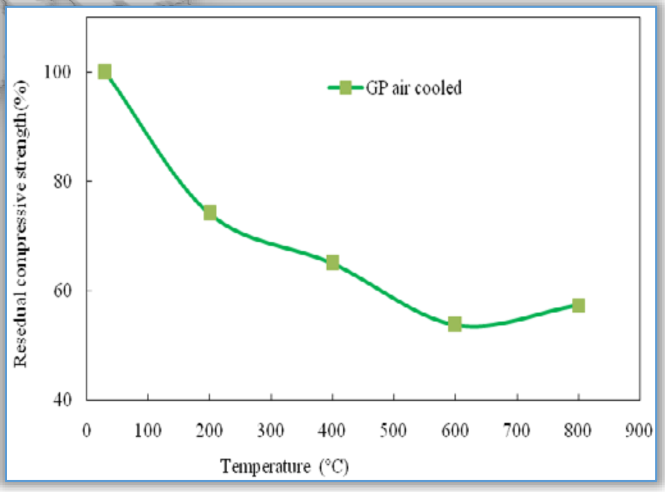

Figure 4. Variation of residual compressive strength of GP concrete with temperature exposure

Also, while the FTIR spectrum of GP paste shows marginal reduction in the peak intensities over the Si-O-Al and Si-O-Si region (h-d) for the temperature exposure between 200°C and 600°C, the peak intensity corresponding to Si-O-Si linkage increases slightly beyond 600°C, confirming the polymerization of initially unreacteted materials beyond 600°C and this may lead to increase in the compressive strength of GP concrete product beyond 600°C temperature exposure.

Typical variation of compressive strength of GP concrete after exposure to temperatures is presented in Figure 4 and this figure confirms the hypothesis of early strength loss and subsequent strength gain of GP concrete when exposed to elevated temperatures.

XRD Analysis

Figure 5 shows the XRD diagram of fly ash and geopolymer paste at ambient temperature. The amorphous phase in GP paste, as per XRD analysis was 78% while that in fly ash was 41%. This is to say that the geopolymer is more amorphous than the fly ash used in it and this observation is consistent with the observations reported elsewhere [25].

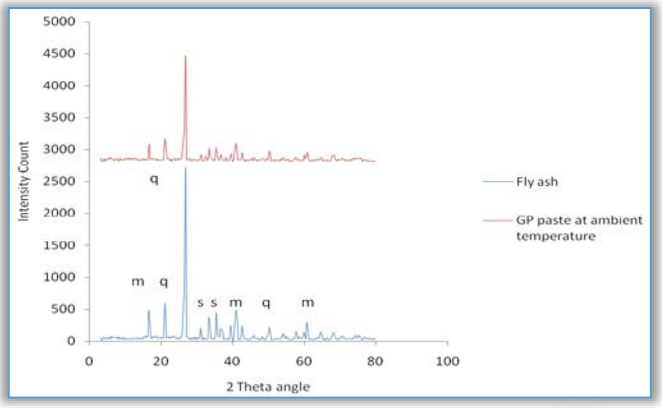

Figure 5. XRD diagram of fly ash and geopolymer paste at ambient temperature

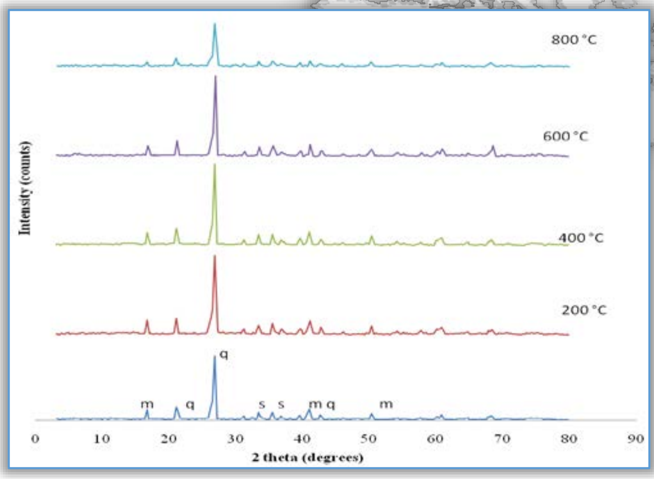

Figure 6. XRD diagram of geopolymer paste after exposed to elevated temperatures

Furthermore, from Figure 5 it is clear (existence of the peaks of Quartz, Mullite and Sellmanite) that, complete dissolution of fly ash due to alkali activation has not taken place at ambient temperature. Figure 6 shows the XRD diagram of GP paste after exposure to elevated temperatures.

From Figure 6, it could be seen that the crystalline materials present in the GP paste has not under gone significant change in its phase up to an exposure temperature of 600°C. However, at 800°C, the crystalline phase got further changed to amorphous phase. This new amorphous content further undergoes polymerization and may cause increased strength in the GP paste.

TGA Analysis

Figure 7 shows the result of the Thermo gravimetric Analysis (TGA) of GP paste.

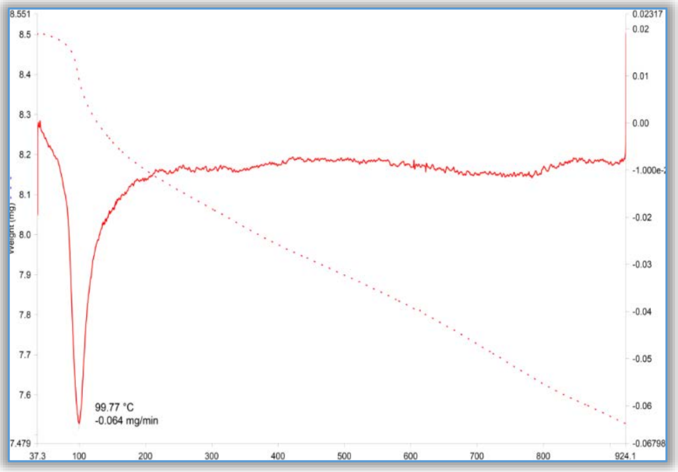

Figure 7. TGA of geopolymer paste exposed to elevated temperatures

A rapid mass loss at 100°C could be seen from Figure 7. Further, the rate of mass loss is more or less constant beyond a temperature of about 200°C. Hence it could be stated that, most of the free water and weakly adsorbed water within the geopolymer paste escape at a temperature below 200°C. This observation is in line with the published literatures [39]. The FTIR analysis presented also justifies the said behaviour. It may further be noted that, the mass loss of OPC specimen at elevated temperature is different from that of GP specimen, primarily due to the difference in the chemical and structural change of OPC specimen at elevated temperatures.

It has been reported elsewhere [40] that the TGA of OPC has three rapid mass loss stages like loss of water due to dehydration of C-S-H between 100°C and 200°C: dehydration of portlandite causing rapid weight loss between 450°C and 500°C; and the decarbonation of Ca_2CO_3 at 750°C.

SEM analysis

The SEM Image study was carried out on GP mortar and OPC mortar taken from their respective concrete samples. The SEM images of GP mortar and OPC mortar specimens were taken after they were exposed to 200°C, 400°C, 600°C and 800°C and air cooled to ambient temperature. These images are compared in Figure 8.

From Figure 8 it could be observed that, at a temperature exposure of 200°C, GP mortar specimen experiences very low crack width (400 nm), compared to the crack width of cement mortar (2.33 μm).

As the exposure temperature increases, both GP and OPC specimen develops wider crack. However, even at 800°C, the crack width of GP specimen is (6.19 mm) lower compared with OPC specimen (16.67).

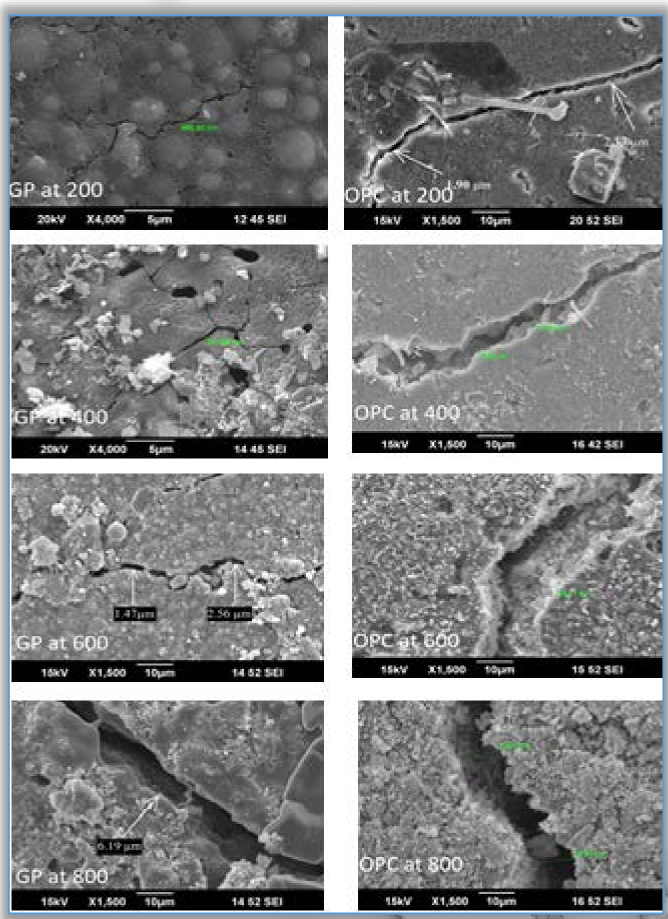

Figure 8. SEM image of GP and OPC mortar after exposure to elevated temperatures

CONCLUSIONS

Following conclusions could be derived based on the experimental study conducted on geopolymer paste and mortar.

a. The geopolymer concrete, when exposed to elevated temperatures, experiences a higher rate of strength loss up to 200°C and gains its strength beyond 600°C.
b. The higher rate of strength loss in the early heating period of geopolymer is contributed due to the reduction in bonding force and decrease in chain length in Si-O-Al and Si-O-Si bond.
c. The strength gain of geopolymer beyond 600°C temperature exposure is primarily due to the polymerization of initially unreacted materials.
d. The materials with crystalline phase in geopolymer tends to change to amorphous phase at temperature above 600°C and undergoes further polymerization; leading to improved strength properties.
e. There is a rapid mass loss in geopolymer at 100°C due to the expulsion of most of the water (free and weakly adsorbed) from the geopolymer. Further, the rate of mass loss beyond 200°C is more or less constant.
f. The mass loss characteristic of geopolymer is different from the mass loss characteristics of OPC paste. The OPC paste undergoes rapid mass loss at three stages when exposed to elevated temperatures (at about 100°C, 450°C and 750°C).
g. The crack developed in geopolymer mortar during early heating period is very much less compared to that of OPC mortar. Even at elevated temperatures, the geopolymer mortar develops only lesser crack width than OPC mortar. In the present study, at 200°C, OPC mortar developed a crack width of about 5.8 times that of geopolymer mortar and at 800°C, the corresponding figure is about 2.7.

Acknowledgements

This project was sponsored by Kerala State Council for Science, Technology and Environment (No. 55/2012/KSCSTE dated 23-01-2012).

Reference

[1.] Davidovits J. High-Alkali Cements for 21st Century Concretes, ACI Special Publication, 1994;144: 383-398.
[2.] Malhotra V M. Making Concrete “Greener” With Fly Ash. Concrete Inter1999: 21(5): 61-66.
[3.] Benny J, George M. Influence of Aggregate content on the Behavior of Fly ash based Geopolymer Concrete. Scientia Iranica 2012; 19(5) : 1188-1194
[4.] Pacheco-Torgal F, Castro-Gomes J, Jalali S. Alkali-activated binders: A review Part 1. Historical background, terminology, reaction mechanisms and hydration products. Constr and Build Mater2008; 22(7):1305–1314.
[5.] Xu H, Van Deventer JSJ. The geopolymerisation of alumino-silicate minerals. Inter Jof Min Proc 2000; 59(3): 247–266.
[6.] Weng L, Sagoe-Crentsil K. Dissolution Processes, hydrolysis and condensation reactions during geopolymer synthesis: Part I- Low Si/Al ratio systems. J Mater Sci 2007; 42(9): 2997-3006.
[7.] Rahier H, Wastiels J, Biesemans M, Willlem R, Van Assche G, Van Mele B. Reaction mechanism, kinetics and high temperature transformations of geopolymers. Journal of Material Science 2007; 42(9): 2982–2996.
[8.] Davidovits J. Geopolymers:Inorganic polymerie new materials. J Therm Ana 1991; 37(8): 1633-1656.
[9.] Barbosa VF, MacKenzie KD, Thaumaturgo C. Synthesis and characterisation of materials based on inorganic polymers of alumina and silica: sodium polysialate polymers. Inter J Inorg Mater 2000; 2(4): 309–317.
[10.] Yang K, Hwang H, Lee S. Effects of Water-Binder Ratio and Fine Aggregate–Total Aggregate Ratio on the Properties of Hwangtoh-Based Alkali-Activated Concrete. J Mater Civil Eng 2010; 22(9): 887-897.
[11.] Ravikumar D, Peethamparan S, Neithalath N. Structure and strength of NaOH activated concretes containing fly ash or GGBFS as the sole binder. Cem Concr Com 2010; 32(6): 399–410.
[12.] Oh JE, Monteiro PJM, Jun SS, Choi S, Clark SM. The evolution of strength and crystalline phases for alkali-activated ground blast furnace slag and fly ash-based geopolymers. Cem Concr Res 2010; 40(2): 189–196.
[13.] Kourti I, Rani DA, Boccaccini AR, Cheeseman, CR Geopolymers from DC Plasma Treated APC Residues, Metakaolin and GGBFS. J Mater Civil Eng 2011; 3(6): 735-740.

[14.]Wongpa J, Kiattikomol K, Jaturapitakku C, Chindaprasirt, P. Compressive strength, modulus of elasticity, and water permeability of inorganic polymer concrete. Materials and Design 2010; 10: 4748–4754.

[15.]He, J., Jie, Y., Zhang, J., Yu, Y., and Zhang, G. Synthesis and characterization of red mud and rice husk ash-based geopolymer composites. Cem Concr Com 2011; 37: 108–118.

[16.]Papakonstantinou G C, Balaguru, PN. Fatigue Behavior of High Temperature Inorganic Matrix Composites. J Mater in Civil Eng 2007: 19(4): 321-328.

[17.]Ranjbar N, Mehdi M, Behnia A, Alengaram UJ, Jumaat MZ. Compressive strength and microstructural analysis of fly ash/palm oil fuel ash based geopolymer mortar. Materials and Design 2014; 59: 532–539.

[18.]Brew DRM, MacKenzie KJD. Geopolymer synthesis using silica fume and sodium aluminate. J Mater Sci2007; 42(11): 3990-3993.

[19.]Jian-xiong C, Han-bin C, Pei X, Lan-fang Z A study on complex alkali-slag environmental concrete. In; International Workshop on Sustainable Development and Concrete Technology 2004; Beijing.

[20.]Lokeshappa B, Dikshit AK. Disposal and Management of Flyash. IPCBEE 2011;3: 11-14.

[21.]Thakur RN, Ghosh S. Effect of Mix Composition on Compressive Strength and Microstructure of Fly Ash Based Geopolymer Composites. ARPN Eng App Sci 2009; 4(4): 68-74.

[22.]Hardjito D, Wallah SE, Sumajouw DMJ Rangan BV. On the Development of Fly - Based Geopolymer Concrete. ACI Mater J 2004; 101(6): 467-472.

[23.]Duxson P, Provis JL, Lukey GC, Mallicoat SW, Kriven WM, van Deventer, JSJ. Understanding the relationship between geopolymer composition, microstructure and mechanical properties. Colloids and Surf A: Physicochemical and Engineering Aspects 2005; 269(1-3): 47–58.

[24.]Xu H, Van Deventer JSJ Effect of Source material on Geopolymerization, Ind and Eng Chem Res 2003; 42(8): 1698-1706.

[25.]Diaz EI, Alloche EN, Eklund S. Factors affecting suitability of fly ash source material for geopolymers. Fuel 2010; 89(5): 992-996.

[26.]Willam K, Xi Y, Lee K, Kim B. Thermal Response of Reinforced Concrete Structures in Nuclear Power Plants. A report submitted at College of Engineering and Applied Science 2009; University of Colorado, Boulder.

[27.]Phan L. Fire Performance of High Strength Concrete: A Report of the State –of-The –Art. Bulding and Fire Research Laboratory, National Institute of Standards, 19996; Maryland.

[28.]Lin W, Lin TD, Powers-Couche LJ. Microstructures of Fire-Damaged Concrete. ACI Mater J 1996; 93(3): 199-205.

[29.]Janotka, I., Bagel L. Pore Structures, Permeabilities, and Compressive Strengths of Concrete at Temperatures up to 800 °C. ACI Mater J 2002; 99(2): 196-200.

[30.]Ahmed AE, Al-Shaikh AH, Arafat TI Residual compressive and bond strength of lime stone aggregate concrete subjected to elevated temperatures. Mag concr res 1992; 44 (159): 117-125.

[31.]Kodur VKR, Sultan MA. Effect of Temperature on Thermal Properties of High-Strength Concrete. J Mater Civil Engin 2003;15(2): 101-107.

[32.]Kong DLY, Sanjayan JG. Effect of elevated temperatures on geopolymer paste, mortar and concrete. Cem Concr Res 2010; 40(2): 334–339.

[33.]Palomo A, Grutzeck MW, Blanco MT. Alkali-activated fly ashes A cement for the future. Cem Concr Res 2008;29(8): 1323–1329.

[34.]Ferna´ndez-Jime´nez A, Palomo A. Mid-infrared spectroscopic studies of alkali-activated fly ash structure. Inter J Inorg Mater 2005; 86(1-3):309–317.

[35.]Sugama T, Warren J, Butcher T. Self-degradable Slag/Class F Fly Ash-Blend Cements", Report prepared for The U.S. Department of Energy, Energy Efficiency and Renewable Energy, Geothermal Technologies Program, 2014; 1000 Independence Avenue SW, Washington, D.C. 20585.

[36.]Bakharev T. "Durability of geopolymer materials in sodium and Magnesium sulfate solutions. Cem Concr Res 2005;35(6):1233-1246.

[37.]Guo X, Shi H, Dick W. "Compressive strength and microstructural characteristics of class C fly ash geopolymer. Cem Concre Com 2010; 32(2): pp.142–147

[38.]Yunfen H, Dongmin W, Wenjuan Z, Hongho LU, Lin W. Effect of Activator and Curing mode on Fly ash based Geopolymers. Journal of Wuhan University of Technology-Mater. Sci. Ed. 2009; 24(5): 711-715.

[39.]Kong DLY, Sanjayan JG, Sagoe-Crentsil K., Comparative performance of geopolymers made with metakaolin and fly ash after exposure to elevated temperatures. Cem Concr Res 2007; 37(12): 1583–1589.

[40.]Alarcon-Ruiz L, Platret G, Massieu E, Ehrlacher A. The use of thermal analysis in assessing the effect of temperature on a cement paste", Cem Concr Res 2005: 35(3): 609–613

ISSN:2067-3809

ACTA TECHNICA CORVINIENSIS
– Bulletin of Engineering
Tome X [2017]
Fascicule 2 [April – June]
ISSN: 2067 – 3809

[1.]Mario HIRZ, [2.]Patrick ROSSBACHER

ENHANCED KNOWLEDGE-BASED 3D-CAD METHODS SUPPORTING AUTOMOTIVE BODY-IN-WHITE PRODUCTION ENGINEERING

[1,2.] Graz University of Technology, Institute of Automotive Engineering, Inffeldgasse 11/II, Graz, AUSTRIA

Abstract: Automotive development is based on virtual product and process models and covers both the development of the car itself as well as of the corresponding production and assembling processes. Considering simultaneous engineering approaches, the integration of product-related and production-associated development plays an important role. Based on an exemplary application in automotive body-in-white development, the present paper introduces and discusses the efficient application of enhanced knowledge-based 3D-CAD methods, including data exchange and management. Target is to support data creation and processing through the implementation of specific algorithms. In this way, a continuous method is provided, which closes the gap between different design, simulation, and production engineering processes.
Keywords: automotive body in white, joining technology, enhanced design, knowledge-based engineering

INTRODUCTION

Automotive development has to face numerous challenges, which are resulting from the accelerated change in ecological, technological, economic and social perspectives. Due to growing globalization, vehicle producers and affiliated suppliers focus on profitable market niches in order to react on a rising market saturation. This "search" for niches results in an increasing variety of different vehicle types and so called derivatives, which represent technical variants of a basic vehicle. As a consequence, the development of several car body variants challenges established development processes and requires the introduction of enhanced knowledge-based 3D-CAD methods.

In addition, the need for fuel consumption reduction leads to amplified application of lightweight technologies in automotive body design. This comprises both, lightweight materials and new design solutions including joining technology. Exemplary, the potential of weight reduction with high-strength steel is about 10 % in relation to conventional steel. Aluminum shows potential between 30 – 40 %, and a full carbon fiber body weights about 50 % less than a comparable standard steel body in the same vehicle class.

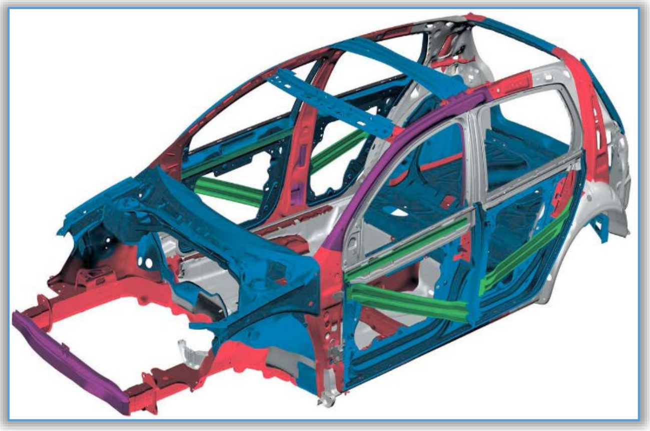

Figure 1 – Steel body structure of the Volkswagen Golf, shown without blanking. The different colors indicate different types of steel [15].

Another important influencing factor for the selection of body material in mass production cars is the cost situation, which can be divided into the consideration of investment costs for production facilities and variable costs for raw material, body panel and parts manufacturing, joining technology, corrosion protection and painting. Details of design, simulation and cost planning in automotive body development can be found in several literature, e.g. [6, 10, 21, 24].

Considering market requirements, lightweight design and development trends, steel bodies show economic advantages in case of larger production sizes above about 100000 pieces per year. But in case of lower numbers of produced car bodies, investment costs for steel deep-drawn and forming tools put this technology in question.

Figure 1 shows an exemplary mass production steel body. Considering investment costs, aluminum body technology comes into play: besides advantageous behavior in view of weight, aluminum space frame design enables the introduction of relatively simple components, which reduces investment costs, but increases costs for assembly and joining techniques.

Figure 2 shows an exemplary space frame aluminum body. Carbon fiber body design represents itself as high technology-solution for sports cars and premium electric cars. The striking physical characteristics of carbon fiber supports development of very stiff and lightweight body structures, which provide leading-edge driving behavior for upscale sport cars, e.g. [3, 13, 14, 19]. Moreover sports cars, one manufacturer has introduced a carbon fiber body for its compact electric car to reduce weight-caused driving resistances, increase driving dynamics and expand the driving range, Figure 3 [4]. Carbon fiber provides advantageous physical behavior, but this technology is the most expensive one for automotive body design by far.

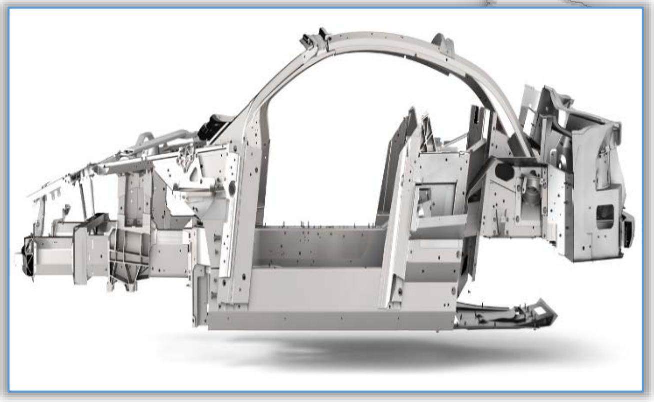

Figure 2 – Aluminum space frame design of the Aston Martin Vanquish, without blanking [13].

Bearing in mind the mentioned aspects of lightweight design, production technology, costs as well as the trend of raising number of car-variants, combinations of different materials will increasingly play an important role in automotive body-in-white design. In this context, joining technology plays a major role for combining components of same or different materials. In automotive steel body production, spot welding plays a major role. A standard car steel body is equipped with about 5000 weld spots, which have to ensure different functional requirements, e.g. body stiffness, durability and crash behavior. In addition, (laser) weld lines come to use in specific applications as well as screws, bolds and rivets. Due to varying material characteristics, aluminum bodies require different design-related solutions and different joining technologies, e.g. (laser) weld lines, bonding, screws, bolds and rivets. The number of weld spots is much lower there.

Figure 3 – Carbon fiber body of the BMW i3 with some adjacent parts [4].

Carbon fiber requires the application of specific joining technology, because of the fundamental different material characteristics, which influence entire body design significantly. In carbon fiber design, the orientation of the fibers within several layers states the basis for advantageous behavior in view of strength, deformation and durability [23]. This anisotropic material behavior must be considered in the structural design as well as in the definition of joining technology. In this way, most components are integrated into the carbon fiber structure, so that an additional joining is not required. In case of adjacent components that have to be mounted, bonding, screws or bolts come to use.

Combining different materials represents the biggest challenge for joining development. Each component pairing has to be optimized in view of functional behavior, lightweight design, production processes and costs. In this context, multi material design requires the application of different, specific joining techniques, which includes all the mentioned technologies with a certain main share of bonding, bolts and screws.

The present publication focuses on the integration of bonding technology into body-in-white development with a focus on the design phase. The design phase plays a major role in automotive development, because the product main characteristics are defined there, [5, 17]. Virtual product models are built-up in computer-aided design (CAD) environment and optimized by use of different types of computer-aided engineering (CAE) applications, [12].

In addition, production-related aspects are considered, and production processes are developed by application of computer-aided manufacturing engineering (CAM) [7, 10]. In digital mock-ups (DMU), the model data are put together and verified for fulfillment of different geometrical, packaging-related and functional requirements.

Figure 4 – Body of Audi R8 e-tron: aluminum space frame technology combined with carbon fiber components, displayed without blanking [1].

The various process steps involve a continuous evaluation and verification of vehicle properties and functions, which is accomplished by the application of proper computer based tools and methods. Within the virtual tool landscape, CAD tools play a key role. Besides the sole geometric description of a part or an assembly, modern 3D-CAD systems provide essential information for subsequent processes, e.g. simulation and production engineering [16]. As illustrated in Figure 5, the consideration of production-related demands and requirements has to start already in the concept phase because of the long preliminary lead-time.

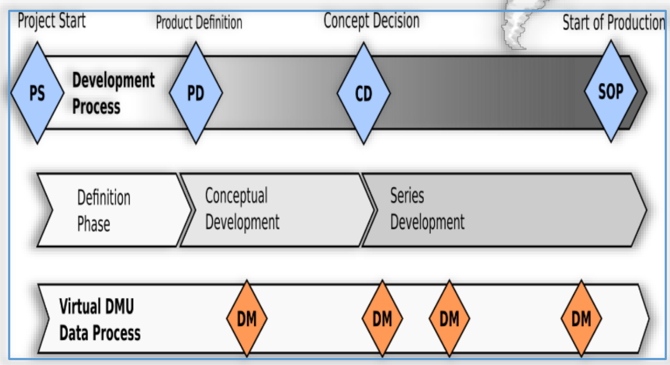

Figure 5 – General schematic overview of a vehicle development process

In order to evaluate and prove the different vehicle properties virtually, a corresponding data process is required, capable of delivering the right data at the right moment with the necessary amount and quality, e.g. for production engineering.

Figure 5 illustrates a schematic data support process with corresponding data milestones (DM). They have to be planned carefully to ensure that the required data can be provided at the right moment with the necessary quality. This forces production requirements to be defined very early in order to be taken into account in data planning. This is a challenging task, since available production tools and mounting elements may vary as a function of global location of the production facility.

INTEGRATION OF PRODUCTION-RELATED ASPECTS INTO JOINING TECHNOLOGY DESIGN IN AUTOMOTIVE BODY-IN-WHITE DEVELOPMENT

A virtual vehicle body model is created in CAD under consideration of technical aspects and simultaneously or subsequently verified within different CAE systems. Examples for CAE-based verification include the simulation process in the course of vehicle stiffness, durability and crash analysis [11, 16]. The calculation programs identify problem areas and then the results lead to optimization cycles of the CAD model. These loops can be run through several times during the development. A similar loop can be found between CAD and computer-aided production engineering. CAD data are passed to the CAM environment, where they are checked regarding manufacturing related aspects. Again, the improvements within CAM are transferred back to the CAD system and may lead to modifications of the CAD models. One goal of process optimization is to improve the communication and data transfer between CAD, CAE and CAM to accelerate the overall development processes, [7].

Joining technology represents a specific area in automotive body-in-white design. It is used to combine different components of an automotive body, e.g. sheet metal parts, but also components made of different materials. In many cases, production engineering of joining techniques has to ensure the accessibility of robots and provide well-arranged configurations for automated processing [18].

In a body-in-white development process, information regarding the applied joining methods is created in CAD by definition of the corresponding flanges at the concerned components, e.g. sheet metal parts, [9]. The CAD model also includes relevant information about the specific joining technology, e.g. weld spots, screw or bond lines. The simulation processes, which verify the stiffness, durability and deformation behavior in case of different crash scenarios, are supplied with the required information regarding joining techniques. Finally, production engineering is also supplied by the CAD-model with required information, e.g. positions and dimensions, the unambiguous definition of involved components and material information.

During data transfer between these different disciplines of development, the CAD model provides central information of the entire development process chain. Besides a considerable effort for the creation of joining techniques models, the definition of metadata, which cannot be provided geometrically leads to amplified engineering workload. Among others, metadata include

the type of connection, the involved components, and the number of circuit of the connections. In joining pairings, the position of the connection surfaces is of great importance, because they provide information about durability and safety-relevant areas.
Due to the increasing importance of specific joining technologies for automotive multi material body development, this publication exemplary focuses on the development process of adhesive technologies within CAD environment [20, 22]. Besides spot welding, weld seams, screws, bolts and rivets, the bonding technology plays a major role because of advantages in view of lightweight design, functional characteristics, lean production as well as low costs. New bonding materials enable powerful connection with an advantageous durability behavior. In addition, different materials can be connected together, which is important for the realization of multi-material design [2].
Figure 6 shows an approach for the efficient integration of bonding technology in virtual automotive body development. The approach includes a comprehensive CAD template model, which provides both technology and process-related information. Within the CAD-model, all relevant connectivity information, as well as the created geometry are prepared for visibility in the connection technique part. This joining technique oriented CAD model includes a specific model structure, which holds the entire data structure of geometry and additional metadata. The structure is used for better overview during development and it also enables to distinguish between different types of joining measures.
The implemented tool supports design engineers when processing data from existing components. After selection of the elements to be joined, material properties and wall thickness of the respective flanges are analyzed and tracked as parameters in a designated area in the model structure. The CAD model supports during processing of existing (delivered) information, and it also allows access to additional joining technique related information. All metadata are handled with the help of specific GUIs (graphical user interfaces), which are programmed within the applied CAD software. These GUIs are prepared for the different types of joining technology differently (welding, bonding, screws and rivets), so that all relevant information can be managed.
In addition to the functional aspects of the software, the tool enables an unambiguous denotation and numbering of the various types of applied joining techniques. The nomination considers the specific components, which are combined in the bonding process, the materials and other related aspects. In this way, the design engineer defines the each bonding surface. After that, the numbers of affected surface are defined automatically for the subsequent components. Finally, all connection elements with the previously defined number ranges are labeled with annotations automatically. This text flags support the creation of 2D-drawings, which provide all required information for further simulation processing and production engineering.
Finally, an automated algorithm elects the previously created data. This data monitoring takes place in a neutral format that is transferred to the involved simulation programs. The data bundle not only includes the required parameters, but also the concerned geometry models.
As important information, all coordinate data and geometrical extensions of each bonding surface is included. This information is saved in a predefined structure as it is exemplary shown in Figure 6. For the transfer to the CAE environment, e.g. for simulation purpose, a pre-defined data format is used. That format includes the type of the connection in a predefined way, so that it can be proceeded by the calculation program automatically.
The same applies to functional characteristics, e.g. identification number, safety relevance, materials of component pairings, wall thickness and part-IDs of the joined components. In addition, another format comes to use, which provides information for data transfer into CAM environments.

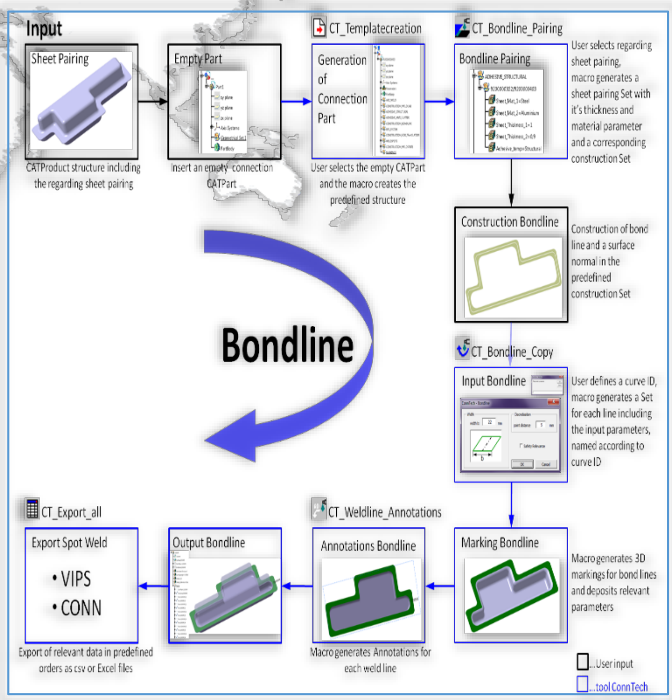

Figure 6 – Exemplary process of bonding in automotive body-in-white development by application of the presented approach.

All the information is specifically tailored for these formats, so that the calculation program or the CAM program prepares no longer obstacles by reading-in the relevant data, supporting effective data transfer.

Respective modifications that may arise during simulation-based investigations in CAE are discharged in a neutral format and transferred back into the CAD environment for further modifications of the design models. The data feedback to the CAD program provides uniform and consistent process results.

The described approach has been implemented in an industrial application, to support the creation, optimization and verification of joining techniques in automotive body-in-white design. The tool is realized as a VBA (visual basic for applications) macro, which is implemented in commercial CAD software [8]. The integration into a commercial software package enables an efficient combination of standard functions for geometry creation and data management with specific programmed operations for the treatment of joining techniques.

CONCLUSION

Taking into account steady decreasing development times in automotive industry, automated processes are becoming increasingly important to support engineers in both product development and data management. In this context, automation is able to accelerate development processes significantly, but it also contributes to process reliability.

By a combination of knowledge-based engineering and structured template geometry models in standard CAD systems, a method has been presented, which maintenances creation and structuring of joining technique-related geometry in automotive body-in-white design. It also supports the CAD-based preparation of relevant data for simulation processes and production engineering.

The paper points out new possibilities for improvement of the entire development process of joining techniques by provision of a comprehensive data model, enabling the integration of styling, design, simulation and production engineering. In this way, the application leads to both, reduced development effort as well as increasing data quality.

Note

This paper is based on the paper presented at The International Conference Management of Technology – Step to Sustainable Production (MOTSP 2016), organized by the Faculty of Mechanical Engineering and Naval Architecture, Croatian Association for PLM and the University of North, in Porec/Parenzo, Istria, CROATIA, June 01–03, 2016.

References

[1] Audi Media center, www.audi-mediacenter.com/en/photos/detail/audi-r8-lms-20154, date of access: 2016-02-15.

[2] Bhowmik, S., Benedictus, R., Dan, Y.: Adhesive Bonding Technology, Handbook of Manufacturing Engineering and Technology, 765-784.

[3] BMW i8, www.bmw.com/com/en/newvehicles/i/i8/2014/showroom/index.html, 2016-02-15.

[4] BMW i3, www.bmw.com/com/en/newvehicles/i/i3/2015/showroom/index.html, 2016-02-15.

[5] Bonitz, P.: Freiformflächen in der rechnerunterstützten Karosseriekonstruktion und im Industriedesign, Springer Publisher, 2009.

[6] Bubna, P.: Impact of light-weight design on manufacturing cost – a review of BMW i3 and Toyota Corolla body components, SAE 2016 World Congress and Exhibition, USA, 2016.

[7] Burr, H.: Informationsmanagement an der Schnittstelle zwischen Entwicklung und Produktionsplanung im Karosserierohbau, Lehrstuhl für Konstruktionstechnik/CAD an der Universität des Saarlandes, 2008.

[8] Dassault Systems, www.3ds.com/products/catia, 2016-01-20.

[9] Frener, G., Thum, K., Hirz, M., Harrich, A.: An application of enhanced 3D-CAD methods with integrated geometry creation algorithms for PVC-seams in automotive body in white design, Journal 3D Research, Springer, 2012.

[10] Grabner, J., Nothhaft, R.: Konstruieren von Pkw-Karosserien, Springer, 2006

[11] Hiermaier, S.: Structures Under Crash and Impact, Springer, 2008.

[12] Hirz, M., Gfrerrer, T., Lang, J., Dietrich, W.: Integrated Computer-Aided Design in Automotive Development - Development processes, Geometric Fundamentals, Methods of CAD, Knowledge Based Data Management, Springer, 2013.

[13] www.astonmartin.com, 2016-02-15.

[14] McLaren Automotive, www.mclaren.com2016-02-10.

[15] Volkswagen AG, www.volkswagenag.com2016-02-10.

[16] Meywerk, M.: CAE-Methoden in der Fahrzeugtechnik, Springer, 2007.

[17] Pahl, G., Beitz, W.: Engineering Design: A Systematic Approach, K. Wallace (editor), Springer Publisher,

[18] Pires, J. N.; Loureiro, A.; Bölmsjo, G.: Welding Robots, Technology, System Issues and Application, Springer, 2006.

[19] Porsche Spyder, www.porsche.com/uk/models/918/, 2016-02-10.

[20] Rossbacher, P., Hirz, M., Harrich, A., Dietrich, W. et al.: The Potential of 3D-CAD Based Process – Optimization in the Automotive Concept Phase, SAE International Journal of Materials and Manufacturing 2, 2009.

[21] Tecklenburg, G.: Karosseriebautage Hamburg, Wie Leichtbau und Elektromobilität nachhaltig die Karosserien beeinflussen, Springer, 2014.

[22] Thum, K., Hirz, M., Mayr, J.: An integrated approach supporting design, simulation and production engineering of connection techniques in automotive

body-in-white development, Journal Computer-Aided Design and Applications, 2013.
[23] Wisner, G., Stammen, E., Dilger, K., Behrens, B.-A.: Adhesively Bonded Blanks for local reinforcements in body-in-white manufacturing, The Journal of Adhesion, Taylor and Francis, December 2015.
[24] Wallentowitz, H.: Freialdenhoven, A., Olschewski, I.: Strategien in der Automobilindustrie, Technologietrends und Marktentwicklungen, Springer, 2009.

ISSN:2067-3809

ACTA TECHNICA CORVINIENSIS
– Bulletin of Engineering
Tome X [2017]
Fascicule 2 [April – June]
ISSN: 2067 – 3809

[1.]Annamária BEHÚNOVÁ, [2.]Lucia KNAPČÍKOVÁ, [3.]Marcel BEHÚN

ECONOMICAL AND ENVIRONMENTAL ADVANTAGES OF MATERIALS MANUFACTURED FROM WASTE TIRES

[1,2.]Technical University of Košice, Faculty of Manufacturing Technologies in Prešov, Bayerova 1, Prešov, SLOVAKIA
[3.]Technical University of Košice, Faculty of Mining, Ecology, Process Control and Geotechnology, Letná 9, Košice, SLOVAKIA

Abstract: Presently, there are known various technologies for processing of waste tires and their components. Rubber materials are by separating devices processed into small pieces or granules, which are added to asphalt, concrete products and in railway sleepers. One disadvantage of these technology solutions is inefficient rubber materials evaluation and potential environmental hazards at their disposal. The paper is focused on therefore reducing the economic and environmental impact on the environment using fabrics components from waste tires. Recycling by itself plays an important role in meeting the objectives of the EU as regards the use of secondary raw materials, namely the reduction of energy consumption and their applications to the new material. Currently, processors of waste recycling systems are motivated to recovery for environmental solutions. There are research companies seeking to develop new more appropriate methods of processing waste tires, and the use of known methods of recovery and their constant innovation.
Keywords: Saving cost, waste tires, secondary raw materials, environment

INTRODUCTION

The current situation in Europe point out highlights the increased activity in the field of waste management of used tires. According to the Slovak Law about "Waste", the waste holder is required to dispose of waste as far as possible be recovered, priority must be given to energy assessment material utilization (combustion). [1] Currently, processors of waste recycling systems are motivated to recovery for environmental solutions. There are research companies seeking to develop new more appropriate methods of processing waste tires, and the use of known methods of recovery and their constant innovation. [2] Slovakia is currently implementing projects with investment aid Recycling Fund to implement environmental objectives. [1] [3] The use of waste tires only for the actual recycling does not make sense. The whole of Europe is engaged in recycling of tires more than 100 independent companies in all Member States. Companies dealing with collection and processing of information on the recovery or disposal of used tires in the world and particularly in Europe, is a lot. One of the main organizations, the company ETRA "European Tire Recycling Association", which gathers information, processes them statistically, evaluate and inform the public about the new possibilities of recovery and subsequent use of the commodity. The individual components of the recovered tires are still defined as a valuable source of raw materials, as well as a viable means to achieve sustainable growth and development. [3] The market for these materials has been shown to be regarded as the most suitable and usable for a wide range of applications. [4] Recent research at the Technical University in Vienna under the guidance of prof. Marini, helped identify a broad range of new products and applications that rely on the chemical and physical properties of recycled tires, especially with regard to cleaning of fabrics components and the use of the separated components. [4], [5], [6]

WASTE TIRES AND THEIR ECONOMICAL AND ENVIRONMENTAL IMPACT

Recycling by itself plays an important role in meeting the objectives of the EU as regards the use of secondary raw materials, namely the reduction of energy consumption and their applications to the new material. [6], [7] Waste tires are a big potential material with saving cost impact on the company. The existing and potential users like to have the use of secondary materials, compared to traditional, often they find that it is significantly more economical and there is thus a reduced environmental impact. Effective recycling of tires a product recycling tries to copy the properties of natural materials. In 2015 the European Union (Figure 1) has been processed by recycling nearly 5 000 000 tons of passenger and truck tires represents almost one third of annual output in 25 emerging countries.

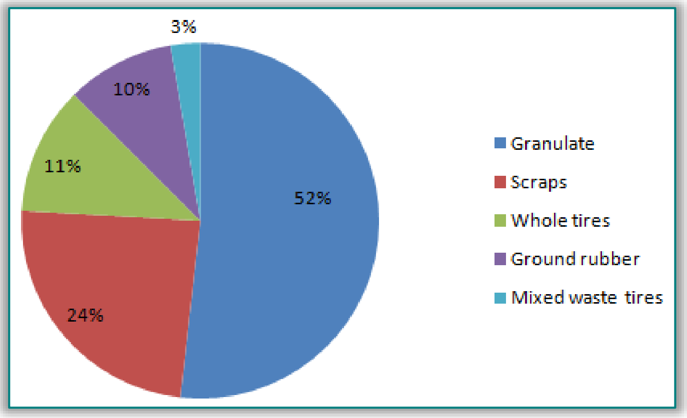

Figure 1. Material production of waste tires in the European Union, year 2015 [5]

Today about 12% of the total quantity of tires is subjected to a treatment such as pressing, removal of wires, the sidewalls, or simple cutting, for use in various applications. [8] About 76% of tires collected for recycling is processed into three broad categories of materials, such as:

≡ Scraps,
≡ Granulate,
≡ Ground rubber (size of 300 mm and ± 500 microns) [5], [9]

Today is very interested in the tire as a valuable source of raw material (Figure 2) is mainly about their final destination. It focuses on the emerging material from amounts collected or processes. [8], [10] For most materials, some percentage of the input material is lost during processing, due to removal of the rubber component, a metal fabric.

It can be says that the indivisible scrap of tires is minimal loss of about 5%. This applies to metals and fabrics. Granulate (about 7–12 mm), may lose approximately 30% of the material, while the loss of a smaller fraction of the rubber granulate or powder may be from 40% to 60%. This depends on the desired size and separation of the impurities. Products and applications using these smaller fractions of materials, generally require that the output product practically free of impurities, a limit of ± 1–5%, with respect to the content of metal or fabrics. Obviously, the greater demand for materials and has specific products which require less treatment before use. This research has led to increased use of whole tires, scrap, gravel, dust and rubber for a variety of engineering applications.

APPLICATION OF WASTE TIRES TO THE INDUSTRY

The paper deals with the production of waste tires component in the composite industry using, secondary raw materials, where the main objective is conservation of raw materials and economical and environmental advantages. Use of this material is mainly in the field of construction, garden and automotive engineering, as finished product or in semi–manufactured forms – granules. Saving the input cost of primary raw material in the production process is currently at the forefront of sustainable development of each country. The effort is used to produce materials with comparable properties and characteristics.

Figure 2. Components after tire recycling (from up to down: steel, granulate, fabrics) [8]

USING WASTE TIRES COMPONENTS IN THE COMPOSITE MANUFACTURE

Fabrics from waste tires are material with high sorption capacity, flexibility and elasticity, excellent sound absorption and thermal insulation properties. At present it is known the use of this raw material in many fields of industry, for example, the production of noise elements in construction, transport (asphalt) and in agriculture (floors in stables). [5] Matrix is a thermoplastic polyvinyl butyral (PVB). Composite materials using two secondary materials–first is fabric from waste tires and second, a matrix is recycled polyvinyl butyral (Figure 3). Company Kurraray (2015) definite a PVB as a thermoplastic, which is typically used for applications requiring strong chemical bonding, optical properties (transparency), and adhesion to the surface of various materials, strength and flexibility. Separation methods there to perfect grinding of windshields using the input line, which is equipped with a highly functional shredder. After reduction comes the conveyors and separators that sorted out metals and other impurities contained in car–glass. Small fragments are further transported to the system of optical sensors, with their help remove debris from the rubble, scrap foils, rubber, etc. displacement. PVB film ensures safety feature in car–glass. PVB film is in the flakes form, which are actually crushed and chopped recycled foil size approx. 20–30 mm. Fibres was obtain from recovery of used tires.

Figure 3. Composite materials after the homogenization [5]

Authors Knapčíková et al. [8] in their research worked on the entrance commodity for the technological process of recovery used tires into which the passenger tires without the necessary pre–treatment and expensive all steel tires. From these tires must be removed heel rope. Heel ropes are removed to dilute the unbroken and knives input device technology line. Tires also are cut, broken into size of about 250 mm x 250 mm. [3], [7] Slashed tires of the conveyor belt, proceed to the second part of the technological line, which are cut in half, from 18 mm to 20 mm. At the end of the crusher magnetic separator, this captures the metal deposited in collection containers. Force captured metal is approx. 90%. The remaining portion which is separated goes along with rubber and cloth in fine granulator. [8] Material passes through a magnetic separator to remove part of the metal residue. When this unit is plugged exhaust system, whose job is to suck fabric section, which is lighter than granules. Cylindrical magnet captures the remaining metal and fibres exhaust system. The composite contains fibres from used tire and recycled polyvinyl butyral after separation by vibrating screens on fabric (fabric purity is 57, 29%). Separation was performed on a vibrating machine, which are wearing stacked sieves with a mesh diameter of 0,9mm to 0,09mm.

The separation is permanent, conducted in 2 phases after 15 min. In the first stage, coarse fabric cleansed from impurities and the second stage is polishing. [8],[9]

CONCLUSIONS

Components from waste tires have a different applicability as a new material in the automotive industry in the motor section, in wheel arches – noise control, mud flaps – corrosion property, resistance to water, snow, aggressive (in winter – gritted road), insulation hood – control noise, vibration capacity, fire resistance. In part of the passenger esp. in car interior, rubber car mats – extra edge protection against seepage of water into the base fabric, door panels – side bar (stainless material property). Second material application in the construction industry in the indoor use as the backing layer underneath wood, laminate flooring, protection against impact sound, floor anti–vibration ability. Other material application is in the construction industry, in garden engineering as curbs, pots, protection against weeds, protection against undesired growth of roots, pools, as a protection, preventing breakage of the release liner pools. Possibility of material application is in civil engineering too, by rail crossings, cushioning materials under the rails, bumps, noise barriers at busy roads.

References

[1.] CHMIELEWSKA E., KURUC J.: Odpady. EPOS, Bratislava, 199–201,2008, ISBN 978–80–8057771–1
[2.] CRAWFORD R.J. : Plastics Engineering, Pergsmon Press, England. 1987Barry, C.M.F.–Orroth, S.A.:Processing of thermoplastics, In: Harper, CH.A.: Modern Plastics Handbook, USA,2000, ISBN 0–07–026714–6
[3.] ZAJAC, J., SMETANKA, Ľ., PAŠKO, J., HATALA, M., HRIN, M.: Systém dezintegrácie pneumatík In: Doprava a logistika. č. 18 (2010), s. 77–90.ISSN1451–107X
[4.] DIN Taschenbuch 18, Kunststoffe– Mechanische und thermische Eingeschaften, s. 251, ISBN 3–410–13421–2
[5.] KNAPČÍKOVÁ, L. – HUSÁR, J. – FEDÁK, M.: Opotrebovaná pneumatika –materiál budúcnosti,

Tribun EU – 2016. – 90 p.. – ISBN 978–80–263–1068–6.
[6.] LIPTÁKOVÁ T.– ALEXY P. a kol.: Polymérne technické materiály, Vysokoškolská učebnica, 2009
[7.] VASILIEV V.V., MOROZOV E.V.: Mechanics and analysis of composite materials, Elsevier, ISBN 0–08–042702–2, 2001
[8.] KNAPČÍKOVÁ L., HERZOG M., ORAVEC, P.: Material characterization of composite materials from used tires, In: Výrobné inžinierstvo. č. 4 (2010), s. 31–34. – ISSN 1335–7972 <www.tuke.sk/fvtpo/casopis>
[9.] KNAPČÍKOVÁ L, PEŠEK, L.: Kompozitný materiál z recyklovaných textílií, úžitkový vzor č. 6907 : Vestník ÚPV SR č.: 052014 – Banská Bystrica : ÚPV SR – 2014. – 8 s..

ISSN:2067-3809

ACTA TECHNICA CORVINIENSIS
– Bulletin of Engineering
Tome X [2017]
Fascicule 2 [April – June]
ISSN: 2067 – 3809

[1.]Biljana MARKOVIĆ, [2.]Miodrag DIVČIĆ

CALCULATION OF THE BEARING MODIFIED RATING LIFE DURING NEW BEARING DESIGN

[1.]Faculty of Mechanical Engineering, University of East Sarajevo, BOSNIA & HERZEGOVINA
[2.]ORAO a.d. za proizvodnju i remont, Bijeljina, Republika Srpska, BOSNIA & HERZEGOVINA

Abstract: Bearings, as a mechanical elements that allow relative movement of rotating parts while transferring loads between them, are primary in the most demanding sectors of machine industry, as automotive and aerospace industry, and they are required to have extremely high level of accuracy of manufacturing and meet the requirements prescribed by international standards. Producers specialized in the production of highly demanding types of bearings must prove eligibility criteria defined in ISO 281:2007 and ISO/TS 16281/2008 specification. This paper deals with the bearing testing results by manufacturer and research of the basic and modified rating life of bearings, the winning of new types of bearings, in accordance with the relevant specifications.
Keywords: bearings, modified reference rating life, testing

INTRODUCTION

It is well known the role of bearings in the engineering industry, as well as elements for rotary motion, which are represented in almost all types of machines where rotation is the basic movement of the craft. Primarily used for supporting the shaft, thereby allowing rotation of the sleeve relative to the fixed support, while the transfer of appropriate load. Of course, the application is wider at the junctions with straight and helical motion, for example threaded couple. Manufacture of bearings, especially rolling, belongs to the standard way of mass production, defined by following features of standard bearings, which can be found in any literature related to bearings or marketing material of producers, in the case of standard types of bearings.

However, the production of special-purpose bearings or bearings of high accuracy and hybrid types of bearings, which are primarily designed for the automotive or aerospace industry is a particular challenge for manufacturers. Therefore, now there is a relatively small bearing manufacturers with increase accuracy in terms of ex Yugoslavia and beyond, who are engaged in this issue and it is very difficult to achieve a higher level of knowledge and experience that is applicable in conquering new types of bearings, which refers to, for example a reduced clearance in bearings, tolerance class 4 or resistance to high temperatures.

Original car or aircraft manufacturers forming separate companies for production bearings exclusively for their needs, on a world scale, and their experience and knowledge are hard to reach for small bearings producers or companies engaged in maintenance, for example maintenance aircraft or aircraft engines. Moreover, in such cases, it is evident the problem of changes in the application of certain types of bearings, when the original manufacturer delivered only a notification (notice) about change to company for maintenance or overhaul, without adequate explanation concerning the reasons for the changes, especially if those relating to the bearing capacity (load) or his rating time.

This paper presents the results of research in the process of conquering new types of bearings for use in the aerospace industry, conditioned by international standards for bearing testing BS ISO 281:2007, Rolling bearings- Dynamic load ratings and rating life and DD ISO/TS 16281:2008, Rolling bearings - Methods for calculating the modified reference rating life for universally loaded bearings.

SPECIFICATION FOR CALCULATION RATING LIFE OF ROLLING BEARINGS

The basic specification regarding rolling bearing is ISO 281:2007, which specifies methods of calculating the basic dynamic load rating of rolling bearings within the size ranges shown in the relevant ISO publications, manufactured from contemporary, commonly used, high quality hardened bearing steel, in accordance with good manufacturing practice and basically of conventional design in regard of the shape of rolling contact surfaces.

This documents also specifies methods of calculating the basic rating life, which is the life associated with 90% reliability, with commonly used high quality material, good manufacturing quality and conventional operating conditions. In addition, it specifies methods of calculating the modified rating life, in which various reliabilities, lubrication conditions, contaminated lubricant and fatigue load of the bearing are taken into account [1].

The basic rating life is given by the life equation:

$$L_h = \left(C_r / P_r\right)^{\alpha} \tag{1}$$

- C_r is basic dynamic load rating
- P_r is dynamic equivalent load
- α - can be 3 or 10/3, depend on bearing type

Detailed calculation is described in ISO 281: 2007, depending on bearing type and and bearing combination (arrangement).

For many years the use of the basic rating life L10 as a criterion of bearing performance has proved satisfactory. However, for many applications it has become desirable to calculate the life for a different level of reliability and/or for a more accurate life calculation under specified lubrication and contamination conditions. With modern high quality bearing steel, it has been found that, under favorable operating conditions and below Hertzian rolling element contact stress, very long bearing lives, compared with the L10 life, can be obtained if the fatigue limit of the bearing steel is not exceeded On the other hand, bearing lives shorter than the L10 can be obtained under unfavorable operating conditions.

A system approach to the fatigue life calculation has been used in this specification and this paper. That means, the influence on the life of the system due to a variation and interaction of interdependent factors is considered by referring all influence to the additional stress they give rise to in the rolling element contacts and under the contact regions [1].

A life modification factor, a ISO is introduced, based on a system approach of life calculation, together with modification factor a1, in this specification. These factors are applied in the modified rating life equation:

$$L_{nm} = a_1\, a_{ISO}\, L_{10} \tag{2}$$

These factors are described in the specification in details. This document does not cover the influence of wear, corrosion and electrical erosion on bearing life.

ISO/TS 16281:2008 is specification which describes methods for calculating the modified reference rating life for universally loaded bearings. This specification taking into consideration lubrication, contamination and fatigue load limit of bearing material, as well as tilting of misalignment, operating clearance of the bearing and internal load distribution on rolling elements. The calculation method provided in this specification covers influencing parameters additional to those described in ISO 281.

It is very important to mention here: this TS (technical specification) is primarily intended to be used for computer programs and together with ISO 281 covers the information needed for life calculation. For accurate life calculation under the operating conditions which has been specified in this specification, it is recommended that either this TS or advanced computer calculation provided by bearing manufacturers, for determining the dynamic equivalent reference load under different loading conditions, to be used [2].

A system approach of the fatigue life calculation is therefore appropriate, as long as the influence on the life of the system from variation and interaction of interdependent factor will be considered. For example, the life modification factor also can be expressed as a function of σ_u/σ, the fatigue stress limit divided by the real stress with as many influencing factors as possible considered.

$$a_{ISO} = f\left(\sigma_u / \sigma\right) \tag{3}$$

But, this ratio can then (in accordance with ISO 76) be sufficiently approximated by the ratio C_u /P, fatigue load limit divided by dynamic equivalent load and the life modification factor can be expressed as

$$a_{ISO} = f\left(C_u / P\right) \tag{4}$$

In the calculation of C_u the following influences have to be considered:

- The type, size and internal geometry of the bearing,
- The profile of rolling elements and raceway
- The manufacturing quality
- The fatigue limit of raceway material

That means, qualified bearing manufacturers can use both of these specifications, together with chosen computer program (as MESYS) for calculating bearing life, under specific testing (load) conditions, defined and provided by manufacturer.

Also, modern technology makes possible to determine a_{ISO} by combining computer supported theory with empirical test and practice experience.

Besides bearing type, fatigue load and bearing load, the factor a_{ISO} considers influence of:

- Lubrication (type of lubrication, viscosity, bearing speed, bearing size, additives)
- Environment (contamination level, seals)
- Contaminant particles (hardness and particle size in relation to bearing size, lubrication method, filtration)
- Mounting (cleanliness during mounting)

That means, modification factor a_{ISO} can be derived from the following equation:

$$a_{ISO} = f\left(e_c c_u / P, \kappa\right) \qquad (5)$$

e_c is contamination factor , κ is viscosity ratio

Simplifying theory regarding rating bearing life which is commonly used for describing and calculating L_{10} is not enough for bearing manufacturer and it can provide wrong calculating results, during first step of bearing design and adopting.

TECHNICAL ACCEPTANCE CONDITIONS FOR TESTING DEEP GROOVE BALL BEARING WITH SOLID BRASS CAGE

In this paper, production and testing of Rolling bearings signed with PLC 04-200, single-row ball bearing with massive brass cage, has been used as a main example for calculating rating life. Bearings provide rotation fit of parts of engine based of principle of rolling friction inside the bearings.

Basic characteristics of material used for bearing production are remelted quality bearing steel with designation 100Cr6 in accordance with ISO 683-17. Technical parameters of cage are not important for this paper.

Table 1. Hardness of components and heat stabilization, load rating and working speed of bearings

Bearing designation	Ring hardness [HRc]	Rolling elements hardness [HRc]	Heat stabilization	Load rating		Working speed RPM [min^{-1}]
				dynamical C_r [kN] ISO281	statical C_{or} [kN] ISO 76	
PLC 04-200	61÷65	61÷65	n/a	9,04	5,53	4 000

n/a-bearing can be used up to 120°C operation environment

Main bearing dimensions and tolerances are part of construction drawing, created by customer (aviation industry). Main parameters of assembled bearing are part of customer requirements, based on specific usage of bearings (specific working conditions and function).

Table 2. Testing parameters for test certificate

Bearing designation	dimensions	Radial play [mm]	Axial Play [mm]	Acceptable vibration	Residual magnetism
PLC 04-200	Δd_{mp}, ΔD_{mp}	Yes	Yes	Yes	Yes

Predominant test is testing of bearings in engine. Range of the tests is prescribed by a costumer. Testing of bearings on testing device of producer are performed based on quality management system testing plan in accordance to customer's order.

Validation tests for standard test of achieving 100% basic dynamical capacity (basic dynamical load rating C based from ISO 281) for each type are provided by manufacturer in range 4-8 pieces selected by a costumer from first batch.

Medium for vibration testing was FAMKORTIL 235 viscosity 40 mm2/sec on 40°C.

TESTING FACILITY

The testing was performed according to bearing test regulations for the manufacturer company, in own test facility. The purpose of the test performed is to verify the function of the bearing design using the test for basic dynamic load capacity (BDLC) of bearings in the manufacturer testing facility.

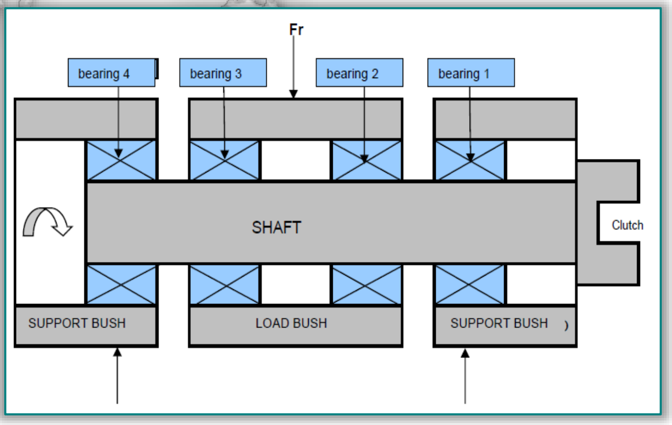

Figure 1. Testing facility station scheme

Table 3. Testing parameters

Parameter	Indication	Value	Unit
Radial Load	F_r	1700	N
Axial Load	F_a	0	N
Equivalent Load	P_r	3,4	bar
Testing ratio		5,3	
Boundary rotational frequency	C_r/F_r	4000	min^{-1}
Test speed	n_k	4800	min^{-1}
Test speed ratio	n_{sk}	0,8	
Calculated resistance %	L_h	522,1	hrs

Figure 2. Testing facility station

To perform the official test under manufacturer Operating procedure, a testing batch of 25 pieces of identical bearings is required, necessary to verify the quality of bearings collected in random selection from production batch. On trial, pcs of bearings PLC 04-200 were delivered by the manufacturer, it is thus a nonstandard testing within the operating procedure and the above mentioned, the test was performed under manufacturer's requirements and decisions stated in the test specification. The test was performed in two testing station (one test station picture 2.) of testing facility in the operating mode of the working week of continues operation , i.e. 24 hours a day, from the beginning of the working week to the end of the working week. On days off, the testing facility was not in operation due to insufficient protection system of its operation.

BEARING TESTING

During the bearing testing, the previously described test bench created by the manufacturer, it was established way of determining the service life of the bearing, by defining C_s% - dynamic load capacity, displayed in%. C_s represents the ratio of dynamic load capacity achieved during the test (tests on the test bench) and the catalogue value of the dynamic load capacity for the type of bearing:

$$C_{s\,\%} = \left(C_S / C_R\right) \cdot 100\% \qquad (6)$$

When the first group of test bearings of the same type, under defined conditions of testing, 8 bearing from each type, 4 bearing on each shaft (picture 1, 2), which are defined and adopted by the manufacturer, is being tested, the method used to calculate the lifetime for terms bearings defined in ISO 281: 2007 specification.

Thus obtained values are compared with the catalogue values for a given type of bearing, and the calculated value of dynamic load capacity C_s.

In this way, the calculated values do not reach 100% capacity, which according to the manufacturer's recommendations are not permitted in the conquest of new types of bearings (Table 4).

Table 4. Load capacity test

P/N	C_r (Kn)	Calculated L_{10} (hrs)	RPM	Achieved C_r
PLC 04-200	10,12	732,5	4000	91,2

Then team (manufacturer and customer participants) analyzed the possible reasons for the appearance of non-conforming bearings, according to the defined acceptance criteria (min. 100% C_s).

Non-conforming bearings were analyzed in two ways:

- Bearing side (material, heat treatment, noise level, produced geometrical parameters)
- Test side (proper loads, RPM, assembly, oil quality)

Also, detailed results analysis are going deeply under bearing side: sample bearing analysis, input control protocol, heat treatment protocol. After that analysis, using theoretical and experimental knowledge, possible failure causes are:

- initial micro - structure before heat treatment
- hardness over 65 HRc – own heat treatment
- failure of inner ring-wrong assembly on the test shaft

Results of analysis gave next results: Input material (annealing state) –reanalysis in manufacturer place gave negative result, no places found with larger cementite particles in original raw material sample. Regarding to heat treatment – hardness was measured under raceway and it increased by deformation reinforcement. Analysis of test side, especially proper loads (load equipment revision), RPM, assembly (bearing assembly plan) and oil quality (check) gave next feedback: Wrong mode assembly on the shaft was rejected. Primary cause of this is rotation connected with pitting on inner ring, which causes rotation move of inner ring and failure on the bore surface.

In the and of previous analysis, results had to give answer on question: Why bearing did not reach 100% capacity, where is the problem? The main answer was: load rating calculation and test calculation.

P/N	Ø IR	Ø OR	R
PLC 04-200	52-52,6%	52-52,6%	3,12 +0,04

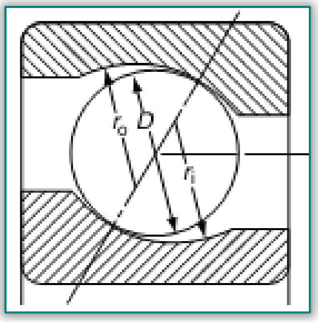

Figure 3. Geometrical parameters of PLC 04-200

Using available information and specifications relating to the subject of the research, it was found that there is a difference in the preferred mode for calculating dynamic load, between the recommendations from specification ISO 281: 2007, which had previously been used, and specification ISO / TS 16281: 2008. It was found that ISO 281 calculation is valid for nominal values and use for initial calculation.

After recalculation of dynamic load capacity, based on specification ISO/TS 16281, used software MESYS, calculated rating life is given in next tables 5 and 6.

Table 5. Load capacity recalculation

P/N	C_r new (kN)	Calculated L_{10} (hrs)	C_r old (kN)	Calculated L_{10} (hrs) old
PLC 04-200	9,04	522,1	10,12	732,5

Table 6. Test results after recalculation

P/N	C_r new (kN)	Calculated L_{10} (hrs)	Achieved C_r %	Achieved C_r old %
PLC 04-200	9,04	522,1	102,1	91,2

CONCLUSIONS

This paper presents the results of tests in the conquest of new types of bearings for industry (aviation use). The characteristics of testing facility, the basic parameters of the tests and the method of bearing testing, according to the manufacturer's recommendations and in accordance with applicable ISO specifications are the basis of this paper.

The main emphasis is put on research of the causes of failing recommended dynamic load bearing capacity (Cs%), while testing bearings on test bench, all in accordance with the requirements of ISO 281: 2007 specification. Research of potential cause of the fault (nonconformity) has been made by the team, in collaboration of manufacturer and the customer participants, and causes that were used for analysis are shown.

At the end of the set of testings that is required to use the technical specification ISO/TS 16281: 2008, which is supplement of the ISO 281: 2007 and gives recommendations for the calculation of the modified rating life, though use of appropriate software package.

All possible known causes of nonconforming due to material, heat treatment and test condition were investigated and rejected.

Finally, team found that difference between standard ISO 281 calculation and adjusted calculation according to ISO/TR 1281 and ISO/TS 16281 gives approx 10% difference for dynamic load rating. Test results after recalculation shows that load capacity of the nonconforming bearings is fulfilled.

These results show that all applicable specifications and technical design specifications, which are related to the production and testing bearing in demanding industries that differ from the standard use, due to the specific conditions of use and function, have to be strictly respected. Also, the causes of the possible occurrence of nonconforming bearing need to be investigated from different aspects in detail, using the available experience and knowledge (usage of best practice), within teamwork. It is very important for the specific bearing usage, especially in aircraft industry.

Note

This paper is based on the paper presented at The 3rd International Scientific Conference on Mechanical Engineering Technologies and Applications (COMETa 2016), organized by the Faculty of Mechanical Engineering, University of East Sarajevo, in Jahorina, Republic of Srpska, BOSNIA & HERZEGOVINA, December 7–9, 2016.

Literatura

[1] BS ISO 281: 2007, Rolling bearings - Dynamic load ratings and rating life;
[2] ISO/TS 16281:2008, Rolling bearings- Methods for calculating the modified reference rating life for universally loaded bearings;
[3] ISO/TR 1281-1, Technical report, Rolling bearings - Explanatory notes on ISO 281
[4] Technical-acceptance conditions for rolling bearings, Test reports for rolling bearings, Kinex bearings, Bytča, Slovakia
[5] Miltenović, V.; Mašinski elementi, oblici, proračun, primena, VII izdanje, 2009, Univerzitet u Nišu

ISSN:2067-3809

We are very pleased to inform that our international and interdisciplinary journal **ACTA TECHNICA CORVINIENSIS ■ Bulletin of Engineering** completed its nine years of publication successfully [**issues of years 2008 – 2016, Tome I–IX**].

In a very short period it has acquired global presence and scholars from all over the world have taken it with great enthusiasm.

Every year, in four online issues (**fascicules 1 – 4**), **ACTA TECHNICA CORVINIENSIS ■ Bulletin of Engineering [e-ISSN: 2067-3809]** publishes a series of reviews covering the most exciting and developing fields of science and technology. Each issue contains papers reviewed by international researchers who are experts in their fields. The result is a journal that gives the scientists and engineers the opportunity to keep informed of all the current developments in their own, and related, areas of research, ensuring the new ideas across an increasingly the interdisciplinary field.

Now, when will celebrate the tenth years anniversary of **ACTA TECHNICA CORVINIENSIS ■ Bulletin of Engineering**, we are extremely grateful and heartily acknowledge the kind of support and encouragement from all contributors and all collaborators!

On behalf of the Editorial Board and Scientific Committees of **ACTA TECHNICA CORVINIENSIS ■ Bulletin of Engineering**, we would like to thank the many people who helped make this journal successful. We thank all authors who submitted their work to **ACTA TECHNICA CORVINIENSIS ■ Bulletin of Engineering**.

ACTA Technica CORVINIENSIS
BULLETIN OF ENGINEERING

ACTA TECHNICA CORVINIENSIS – BULLETIN OF ENGINEERING. Fascicule 1 [JANUARY-MARCH]
ACTA TECHNICA CORVINIENSIS – BULLETIN OF ENGINEERING. Fascicule 2 [APRIL-JUNE]
ACTA TECHNICA CORVINIENSIS – BULLETIN OF ENGINEERING. Fascicule 3 [JULY-SEPTEMBER]
ACTA TECHNICA CORVINIENSIS – BULLETIN OF ENGINEERING. Fascicule 4 [OCTOBER-DECEMBER]

ACTA TECHNICA CORVINIENSIS
– Bulletin of Engineering
Tome X [2017]
Fascicule 2 [April – June]
ISSN: 2067 – 3809

[1.]Sorina SERBAN, [2.]Teodor HEPUT, [3.]Imre KISS

RECYCLING EXPERIMENTS ON PULVEROUS WASTES RESULTED FROM FERROUS INDUSTRY, MINING AND ENERGETIC SECTORS

[1-3.]University Politehnica Timisoara, Faculty of Engineering Hunedoara, ROMANIA

Abstract: The implementation in the industrial practices of the accounting technologies of the ferrous powdery wastes, now stored in the regional ponds of the nearby ferrous industry, mining and energetic sectors, assure in time the repossession of this place occupied by the wastes, to the natural environment. The recovery through pelletizing of the pulverous ferrous wastes stored in the regional ponds can be significant for the environmental protection, given by the increase of recovery for pulverous wastes and reduction of depository spaces for these wastes. The economical aspect is reflected by transferring depositary expenses to other purposes. In the paper some researches and relevant results are presented, regarding the obtaining of the pellets, using wastes resulted from ferrous industry (steel dust, agglomerating–furnace dust), mining (red mud, galvanically sludge) and energetic (thermal power plant ash) sectors. In addition, in the pellets recipes, graphite is used as the reducing agent, respectively bentonite and lime are used as binders.
Keywords: ferrous pulverous wastes, pellets, environmental protection

The deposition of the small and pulverous waste leads to both the pollution of the natural environment by diffuse emissions of harmful compounds and also the contamination of surface and groundwater, areas that go far beyond the perimeters of deposition. Waste recycling processes reduce the negative environmental impact of the deposition.

Recycling is a process to change waste materials into new products to prevent waste of potentially useful materials, reduce the consumption of fresh raw materials and reduce water pollution (from landfilling) by reducing the need for conventional waste disposal. [1–4, 15–20] Recycling of pulverous wastes has emerged as a viable alternative to reduce pressure on the existing reserves of metals. [15–20] It is far more economical for the industries and is also eco–friendly. Therefore, the research suggests that by reusing products, recycling wastes, and making environmentally by–products, businesses can cut costs and increase profits. [15–20] Cost savings take the form of:

- lower waste disposal costs;
- lower waste treatment costs;
- savings on natural materials;
- a reduction in regulatory compliance costs;
- lower storage costs;

Figure 1. Recovery of ferrous wastes strategies

The waste has become a major problem for the various industrial sectors. Concepts like prevention, reuse, recycling, recovery, disposal and their ranking are on the order of the day in the management of the different streams of waste. But the implementation of these

concepts implies the very good knowledge of waste characteristics.
For Romania the recovery of ferrous wastes represents a priority for the durable development strategy because the natural resources of some raw materials categories are poor or insufficient and the resources can substitute part of the raw materials with significant low costs.[1–4, 11] Comparatively with the practice and the world wide manifested tendencies, the Romanian industry registers gaps in the powder wastes collection, transportation and storage area, as well as in that of the recovery technologies area by their recycling or reusing. [5–20] Thereby, the approach of the superior recovery of small and powder ferrous wastes problem was considered necessary and convenient.

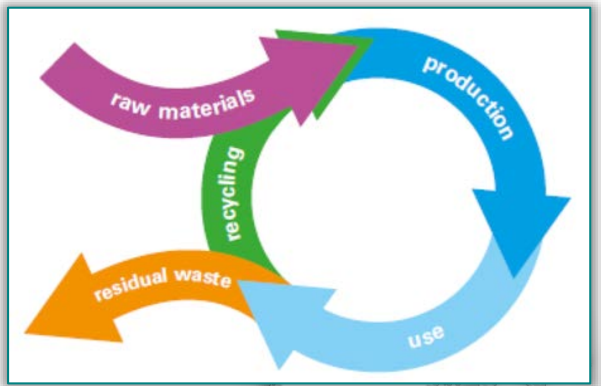

Figure 2. The recycling in the circular economy

The administration of secondary materials must represent a problem of strategy in the internal practice of the company, taking into account the following objectives:
- reducing to the minimal level the quantity of secondary products
- minimizing through recycling the secondary products obtained from a technological process
- increasing the degree of recovery (transforming wastes in useful by–products for other sectors)
- dominating through supervising and control of problems with a negative impact upon the environment, that can occur when treating and transporting wastes.

Today, the man–caused deposits can be equated with the exploitable deposits of natural resources. [1–4] There exist the two ways to increase the volumes of natural resources:
- » by improving the prospecting, delivery and storage methods, deals with the technologies of deposits exploitation, and
- » by increasing the effectiveness of their usage, with the technologies of their usage or the, so called, resource–saving technologies, from the basis of stable development concept.

Expansion of use of secondary raw materials, such as scrap and other ferrous metallurgy wastes, are an important factor of metal industry development from the point of view of its provision with raw materials. Recycling and utilization of wastes with content of useful elements is important not only from the point of view of their usage as an alternative source of raw materials, but regarding the environmental problems also. [1–4, 15–20]
The analysis has allowed us to formulate a scientific problem with the solution in two directions: [1–4, 15–20]
- » On the one hand, waste processing and using it as a relatively cheap raw material for metallurgical manufacture, noticeably lowers expenditures on mix material and improves the quality and competitive strength, and above all lowers the net cost of the finished product. Therefore, recycling and recovery of wastes and their use as low–cost metallurgical raw material entails the considerable reduction of charge costs, increase in the finished products quality, competitiveness and prime cost.
- » On the other hand, the solution of the ecological problem of purification of whole regions where many man–caused waste deposits have been accumulated and reclaiming of current storage of waste of the mentioned above manufactures. Therefore, is a solution for salvation of ecological problems of the entire regions possessing enormous deposits of industrial wastes as well as utilization of current wastes.

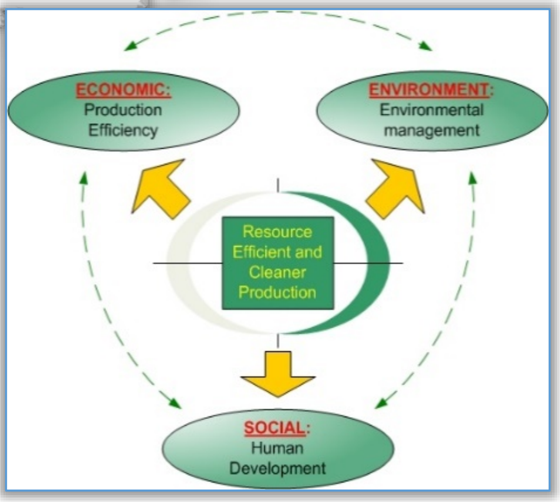

Figure 3. Resource efficient and cleaner production

A mixture charge for use in all kinds of metallurgical processes, ensures the industrial wastes recycling in the form of iron–and–carbon containing pellets ensures a considerable increase in technical and economical characteristics of metal works processes with the simultaneous improvement of ecological situation. [1–4, 15–20]
Recovery and reuse recyclable resources represent the means of give back total settlement of the requirements of the economic growth process and the restrictive character of the resources. At the same time the activity

of recycling deep interferes with the activity of the environment protection, to increase recycling by decreasing the polluting pressure on the environment.

MATERIALS

Our paper presents in the following lines the experiments and the results regarding the re–introduction into the economical circuit of the following ferrous pulverous wastes: steel dust and agglomerating–furnace dust.

The wastes from mining sector (red mud, galvanically sludge) and energetic sector (thermal power plant ash), together with the steel dust and the agglomerating dust were subjects of the pelletizing process, in presence of graphite, used as the reducing agent, respectively bentonite and lime, used as binders. The experiments were put into practice in the iron laboratories of the Faculty of Engineering in Hunedoara. [15–20]

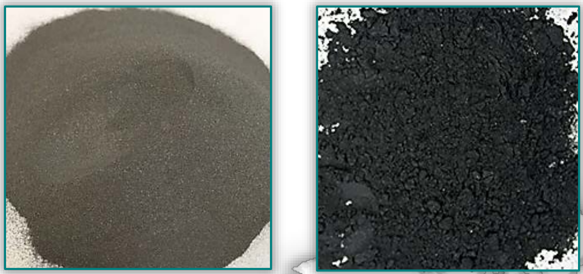

Figure 4. Steel dust and Agglomerating–furnace dust

Figure 5. Galvanically sludge

Figure 6. Red mud

Figure 7. Graphite and Bentonite

Figure 8. Lime and Thermal power plant ash

The recipes compositions for the pelletizing charges in Table 1 are presented. At preparation of the recipes, we have in consideration the following distribution of the components:

- The first four (4) recipes (R1-R4) are prepared without thermal power plant ash (and large variations of other components), as are presented in Table 1 and Figures 9-12.
- The next three (3) recipes (R5-R7) are prepared without graphite (and large variations of other components), as are presented in Table 1 and Figures 13-15.
- The next two (2) recipes (R8-R9) are prepared without thermal power plant ash, graphite and lime (with steel dust or with agglomerating-furnace dust as main component), as are presented in Table 1 and Figures 16-17.
- The next two (2) recipes (R10-R11) are prepared without thermal power plant ash, graphite, lime and red mud (with steel dust or with agglomerating-furnace dust as main component), as are presented in Table 1 and Figures 18-19.
- The last two (2) recipes (R12-R13) are prepared without thermal power plant ash and agglomerating-furnace dust (without red mud or without galvanically sludge), as are presented in Table 1 and Figures 20-21.

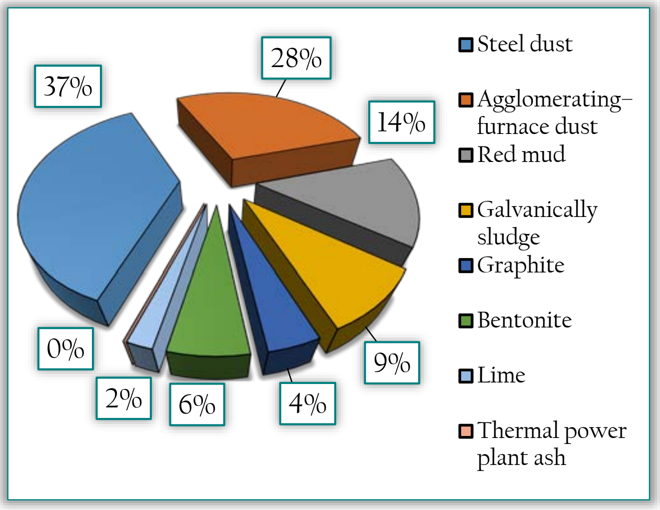

Figure 9. The recipe R1: Without thermal power plant ash (and large variations of other components)

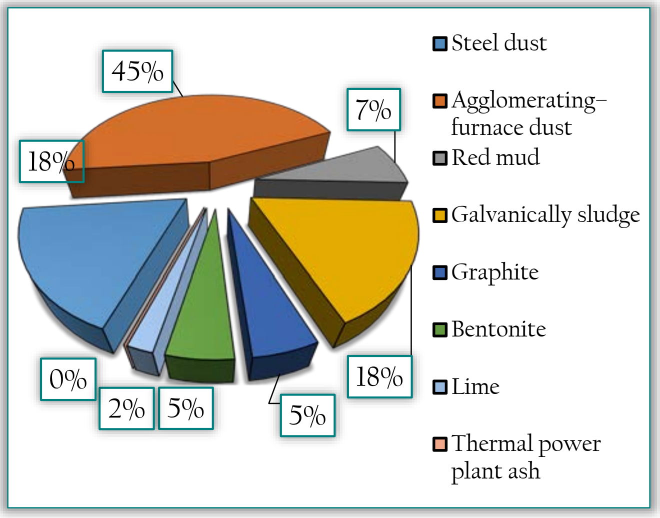

Figure 10. The recipe R2: Without thermal power plant ash (and large variations of other components)

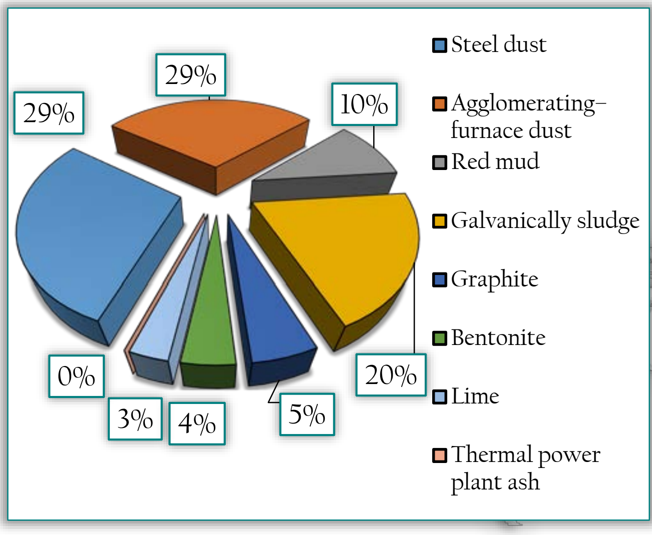

Figure 11. The recipe R3: Without thermal power plant ash (and large variations of other components)

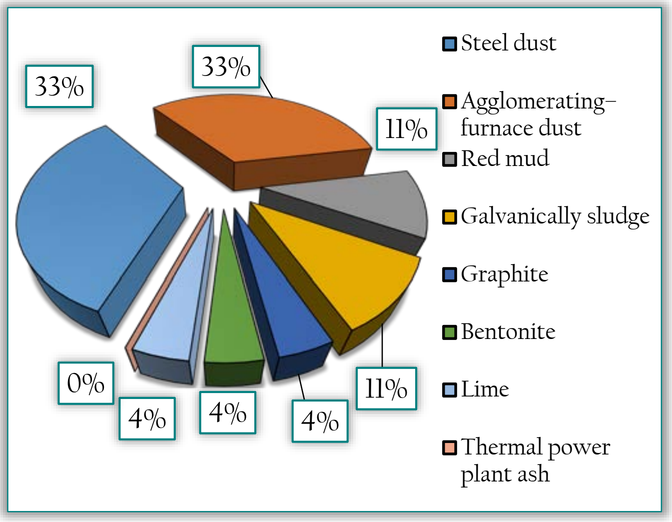

Figure 12. The recipe R4: Without thermal power plant ash (and large variations of other components)

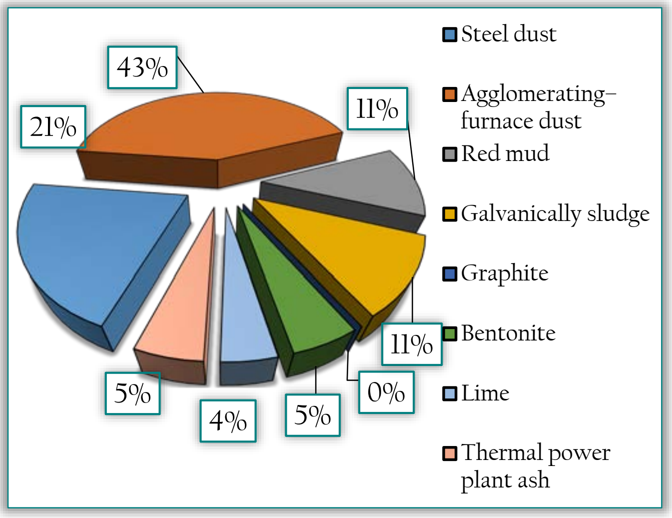

Figure 13. The recipe R5: Without graphite (and large variations of other components)

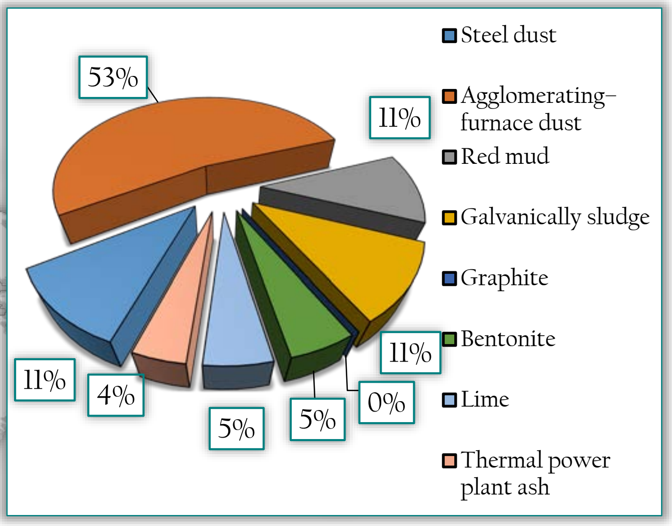

Figure 14. The recipe R6: Without graphite (and large variations of other components)

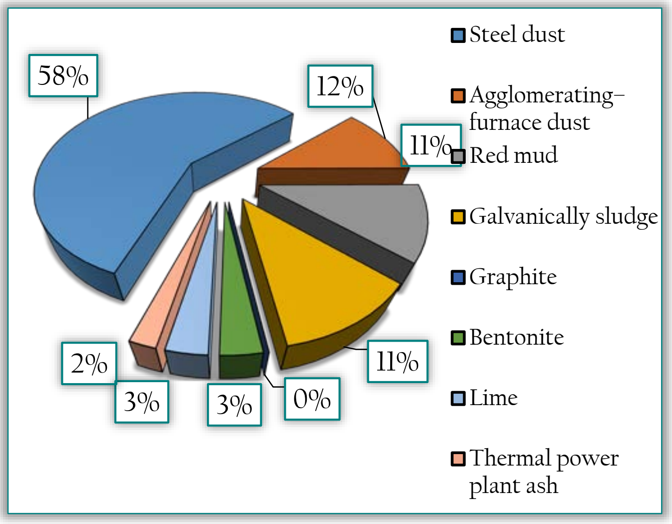

Figure 15. The recipe R7: Without graphite (and large variations of other components)

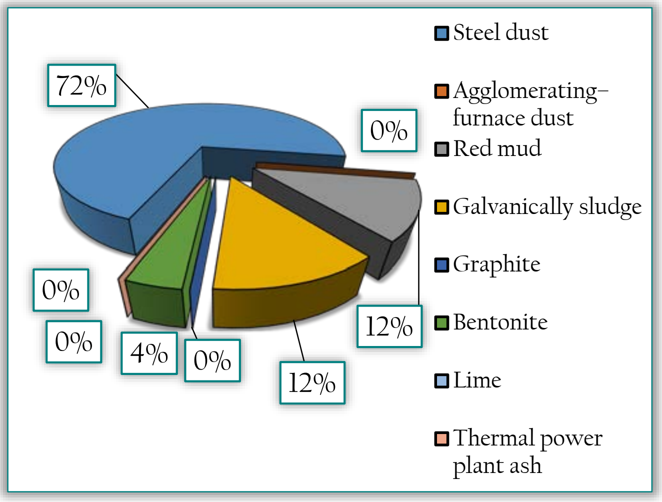

Figure 16. The recipe R8: Without thermal power plant ash, graphite and lime (with steel dust)

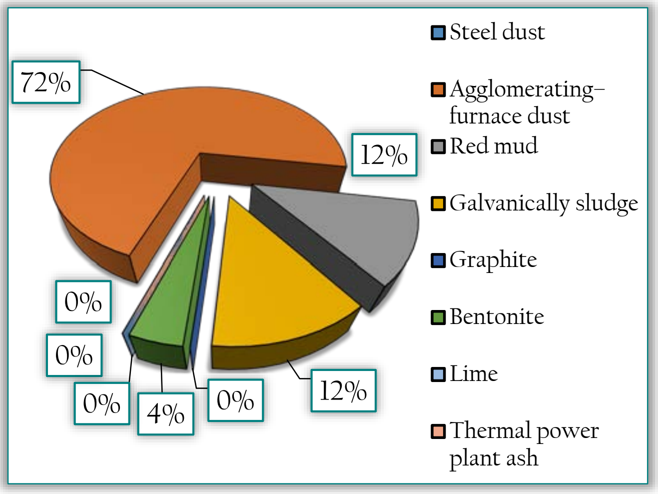

Figure 19. The recipe R11: Without thermal power plant ash, graphite, lime and red mud (with agglomerating-furnace dust)

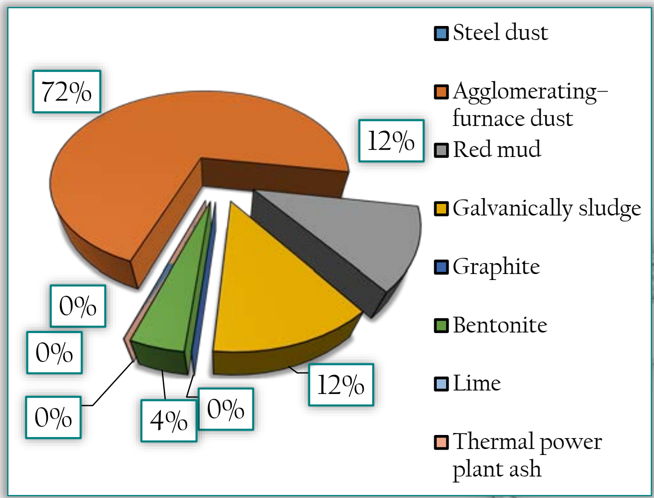

Figure 17. The recipe R9: Without thermal power plant ash, graphite and lime (with agglomerating-furnace dust)

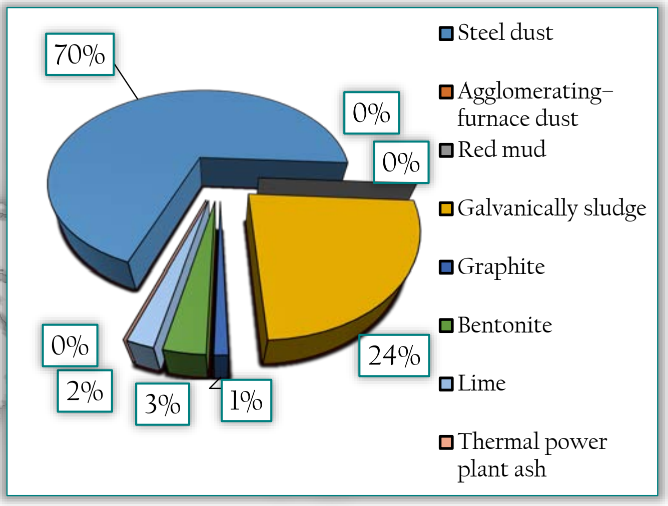

Figure 20. The recipe R12: Without thermal power plant ash and agglomerating-furnace dust (without red mud)

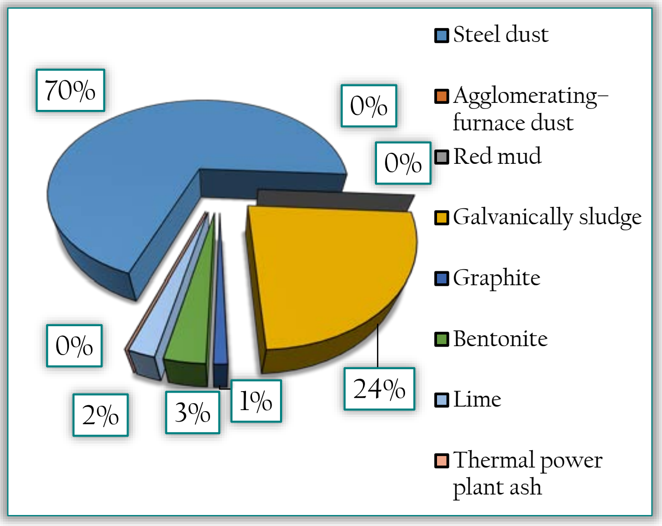

Figure 18. The recipe R10: Without thermal power plant ash, graphite, lime and red mud (with steel dust)

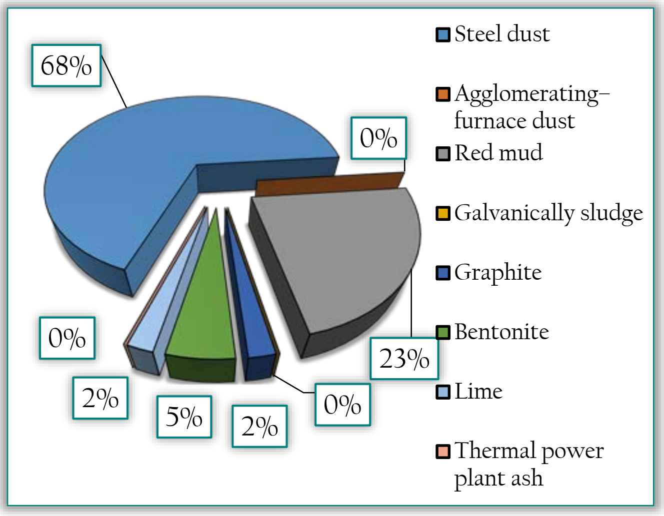

Figure 21. The recipe R13: without thermal power plant ash and agglomerating-furnace dust (without galvanically sludge)

Table 1. The pelletizing recipes, [%]

	Wastes type	R1	R2	R3	R4	R5	R6	R7
1.	Steel dust	37	18	29	32	21	11	57
2.	Agglomerating–furnace dust	28	45	29	32	42	53	11
3.	Red mud	14	7	10	10	11	11	11
4.	Galvanically sludge	9	18	20	10	11	11	11
5.	Graphite	4	5	5	4	–	–	–
6.	Bentonite	6	5	4	4	5	5	3
7.	Lime	2	2	3	4	4	5	3
8.	Thermal power plant ash	–	–	–	–	5	4	2

	Wastes type	R8	R9	R10	R11	R12	R13
1.	Steel dust	72	–	72	–	69	68
2.	Agglomerating–furnace dust	–	72	–	72	–	–
3.	Red mud	12	12	–	–	–	23
4.	Galvanically sludge	12	12	24	24	23	–
5.	Graphite	–	–	–	–	1	2
6.	Bentonite	4	4	4	4	3	5
7.	Lime	–	–	–	–	2	2
8.	Thermal power plant ash	–	–	–	–	–	–

RESULTS

The input pulverous wastes are prepared, blended, mixed and conditioned correctly before being fed in a controlled manner into the pelletizing disc. The material is then granulated to a size and shape that can be tailored to suit each customer's individual requirements. After pelletizing, the pellets were dried (in air stream) the process being guided in such a way as to reach a resistance of a minimal 100 daN/pellet.[11,15–20]

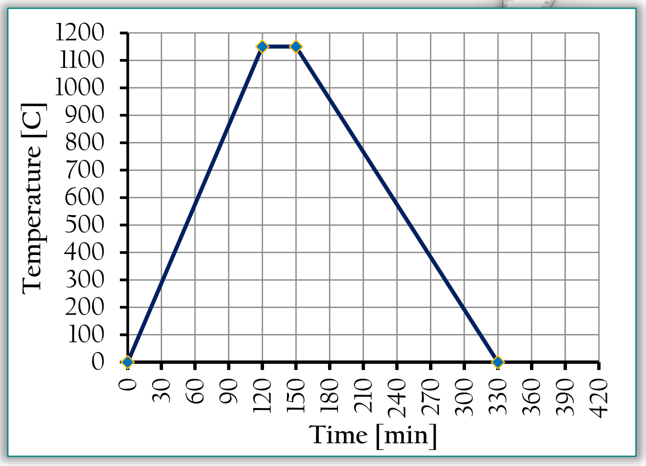

Figure 21. The diagram of hardening processes

The obtained pellets shall be subjected to the hardening processes, initially in the normal atmosphere and subsequently according to the scale of the desirable reduction, in ovens with resistance, heated to 1150°C for 2 hours, holding 0.5 hours and air cooling using a heating – holding – cooling diagram established on the basis of several experiments. (see Figure 22).

Figure 22. Pellets in the calcination oven

Figure 23. Pellets

CONCLUSIONS

The researches and experiments put into practice, led to the following considerations:

≡ two different types of pulverous ferrous wastes (steel dust and agglomerating–furnace dust) are processed through pelletising, together with two wastes from mining sector (red mud, galvanically sludge) and one from the energetic sector (thermal power plant ash), in presence of reducing agent (graphite) and binders (bentonite and lime);

≡ the utilization of these wastes presents an important interest considering the large quantities that are deposited in the ponds (especially the pulverous ferrous wastes). Due to these large quantities there is the danger of their break–down, having severe consequences upon the environment;

≡ the results allow the re–introduction into the economical circuit of some pulverous ferrous wastes which can replace a part of the waste iron, which is a deficitary raw material in the steel making processes;

≡ according to the target had in view (recuperated iron, correction of the slag's chemical composition) the quality of the pellets and the adequate recipe is chosen; technically speaking, the pulverous ferrous additions can be used to produce complex additions, which are very useful for active slag formation;

≡ from the point of view of the compression resistance, the pellets are adequate to be used in the electric arc furnaces which are used in steel making.
≡ a considerable decrease of environmental pollution would be possible in the vicinity of these ponds, and this would an action of considerable social impact (dust draws disappear through air streams, the risk of falling ill decreases, as well as that of soil sliding and water pollution);

In our country there are opportunities to bring in the productive circuit large quantities of pulverous metallic scraps, metallurgical slags and ashes from the thermal power plants that work with coal. They could be used as recycled materials and thus will reduce the quantities of exploited mineral resources. Also the organization of the collection and recovery of such waste can be very effective ways in the reduction of society's pressure upon the non-renewable resources.

The organization and management of more efficient reusable materials in our country should be as a priority from the following preconditions:

¤ the potential of reusable materials is high, which is a prerequisite for ensuring an efficient economy;
¤ the technical and technological level of this activity is modest, but can be improved without special investment efforts;

Therefore, the small and powdery ferrous waste can and must not be reused in their totality, all within the framework of the steel industry. Any tone of recovered ferrous waste and played back in the iron and steel production circuit, leads to a great savings investment and operating expenditure.

References

[1.] Ciocan, A., Turning waste generated in small and powder metallurgy, National Publishing Group Publishing, Bucharest, 2003
[2.] Constantin, N., Nicolae, M., Geanta,V., Butnariu, I., Lepadatu, G., Processes and alternative technologies in steel, Printech, Bucharest, 2009.
[3.] Constantin, N., Nicolae, M., Rucai, V., Research regarding the physical and chemical characteristics of pre–reduced iron ores the analysis of the possibilities of their use in the iron and steel elaborating process, International Conference – Prereduced products and Europe, Milano, Italy, 1996, 230–239.
[4.] *** Pollution Prevention and fighting in the steel making, energy and mining industry areas through the recycling of small–size and powdering Wastes, Program PN2 – Consortium–CO, Research Project No.31– 098/2007.
[5.] Hepuţ T., Kiss I., Raţiu S., Ardelean M., Industrial experiments regarding the ferrous powdery wastes in siderurgy, BuletinulŞtiinţific al UniversităţiiPolitehnicaTimişoara – SeriaMecanică, 46/2, 2001, 113–116
[6.] Hepuţ T., Ardelean E., Kiss I., Raţiu S., Accounting possibilities of ferrous waste from Hunedoara zone – Romania, Annals of the Faculty of Engineering Hunedoara, 1/2, 2003, 89–94
[7.] Hepuţ T., Kiss I., Raţiu S., Ferrous powdery wastes in siderurgy – Possibilities have turning into account through one of the new technologies, Annals of the Faculty of Engineering Hunedoara, 1/2, 2003, 119–124
[8.] Hepuţ T., Kiss I., Raţiu S., Puţan V., Ferrous powdery wastes stored in the ponds and the environments ecology, Annals of the Faculty of Engineering Hunedoara, 1/2, 2003, 125–132
[9.] Hepuţ T., Kiss I., Puţan V., Researches regarding the implementation in the industrial practices of the accounting technologies of the ferrous pulverous wastes, stored in the regional ponds, Annals of the Faculty of Engineering Hunedoara, 1/2, 2003, 71–75
[10.] Hepuţ T., Kiss I., Raţiu S., Possibilities of turning into account the ferrous powdery wastes in siderurgy, Proceedings of the Vth International Symposium of Interdisciplinary Regional Research at Szeged Regional of the Hungarian Academy of Sciences, Szeged, Hungary, 2001
[11.] Socalici A., Harau C., Heput T., Ardelean E., Development of small and powdery waste management, Proceedings of the 6th international conference on Applied Mathematics, Simulation and Modelling – ASM'12 – World Scientific and Engineering Academy and Society (WSEAS), 2012, 156–160
[12.] Hepuţ, T., Socalici, A., Ardelean, E., Ardelean, M., Constantin, N., Buzduga, R., Recovery of ferrous waste and small bulk, Politehnica Publishing House, Timişoara, 2011
[13.] Todorut, A., Socalici, A., Recovery of powdery waste results from technological flows in siderurgy, International Journal of Systems Applications, Engineering & Development, 3(6), 2012, 251–258
[14.] Todoruţ, A., Hepuţ, T., Broadening of raw materials in the steel industry, by recycling wastes, International Conference on Energy, Environmental and Chemical Engineering, 71, Paris, France, 2012, 1466–1472.
[15.] Șerban, S., Hepuţ, T., Ferrous wastes recovery possibilities in the area of steel industry – experiments in the laboratory phase on the briquettes production from fine and pulverous wastes, Acta Technica Corviniensis – Bulletin of Engineering, Fascicule 3 / 2015, 49–56
[16.] Serban, S., Heput, T., Jitian, S., Kiss, I., The Datafit analysis of briquettes manufacturing process from fine and pulverous ferrous wastes, The Vth International Conference Industrial Engineering and Environmental Protection (IIZS 2015), Zrenjanin, Serbia, 2015, 417–422
[17.] Serban, S., Heput, T., Jitian, S., Kiss, I., The Matlab analysis of briquettes manufacturing process from

fine and pulverous ferrous wastes, The Vth International Conference Industrial Engineering and Environmental Protection (IIZS 2015), Zrenjanin, Serbia, 2015, 423–426

[18.] Serban, S., Heput, T., Kiss, I.,The Datafit analysis of small and powdery ferrous wastes destined for the production of briquettes in some laboratory experiments, Acta Technica Corviniensis – Bulletin of Engineering, Fascicule 1 / 2016, 137–142

[19.] Serban, S., Heput, T., Kiss, I., The Matlab analysis of small and powdery ferrous wastes destined for the production of briquettes in some laboratory experiments, Acta Technica Corviniensis – Bulletin of Engineering, Fascicule 1 / 2016, 157–162

[20.] Serban, S., Heput, T., Kiss, I., Recovery possibilities through pelletizing of the pulverous wastes stored in the regional ponds, The VIth International Conference Industrial Engineering and Environmental Protection (IIZS 2016), Zrenjanin, Serbia, 2016, 116–121

ISSN:2067-3809

ACTA TECHNICA CORVINIENSIS
– Bulletin of Engineering
Tome X [2017]
Fascicule 2 [April – June]
ISSN: 2067 – 3809

[1.]Dušan KONIAR, [2.]Libor HARGAŠ, [3.]Zuzana LONCOVÁ,
[4.]František DUCHOŇ, [5.]Peter BEŇO

USAGE OF VIDEO ANALYSIS FOR TRACKING OF LABORATORY ANIMALS

[1-3.]University of Žilina, Faculty of Electrical Engineering, Department of Mechatronics and Electronics, Žilina, SLOVAKIA
[4-5.]Slovak University of Technology, Bratislava, SLOVAKIA

Abstract: This article deals with tracking of laboratory animals (guinea pigs) in cage. Authors collective applied machine vision tools based on global automatic thresholding, adaptive thresholding, differential operators and color matching algorithms. Animal activity and trajectory is significant marker in research of selected pathologies (gastrointestinal diseases in our case). Tracking is done in the huge database of video sequences of healthy animals (reference) and animals with induced gastric pain (gastric ulcer). The solution also be used like non-expensive replacement of radio-frequency laboratory trackers.
Keywords: animal tracking, image segmentation, trajectory, thresholding, differential operators, color matching

INTRODUCTION

Laboratory animals are used in many branches of medical research (drugs testing in pharmacology, efficiency of therapy). Many times, the behavior or activity of animal is significant marker of health status. This fact is used in research of gastrointestinal diseases and influence of selected type of therapy on them (e.g. animal suffering from any kind of gastric pain is generally less vital than healthy one) [1]. Comparison of long-time (hours or days) activity between healthy and ill animals is good feedback in process of optimal therapy setting.

Therefore, it is necessary to develop suitable method for animal activity monitoring or trajectory tracking. The first possibility is to use popular RFID (radio-frequency identification) tracking systems [2] for laboratory cages. This modern solution is slightly invasive: it is necessary to implant RFID tag under the animal skin. RFID tracking system uses specified hardware (RFID pad) and software for animal position processing [3]. Their main disadvantage is high cost. Another group of tracking methods is based on visual systems. Selection of optimal and robust segmentation algorithm is crucial. From the hardware point of view, these tracking methods need "only" camera and video data storage.

In this article we bring some methods for animal tracking in video sequence based on image processing and machine vision and their verification on selected sample video sequences. The length of trajectory is equivalent to animal activity, so we also bring the proposal for trajectory analysis [4]. All algorithms were applied offline but many of them could be used in real-time tracking (e.g. using OpenCV libraries).

MATERIALS

Video sequences for offline analysis were obtained in medical environment (Jessenius Faculty of Medicine, Martin, Slovakia) during experimental phases of gastric diseases therapy. Authors collective were asked for additional animal tracking after the experiments, so offline and machine vision approach was the proper solution for this task. The database contained approximately 200 video sequences with 1 hour duration. The video sequences were captured by color industry IP camera Panasonic in Windows Media Video format.

Figure 1. Scene with animal

The scene (Figure 1) can be divided into basic parts: animal (guinea pig), bowl for food, drinking place (plastic bottle), nest (plastic tube).
On the first sight, we can find and highlight some video sequence features which make the image segmentation process easier and those characteristics which can generate false segmentation results.

Benefits

In a cage, there is always one animal during the tracking process. One animal in a cage is a condition which results from requirements for experiments from medical point of view. Only behavior of one animal is monitored – its activity with and without certain pathology, it is not influenced by any other individual. The animal's environment is natural, standard used during laboratory experiments.
The main components of scene are relatively different in color (bowl is dark brown, nest is gray, animal is always white). In all experiments, the medical specialists used white guinea pigs. Lab technicians who prepared this experiment selected only white guinea pigs. This selection was probably made in order to fulfill set genetic criteria which are connected to research of pathologies of gastrointestinal tract (for instance, features such as genealogy, weight, age, etc.). Animal selection was done before processing of obtained videos and was not connected with used visual methods for trajectory detection. This means that authors solved only the task of animals' tracking, they could not influence their appearance. The color of animal is not important in the case of differential methods of tracking, but is very important in color matching (location).

Cons

The scene is non-uniform illuminated. Cage borders generate shadows (darker places). This fact is not important for adaptive thresholding-based methods or differential methods, but important for global ones and color location.
The covering grid is not removed from the top of the cage and generates reflections.
Despite of these crucial cons, "bad" features in the image created a challenge to authors to do the robust algorithm for tracking task.

METHODS

The main idea of animal tracking is based on animal segmentation, defining the object representative point (center of mass, centroid e.g.) and building the trajectory from these points. We selected three groups of algorithms: differential methods, thresholding-based methods and color matching (location) methods.

Differential methods

Differential methods integrate basic and advanced methods for motion detection using frame subtraction or static background removal [5]. Detection of laboratory animal motion can be defined as a change in position of the animal relative to its surroundings. Area with significant motion (changes) between adjacent video frames is represented in a resulting image as an area with higher intensity levels. Such an area is then transformed to the binary object in order to calculate the centroid (representative point of animal). There is only one single animal in the cage (scene) and the background is static. This fact brings a tremendous advantage for this method, which means that the resulting differential image is composed from one huge object representing animal and isolated small particles generated by noise processes. These small particles can be removed by morphological operators.
The simplest differential method is based on subtracting of relevant video frames. In our case, we can create reference frame ("empty cage", background model) and subtract it from the actual frame or we can subtract two following frames. The mathematical formula for simple difference is as follows:

$$d(n) = \left| f(n) - f(n-1) \right| \qquad (1)$$

where f(n) is actual frame and f(n-1) is previous frame; or:

$$d(n) = \left| f(n) - f_{ref} \right| \qquad (2)$$

where f_{ref} is reference image (empty scene).
Formula (2) is applicable for short-time sequences and analysis due to possible changes of background model (changing lighting conditions).
Advanced method [6] of simple differential was used for remove ghosting effect. This method is in experimental part called *Differential method #1.* Advanced differential method operates with three adjacent video frames: current frame (CF), next frame (NF) and previous frame (PF) (Figure 2a, 2b, 2c). Differential image is then:

$$d(n) = (PF - NF) AND (CF - NF) \qquad (3)$$

After differentiation, resulting pixels are thresholded using global thresholding (Figure 2d). Finding global thresholding is crucial to remove small particles generated by noise processes.

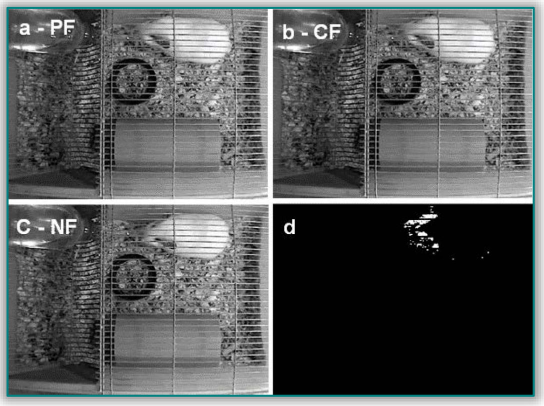

Figure 2. Advanced differential method #1: a) previous frame, b) current frame, c) next frame, d) thresholded differential image

To filter noise particles from thresholded differential image, we can compute standard deviation (StdDev) or variance of pixels and filter those with maximal value of given parameter; or we can use morphological operators for removing small particles. Resulting cluster of pixels is replaced with centroid and this is a single point of trajectory.

As *Differential Method #2* we used advanced static background removal method working in following steps:

» Creating background model from a part of video sequence or entire video sequence. The simplest way is to do the average of all frames or use advanced method [7], [8].
» Subtracting current video frame form background model and blurring the resulting image to remove small particles (Figure 3a). Blurring can be done through spatial scaling down the image and consequent resampling to original size or using blurring spatial filter (Gauss e.g.).
» Thresholding the difference image by Otsu's method [9]. After thresholding, small details are filtered out using erosion and dilation (Figure 3b). If total number of white pixels in the image is greater than MAX value or lower than MIN value, it is considered as false detection and the current frame is discarded. Position coordinates of the object in this frame is then set to predefined value or value from previous frame.

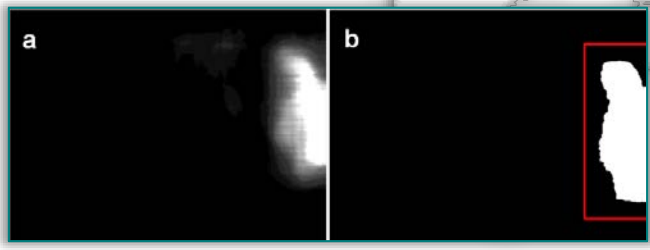

Figure 3. Advanced differential method #2: a) background removal, b) morphological filtering and construction of bounding box

Finally, in image processing lots of other combinations of subtracting two images are known. Some of the differential methods are quite simple and usually they are sensitive to the noise and ghosting [10].

Thresholding-based methods

Compared to differential methods, thresholding-based methods do not use the subtraction of neighboring frames in the video sequence but they work with frames separately. These methods suppose that the object is well separable from background (because of color or intensity). In this work we tested automatic global thresholding method based on entropy and local (adaptive) thresholding method called Background correction method.

Before using global thresholding based on entropy we converted color image from RGB space to HSI space, which is more suitable for computer vision applications. Intensity (I) layer concentrates most of image information content. Global threshold k divides image pixels into two groups: background and foreground. The entropy (information associated with black or white pixels) of background (H_b) and foreground (H_w) is then defined as [11]:

$$H_b = -\sum_{i=0}^{k} P_b(i).\log_2 P_b(i) \qquad (4)$$

$$H_w = -\sum_{i=k+1}^{N-1} P_w(i).\log_2 P_w(i) \qquad (5)$$

where i is gray level (0 - 255), P_b is probability (relative area) of background and P_w is probability (relative area) of foreground. Optimal threshold k maximizes following expression:

$$H_b + H_w \qquad (6)$$

Additional morphology and binary filtering after global thresholding is often needed to remove small particles or filling holes in the object(s) (Figure 4c, 4d).

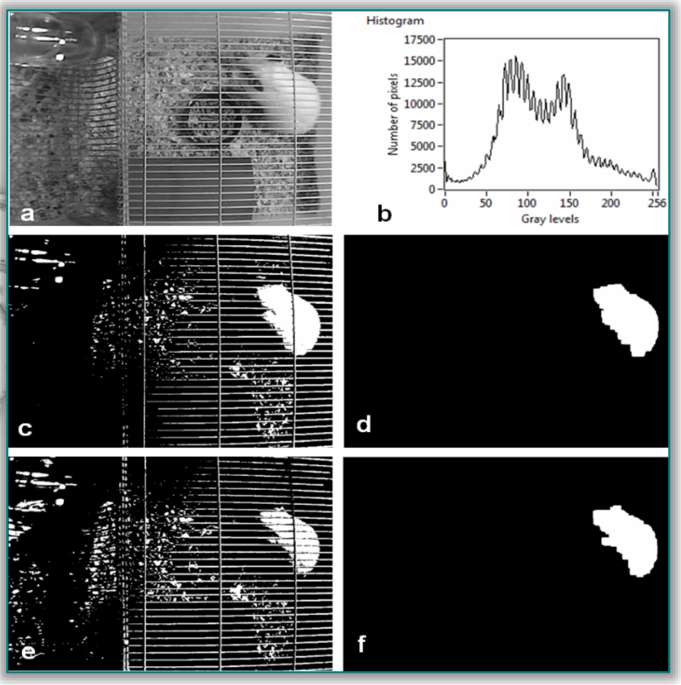

Figure 4. Global and adaptive thresholding: a) Intensity layer of actual frame, b) image histogram, c) result of thresholding using entropy, d) morphological enhancement of c), e) result of adaptive thresholding using Background correction, f) morphological enhancement of e)

Background correction algorithm combines local (adaptive) and global thresholding concepts for image segmentation [11]. In the first phase algorithm computes corrected image B(i;j):

$$B(i;j) = I(i;j) - m(i;j) \qquad (7)$$

where I(i;j) is pixel value at position (i;j) in the frame and m(i;j) is average pixel value in the window centered at pixel I(i;j). Standard window size is 33x33 pixels. Corrected image is then thresholded by global technique (Otsu). Example of adaptive thresholding is in Figure 4e. Additional morphological filtering is needed (Figure 4f).

In both cases, the centroids of filtered objects are points of animal's trajectory.

Color location (Color Matching)

Color matching algorithm uses color template for which searches for in the inspected image. Algorithm determines

a level of similarity (matching score, in range 0 - 1000) between color spectrum of template and classified region in image (Figure 6). The details how to create a color spectrum of image region of interest (ROI) is in [11]. Simplified algorithm of color matching is shown in Figure 5. Key element of this method is in proper selection of template. In our case we created three variations of "animal's texture" for various lighting conditions. Algorithm tests the image ROIs for all the templates and resulting matching score is the maximum value.

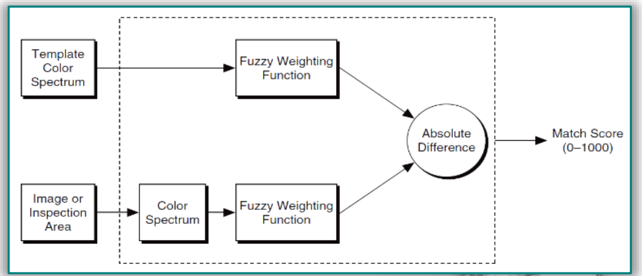

Figure 5. Block diagram of color matching algorithm

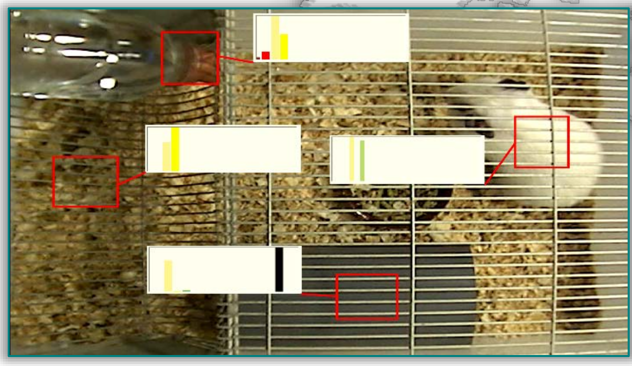

Figure 6. Examples of color spectrums in various image areas

Color matching method can work in two different ways. In the first mode, window with same size as template shifts across the image and color spectrum comparison is done at each position. If the matching score is higher than threshold value (750 e.g.), the central pixel of window is set to 1 or vice versa. The second mode searches only for 1 or some (as set) place(s) in the inspected image with the maximum matching score.

EXPERIMENTAL RESULTS

For experimental verification of laboratory animals tracking we selected 5 methods (2 differential, 2 thresholding-based and 1 color matching). Then we selected 5 representative video sequences (3 color for day mode and 2 infrared – IR - monochromatic for night mode). Color matching was tested only on color – day mode videos, because the IR videos do not contain color information. Duration of each test sequence was 1 minute. The first, we created reference trajectories. All video sequences were segmented manually by constructing bounding rectangle frame by frame around the guinea pig. Centroids for each bounding rectangle were inserted into an array for constructing the reference trajectory. After applying all 5 methods to the samples, the absolute difference between the coordinates from the reference trajectory and the coordinates generated from particular methods for adequate frames was evaluated. The example of experimental testing for each method is as follows:

1. Creating of reference trajectory (common for all methods) – Figure 7;
2. Applying the tracking method to the selected video sample (generating the new trajectory) – Figure 8;
3. Comparison of reference trajectory and the trajectory generated by the method – Figure 9;
4. Evaluation of absolute differences in pixels or relative difference in % – Tab. I.

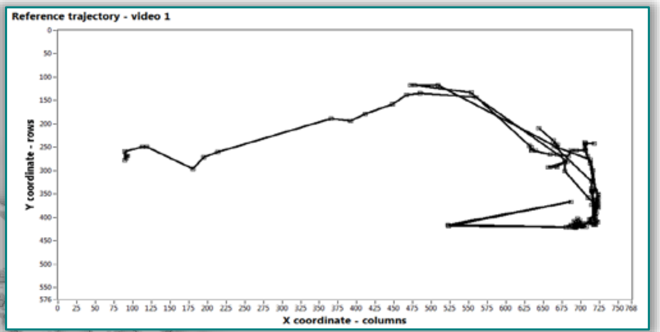

Figure 7. Reference trajectory for video sample #1

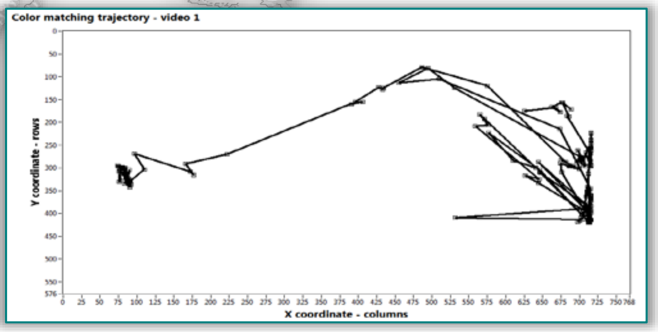

Figure 8. Trajectory for video sample #1 obtained by color matching

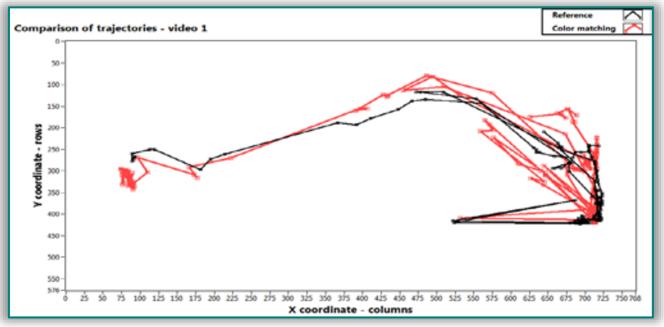

Figure 9. Comparison of reference (black) and measured (red) trajectory

According to Table 1 we can define:

- Δx [%] – average difference in x coordinate between reference and tested videos per one frame (error rate for x coordinate for each method);
- Δy [%] – average difference in y coordinate between reference and tested videos per one frame (error rate for y coordinate for each method).

Table 1. Methods Comparison

Tested video samples		Sample 1	Sample 2	Sample 3	Sample 4	Sample 5
Entropy	Δx [%]	11.60	6.28	83.79	10.75	8.08
	Δy [%]	2.96	3.85	16.57	11.75	2.37
Color matching	Δx [%]	8.42	4.62	4.12		
	Δy [%]	2.93	7.91	6.75		
Background correction	Δx [%]	13.38	12.03	3.59	5.45	8.33
	Δy [%]	4.00	7.13	1.37	7.15	1.40
Differential method - 1	Δx [%]	12.17	2.57	4.13	3.88	3.35
	Δy [%]	16.26	8.47	8.90	4.07	5.08
Differential method - 2	Δx [%]	2.15	2.28	1.41	3.47	3.50
	Δy [%]	2.04	1.50	1.85	2.73	2.13

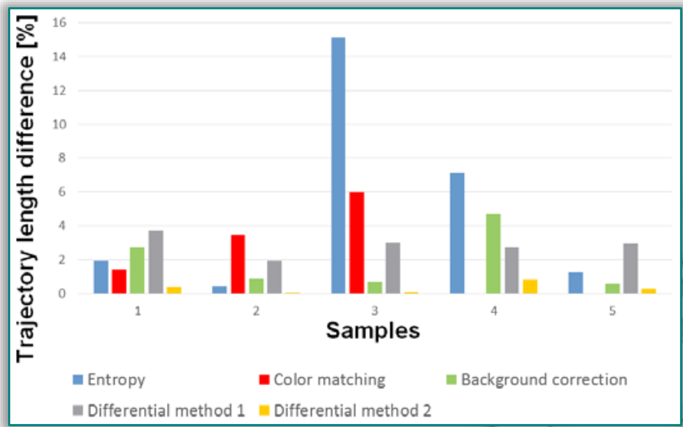

Figure 10. Comparison of methods accuracy

After trajectory points connection, we can compute absolute trajectory length. This parameter is the key element in the process of computation of single methods accuracy (Figure 10). Each trajectory length is compared with relevant reference one. In addition, if camera system is calibrated, trajectory length can be computed in real world units (cm or m e.g.).

DISCUSSION AND CONCLUSIONS

The first, we must underline that selected representative video sequences contain the natural guinea pig's scene without any preliminary modifications. The covering grid was not removed from the cage's top, the lighting was non-homogenous and so lots of shadows and reflections were presented at the scene – in order to verify the robustness of the motion detection algorithms (especially the thresholding-based methods). The entropy method was the most suitable thresholding technique for our application from the family of global thresholding techniques.

When testing the usage of global thresholding method several difficulties were undergone. In video sequences with poor lighting conditions (Sample 3), the entropy threshold value was not optimal and so that only the detection of guinea pig in certain part of its cage was possible (the well-lighted one). In order to bring the method to operate exactly, the scene in each video could be divided into two approximately homogenous parts (the well-lighted one and the one with worse lighting). Worse lighting conditions in the video sequence were obtained during the evening and were caused by combination of day light and artificial lighting (e.g. lamp). Bad accuracy of entropy technique is improved using adaptive background correction method. The accuracy of background correction is approximately at the same level for day video sequences as entropy accuracy, but much better for evening and night video sequences. It was proven that in order to bring this technique to work properly, it is necessary to consider the window size comparable with the size of sought object (guinea pig). In our application the windows size was set to 200x200 pixels for this purpose.

In moments of the video in which the guinea pig was hidden in its nest, its detected position was set into the middle of it automatically.

Detected objects whose area was less than 4000 pixels were considered as false-positive detections in moments of the video when the Guinea pig was hidden in its nest, so such small objects were excluded and the right detected position was set into the middle of the nest instead. Also the possibility of setting the ROI improved the correctness of this algorithm. Setting of the morphology operations did not change, they were the same for both entropy and background correction thresholding techniques.

Differential methods are significant with the stability of results for each sample. This is achieved by frame subtraction (Differential method #1) or static background removal (Differential method #2). In case that there was only one simple moving object in the scene, the background removal achieved the best results. Differential methods presented the best results. Due to their relative simplicity, these methods (with thresholding-based techniques) are suitable for real-time animal tracking.

Color matching operates with a chosen template containing a searched color which is normally of a small area (ca. 50 x 50 pixels), in our case it was part of guinea pig's white/bright fur. It was experimentally proven, that the method works much better if the image of the scene without the guinea pig ("empty cage") is first subtracted from each evaluated video frame. This eliminates the false-positive detection of parts of the scene, which also appear as bright ones (reflections on plastic drinking bottle). Color matching techniques are suitable for offline tracking (recording analysis) due to their computational difficulty.

All the results (trajectory lengths and deviations) are presented in pixels. Pixel units can be easily converted to real-world units (mm, cm, ...) after image calibration (with length reference) based on the fact, that camera has constant distance from the recorded scene.

Notable deviations in tracked length of animal's trajectory, is caused by varying of the centroid position. Centroid moves a little also in the situations, when guinea pig doesn't move (head moves, rotation by little angle etc.). This centroid varying can be successfully filtered by mean or median filtering e.g.

Generally, all methods have similar results in first and second sample. This was due to a relatively small movement of the guinea pig. In third sample, entropy thresholding and color matching failed. This was due to a greater amount of movement of guinea pig. Moreover, guinea pig moved also the nest and this was a significant source of error based on the nature of these methods. The last samples were obtained in IR mode. Especially in fourth sample each method achieved worse results. This was caused by the impacting noise. Differential methods are able to cope with this, as they compare the current image with previous. The best results for the whole sample set were achieved by differential methods, which subtract the background from the image. However, this may be caused by appropriate image post-processing (mathematical morphology and adaptive thresholding). All of the tested methods are based on simple image processing and can be easily implemented into any hardware. It makes these methods robust for other usage in animal trajectory tracking.

Acknowledgment

Results of this work are supported by grant APVV-15-0462: Research on sophisticated methods for analyzing the dynamic properties of respiratory epithelium's microscopic elements.

Note

This paper is based on the paper presented at The 11th International Conference ELEKTRO 2016, organized by University of Žilina, Faculty of Electrical Engineering, in Štrbské Pleso – High Tatras, SLOVAKIA, May 16–18, 2016

References

[1] J. Halička, M. Tatár, "Upper Gastrointenstinal Visceral Pain Models In Guinea-pigs (mini-review)", Acta Medica Martiniana, 2013, Suppl. 1, DOI: 10.2478/acm-2013-0005

[2] A. Gmiterko, M. Kelemen, I. Virgala, R. Surovec, and M. Vacková, „Modeling of a snake-like robot rectilinear motion and requirements for its actuators," in Proceedings of 15th International Conference on Intelligent Engineering Systems, 2011.

[3] L. Catarinucci, R. Colella, L. Mainetti, L. Patrono, S. Pieretti, I. Sergi, L. Tarricone: "Smart RFID Antenna System for Indoor Tracking and Behaviour Analysis of Small Animal in Colony Cages". IEEE Sensors Journal, Vol. 14, No. 4, April 2014, pp. 1198-1206.

[4] Ľ. Miková, F. Trebuňa, and M. Kelemen, „Concept of locmotion mobile undercarriage structure control for the path tracking". In Solid State Phenomena, Vol. 198, 2013, pp. 79-83.

[5] Isaac N. Bankman: Handbook of Medical Image Processing and Analysis (2nd edition). Elsevier Inc., 2009, ISBN 978-0-12-373904-9.

[6] R. T. Collins, R. Gross, and S. Jianbo, "Silhouette-based human identification from body shape and gait," in Proceedings of 5th IEEE International Conference on Automatic Face Gesture Recognition, 2002.

[7] Sobral, Andrews. BGSLibrary: An OpenCV C++ Background Subtraction Library. IX Workshop de Visão Computacional (WVC'2013), Rio de Janeiro, Brazil, Jun. 2013. https://github.com/andrewssobral/bgslibrary.

[8] Piccardi, M. (2004, October). Background subtraction techniques: a review. In Systems, man and cybernetics, 2004 IEEE international conference on (Vol. 4, pp. 3099-3104). IEEE.

[9] Nobuyuki Otsu (1979). "A threshold selection method from gray-level histograms". IEEE Trans. Sys., Man., Cyber. 9 (1): 62–66. doi:10.1109/TSMC.1979.4310076.

[10] L. Zheng, S. Zhang, J. Zhang, Y. Zhang, „Dynamic image mosaic via SIFT and dynamic programming", in Machine Vision and Applications, 2014, vol.25, pp. 1271-1282.

[11] National Instruments, NI Vision Concepts Help, June 2013.

ISSN:2067-3809

ACTA TECHNICA CORVINIENSIS
– Bulletin of Engineering
Tome X [2017]
Fascicule 2 [April – June]
ISSN: 2067 – 3809

1.Snežana DRAGIĆEVIĆ, 2.Brankica ŠUTIĆ, 3.Milan PLAZINIĆ

IMPROVING ENERGY EFFICIENCY IN PUBLIC BUILDING IN THE MUNICIPALITY OF ČAČAK

1-3.University of Kragujevac, Faculty of Technical Sciences in Čačak, SERBIA

Abstract: There are a lot of important factors that influence building energy consumption. The building energy saving effect is an integrated acting result, it has a relationship between thermal characteristics of the building envelope, ventilation ways, efficiency of heating system, and the increasing range of energy saving rate will be different as the energy saving measures are different. In this paper, the public building in the municipality of Čačak was analyzed in order to examine the impact of different retrofitting measures on heating energy consumption. In terms of retrofitting to study, various energy efficiency measurements have been considered such as improving levels of insulations of different building envelope elements. Results show that the annual heating energy consumption could be reduced up to 61 %.
Keywords: energy efficiency, public building, saving energy

INTRODUCTION

Improving energy efficiency in buildings is one of the most cost-effective ways across all sectors to reduce energy consumption and hence greenhouse gas emissions. More than a third of the primary energy used in developed countries is used to heat, cool, and light buildings or is utilized within buildings. Energy efficiency is at the cornerstone of the European energy policy and one of the main targets of the Europe 2020 Strategy for smart, sustainable and inclusive growth adopted by the European Council in June 2010. This includes the objective for a 20% reduction in primary energy consumption by 2020. As energy related emissions account for almost 80% of total EU greenhouse gas emissions, the efficient use of energy can make an important contribution to achieving a low-carbon economy and combating climate change, [1-3].

Public policies in the most countries to promote building energy efficiency have addressed many of the same issues. These include: Building codes, Energy efficiency certificates, Promoting energy efficiency in public buildings, Training and certification of experts and White-certificate programs. Building codes have been effective in improving energy efficiency in new buildings and in some buildings undergoing major refurbishments, because they are mandatory and generally quite specific about requirements. Energy certification of buildings is a key policy instrument for reducing the energy consumption and improving the energy performance of new and existing buildings, [4,5].

One way to improve energy efficiency is to modernise public buildings because hospitals and schools are among the most important public facilities in Serbia. In this paper the possibilities of improving energy efficiency of public facility which is owned by the city of Cacak is analyzed. The current energy condition of the object have been proposed, than measures to increase energy efficiency and the energy state of the object after the application of the proposed measures are shown.

MATERIAL AND METHODS

Case study

The subject of analysis is a public facility Medical Health Care Center Čačak. Location is in the urban area of Čačak and it is free to all four sides. The floors of the building are Su + P + 1 with a total area of 3579,09 m^2, as shown in Figure 1.

To build a site the standard structure for this type of object is used. Horizontal bearing elements are "Avramenko" concrete ceiling, whose overall height from the floor and ceiling is 45 cm. All vertical bearing elements are reinforced-concrete columns. Roof construction is wooden with supporting beams and pillars, which relies on reinforced-concrete construction, which is set for thermal insulation of durisol panels. Over these elements beds, wall panelling, plating of boards, tar paper and tin covers are set up. On the outside of the roof structure was set up copper sheet thickness of 1 mm, while inner roof planes are made of tin plated copper.

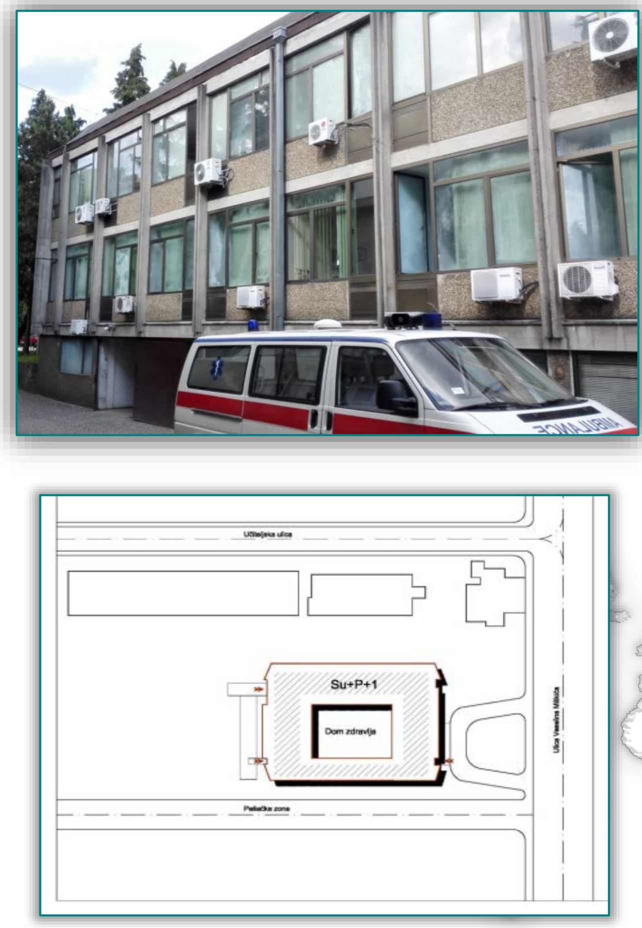

Figure 1. The external appearance of the building and the view of situation of the Medical Health Care Center Čačak

Facade walls are constructed of brick or hips of the slag thickness from 25 to 38 cm depending on the position, while the partition walls constructed of hollow brick thickness of 7 cm. The walls are derived, without thermal insulation. All parapet walls are made of the hollow and clay brick, thickness 25 cm. Flooring in the areas are covered with linoleum, ceramic tiles or concrete. Thermal envelope of the building has an area of 6442,37 m^2. The building is attached to a remote system of heating with individual gas boiler room that is located in the courtyard in the Health center.

Present state energy audit

The analyzed object belongs to the category of objects for health care and social protection, as defined by the State Regulations on energy efficiency in buildings. This building is an existing building and it applies energy rehabilitation, which is also defined in the Regulations. The program KnaufTerm2 PRO S, version 27.2 was used for energy efficiency analysis of the Health Center building in the current state.

Based on the conducted investigation, it is possible to analyze and evaluate the energy efficiency of the building of the Health Centre in Cacak in the current state. The results show that the annual transmission heat losses through certain parts of the building envelope in the current situation are:

1. External walls: 112417,16 kWh;
2. Pitched roof: 97916,75 kWh;
3. Window and curtain wall: 140545,99 kWh;
4. Partition walls towards the unheated area: 11102,92 kWh;
5. Ceiling below unheated space: 161805,10 kWh;
6. Floor above unheated space: 8987,82 kWh;
7. Ground walls (basement): 46842,85 kWh;
8. Ground floors: 111551,21 kWh.

The Figure 2 shows the heat loss percentage through certain components of the facility in the total heat losses.

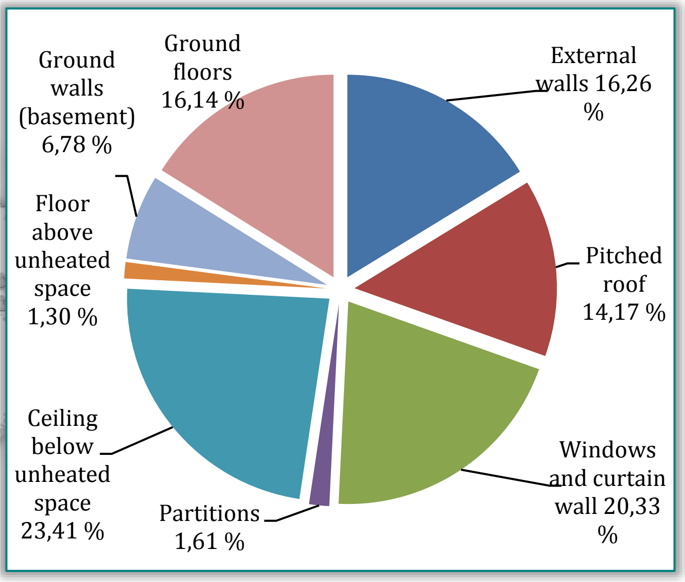

Figure 2. Percentage shares losses through the envelope building elements in the total heat losses in the present state of building

The analysis of heat losses shows that the greatest heat loss is through the basic ceiling below unheated space located below the ceiling, as this surface is the largest of all the areas that make up the thermal envelope of the object and which accounts for 18,5 %, and was conducted without heat insulation. Then the greatest heat losses are through windows and curtain wall, although their surfaces 11,78 % of the total thermal envelope. Losses through the exterior walls and under the floor of the facility amount to about 16 % of total heat loss. By analyzing the characteristics of the circuits forming the thermal envelope of the building, it was noted that the heat transfer coefficients of all the areas that make up the thermal envelope of the object is greater than the allowable values that are defined in the State Regulations on the energy efficiency of buildings. It was also observed that the thermal envelope assemblies such as external slanted walls and a piece of the roof above the heated area leads to the formation of condensation.

Total energy demand for transmission losses of the building is 733,77 MWh and for ventilation losses 229,86 MWh, in its present state. Annual energy building gains in the current state are:

1. Solar gains: 91,37 MWh;
2. Gains from energy consumption: 23,84 MWh;
3. Gains heat from electrical appliances: 45,36 MWh.

Annual energy consumption for heating the building in its present state, using the central gas heating system is 803 MWh, while specific annual heat consumption for heating is 276,48 kWh/m^2. Since the adoption of energy-class benefits of the specific thermal energy for heating systems operating with a recess, on the basis of which this building belongs to the energy class F. Regulations on the energy efficiency of buildings stipulates that the maximum allowed annual consumption of energy for heating buildings allocated to health care and social protection 120 kWh/m^2. Based on the results of the analysis can be concluded that the annual energy consumption for heating of the Health Centre in Čačak 2.3 times higher than allowed for the analyzed object.

Review of measures to improve energy efficiency

Based on the analysis of energy efficiency of the building, it was noted that it is necessary to improve the thermal characteristics of all the components that make up the building envelope and proposes the implementation of the following measures, [6]:

1. On the external walls add a thermal insulation Knauf Insulation FKD-S Thermal 7 cm thickness and on the side walls add thermal insulation Knauf Insulation NaturBoard FIT-G PLUS 8 cm thickness, both on the outside of the building wall;
2. In order to prevent condensation in the roof structure is necessary to reconstruct the roof and replace the covers. On the roof, under the roof construction, install vapor permeable film layer Knauf Insulation LDS 0.02, then a layer of Termal mineral wool Knauf Insulation Unifit 035 thickness of 18 cm and a vapor barrier Homeseal Knauf Insulation LDS 5 Silk. Aluminum replaced with the cover tiles;
3. It is necessary to substitute the existing five-chamber PVC windows and curtain wall with double-layer glass thickness of 4 mm filled with air thickness of 12 mm with six chamber PVC windows with low-emission double-layer glass (4 + 12 + 4) with krypton;
4. On the walls towards the unheated space should be placed insulation rock mineral wool Knauf Insulation NaturBoard FIT-G PLUS thickness of 5 cm;
5. From the floor joists above unheated spaces to remove a layer of cod and the underside of the installed thermal insulation rock mineral wool Knauf Insulation CLT C1 8 cm thick and a layer of vapor permeable film;
6. On the basic ceiling below an unheated attic space on the bottom side install thermal insulation of mineral wool Knauf Insulation Unifit 035 8 cm thickness and a layer of vapor permeable film;
7. On the brick walls in the ground, basement, which are oriented to the south, add insulation rock mineral wool Knauf Insulation FKD-S Thermal 4 cm thickness and on the other basement walls made of concrete in the ground, it is necessary to add on the inner side the same insulation thickness of 5 cm and a layer of vapor permeable film;
8. On the floors of the facility in working spaces in the basement proposes to install a slab of rock mineral wool Knauf Insulation NaturBoard POD EXTRA thickness of 9 cm and utility rooms and 8 cm thickness cement screed.

Table 1. Review of the heat transfer coefficients through the thermal envelope of the building of the Health Centre in Čačak

Building envelope structure	Umax (W/m^2 K)	Present state		Proposed state	
		U (W/m^2 K)	Satisfied	U (W/m^2 K)	Satisfied
External walls	0,40	1,595	No	0,379	Yes
External slanted walls, north-south oriented	0,40	3,378	No	0,400	Yes
Pitched roof above heated area	0,20	1,464	No	0,152	Yes
Window and curtain wall	1,50	2,800	No	1,300	Yes
Partition walls towards the unheated area	0,55	2,294	No	0,546	Yes
Ceiling below unheated space	0,40	2,564	No	0,374	Yes
Floor above unheated space	0,40	0,544	No	0,361	Yes
Ground wall, south oriented	0,50	1,013	No	0,461	Yes
Ground wall, other	0,50	1,592	No	0,485	Yes
Ground flor - utility rooms	0,40	2,375	No	0,395	Yes
Ground flor – working spaces	0,40	3,155	No	0,376	Yes

* According to the Regulations on energy efficiency in buildings

Proposed measures to improve energy efficiency of the object can be achieved by using elements (material) Knauf systems that are tailored to each individual site which can improve and meet the requirements defined in the Regulations for the Energy Efficiency Facility for existing buildings for this purpose.

Implementation of the proposed measures to increase the energy efficiency of the building is fully justified. Table 1 provides an overview of the coefficient of heat transfer through the thermal envelope of the building in its present condition and after the implementation of measures to improve the energy rating of the building. After the application of the proposed measures will not come to the formation of condensation in all the assemblies of the building.

RESULTS AND DISCUSSION

After the implementation of measures to improve energy efficiency of the building annual transmission heat losses through certain parts of the building envelope should have the following values:

1. External walls: 20386,27 kWh
2. Pitched roof: 10166,22 kWh
3. Window and curtain wall: 65253,50 kWh
4. Partition walls towards the unheated area: 2642,63 kWh
5. Ceiling below unheated space: 23601,84 kWh
6. Floor above unheated space: 5964,35 kWh
7. Ground walls (basement): 15890,35 kWh
8. Ground floors: 15143,94 kWh.

Figures 3 and 4 show a comparative analysis of transmission heat losses data and their percentage share in the total heat loss of the building, for the present and the proposed case. The analysis results showed that after the implementation of measures for improvement of building energy efficiency the transmission losses through all the elements decrease, but their share in total losses changed.

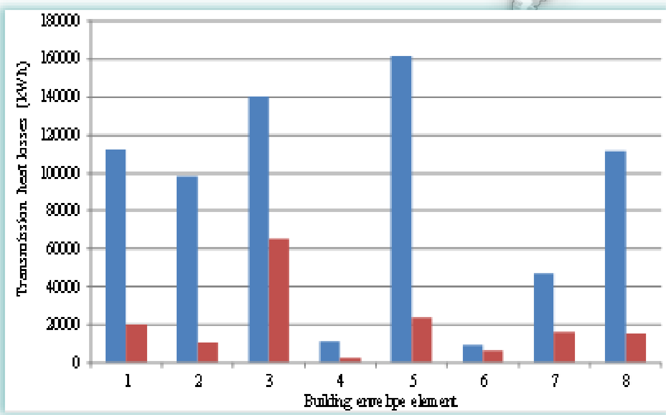

Figure 3. Transmission heat losses for present v.s propose state: 1 – External walls, 2 – Pitched roof, 3 – Window and curtain wall, 4 – Partition walls towards the unheated area, 5 – Ceiling below unheated space, 6 - Floor above unheated space, 7 – Ground walls, 8 – Ground floors;

After the application of the proposed measures for improving energy efficiency the greatest reduction in transmission losses could be expected in pitched roof in which the losses can be reduced by up to 90 %, while the floors on the ground and floors below an unheated area can be achieved reduction of heat loss up to 85%.

Reduction of heat transmission losses through the exterior walls could be up to 82 % and by replacement of a window can be achieved energy savings up to 53%. Total energy use for compensation of transmission losses of the building in the present case amounts to 202 MWh.

The application of the proposed measures can be achieved annual energy savings up to 73 % for the entire object. Solar heat gain in the present case was reduced by 46 % and amounted to 49,10 MWh, while the gains from energy consumption and electrical appliances remained unchanged. Annual energy consumption for building heating in the present state is 313 MWh, which is 61 % less than it consumes in its present condition.

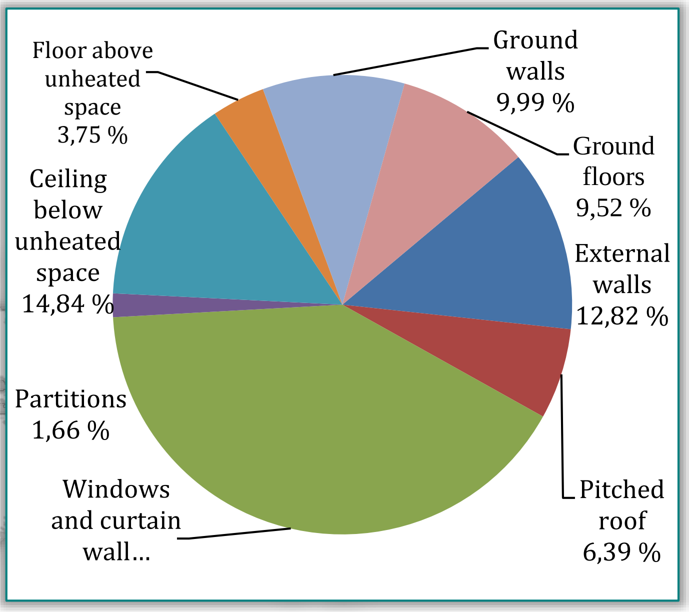

Figure 4. Percentage shares losses through the envelope building elements in the total heat losses for the propose state of building after implementation of measures for energy efficiency improvements

For the proposed state of the building specific annual heat consumption will be 107,83 kWh/m^2, which is below the 120 kWh/m^2, which represents the maximal value of heat energy specific consumption of existing buildings allocated to health care, according to the Regulations for energy efficiency in buildings Republic Serbia. After implementation of measures for improvement of energy efficiency, analyzed object belongs to C energy class, which is two ranges up according to present state.

CONCLUSION

This paper considered the impact of retrofit schedule influence on energy use. The research suggests that improving all building envelope elements insulation level helped significant heating energy reduction. Results show that after applying the proposed measures CO_2 emission can be reduced from 192 CO_2/year t to 75 t CO_2/year. Plenty of studies have considered the effect of improving fabrics' thermal property on heating energy consumption and some provided strong evidences why we need to improve public building energy efficiency. However, even in objects that have achieved specific standards, the energy consumption may be dramatically different depending on the occupants' energy use behavior, and any extensions or alterations they make to the objects. More research is needed into the effects of occupant's behavior on energy use which will allow for more targeted interventions to be applied.

ACKNOWLEDGEMENTS

The paper is a result of the research conducted within "Study on energy efficiency of Health Care Center in Čačak", which is funded by the Municipalitie of Čačak and Public Enterprise Municipal Housing Agency in Čačak, 2016.

Note

This paper is based on the paper presented at The VIth International Conference Industrial Engineering and Environmental Protection 2016 – IIZS 2016, organized by University of Novi Sad, Technical Faculty "Mihajlo Pupin" Zrenjanin, in Zrenjanin, SERBIA, October 13–14, 2016, referred here as [7].

References

[1] Ries, C., Jenkins, J., Wise, O., Improving the energy performance of buildings: learning from the European Union and Australia, Technical report (Rand Corporation), TR-728-RER, Santa Monica, CA : RAND, 2009.

[2] Pe´rez-Lombard, L., Ortiz, J., Pout, C., A review of building energy consumption information, Energy and Buildings, 40, pp.394–398, 2008.

[3] Eftimie, E., Costing energy efficiency improvements in buildings Case study: Braşov, Romania, International Journal of Energy and Environment, Vol. 6, No. 1, pp.47-60, 2015.

[4] Mishra, S., Usmani, J.A., Varshney, S., Energy Saving Analysis In Building Walls Through Thermal Insulation System, International Journal of Engineering Research and Applications, Vol 2, No. 5, pp.128-135, 2012.

[5] Shetal, W., Sharples, S., A Building Simulation Sustainability Analysis to Asess Dwellings in a New Cairo Development, 4th National Conference of IBPSA, New York City, USA, August 11 – 13, pp.94-101, 2010.

[6] Krstić, A., Osnove materijalizacije savremenih industrijalizovanih objekata, Arhitektonski fakultet Univerziteta u Beogradu, Beograd, 2000.

[7] Dragićević, S., Šutić, B., Plazinić, M., Improving energy efficiency in public building in the municipality of Čačak, The VIth International Conference Industrial Engineering and Environmental Protection 2016 – IIZS 2016, Zrenjanin, Serbia, 2016

ISSN:2067-3809

10TH ANNIVERSARY

We are very pleased to inform that our international and interdisciplinary journal **ACTA TECHNICA CORVINIENSIS ■ Bulletin of Engineering** completed its nine years of publication successfully [**issues of years 2008 – 2016, Tome I–IX**].

In a very short period it has acquired global presence and scholars from all over the world have taken it with great enthusiasm.

Every year, in four online issues (**fascicules 1 – 4**), **ACTA TECHNICA CORVINIENSIS ■ Bulletin of Engineering [e-ISSN: 2067-3809]** publishes a series of reviews covering the most exciting and developing fields of science and technology. Each issue contains papers reviewed by international researchers who are experts in their fields. The result is a journal that gives the scientists and engineers the opportunity to keep informed of all the current developments in their own, and related, areas of research, ensuring the new ideas across an increasingly the interdisciplinary field.

Now, when will celebrate the tenth years anniversary of **ACTA TECHNICA CORVINIENSIS ■ Bulletin of Engineering**, we are extremely grateful and heartily acknowledge the kind of support and encouragement from all contributors and all collaborators!

On behalf of the Editorial Board and Scientific Committees of **ACTA TECHNICA CORVINIENSIS ■ Bulletin of Engineering**, we would like to thank the many people who helped make this journal successful. We thank all authors who submitted their work to **ACTA TECHNICA CORVINIENSIS ■ Bulletin of Engineering**.

ACTA Technica CORVINIENSIS
BULLETIN OF ENGINEERING

ACTA TECHNICA CORVINIENSIS – BULLETIN OF ENGINEERING. Fascicule 1 [JANUARY-MARCH]
ACTA TECHNICA CORVINIENSIS – BULLETIN OF ENGINEERING. Fascicule 2 [APRIL-JUNE]
ACTA TECHNICA CORVINIENSIS – BULLETIN OF ENGINEERING. Fascicule 3 [JULY-SEPTEMBER]
ACTA TECHNICA CORVINIENSIS – BULLETIN OF ENGINEERING. Fascicule 4 [OCTOBER-DECEMBER]

ACTA TECHNICA CORVINIENSIS
– Bulletin of Engineering
Tome X [2017]
Fascicule 2 [April – June]
ISSN: 2067 – 3809

MANUSCRIPT PREPARATION – GENERAL GUIDELINES

Manuscripts submitted for consideration to **ACTA TECHNICA CORVINIENSIS – Bulletin of Engineering** must conform to the following requirements that will facilitate preparation of the article for publication. These instructions are written in a form that satisfies all of the formatting requirements for the author manuscript. Please use them as a template in preparing your manuscript. Authors must take special care to follow these instructions concerning margins.

INVITATION

We are looking forward to a fruitful collaboration and we welcome you to publish in our **ACTA TECHNICA CORVINIENSIS – Bulletin of Engineering**. You are invited to contribute review or research papers as well as opinion in the fields of science and technology including engineering. We accept contributions (full papers) in the fields of applied sciences and technology including all branches of engineering and management.

ACTA TECHNICA CORVINIENSIS – Bulletin of Engineering publishes invited review papers covering the full spectrum of engineering and management. The reviews, both experimental and theoretical, provide general background information as well as a critical assessment on topics in a state of flux. We are primarily interested in those contributions which bring new insights, and papers will be selected on the basis of the importance of the new knowledge they provide.

Submission of a paper implies that the work described has not been published previously (except in the form of an abstract or as part of a published lecture or academic thesis) that it is not under consideration for publication elsewhere. It is not accepted to submit materials which in any way violate copyrights of third persons or law rights. An author is fully responsible ethically and legally for breaking given conditions or misleading the Editor or the Publisher.

ACTA TECHNICA CORVINIENSIS – Bulletin of Engineering is an international and interdisciplinary journal which reports on scientific and technical contributions. Every year, in four online issues (fascicules 1 – 4), **ACTA TECHNICA CORVINIENSIS – Bulletin of Engineering [e-ISSN: 2067-3809]** publishes a series of reviews covering the most exciting and developing areas of engineering. Each issue contains papers reviewed by international researchers who are experts in their fields. The result is a journal that gives the scientists and engineers the opportunity to keep informed of all the current developments in their own, and related, areas of research, ensuring the new ideas across an increasingly the interdisciplinary field. Topical reviews in materials science and engineering, each including:

- ✓ surveys of work accomplished to date
- ✓ current trends in research and applications
- ✓ future prospects.

As an open-access journal **ACTA TECHNICA CORVINIENSIS – Bulletin of Engineering** will serve the whole engineering research community, offering a stimulating combination of the following:

- ✓ Research Papers – concise, high impact original research articles,
- ✓ Scientific Papers – concise, high impact original theoretical articles,
- ✓ Perspectives – commissioned commentaries highlighting the impact and wider implications of research appearing in the journal.

ACTA TECHNICA CORVINIENSIS – Bulletin of Engineering encourages the submission of comments on papers published particularly in our journal. The journal publishes articles focused on topics of current interest within the scope of the journal and coordinated by invited guest editors. Interested authors are invited to contact one of the Editors for further details.

BASIC INSTRUCTIONS AND MANUSCRIPT REQUIREMENTS

The basic instructions and manuscript requirements are simple:

- Manuscript shall be formatted for an A4 size page.
- The all margins (top, bottom, left, and right) shall be 25 mm.
- The text shall have both the left and right margins justified.
- Single-spaced text, tables, and references, written with 11 or 12-point Georgia or Times Roman typeface.
- No Line numbering on any pages and no page numbers.
- Manuscript length must not exceed 15 pages (including text and references).
- Number of figures and tables combined must not exceed 20.
- Manuscripts that exceed these guidelines will be subject to reductions in length.

The original of the technical paper will be sent through e-mail as attached document (*.doc, Windows 95 or higher). Manuscripts should be submitted to e-mail: redactie@fih.upt.ro, with mention **"for ACTA TECHNICA CORVINIENSIS – Bull. of Eng."**.

STRUCTURE

The manuscript should be organized in the following order: Title of the paper, Authors' names and affiliation, Abstract, Key Words, Introduction, Body of the paper (in sequential headings), Discussion & Results, Conclusion or Concluding Remarks, Acknowledgements (where applicable), References, and Appendices (where applicable).

THE TITLE

The title is centered on the page and is CAPITALIZED AND SET IN BOLDFACE (font size 14 pt). It should adequately describe the content of the paper. An abbreviated title of less than 60 characters (including spaces) should also be suggested. Maximum length of title: 20 words.

AUTHOR'S NAME AND AFFILIATION

The author's name(s) follows the title and is also centered on the page (font size 11 pt). A blank line is required between the title and the author's name(s). Last names should be spelled out in full and succeeded by author's initials. The author's affiliation (in font size 11 pt) is provided below. Phone and fax numbers do not appear.

ABSTRACT

State the paper's purpose, methods or procedures presentation, new results, and conclusions are presented. A nonmathematical abstract, not exceeding 200 words, is required for all papers. It should be an abbreviated, accurate presentation of the contents of the paper. It should contain sufficient information to enable readers to decide whether they should obtain and read the entire paper. Do not cite references in the abstract.

KEY WORDS

The author should provide a list of three to five key words that clearly describe the subject matter of the paper.

TEXT LAYOUT

The manuscript must be typed single spacing. Use extra line spacing between equations, illustrations, figures and tables. The body of the text should be prepared using Georgia or Times New Roman. The font size used for preparation of the manuscript must be 11 or 12 points. The first paragraph following a heading should not be indented. The following paragraphs must be indented 10 mm. Note that there is no line spacing between paragraphs unless a subheading is used. Symbols for physical quantities in the text should be written in italics. Conclude the text with a summary or conclusion section. Spell out all initials, acronyms, or abbreviations (not units of measure) at first use. Put the initials or abbreviation in parentheses after the spelled-out version. The manuscript must be writing in the third person ("the author concludes... ").

FIGURES AND TABLES

Figures (diagrams and photographs) should be numbered consecutively using Arabic numbers. They should be placed in the text soon after the point where they are referenced. Figures should be centered in a column and should have a figure caption placed underneath. Captions should be centered in the column, in the format "Figure 1" and are in upper and lower case letters.

When referring to a figure in the body of the text, the abbreviation "Figure" is used Illustrations must be submitted in digital format, with a good resolution. Table captions appear centered above the table in upper and lower case letters.

When referring to a table in the text, "Table" with the proper number is used. Captions should be centered in the column, in the format "Table 1" and are in upper and lower case letters. Tables are numbered consecutively and independently of any figures. All figures and tables must be incorporated into the text.

EQUATIONS & MATHEMATICAL EXPRESSIONS

Place equations on separate lines, centered, and numbered in parentheses at the right margin. Equation numbers should appear in parentheses and be numbered consecutively. All equation numbers must appear on the right-hand side of the equation and should be referred to within the text.

CONCLUSIONS

A conclusion section must be included and should indicate clearly the advantages, limitations and possible applications of the paper. Discuss about future work.

Acknowledgements

An acknowledgement section may be presented after the conclusion, if desired. Individuals or units other than authors who were of direct help in the work could be acknowledged by a brief statement following the text. The acknowledgment should give essential credits, but its length should be kept to a minimum; word count should be <100 words.

References

References should be listed together at the end of the paper in alphabetical order by author's surname. List of references indent 10 mm from the second line of each references. Personal communications and unpublished data are not acceptable references.

Journal Papers: Surname 1, Initials; Surname 2, Initials and Surname 3, Initials: Title, Journal Name, volume (number), pages, year.

Books*:* Surname 1, Initials and Surname 2, Initials: Title, Edition (if existent), Place of publication, Publisher, year.

Proceedings Papers: Surname 1, Initials; Surname 2, Initials and Surname 3, Initials: Paper title, Proceedings title, pages, year.

ACTA TECHNICA CORVINIENSIS – Bulletin of Engineering is an international and interdisciplinary journal which reports on scientific and technical contributions. The **ACTA TECHNICA CORVINIENSIS – Bulletin of Engineering** advances the understanding of both the fundamentals of engineering science and its application to the solution of challenges and problems in engineering and management, dedicated to the publication of high quality papers on all aspects of the engineering sciences and the management.

You are invited to contribute review or research papers as well as opinion in the fields of science and technology including engineering. We accept contributions (full papers) in the fields of applied sciences and technology including all branches of engineering and management. Submission of a paper implies that the work described has not been published previously (except in the form of an abstract or as part of a published lecture or academic thesis) that it is not under consideration for publication elsewhere. It is not accepted to submit materials which in any way violate copyrights of third persons or law rights. An author is fully responsible ethically and legally for breaking given conditions or misleading the Editor or the Publisher.

The Editor reserves the right to return papers that do not conform to the instructions for paper preparation and template as well as papers that do not fit the scope of the journal, prior to refereeing. The Editor reserves the right not to accept the paper for print in the case of a negative review made by reviewers and also in the case of not paying the required fees if such will be fixed and in the case time of waiting for the publication of the paper would extend the period fixed by the Editor as a result of too big number of papers waiting for print. The decision of the Editor in that matter is irrevocable and their aim is care about the high content-related level of that journal.

The mission of the **ACTA TECHNICA CORVINIENSIS – Bulletin of Engineering** is to disseminate academic knowledge across the scientific realms and to provide applied research knowledge to the appropriate stakeholders. We are keen to receive original contributions from researchers representing any Science related field.

We strongly believe that the open access model will spur research across the world especially as researchers gain unrestricted access to high quality research articles. Being an Open Access Publisher, Academic Journals does not receive payment for subscription as the journals are freely accessible over the internet.

GENERAL TOPICS

ENGINEERING

- ✓ Mechanical Engineering
- ✓ Metallurgical Engineering
- ✓ Agricultural Engineering
- ✓ Control Engineering
- ✓ Electrical Engineering
- ✓ Civil Engineering
- ✓ Biomedical Engineering
- ✓ Transport Engineering
- ✓ Nanoengineering

CHEMISTRY

- ✓ General Chemistry
- ✓ Analytical Chemistry
- ✓ Inorganic Chemistry
- ✓ Materials Science & Metallography
- ✓ Polymer Chemistry
- ✓ Spectroscopy
- ✓ Thermo-chemistry

ECONOMICS

- ✓ Agricultural Economics
- ✓ Development Economics
- ✓ Environmental Economics
- ✓ Industrial Organization
- ✓ Mathematical Economics
- ✓ Monetary Economics
- ✓ Resource Economics
- ✓ Transport Economics
- ✓ General Management
- ✓ Managerial Economics
- ✓ Logistics

AGRICULTURE

- ✓ Agricultural & Biological Engineering
- ✓ Food Science & Engineering
- ✓ Horticulture

INFORMATION SCIENCES
- ✓ Computer Science
- ✓ Information Science

EARTH SCIENCES
- ✓ Geodesy
- ✓ Geology
- ✓ Hydrology
- ✓ Seismology
- ✓ Soil science

ENVIRONMENTAL
- ✓ Environmental Chemistry
- ✓ Environmental Science & Ecology
- ✓ Environmental Soil Science
- ✓ Environmental Health

BIOTECHNOLOGY
- ✓ Biomechanics
- ✓ Biotechnology
- ✓ Biomaterials

MATHEMATICS
- ✓ Applied mathematics
- ✓ Modeling & Optimization
- ✓ Foundations & Methods

ACTA TECHNICA CORVINIENSIS – Bulletin of Engineering has been published since 2008, as an online supplement of the **ANNALS of FACULTY ENGINEERING HUNEDOARA – International Journal of Engineering**. Now, the **ACTA TECHNICA CORVINIENSIS – Bulletin of Engineering** is a free-access, online, international and multidisciplinary publication of the Faculty of Engineering Hunedoara. **ACTA TECHNICA CORVINIENSIS – Bulletin of Engineering** exchange similar publications with similar institutions of our country and from abroad.

ISSN:2067-3809

Edited by:

FACULTY OF ENGINEERING HUNEDOARA
UNIVERSITY POLITEHNICA TIMISOARA

with kindly supported by:

THE GENERAL ASSOCIATION OF ROMANIAN ENGINEERS (AGIR)
– branch of HUNEDOARA

Editor / Technical preparation / Cover design:

Assoc. Prof. Eng. KISS Imre, PhD.
UNIVERSITY POLITEHNICA TIMISOARA,
FACULTY OF ENGINEERING HUNEDOARA

Commenced publication year:
2008

fascicule 2
[April - June]
tome X
[2017]
ISSN:2067-3809

ACTA Technica CORVINIENSIS
BULLETIN OF ENGINEERING

10th years
ANNIVERSARY

ISSN:2067-3809